U.S. DEPARTMENT OF COMMERCE
National Technical Information Service

PB-246 576

EVALUATION OF MATHEMATICAL MODELS FOR TEMPERATURE PREDICTION IN DEEP RESERVOIRS

VANDERBILT UNIVERSITY

PREPARED FOR

PACIFIC NORTHWEST ENVIRONMENTAL RESEARCH LABORATORY

JUNE 1975

KEEP UP TO DATE

Between the time you ordered this report—which is only one of the hundreds of thousands in the NTIS information collection available to you—and the time you are reading this message, several *new* reports relevant to your interests probably have entered the collection.

Subscribe to the **Weekly Government Abstracts** series that will bring you summaries of new reports *as soon as they are received by NTIS* from the originators of the research. The WGA's are an NTIS weekly newsletter service covering the most recent research findings in 25 areas of industrial, technological, and sociological interest—invaluable information for executives and professionals who must keep up to date.

The executive and professional information service provided by NTIS in the **Weekly Government Abstracts** newsletters will give you thorough and comprehensive coverage of government-conducted or sponsored research activities. And you'll get this important information within two weeks of the time it's released by originating agencies.

WGA newsletters are computer produced and electronically photocomposed to slash the time gap between the release of a report and its availability. You can learn about technical innovations immediately—and use them in the most meaningful and productive ways possible for your organization. Please request NTIS-PR-205/PCW for more information.

The weekly newsletter series will keep you current. But *learn what you have missed in the past* by ordering a computer **NTISearch** of all the research reports in your area of interest, dating as far back as 1964, if you wish. Please request NTIS-PR-186/PCN for more information.

WRITE: Managing Editor
5285 Port Royal Road
Springfield, VA 22161

Keep Up To Date With SRIM

SRIM (Selected Research in Microfiche) provides you with regular, automatic distribution of the complete texts of NTIS research reports *only* in the subject areas you select. SRIM covers almost all Government research reports by subject area and/or the originating Federal or local government agency. You may subscribe by any category or subcategory of our WGA **(Weekly Government Abstracts)** or **Government Reports Announcements and Index** categories, or to the reports issued by a particular agency such as the Department of Defense, Federal Energy Administration, or Environmental Protection Agency. Other options that will give you greater selectivity are available on request.

The cost of SRIM service is only 45¢ domestic (60¢ foreign) for each complete microfiched report. Your SRIM service begins as soon as your order is received and processed and you will receive biweekly shipments thereafter. If you wish, your service will be backdated to furnish you microfiche of reports issued earlier.

Because of contractual arrangements with several Special Technology Groups, not all NTIS reports are distributed in the SRIM program. You will receive a notice in your microfiche shipments identifying the exceptionally priced reports not available through SRIM.

A deposit account with NTIS is required before this service can be initiated. If you have specific questions concerning this service, please call (703) 451-1558, or write NTIS, attention SRIM Product Manager.

This information product distributed by

NTIS U.S. DEPARTMENT OF COMMERCE
National Technical Information Service
5285 Port Royal Road
Springfield, Virginia 22161

325205

PB 246 576

EPA-660/3-75-038
JUNE 1975

Ecological Research Series

UNITED STATES ENVIRONMENTAL PROTECTION AGENCY

RESEARCH REPORTING SERIES

Research reports of the Office of Research and Development, U.S. Environmental Protection Agency, have been grouped into five series. These five broad categories were established to facilitate further development and application of environmental technology. Elimination of traditional grouping was consciously planned to foster technology transfer and a maximum interface in related fields. The five series are:

1. Environmental Health Effects Research
2. Environmental Protection Technology
3. Ecological Research
4. Environmental Monitoring
5. Socioeconomic Environmental Studies

This report has been assigned to the ECOLOGICAL RESEARCH STUDIES series. This series describes research on the effects of pollution on humans, plant and animal species, and materials. Problems are assessed for their long- and short-term influences. Investigations include formation, transport, and pathway studies to determine the fate of pollutants and their effects. This work provides the technical basis for setting standards to minimize undesirable changes in living organisms in the aquatic, terrestrial and atmospheric environments.

EPA REVIEW NOTICE

This report has been reviewed by the Office of Research and Development, EPA, and approved for publication. Approval does not signify that the contents necessarily reflect the views and policies of the Environmental Protection Agency, nor does mention of trade names or commercial products constitute endorsement or recommendation for use.

TECHNICAL REPORT DATA
(Please read Instructions on the reverse before completing)

1. REPORT NO. EPA-660/3-75-038	2.	3. RECIPIENT'S ACCESSION NO. PB 246 576
4. TITLE AND SUBTITLE Evaluation of Mathematical Models for Temperature Prediction in Deep Reservoirs		5. REPORT DATE June, 1975
		6. PERFORMING ORGANIZATION CODE
7. AUTHOR(S) Frank L. Parker, Barry A. Benedict, Chii-ell Tsai		8. PERFORMING ORGANIZATION REPORT NO.
9. PERFORMING ORGANIZATION NAME AND ADDRESS Vanderbilt University Nashville, Tennessee 37235		10. PROGRAM ELEMENT NO. 1BA032
		11. CONTRACT/GRANT NO. R-800613
12. SPONSORING AGENCY NAME AND ADDRESS Pacific Northwest Environmental Research Laboratory National Environmental Research Center Corvallis, Oregon 97330		13. TYPE OF REPORT AND PERIOD COVERED
		14. SPONSORING AGENCY CODE

15. SUPPLEMENTARY NOTES

16. ABSTRACT

The deep reservoir model with one-dimensional assumptions can be applied to a reservoir or lake where the principal variation of flow characteristics is in the vertical direction. Among the models evaluated, the MIT deep reservoir model appears to be most easily used and to give results most compatible with the measured temperatures. The temperature predicted is strongly dependent upon the magnitude of the absorption coefficient of water, and the diffusion coefficient. However, our sensitivity analysis shows that an absorption coefficient of about $0.75 m^{-1}$ and a diffusion coefficient of 15 to 20 times molecular diffusion are appropriate choices for the seven TVA reservoirs studied. The determination of whether or not a reservoir model depends on the Densimetric Froude number. However, the representativeness of the result is not solely dependent upon the Densimetric Froude number. By the use of a fitted curve to the measured temperatures, it was possible to determine the maximum standard error of estimate for the predicted outlet level temperature, 1.6°C. Temperatures on individual days may exceed these values and they surely are exceeded at other depths in the reservoir. These limits are suggested as the limit of accuracy of these types of models.

17. KEY WORDS AND DOCUMENT ANALYSIS

a. DESCRIPTORS	b. IDENTIFIERS/OPEN ENDED TERMS	c. COSATI Field/Group
Thermal pollution, reservoirs, mathematical models, sensitivity analysis, Tennessee Valley Authority Projects	Deep reservoir models, Massachusetts Insitute of Technology, Water Resources Engineers, Cornell Aeronautical Laboratory	

PRICES SUBJECT TO CHANGE

18. DISTRIBUTION STATEMENT	19. SECURITY CLASS *(This Report)*	21. NO. OF PAGES 227
	20. SECURITY CLASS *(This page)*	22. PRICE $8.00 - 2.25

EPA Form 2220-1 (9-73)

☆ U.S. GOVERNMENT PRINTING OFFICE 1975—699-073 /15 REGION 10

EPA-660/3-75-038
JUNE 1975

EVALUATION OF MATHEMATICAL MODELS FOR TEMPERATURE PREDICTION IN DEEP RESERVOIRS

By

Frank L. Parker
Barry A. Benedict
Chii-ell Tsai

Vanderbilt University
Nashville, Tennessee

Grant No. R-800613
Program Element 1BA032
ROAP 21AJH/Task 12

Project Officer

Bruce Tichenor
Pacific Northwest Environmental Research Laboratory
National Environmental Research Center
Corvallis, Oregon 97330

NATIONAL ENVIRONMENTAL RESEARCH CENTER
OFFICE OF RESEARCH AND DEVELOPMENT
U. S. ENVIRONMENTAL PROTECTION AGENCY
CORVALLIS, OREGON 97330

For sale by the Superintendent of Documents, U.S. Government Printing Office, Washington, D.C. 20402

ia

ABSTRACT

The deep reservoir model with one-dimensional assumptions can be applied to a reservoir or lake where the principal variation of flow characteristics is in the vertical direction. Among the models evaluated, the MIT deep reservoir model appears to be most easily used and to give results most compatible with the measured temperatures. The temperature predicted is strongly dependent upon the magnitude of the absorption coefficient of water, and the diffusion coefficient. However, our sensitivity analysis shows that an absorption coefficient of about $0.75m^{-1}$ and a diffusion coefficient of 15 to 20 times molecular diffusion are appropriate choices for the seven TVA reservoirs studied. The determination of whether or not a reservoir model depends on the Densimetric Froude number. However, the representativeness of the result is not solely dependent upon the Densimetric Froude number. By the use of a fitted curve to the measured temperatures, it was possible to determine the maximum standard error of estimate for the predicted outlet level temperature, 1.6°C. Temperatures on individual days may exceed those values and they surely are exceeded at other depths in the reservoir. These limits are suggested as the limit of accuracy of these types of models.

This report was submitted in fulfillment of Grant R-800613 by Vanderbilt University, Nashville, Tennessee, under the sponsorship of the Environmental Protection Agency. Work was completed as of June, 1975.

TABLE OF CONTENTS

Page

List of Figures v

List of Tables xvii

Section I

Conclusions 1

Section II

Recommendations 3

Section III

Introduction. 4

Section IV

- Analysis of Deep Reservoir Models 8
- General Description of Deep Reservoir Models. 9
- Water Resources Engineers' Model. 24
  - Principal Assumptions. 25
  - Factors Considered and the Basic Equations 25
  - Direct Absorption of Solar Radiation 25
  - Selective Withdrawal 26
  - Depth and Velocity Distribution of Inflow. 27
  - Internal Mixing. 28
  - Governing Equation 29
  - Verification 33
  - Results of Test Run. 33
- MIT Model 39
  - Principal Assumptions. 39
  - Factors Considered and the Basic Equations 43
  - Varification 48
  - Sensitivity Analysis 48
- Cornell Model 48
  - Assumptions. 48
  - Basic Equations. 49
  - Verification 52
  - Results of Test Run. 53
- Problems with Deep Reservoirs Models. 58

Section V

- Sensitivity Analysis. 64
- Fontana Reservoir 69
- Douglas Reservoir 91
- Cherokee Reservoir. 109
- Norris Reservoir. 126
- South Holston Reservoir 140

Hiwasee Reservoir 158
Fort Loudon Reservoir 176

Section VI

Analysis of Data. 197

References 204

LIST OF FIGURES

		Page
Figure 1	Reservoir Representation	11
Figure 2	WRE Model -- Effect of Thickness of Horizontal Layer (July 6, 1966)	35
Figure 3	WRE Model -- Effect of Thickness of Horizontal Layer (Sept. 1, 1966)	36
Figure 4	WRE Model -- Effect of Thickness of Horizontal Layer (Dec. 1, 1966)	37
Figure 5	WRE Model -- Effects of Diffusion Coefficient (July 6, 1966)	40
Figure 6	WRE Model -- Effects of Diffusion Coefficient (Sept. 1, 1966)	41
Figure 7	WRE Model -- Effects of Diffusion Coefficient (Dec. 1, 1966)	42
Figure 8	Cornell Model Test Run Results July 6, 1966	55
Figure 9	Cornell Model Test Run Results Septemper 1, 1966	56
Figure 10	Cornell Model Test Run Results December 1, 1966	57
Figure 11	Surface Layer Schematic	61
Figure 12	Fontana Reservoir - Measured Temperature Profile	72
Figure 13	Fontana Reservoir - Computed Temperature Profile	72
Figure 14	Fontana Reservoir - Computed Outflow Temperature	76
Figure 15	Fontana Reservoir - Layer Thickness Sensitivity Day 75	76
Figure 16	Fontana Reservoir - Layer Thickness Sensitivity Day 132	77

Figure 17 Fontana Reservoir - Layer Thickness Sensitivity Day 187 77
Figure 18 Fontana Reservoir - Layer Thickness Sensitivity Day 215 78
Figure 19 Fontana Reservoir - Layer Thickness Sensitivity Day 244 78
Figure 20 Fontana Reservoir - Layer Thickness Sensitivity Day 285 79
Figure 21 Fontana Reservoir - Layer Thickness Sensitivity Day 335 79
Figure 22 Fontana Reservoir - Absorption Coefficient Sensitivity, Day 75 80
Figure 23 Fontana Reservoir - Absorption Coefficient Sensitivity, Day 132 80
Figure 24 Fontana Reservoir - Absorption Coefficient Sensitivity, Day 187 81
Figure 25 Fontana Reservoir - Absorption Coefficient Sensitivity, Day 215 81
Figure 26 Fontana Reservoir - Absorption Coefficient Sensitivity, Day 244 82
Figure 27 Fontana Reservoir - Absorption Coefficient Sensitivity, Day 285 82
Figure 28 Fontana Reservoir - Absorption Coefficient Sensitivity, Day 335 83
Figure 29 Fontana Reservoir - Extinction Coefficient Sensitivity, Day 75 83
Figure 30 Fontana Reservoir - Extinction Coefficient Sensitivity, Day 132 84
Figure 31 Fontana Reservoir - Extinction Coefficient Sensitivity, Day 187 84
Figure 32 Fontana Reservoir - Extinction Coefficient Sensitivity, Day 215 85
Figure 33 Fontana Reservoir - Extinction Coefficient Sensitivity, Day 244 85

Figure 34 Fontana Reservoir - Extinction Coefficient Sensitivity, Day 285 86

Figure 35 Fontana Reservoir - Extinction Coefficient Sensitivity, Day 335 86

Figure 36 Fontana Reservoir - Diffusion Coefficient Sensitivity, Day 75 87

Figure 37 Fontana Reservoir - Diffusion Coefficient Sensitivity, Day 132 87

Figure 38 Fontana Reservoir - Diffusion Coefficient Sensitivity, Day 187 88

Figure 39 Fontana Reservoir - Diffusion Coefficient Sensitivity, Day 215 88

Figure 40 Fontana Reservoir - Diffusion Coefficient Sensitivity, Day 244 89

Figure 41 Fontana Reservoir - Diffusion Coefficient Sensitivity, Day 285 89

Figure 42 Fontana Reservoir - Diffusion Coefficient Sensitivity, Day 335 90

Figure 43 Douglas Reservoir - Computed Temperature Profile 93

Figure 44 Douglas Reservoir - Computed Outflow Temperature 96

Figure 45 Douglas Reservoir - Layer Thickness Sensitivity, Day 69 96

Figure 46 Douglas Reservoir - Layer Thickness Sensitivity, Day 121 97

Figure 47 Douglas Reservoir - Layer Thickness Sensitivity, Day 186 97

Figure 48 Douglas Reservoir - Layer Thickness Sensitivity, Day 218 98

Figure 49 Douglas Reservoir - Layer Thickness Sensitivity, Day 250 98

Figure 50 Douglas Reservoir - Layer Thickness Sensitivity, Day 276 99

Figure 51	Douglas Reservoir - Absorption Coefficient Sensitivity, Day 69	99
Figure 52	Douglas Reservoir - Absorption Coefficient Sensitivity, Day 121	100
Figure 53	Douglas Reservoir - Absorption Coefficient Sensitivity, Day 186	100
Figure 54	Douglas Reservoir - Absorption Coefficient Sensitivity, Day 218	101
Figure 55	Douglas Reservoir - Absorption Coefficient Sensitivity, Day 250	101
Figure 56	Douglas Reservoir - Absorption Coefficient Sensitivity, Day 276	102
Figure 57	Douglas Reservoir - Extinction Coefficient Sensitivity, Day 69	102
Figure 58	Douglas Reservoir - Extinction Coefficient Sensitivity, Day 121	103
Figure 59	Douglas Reservoir - Extinction Coefficient Sensitivity, Day 186	103
Figure 60	Douglas Reservoir - Extinction Coefficient Sensitivity, Day 218	104
Figure 61	Douglas Reservoir - Extinction Coefficient Sensitivity, Day 250	104
Figure 62	Douglas Reservoir - Extinction Coefficient Sensitivity, Day 276	105
Figure 63	Douglas Reservoir - Diffusion Coefficient Sensitivity, Day 69	105
Figure 64	Douglas Reservoir - Diffusion Coefficient Sensitivity, Day 121	106
Figure 65	Douglas Reservoir - Diffusion Coefficient Sensitivity, Day 186	106
Figure 66	Douglas Reservoir - Diffusion Coefficient Sensitivity, Day 218	107
Figure 67	Douglas Reservoir - Diffusion Coefficient Sensitivity, Day 250	107

Figure 68	Douglas Reservoir - Diffusion Coefficient Sensitivity, Day 276	108
Figure 69	Cherokee Reservoir - Computed Temperature Profile	112
Figure 70	Cherokee Reservoir - Computed Outflow Temperature	113
Figure 71	Cherokee Reservoir - Layer Thickness Sensitivity, Day 66	113
Figure 72	Cherokee Reservoir - Layer Thickness Sensitivity, Day 123	114
Figure 73	Cherokee Reservoir - Layer Thickness Sensitivity, Day 186	114
Figure 74	Cherokee Reservoir - Layer Thickness Sensitivity, Day 213	115
Figure 75	Cherokee Reservoir - Layer Thickness Sensitivity, Day 248	115
Figure 76	Cherokee Reservoir - Layer Thickness Sensitivity, Day 277	116
Figure 77	Cherokee Reservoir - Absorption Coefficient Sensitivity, Day 66	116
Figure 78	Cherokee Reservoir - Absorption Coefficient Sensitivity, Day 123	117
Figure 79	Cherokee Reservoir - Absorption Coefficient Sensitivity, Day 186	117
Figure 80	Cherokee Reservoir - Absorption Coefficient Sensitivity, Day 213	118
Figure 81	Cherokee Reservoir - Absorption Coefficient Sensitivity, Day 248	118
Figure 82	Cherokee Reservoir - Absorption Coefficient Sensitivity, Day 277	119
Figure 83	Cherokee Reservoir - Extinction Coefficient Sensitivity, Day 66	119
Figure 84	Cherokee Reservoir - Extinction Coefficient Sensitivity, Day 123	120

Figure 85 Cherokee Reservoir - Extinction Coefficient Sensitivity, Day 186 120

Figure 86 Cherokee Reservoir - Extinction Coefficient Sensitivity, Day 213 121

Figure 87 Cherokee Reservoir - Extinction Coefficient Sensitivity, Day 248 121

Figure 88 Cherokee Reservoir - Extinction Coefficient Sensitivity, Day 277 122

Figure 89 Cherokee Reservoir - Extinction Coefficient Sensitivity, Day 66 122

Figure 90 Cherokee Reservoir - Diffusion Coefficient Sensitivity, Day 123 123

Figure 91 Cherokee Reservoir - Diffusion Coefficient Sensitivity, Day 186 123

Figure 92 Cherokee Reservoir - Diffusion Coefficient Sensitivity, Day 213 124

Figure 93 Cherokee Reservoir - Diffusion Coefficient Sensitivity, Day 248 124

Figure 94 Cherokee Reservoir - Diffusion Coefficient Sensitivity, Day 277 125

Figure 95 Norris Reservoir - Computed Temperature Profile 127

Figure 96 Norris Reservoir - Computed Outflow Temperature 129

Figure 97 Norris Reservoir - Layer Thickness Sensitivity, Day 106 129

Figure 98 Norris Reservoir - Layer Thickness Sensitivity, Day 139 130

Figure 99 Norris Reservoir - Layer Thickness Sensitivity, Day 183 130

Figure 100 Norris Reservoir - Layer Thickness Sensitivity, Day 225 131

Figure 101 Norris Reservoir - Layer Thickness Sensitivity, Day 252 131

Figure 102 Norris Reservoir - Absorption Coefficient Sensitivity, Day 106 132

Figure 103 Norris Reservoir - Absorption Coefficient Sensitivity, Day 106 132

Figure 104 Norris Reservoir - Absorption Coefficient Sensitivity, Day 183 133

Figure 105 Norris Reservoir - Absorption Coefficient Sensitivity, Day 225 133

Figure 106 Norris Reservoir - Absorption Coefficient Sensitivity, Day 252 134

Figure 107 Norris Reservoir - Extinction Coefficient Sensitivity, Day 106 134

Figure 108 Norris Reservoir - Extinction Coefficient Sensitivity, Day 139 135

Figure 109 Norris Reservoir - Extinction Coefficient Sensitivity, Day 183 135

Figure 110 Norris Reservoir - Extinction Coefficient Sensitivity, Day 225 136

Figure 111 Norris Reservoir - Extinction Coefficient Sensitivity, Day 252 136

Figure 112 Norris Reservoir - Diffusion Coefficient Sensitivity, Day 106 137

Figure 113 Norris Reservoir - Diffusion Coefficient Sensitivity, Day 139 137

Figure 114 Norris Reservoir - Diffusion Coefficient Sensitivity, Day 183 138

Figure 115 Norris Reservoir - Diffusion Coefficient Sensitivity, Day 225 138

Figure 116 Norris Reservoir - Diffusion Coefficient Sensitivity, Day 252 139

Figure 117 South Holston Reservoir - Measured Temperature Profile 142

Figure 118 South Holston Reservoir - Computed Temperature Profile 145

Figure 119 South Holston Reservoir - Computed Outflow Temperature 145
Figure 120 South Holston Reservoir - Layer Thickness Sensitivity, Day 78 146
Figure 121 South Holston Reservoir - Layer Thickness Sensitivity, Day 142 146
Figure 122 South Holston Reservoir - Layer Thickness Sensitivity, Day 203 147
Figure 123 South Holston Reservoir - Layer Thickness Sensitivity, Day 245 147
Figure 124 South Holston Reservoir - Layer Thickness Sensitivity, Day 299 148
Figure 125 South Holston Reservoir - Layer Thickness Sensitivity, Day 362 148
Figure 126 South Holston Reservoir - Absorption Coefficient Sensitivity, Day 78 149
Figure 127 South Holston Reservoir - Absorption Coefficient Sensitivity, Day 142 149
Figure 128 South Holston Reservoir - Absorption Coefficient Sensitivity, Day 203 150
Figure 129 South Holston Reservoir - Absorption Coefficient Sensitivity, Day 245 150
Figure 130 South Holston Reservoir - Absorption Coefficient Sensitivity, Day 299 151
Figure 131 South Holston Reservoir - Absorption Coefficient Sensitivity, Day 362 151
Figure 132 South Holston Reservoir - Extinction Coefficient Sensitivity, Day 78 152
Figure 133 South Holston Reservoir - Extinction Coefficient Sensitivity, Day 142 152
Figure 134 South Holston Reservoir - Extinction Coefficient Sensitivity, Day 203 153
Figure 135 South Holston Reservoir - Extinction Coefficient Sensitivity, Day 245 153
Figure 136 South Holston Reservoir - Extinction Coefficient Sensitivity, Day 299 154

Figure 137 South Holston Reservoir - Extinction Coefficient Sensitivity, Day 362 154

Figure 138 South Holston Reservoir - Diffusion Coefficient Sensitivity, Day 78 155

Figure 139 South Holston Reservoir - Diffusion Coefficient Sensitivity, Day 142 155

Figure 140 South Holston Reservoir - Diffusion Coefficient Sensitivity, Day 203 156

Figure 141 South Holston Reservoir - Diffusion Coefficient Sensitivity, Day 245 156

Figure 142 South Holston Reservoir - Diffusion Coefficient Sensitivity, Day 299 157

Figure 143 South Holston Reservoir - Diffusion Coefficient Sensitivity, Day 362 157

Figure 144 Hiwassee Reservoir - Measured Temperature Profile 162

Figure 145 Hiwassee Reservoir - Computed Temperature Profile 162

Figure 146 Hiwassee Reservoir - Computed Outflow Temperature 163

Figure 147 Hiwassee Reservoir - Layer Thickness Sensitivity, Day 80 163

Figure 148 Hiwassee Reservoir - Layer Thickness Sensitivity, Day 148 164

Figure 149 Hiwassee Reservoir - Layer Thickness Sensitivity, Day 209 164

Figure 150 Hiwassee Reservoir - Layer Thickness Sensitivity, Day 267 165

Figure 151 Hiwassee Reservoir - Layer Thickness Sensitivity, Day 302 165

Figure 152 Hiwassee Reservoir - Layer Thickness Sensitivity, Day 364 166

Figure 153 Hiwassee Reservoir - Absorption Coefficient Sensitivity, Day 80 166

Figure 154 Hiwassee Reservoir - Absorption Coefficient Sensitivity, Day 148 167

Figure 155 Hiwassee Reservoir - Absorption Coefficient Sensitivity, Day 209 167

Figure 156 Hiwassee Reservoir - Absorption Coefficient Sensitivity, Day 267 168

Figure 157 Hiwassee Reservoir - Absorption Coefficient Sensitivity, Day 302 168

Figure 158 Hiwassee Reservoir - Absorption Coefficient Sensitivity, Day 364 169

Figure 159 Hiwassee Reservoir - Extinction Coefficient Sensitivity, Day 80 169

Figure 160 Hiwassee Reservoir - Extinction Coefficient Sensitivity, Day 148 170

Figure 161 Hiwassee Reservoir - Extinction Coefficient Sensitivity, Day 209 170

Figure 162 Hiwassee Reservoir - Extinction Coefficient Sensitivity, Day 267 171

Figure 163 Hiwassee Reservoir - Extinction Coefficient Sensitivity, Day 302 171

Figure 164 Hiwassee Reservoir - Extinction Coefficient Sensitivity, Day 364 172

Figure 165 Hiwassee Reservoir - Diffusion Coefficient Sensitivity, Day 80 172

Figure 166 Hiwassee Reservoir - Diffusion Coefficient Sensitivity, Day 148 173

Figure 167 Hiwassee Reservoir - Diffusion Coefficient Sensitivity, Day 209 173

Figure 168 Hiwassee Reservoir - Diffusion Coefficient Sensitivity, Day 267 174

Figure 169 Hiwassee Reservoir - Diffusion Coefficient Sensitivity, Day 302 174

Figure 170 Hiwassee Reservoir - Diffusion Coefficient Sensitivity, Day 364 175

Figure 171	Fort Loudon Reservoir - Measured Temperature Profile	178
Figure 172	Fort Loudon Reservoir - Computed Temperature Profile	181
Figure 173	Fort Loudon Reservoir - Computed Outflow Temperature	181
Figure 174	Fort Loudon Reservoir - Layer Thickness Sensitivity, Day 76	182
Figure 175	Fort Loudon Reservoir - Layer Thickness Sensitivity, Day 132	182
Figure 176	Fort Loudon Reservoir - Layer Thickness Sensitivity, Day 204	183
Figure 177	Fort Loudon Reservoir - Layer Thickness Sensitivity, Day 226	183
Figure 178	Fort Loudon Reservoir - Layer Thickness Sensitivity, Day 253	184
Figure 179	Fort Loudon Reservoir - Layer Thickness Sensitivity, Day 280	184
Figure 180	Fort Loudon Reservoir - Layer Thickness Sensitivity, Day 343	185
Figure 181	Fort Loudon Reservoir - Absorption Coefficient Sensitivity, Day 76	185
Figure 182	Fort Loudon Reservoir - Absorption Coefficient Sensitivity, Day 132	186
Figure 183	Fort Loudon Reservoir - Absorption Coefficient Sensitivity, Day 204	186
Figure 184	Fort Loudon Reservoir - Absorption Coefficient Sensitivity, Day 226	187
Figure 185	Fort Loudon Reservoir - Absorption Coefficient Sensitivity, Day 253	187
Figure 186	Fort Loudon Reservoir - Absorption Coefficient Sensitivity, Day 280	188
Figure 187	Fort Loudon Reservoir - Absorption Coefficient Sensitivity, Day 343	188

Figure 188 Fort Loudon Reservoir - Extinction Coefficient Sensitivity, Day 76 189

Figure 189 Fort Loudon Reservoir - Extinction Coefficient Sensitivity, Day 132 189

Figure 190 Fort Loudon Reservoir - Extinction Coefficient Sensitivity, Day 204 190

Figure 191 Fort Loudon Reservoir - Extinction Coefficient Sensitivity, Day 226 190

Figure 192 Fort Loudon Reservoir - Extinction Coefficient Sensitivity, Day 253 191

Figure 193 Fort Loudon Reservoir - Extinction Coefficient Sensitivity, Day 280 191

Figure 194 Fort Loudon Reservoir - Extinction Coefficient Sensitivity, Day 343 192

Figure 195 Fort Loudon Reservoir - Diffusion Coefficient Sensitivity, Day 76 192

Figure 196 Fort Loudon Reservoir - Diffusion Coefficient Sensitivity, Day 132 193

Figure 197 Fort Loudon Reservoir - Diffusion Coefficient Sensitivity, Day 204 193

Figure 198 Fort Loudon Reservoir - Diffusion Coefficient Sensitivity, Day 226 194

Figure 199 Fort Loudon Reservoir - Diffusion Coefficient Sensitivity, Day 253 194

Figure 200 Fort Loudon Reservoir - Diffusion Coefficient Sensitivity, Day 280 195

Figure 201 Fort Loudon Reservoir - Diffusion Coefficient Sensitivity, Day 343 195

LIST OF TABLES

		Page
Table 1	Assumptions	14, 15
Table 2	Input Parameters	16, 17, 18, 19
Table 3	Factors Involved in Analysis	20, 21
Table 4	Model Construction	22, 23
Table 5	Parameters Varied in Sensitivity Analysis	66
Table 6	Frequency Analysis of the Wind Speed	70
Table 7	Legend for Figures 12-201	71
Table 8	Statistical Analysis for the Predicted Water Temperature at Outlet Level - Fontana Reservoir, 1966	73
Table 9	Statistical Analysis for the Predicted Surface Water Temperature - Fontana Reservoir, 1966	74
Table 10	Statistical Analysis for the Predicted Water Temperature at Outlet Level - Douglas Reservoir, 1969	94
Table 11	Statistical Analysis for the Predicted Surface Water Temperature - Douglas Reservoir, 1969	95
Table 12	Statistical Analysis for the Predicted Water Temperature at Outlet Level - Cherokee Reservoir, 1967	110
Table 13	Statistical Analysis for the Predicted Surface Water Temperature - Cherokee Reservoir, 1967	111
Table 14	Statistical Analysis for the Predicted Surface Water Temperature - Norris Reservoir, 1972	128
Table 15	Statistical Analysis for the Predicted Water Temperature at Outlet Level - South Holston Reservoir, 1953	143
Table 16	Statistical Analysis for the Predicted Surface Water Temperature - South Holston Reservoir, 1953	144

Table 17 Statistical Analysis for the Predicted Water Temperature at Outlet Level - Hiwassee Reservoir, 1947 160

Table 18 Statistical Analysis for the Predicted Surface Water Temperature - Hiwassee Reservoir, 1947 161

Table 19 Statistical Analysis for the Predicted Water Temperature at Outlet Level - Fort Loudon Reservoir, 1971 179

Table 20 Statistical Analysis for the Predicted Surface Water Temperature - Fort Loudon Reservoir, 1971 180

Table 21 Least Squares Curve Fit for Measured Surface Water Temperature 198

Table 22 Least Squares Curve Fit for Measured Water Temperature at Outlet Level 199

Table 23 Densimetric Froude Numbers for Some TVA Reservoirs 203

SECTION I

CONCLUSIONS

1. This study using field data indicates that the deep reservoir model with one-dimensional assumptions can be applied to a reservoir or lake where the principal variation of flow characteristics is in the vertical direction. The factors considered in the heat transport equation must include the heat gained or lost through the water surface, heat transported by inflow, outflow and vertical advection, and the mixing mechanism due to diffusion and convection.

2. Among the models evaluated, the MIT deep reservoir model appears to be most easily used and to give results most compatible with the measured temperatures.

3. The temperature predicted is strongly dependent upon the magnitude of the absorption coefficient of water, and the diffusion coefficient. However, our sensitivity analysis shows that the value of about $0.75 m^{-1}$ and a diffusion coefficient of 15 to 20 times molecular diffusion are appropriate choices for the seven TVA reservoirs studied.

4. The Densimetric Froude number is an important parameter to indicate the degree of stratification of a body of water. The determination of whether or not a reservoir or lake is suitable for the application of a deep reservoir model depends on the Densimetric Froude number.

However, the representativeness of the result is not solely dependent upon the Densimetric Froude number.

5. Perhaps, the most important water temperatures are those at the surface and in the withdrawal layer. By the use of a fitted curve to the measured temperatures at these elevations, it was possible to determine the maximum standard error of estimate for the predicted surface temperature, $1.2^{o}C$, and of the predicted outlet level temperature, $1.6^{o}C$. Temperature variations on individual days may exceed these values and they surely are exceeded at other depths in the reservoir. These limits are suggested as the limit of accuracy of these types of models.

6. In a reservoir where the temperature goes below $4^{o}C$, the density instead of temperature, should be used for the determination of the entrance level of inflow, the thickness of withdrawal layer and the condition for the convection to occur. The models evaluated, MIT, WRE and Cornell must be modified before they can be applied to such conditions.

SECTION II

RECOMMENDATIONS

1. Though it is possible to further refine the mathematical models used in temperature predictions for deep reservoirs, it appears that at this time it would be advisable for operational purposes to utilize the existing models, such as the MIT model, which have been most thoroughly verified.
2. Though an analysis of the reservoir temperatures has been made for a series of the TVA reservoirs, no analysis has yet been made for the temperature distribution of a single reservoir over a period of years to determine the proper coefficients to be used in the model. This should be done.
3. An intensive thermal analysis of reservoirs in the southeast section of the United States has been made. Such an analysis needs to be made for other sections of the country to determine if the coefficients most suitable for the southeastern section of the United States are also most suitable for the other sections.
4. For a better theoretical and emperical understanding of thermal regimes in reservoirs, further detailed laboratory and field studies on the effects of multiple inflows on the assumption of horizontal homogeneity need to be carried out. In addition, further field studies on withdrawals is required to determine the layers affected and the internal currents induced by the intermittent releases.

SECTION III

INTRODUCTION

Water quality is one of the major considerations in water resources planning, and water temperature is a key factor in determining water quality. Due to the influence of temperature on the physical and chemical properties of water and on the aquatic life within a water body, a reasonable prediction of the temporal and spatial variation of the thermal structure within the reservoir is essential for successful management. This has become even more evident with passage of PL 92-500, Federal Water Pollution Control Act Amendments of 1972, where thermal water quality standards are specifically included in the term "water quality standards" (Section 303-h).

Relief from these standards may be obtained under Section 316 if the petitioner can show that the effluent limitations are "more stringent than necessary to assure the projection and propagation of a balanced, indigenous population of shellfish, fish and wildlife in and on the body of water into which the discharge is to be made ...".

With the increase in the size of power production units and plants and the trend to nuclear power, the prediction of the thermal structure in receiving waters is even more so a necessity. Consequently, a large number of mathematical models have been constructed but most have had only very limited field verification. All of the models have certain features in common and it has, therefore, become more important to verify the models' field results and obtain the range and mean of the necessary coefficients than to further elaborate on the details of the models themselves. For practical field applications, this is especially true. For research purposes some of the phenomena should be disaggregated and be more intensively studied but for purposes of meeting the legal requirements of Section 316, determination with greater confidence of the coefficients of the aggregated phenomena is more important.

Therefore, a series of comparative studies of mathematical models of typical thermal systems have been commissioned by EPA. These include a comparative study of the local thermal structure of submerged discharges into large bodies of water[1], of the local thermal structure of surface discharges into large bodies of water[2], and this work on the thermal structure of large, deep bodies of water (i.e., reservoirs or lakes).

The distinction between a deep reservoir or lake and a shallow, run of the river reservoir is the maintenance of horizontal isotherms and a strong stratification during summer. Also deep reservoirs usually have a low annual through-flow to volume ratio.

Though there are many mathematical models available today for calculation of temperature rises in reservoirs, few of them have been so thoroughly explicated that they can be used easily except by a specialist in the field. Though many of the models have been developed under EPA contracts, there is no detailed evaluation and comparison of the various models. Therefore, it is not possible to know beforehand what information is required for the computer program evaluation, which factors are considered in the models, the sensitivity of the models to changes in the variables nor how the results would differ from one another if the various models were used.

Therefore, the most widely known and used models, Water Resources Engineers (Orlob)[3], MIT (Harleman-Huber-Ryan)[4], Cornell Aeronautical Laboratory (Sundaram)[5], Colheat (Jaske)[6] and Corps of Engineers (Beard)[7] have been collected and evaluated. After preliminary analysis only three models, WRE, MIT and Cornell were further evaluated. The Colheat Model was developed primarily to simulate the thermal properties of a flowing water body where the vertical stratification is very weak or nonexistent. The assumption that convection is restricted only to the longitudinal direction makes it unsuitable for use for deep reservoir analysis. The Corps of Engineers' model simulates thermal properties within a reservoir on a monthly basis. This time span is too large for the detail required in this study.

The purposes of this study are:

1. To review each model, including analysis of available documentation and computer codes, tabulation of assumptions and factors involved in analysis, listing of input parameters required and the criteria for application to prototype in an explicit form.
2. To analyze the major differences between models.
3. To verify each model using numerous reservoirs' field data.
4. To perform sensitivity analysis of the most important input parameters.
5. To recommend criteria for choosing suitable input parameters required to run the predictive models based on the field data verification and sensitivity analysis.

It was anticipated that this study would provide clues in choosing a suitable model, provide the necessary information about the proper use of each model and lessen the difficulties one may encounter in running such programs, to the extent that a new investigator in the field will not be tempted to build his own program, but would further detail and verify the existing programs.

SECTION IV

ANALYSIS OF DEEP RESERVOIR MODELS

In temperate zones, the spring heating, primarily by the absorption of the solar and atmospheric radiation, tends to warm up the waters closest to the surface. However, surface cooling, due to back radiation, evaporation and conduction, and wind-induced turbulence will cause mixing whenever the density gradient is too shallow and too weak to maintain a stable condition. During this period the temperature distribution is only weakly stratified. The heat in the surface layers is transported slowly down to the deep water primarily by advection. As solar heating continues, the temperature of the upper region, epilimnion, increases, while the lower region, hypolimnion, remains cool and relatively undisturbed. A zone in between the two regions in which the temperature gradient is the largest is called the thermocline. This steep density gradient tends to inhibit the transfer of heat and momentum between the warm upper layer, and the underlying cooler waters. The tributary inflows, which tend to be warmer than the lower reservoir waters during the summer season, mix and enter the reservoir water column at the elevation where its density is equal to that in the water column.

Thermal stratification affects not only the extent of dilution and mixing of the inflow waters, but also the quality of the water in hypolimnion. The development of deficits in the hypolimnetic dissolved oxygen concentration usually follows the establishment of thermal stratification. After its formation, the thermocline moves downward as the stratification increases. When the surface water attains its maximum temperature and then begins to cool, the epilimnion tends to become more dense and unstable with respect to the lower, less dense waters. The thermocline sinks rapidly as the epilimnion cools further until the whole reservoir mixes or overturns and is isothermal. In climates where the temperature falls below 4°C, two overturns may occur per year. The reservoir then is isothermal in the early spring as well.

The cycle of stratification is very complicated. The solution of this problem must consider all the influences from the meteorologic, hydraulic and hydrodynamic factors and the thermal and density properties of the water.

GENERAL DESCRIPTION OF DEEP RESERVOIR MODELS

The basic equation, 1[8], relating all the energy inputs to a body of water can be solved for reservoirs, rivers and estuaries and coastal regions.

$$Q_s - Q_r + Q_a - Q_{ar} - Q_{bs} + Q_v - Q_e \mp Q_h - Q_w = Q \qquad (1)$$

Where:

Q_s = shortwave radiation incident to the water surface;

Q_r = reflected shortwave radiation;

Q_a = incoming longwave radiation from the atmosphere;

Q_{ar} = reflected longwave radiation;

Q_{bs} = longwave radiation emitted by the body of water;

Q_v = net energy brought into the body of water in inflow, including precipitation, and accounting for outflow;

Q_e = energy utilized by evaporation;

Q_h = energy conducted from the body of water as sensible heat;

Q_w = energy carried away by the evaporated water;

Q = increase in energy stored in the body of water.

A three-dimensional analysis is so complicated that it is usually not justified by the increased accuracy of the results. In most practical problems, one or two dimensional analyses will describe adequately all the principal factors. The existence of horizontal isotherms, although sometimes tilted slightly by the wind action and/or the effect of lag time of inflow, and the much faster dispersion in the horizontal direction than in the vertical direction, ensure that the assumption of horizontal homogeniety of physical properties in the model is compatible with the prototype. Most mathematical models are based on the one-dimensional vertical motion assumption and can predict the thermal structure of reservoirs that are in good agreement with the measured values.

In a stratified reservoir, the body of water must be segmented into a series of discrete horizontal elements to compute the vertical variation of temperature. Therefore, heat flux due to vertical advection, and diffusion between elements is added to Eq. 1 and applied to each element. A schematic of the reservoir model considered is shown in Figure 1. For simplicity, the elements except for the top and bottom are usually of equal thickness. The basic heat transport equation and the continuity equation are written for an element. At the beginning of the calculation, the surface elevation is determined either from a measured surface elevation or calculated from measured inflow and outflow rates. The inflow and outflow distribution in each layer is evaluated according to certain

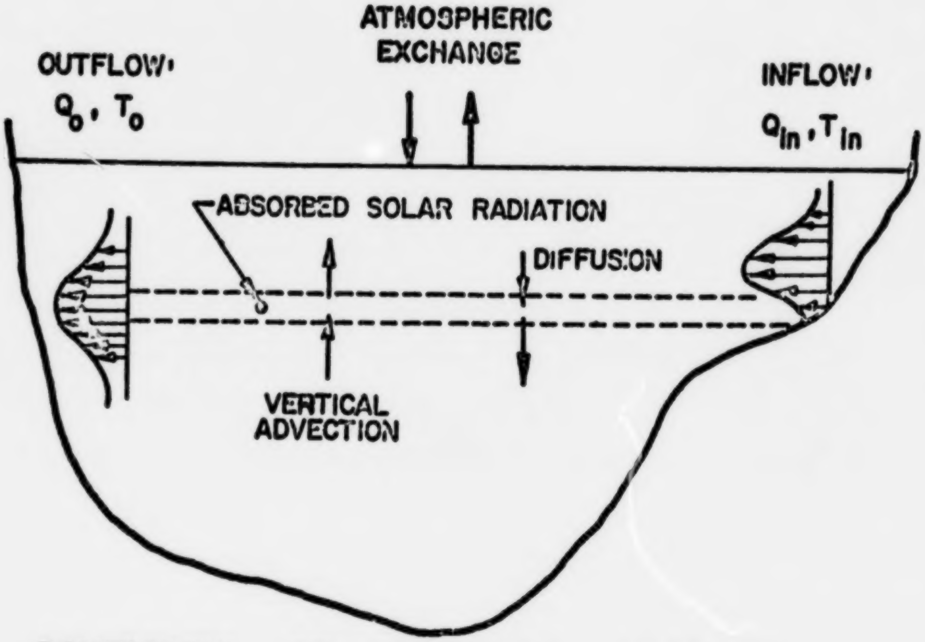
ATMOSPHERIC EXCHANGE
OUTFLOW: Q_o, T_o
INFLOW: Q_{in}, T_{in}
ABSORBED SOLAR RADIATION
DIFFUSION
VERTICAL ADVECTION

SCHEMATIC OF RESERVOIR PROBLEM

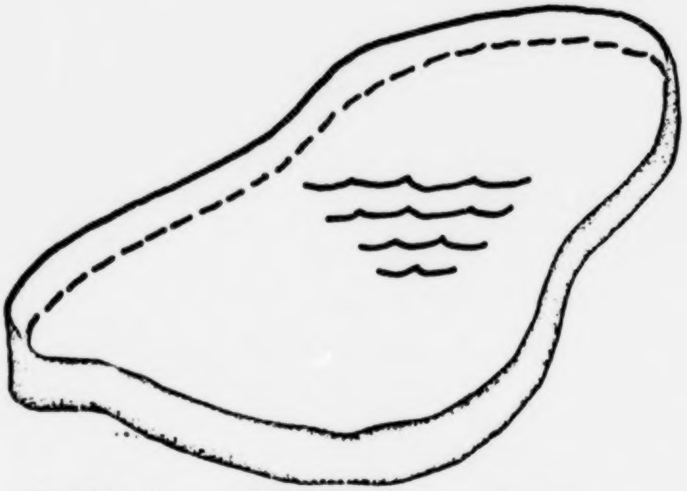

TYPICAL HORIZONTAL SLICE FROM RESERVOIR

Figure 1. Reservoir representation

formula or criteria. Applying the continuity equation to each control volume, beginning with the bottom element, the vertical advection across the bounding surfaces can easily be found.

For a chosen period of time, Δt, the net change of heat content, or the rate of heat change, in the control volume is evaluated. The heat fluxes considered include that from inflow, outflow, vertical advection, diffusion, and absorption of radiation energy for an internal element. In addition to these, surface absorbed energy and surface heat losses, due to evaporation, conduction, and longwave back radiation must also be included in the surface layer heat balance. From the rate of heat change, the final temperatures are obtained.

Each of the models is essentially an accounting procedure of the energy budget over a period of time. The procedure iterates until balance is achieved and stability criteria are satisfied, and proceeds to the next time step.

The differences in solution method relate primarily to: a) the handling of Q_v, the net energy brought into the body of water in inflow, including precipitation, and accounting for outflow; b) the use of directly measured or internally calculated meteorologic data, to account for solar radiation, back radiation, conduction and evaporation (the latter parameter includes the selection of the formula, and coefficients from relevant meteorologic input); and c) the mathematical scheme for numerical calculation.

The models differ in how they handle the inflow to and the outflow from the reservoir (whether it entered or discharged at one or more levels, how it is distributed over the vertical cross-sectional area, and the entrance mixing); and in determining whether or not there should be a time delay in the water inflow input to take into account time of flow in the reservoir; in determining whether the horizontal segments should not also be divided into fast flowing and slower flowing sectors.

The physical aspects of solar radiation, back radiation, conduction and evaporation, etc. do not, of course, change. However, not all of the measured meteorologic data are available or even feasible or economic to measure on a daily basis. Some of them must be evaluated from relevant input data (for example, the evaporation calculated from wind speed, relative humidity or dew point temperature etc.). The models may differ in the formulas used; in the coefficients chosen; in the mechanism of testing for stability in the horizontal slices and thereby initiating the thermocline; and in the mechanisms determining the heat transfer in the vertical directions.

The models also differ in the thickness of the top and bottom layers, and the time increments iterated.

Tables 1-4 illustrate the major differences between models as determined by reading the documentation and the computer program listings and test runs on the data furnished with the model and/or test runs on data prepared from Fontana Reservoir if original model test data is not available. The assumptions made are shown in Table 1; the input parameters in Table 2; the factors involved in the analysis in Table 3; and the model construction in Table 4. Some difficulty (due to program mistakes or inadequate information provided in the model) was experienced in getting some of the programs to run and in obtaining full documentation on each model.

Table 1. ASSUMPTIONS

Assumptions	Cornell Model	MIT Model	Water Resources Engineering Model
Horizontal homogeneity	Yes--one dimensional stratification in vertical direction only	Yes--one dimensional stratification in vertical direction only	Yes--one dimensional[1] stratification in vertical direction only
Primary mechanism for the formation of thermocline	Nonlinear interaction between wind induced turbulence and buoyancy gradient[2]	Differential absorption of incoming solar radiation	Differential absorption of incoming solar radiation
Surface boundary conditions	one of the three is specified in a sinusoidal form[3] i) water surface temperature T_S ii) heat flux at surface q_S iii) equilibrium temperature T_E usually T_E is specified	Meteorologic Input Water surface temperature calculated	Meteorologic Input Water surface temperature calculated
Bottom boundary condition (no flux)	Yes	Yes	Yes
Water budget (water losses due to evaporation and gains to rainfall)	No	No (the reservoir surface elevation is calculated as a function of initial surface level and the cumulative inflow and outflow; the input measured pool elevations has never been used)	Not directly; however the measured daily surface elevations are used as pool level for each simulation day. The water budget implies evaporation, rainfall and possible leakage
Advective heat (add or subtracted)	No	Yes	Yes

Table 1 (continued). ASSUMPTIONS

1. The reservoir system can be represented by more than one segment, with thermal simulation carried downstream segment by segment, to achieve a quasi two dimensional solution from a series of one dimensional solutions.
2. The assumption that the bulk of incoming solar radiation is absorbed within a small layer near the surface is implicit in the governing equations.
3. $A + B \sin (\frac{2\pi}{365} t + \phi)$

where A - mean value

B - amplitude

t - time in day, t = o corresponding to the time when reservoir temperature profile is isothermal

ϕ - phase angle

Table 2. INPUT PARAMETERS

Input Parameters	Cornell Model	MIT Model	Water Resources Engineering Model
Unit	Input data in specified units only	Input data in specified units only	can be in any units user supplies conversion factors, standard units as indicated
Short wave Solar radiation	No[3]	Yes (net flux) kcal/m^2 - day	Yes[1,2,4,8] (gross flux i.e. no reflection) kcal/m^2 - sec
Net Long-wave atmosphere radiation	No	Yes[1,2,7] kcal/m^2 - day	No (calculated)
Wind speed	No[3,10]	Yes m/sec	Yes[8] m/sec
Air Temperature	No[3]	Yes °c	Yes[8] °c
Cloud Cover	No[3]	Yes[2,6] decimal	Yes[8] decimal
Atmospheric Pressure	No[3]	No	Yes[1,2,8] mb
Relative Humidity	No[3]	Yes decimal	Yes[2,5,8] decimal
Wet Bulb Temperature	No	No	Yes[2,5,8] °c
Dew Point Temperature	No	No	Yes[2,5,8] °c
Equilibrium Temperature	Yes[12] (in terms of mean value, amplitude and phase angle in a sinusoidal form)°c	No	No

Table 2 (Continued). INPUT PARAMETERS

Input Parameters	Cornell Model	MIT Model	Water Resources Engineering Model
Evaporation	No	No (Input constant for built-in formula to calculate heat loss)	No (input evaporation coefficient to calculate heat loss)
Precipitation	No	No	No
Outlet elevation	Yes (depth of intake for power plant) ft	Yes m	Yes m
Inflow rate	No[9]	Yes m^3/day	Yes (daily avg.) m^3/sec
Inflow Temperature	No[9]	Yes °c	Yes (daily avg.) °c
Initial Reservoir (i) temperature (ii) rate of temperature change	(i) Yes (isothermal) °c (ii) (isothermal)	(i) Yes (isothermal only) °c (ii) (isothermal)	(i) Yes (either isothermal or variable) °c (ii) Yes (by default use 1×10^{-9} °c/sec)
Reservoir surface elevation	Yes (constant reservoir depth) ft	Yes (used for comparison only, the actual value is evaluated from continuity) m	Yes (daily avg.) m
Reservoir Geometry (i) Length v s. elevation (ii) Horizontal cross-section area v s. elev.	(i) No (ii) No[11]	(i) Yes m m (ii) Yes m^2 m	(i) No (ii) Yes m^2 m
Fraction of solar radiation absorbed at the water surface	No	Yes (0.4 = 0.5 recommended)	No (Assume equal to 0.4 internally for the top 0.3m layer)
Outflow rate	No[9]	Yes m^3/day	Yes (daily avg.) m^3/sec

Table 2 (Continued). INPUT PARAMETERS

Input Parameters	Cornell Model	MIT Model	Water Resources Engineering Model
Friction velocity	Yes (in terms of mean, amplitude and phase angle in a sinusoidal form[3]) ft/sec	No	No
Short wave radiation extinction coefficient	No	Yes 1/m	Yes in terms of extinction depth (m) coefficient = 6.908/extinction depth
Diffusion coefficient	Yes [in terms of $(C_1 + C_2 Z)\ w^*$] (upper and lower bound of the coefficient are also inputed) ft^2/day	Yes m^2/day	Yes, empirical determined constants A_1, A_2, and A_3 (i) $D_c = A_1$ for $E < E_c$ (ii) $D_c = A_2 E^{A_3}$ for $E \geq E_c$ $E = -\frac{1}{\rho}\frac{\Delta\rho}{\Delta z}$ stability of the water column m^2/sec
Heat exchange coefficient	Yes Btu/ft^2-day-°c	No	No

1. May be calculated internally by program
2. May or may not have to be inputed
3. Wind speed, air temperature, vapor pressure, humidity, short-wave solar radiation and cloud cover are necessary data for external calculation of of the equilibrium temperature
4. Calculated internally both with and without reflection. If data are in input, the net flux = Input flux x $\frac{\text{cal.flux (with reflection)}}{\text{cal. flux (no reflection)}}$, if not in input, the net flux = cal. flux (with reflection)

Table 2 (Continued). INPUT PARAMETERS

5. Only one of the three parameters is used. If more than one are presented the last read in has the priority. But at least one of them should be presented in input data
6. To be read in only when atmospheric radiation is to be calculated internally by program
7. If calculated by program cloud cover should be known
8. Meteorologic data provide at least one observation per day, constant values such as average monthly meteorologic conditions should be avoided.
9. Taking account of the power plant cooling water only and in terms of heat, q_p, per unit area per unit time added by power plant
10. Also used for friction velocity calculation externally
11. A constant surface area is needed for calculating q_p (see 9)
12. Either surface temperature (^{0}c) or heat flux at surface (Btu/ft^2-day) can be used to replace equilibrium temperature
13. $A + B \sin (\frac{2\pi}{365} t + \phi)$

Table 3. FACTORS INVOLVED IN ANALYSIS

Factors	Cornell Model	MIT Model	Water Resources Engineering Model
Diffusivity	Eddy diffusivity Eddy diffusivity >> molecular diffusivity	Molecular diffusion (constant) neglects turbulent diffusion	So called "effective diffusion" accounts for turbulent diffusion and convective mixing calculated from temperature profile $D_c = A_1$ for $E < E_c$ $D_c = A_2 E^{A_3}$ for $E \geq E_c$ where $E = \frac{-1}{\rho} \frac{\Delta\rho}{\Delta z}$ stability of the water column, E_c = some critical value of stability
Stability mixing process	Free convection if stratification is unstable	Convective mixing if negative temperature gradient occurs $\frac{\partial T}{\partial y} < 0$ (T - temperature, y - elevation, positive upward)	Convective mixing if negative temperature gradient occurs $\frac{\partial T}{\partial y} < 0$ (T - temperature, y - elevation, positive upward)
Heat transfer in control volume (horizontal layer)			
1. Direct absorption	1. No	1. Yes	1. Yes
2. Diffusion	2. Yes	2. Yes	2. Yes
3. Vertical advection	3. No	3. Yes	3. Yes
4. Horizontal advection	4. No	4. Yes	4. Yes

Table 3 (Continued). FACTORS INVOLVED IN ANALYSIS

Factors	Cornell Model	MIT Model	Water Resources Engineering Model
Heat transfer across water surface 1. short wave solar radiation 2. Net long-wave radiation 3. Evaporation 4. Conductions	In terms of heat flux $q_s = K(T_E - T_s)$ where K - heat exchange coefficient T_E - equilibrium temperature T_s - water surface temperature	1. Yes 2. Yes 3. Yes 4. Yes	1. Yes 2. Yes 3. Yes 4. Yes
Inflow consideration 1. enter at the level of equal temperature 2. distribution in vertical direction	1. Yes 2. No (spread instantaneously into a thin horizontal sheet)	1. Yes 2. Gaussian velocity distribution either with or without entrance mixing	1. Yes 2. uniform velocity distribution over the interflow thickness determined by Debler's critera
Withdrawal consideration 1. level 2. distribution in vertical direction 3. limit on withdraw zone	1. single level outlet 2. No (uniformly distributed at the level of withdraw) 3. No	1. selective withdrawal 2. withdrawal layer thickness & Gaussian velocity distribution in withdrawal layer 3. Yes (withdrawal layer never extended over the region with temperature gradient equal or greater than cut-off gradient) of $\frac{\Delta T}{\Delta y} = 0.05$	1. selective withdrawal 2. withdrawal layer thickness and uniform velocity distribution over withdrawal layer determined by Debler's criteria 3. Yes withdrawal zone always on top or underneath the thermocline

Table 4. MODEL CONSTRUCTION

Parameters	Cornell Model	MIT Model	Water Resources Engineering Model
Mathematical scheme of approximation	Explicit finite difference scheme	Explicit finite difference scheme	Implicit finite difference scheme
Stability criteria for use		$D \frac{\Delta t}{(\Delta y)^2} \leq \frac{1}{2}$ --(1) $V \frac{\Delta t}{\Delta y} \leq 1$ -----(2)	$R_a = \frac{Q(\text{element}) \cdot \Delta t}{V(\text{element})} < .5$ recommended $R_a < 1$ always
Applicability criteria	deep, stratified turbid lake	stratified[2] $F_D < \frac{1}{\pi} = 0.32$	strongly stratified[2] $F_D \ll 0.1$
Time step (Δt)	Variable $\Delta t_{k+1} = C_t \frac{(\Delta y)^2}{(K_H)_{max}}$ $0 < C_t < .5$ K_H - diffusivity	Constant (i) Determine Δt max. from $E_q(1)$ (ii) guided by time step of input data (iii) must satisfy stability criteria[3]	Constant (i) 1 hr. $\leq \Delta t \leq$ 1 day (ii) guided by time step of input data
Depth Interval (Δy)	Constant (i) maximum 100 intervals	Constant (i) 50 intervals or less is recommended (ii) min. 20 intervals	Constant (i) 1 meter recommended (ii) max.number of steps is 200
Test Case	Cayuga Lake 400 days	Fontana Reservoir 3/1/66 to 12/31/66	Fontana Reservoir 3/1/66 to 12/31/66

Table 4 (Continued). MODEL CONSTRUCTION

Parameters	Cornell Model	MIT Model	Water Resources Engineering Model
Running[1] time for test case	(400 days) 13 min. for Δy = 5 ft.	(300 days) 1.4 min. for $\Delta y = 2.0^m$ Δt = 1 day 2.0 min. for $\Delta y = 1.0^m$ Δt = 1 day	(300 days) 2.6 min. for Δy = 2.0m Δt = 1 day 3.1 min. for Δy = 1.0m Δt = 1 day

1. the program compiling time is not included
2. the densimetric Fronde number in defined as

$$F_o = \frac{LQ}{DV}\sqrt{\frac{\rho_o}{g\beta}}$$

where L - reservoir length

Q - volumetric discharge through the reservoir

D - mean reservoir depth

V - reservoir volume

ρ_o- reference density

β - average density gradient $= \frac{-d\rho}{dy}$

g - gravitational acceleration

3. Check by stability criteria, Equation (2), internally and the input Δt is subdivided if necessary in that particular time step.

A brief description of each model evaluated is given in the following sections.

WATER RESOURCES ENGINEERS' MODEL

The WRE model has been developed by Water Resources Engineers, Inc., through a series of studies for various agencies [3,9]. It was the first comprehensive model proposed for predicting the thermal structure in reservoirs. The computer program of WRE model used for this study is the modified EPA version. Although this model has many versions and is widely used, most users indicate that an intensive effort is needed to have this model run properly. This is partially due to the difficulty of acquiring full documentation and partially to some computer coding problems. Several errors were detected during this study. The most serious one is the concept of 'effective' diffusion, based on the numerical evaluation of the eddy conductivity coefficient from the measured temperature profile in a reservoir. By comparing the rederived heat transport equation, as shown later in this section, with the WRE's computer program, a mistake in the computer code related to the diffusion term was discovered. The density of water, ρ, appears to have been omitted from the diffusion term. Since the MKS system is used, the actual diffusion is approximately one thousandth (1/1000) of the 'effective' diffusion, as defined by WRE. After correction of this error, the magnitude of the 'effective' diffusion coefficient is then of the same order of magnitude as the molecular diffusion coefficient.

Other difficulties in using the WRE model were related to the numerical scheme for evaluation of the heat flow term at the top layer. This general problem will be discussed in detail in a separate section.

We were unable to acquire the original WRE test run data. Therefore, Fontana Reservoir data used in the evaluation were prepared from TVA measured field data.

Principal Assumptions

(a) There is horizontal homogeneity, i.e., stratification is in the vertical direction only.

(b) Effective diffusion accounts for the heat transfer due to wind mixing turbulent motion and reservoir instability.

(c) There is differential absorption of incoming solar radiation.

(d) There is no flux, of volume or heat, through the reservoir bottom or sides except that due to inflow and outflow.

Factors Considered and the Basic Equations

Since the heat transport equations used in the computer program are different than those indicated in WRE report, the heat transport equations were rederived. The set of implicit equations were solved by the Thomas Alogrithm, and are shown below.

Direct absorption of solar radiation ---

$$\phi(z) = \phi_o (1-\beta)\, e^{-\eta(z_s-0.3-z)} \qquad (2)$$

where ϕ_o = net short wave radiation at water surface

$\phi(z)$ = short wave radiation at elevation z

z_s = elevation of water surface

β = fraction of solar radiation absorbed at the water surface (β=0.4 is assumed)

η = radiation extinction coefficient, m^{-1}

Selective withdrawal---

(i) Up to five outlets are allowed

(ii) Based on Debler's experimental results$^{(10)}$ the critical Froude number, F_c, is 0.24, therefore:

$$0.24 = \frac{q}{d^2} \left[\frac{\rho_o}{-g \frac{\partial\rho}{\partial z}} \right]^{\frac{1}{2}} \qquad (3)$$

The withdrawal depth in meters, then is:

$$d = 2.0 \left[\frac{q^2}{\frac{-g}{\rho_o} \frac{\partial\rho}{\partial z}} \right]^{\frac{1}{4}} = 2.0 \frac{q^{\frac{1}{2}}}{(g\varepsilon)^{\frac{1}{4}}} \qquad (4)$$

where $q = \frac{\frac{1}{2}Q}{w}$, one half of the discharge per unit width,

and w is the reservoir width

$\varepsilon = \frac{-1}{\rho_o} \frac{\partial\rho}{\partial z}$, normalized density gradient

(iii) The velocity is uniform within the withdrawal zone

(iv) The principle of superposition is applied for the regions in which withdrawal layers overlap

(v) Withdrawal layers never extend through the thermocline, or physical boundaries.

(vi) At the onset of fall cooling, when the epilimnetic region is well-mixed and isothermal Debler's criteria do not hold for withdrawals from the epilimnion and Craya's approach$^{(11)}$ is used. The flow is withdrawn from epilimnion until the discharge is larger than Craya's critical flow given by:

$$q_c = 1.52 \sqrt{gh^3 \frac{\Delta\rho}{\rho}}, \qquad 2h < d_t \text{ for submerged outlets} \qquad (5)$$

and

$$q_c = 0.75 \sqrt{gd_t^3 \frac{\Delta\rho}{\rho}} \qquad \text{for surface outlets} \qquad (6)$$

where d_t = depth to bottom of thermocline

h = thickness of thermocline

ρ = density above thermocline

$\rho+\Delta\rho$ = density below thermocline

At greater discharges water will begin to be withdrawn from the hypolimnion.

Depth and velocity distribution of inflow ---

(i) The inflow is centered at the equivalent water density of the reservoir.

(ii) The inflow layer thickness is determined from measured inflow data by using Debler's criterion.

(iii) The distribution of inflow is proportional to the volume of each horizontal layer within the inflow zone.

(iv) The inflow, Q_i, is calculated from the continuity equation:

$$Q_i = \frac{dV}{dt} + Q_o \qquad (7)$$

where V = volume of reservoir

Q_o = outflow rate

(v) The distribution of inflow in each layer is then modified by multiplying the ratio of calculated inflow rate to the measured inflow rate.

Internal mixing ---

(i) Free convection occurs if stratification is unstable.

(ii) The heat transport, H, due to diffusion can be written as:

$$H = \rho c \cdot D(z,t) \cdot \frac{\partial T(z,t)}{\partial z} \qquad (8)$$

The general properties of diffusion coefficient D are as follows:

(a) It is usually greatest near the surface but declines rapidly with depth and attains the minimum at thermocline.

(b) In the hypolimnion, it increases with depth in an erratic manner, reaching a maximum at about mid-depth, thereafter decreases as the bottom is approached.

(iii) The form of the diffusion coefficient used is:

$$D = A_1 \text{ (constant)}, \qquad E < E_c \qquad (9)$$

$$D = A_2 E^{A_3}, \qquad E \geq E_c \qquad (10)$$

where E = stability of the water column

$$E = -\frac{1}{\rho}\frac{\Delta\rho}{\Delta z} \qquad (11)$$

E_c = critical stability parameter

The following values are suggested:

$A_1 = 2.5 \times 10^{-4}\ m^2/sec$

$A_2 = 1.5 \times 10^{-8}\ m^{1.3}/sec$

$A_3 = -0.7$

$E_c = 1.0 \times 10^{-6}\ m^{-1}$

Governing equation ---

The time rate of change of thermal energy H in a control volume of thickness Δz, is:

$$\frac{\partial H_j}{\partial t} = (h_I - h_o)_j + (h_{sw})_j + (h_v)_j - (h_v)_{j+1} + (h_d)_j - (h_d)_{j+1} \quad (12)$$

where subscript j indicates the increment of depth; $j = 1$ at
bottom surface

H = The heat energy stored in the control volume (kcal)

h_I = Heat flow associated with inflowing water (kcal/sec)

h_o = Heat flow associated with outflowing water (kcal/sec)

h_v = Heat flow by advection (kcal/sec)

h_d = Heat flow by diffusion (kcal/sec)

h_{sw} = Heat flow by short wave solar radiation (kcal/sec)

In terms of temperature T, Eq. 12 can be written as:

$$\bar{\rho}_j \ c\bar{A}_j \ \Delta z \frac{\partial T_{j+\frac{1}{2}}}{\partial t} = \bar{\rho}_j \ c \ (T_I)_j \ (q_I)_j - \bar{\rho}_j c \ (T_o)_j \ (q_o)_j + h_j \ \bar{A}_j$$
$$+ \rho_j \ c \ v_j A_j T_j - \rho_{j+1} c v_{j+1} A_{j+1} T_{j+1} + \rho_j c D_j A_j \frac{\partial T_j}{\partial z} - \rho_{j+1} \ c D_{j+1}$$
$$A_{j+1} \frac{\partial T_{j+1}}{\partial z} \quad (13)$$

or

$$\rho_j \ c\Delta\nabla_j \dot{T}_{j+\frac{1}{2}} = \bar{\rho}_j c(T_I)_j \ (q_I)_j - \bar{\rho}_j c(T_o)_j \ (q_o)_j + h_j \ \bar{A}_j$$
$$+ \ \rho_j c v_j A_j T_j - \rho_{j+1} c v_{j+1} A_{j+1} T_{j+1} - \rho_j c D_j A_j \frac{T_{j+\frac{1}{2}} - T_{j-\frac{1}{2}}}{\Delta z}$$
$$+ \rho_{j+1} c D_{j+1} A_{j+1} \frac{T_{j+3/2} - T_{j+\frac{1}{2}}}{\Delta z} \quad (14)$$

$$= P_j + Q_j + \rho_j c \frac{D_j A_j}{\Delta z} T_{j-\frac{1}{2}} - (\rho_j c \frac{D_j A_j}{\Delta z} + \rho_{j+1} c \frac{D_{j+1} A_{j+1}}{\Delta z}) T_{j+\frac{1}{2}}$$

$$+ \rho_{j+1} c \frac{D_{j+1} A_{j+1}}{\Delta z} T_{j+{}^3/_2} \qquad (15)$$

where

P_j = $\bar{\rho}_j c (T_I)_j (q_I)_j - \bar{\rho}_j c (T_o)_j \; (q_o)_j + h'_j \bar{A}_j$ (16)

Q_j = $\rho_j c v_j A_j T_j - \rho_{j+1} c v_{j+1} A_{j+1} T_{j+1}$ (17)

T = water temperature (^{o}c)

T_I = inflow temperature (^{o}c)

q_I = inflow rate (m^3/sec) into control volume

T_o = outflow temperature (^{o}c)

q_o = outflow rate (m /sec) from control volume

h' = net insolation heat flux per unit area (kcal/m^2-sec)

D = diffusion coefficient (m^2/sec)

v = vertical advection velocity (m/sec)

Δz = thickness of control volume (m)

$\bar{\rho}$ = average density of water (kg/m^3)

ρ = density of water (kg/m^3)

ΔV_j = $\bar{A}_j \cdot \Delta z$ volume of jth control volume (m^3)

z = vertical axis, positive upward (m)

A_j = cross-section area at depth step j (m^2)

$\bar{A}_j$ = $(A_j + A_{j+1})/2$ (18)

$\bar{T}$ = mean water temperature of jth control volume (^{o}c)

c = specific heat of water (= 1 kcal/kg-^{o}c) since

$$T_{j-\frac{1}{2}} = \bar{T}_{j-1} \qquad (19)$$

$$T_{j+\frac{1}{2}} = \bar{T}_{j} \qquad (20)$$

$$T_{j+{}^{3}/_{2}} = \bar{T}_{j+1} \qquad (21)$$

Equation 15 becomes:

$$\bar{\rho}_j c \Delta \bar{v}_j \dot{\bar{T}}_j + K_{j,\,1}\, \bar{T}_{j-1} + K_{j,2}\bar{T}_j + K_{j,3}\bar{T}_{j+1} = P_j + Q_j \qquad (22)$$

where

$$K_{j,1} = -\rho_j c \frac{D_j A_j}{\Delta z} \qquad (23)$$

$$K_{j,2} = \rho_j c \frac{D_j A_j}{\Delta z} + \rho_{j+1} c \frac{D_{j+1} A_{j+1}}{\Delta z} = -(K_{j,1} + K_{j,3}) \qquad (24)$$

$$K_{j,3} = -\rho_{j+1} c \frac{D_{j+1} A_{j+1}}{\Delta z} \qquad (25)$$

Taylor series of 2nd order

$$T(t+\Delta t) = T(t) + T(t)\Delta t + \ddot{T}\,(t)\,\frac{\Delta t^2}{2} \qquad (26)$$

and by definition of derivative

$$\ddot{T}\,(t) = \lim_{\Delta t \to o} \frac{\dot{T}(t+\Delta t) - \dot{T}(t)}{\Delta t} \qquad (27)$$

for small Δt

$$T(t+\Delta t) = T(t) + \dot{T}(t)\frac{\Delta t}{2} + \dot{T}(t+\Delta t)\,\frac{\Delta t}{2} \qquad (28)$$

or use superscript k to indicate time step

$$T^{(k+1)} = T^{(k)} + \dot{T}^{(k)}\,\frac{\Delta t}{2} + \dot{T}^{(k+1)}\,\frac{\Delta t}{2} = \alpha^{(k)} + \dot{T}^{(k+1)}\,\frac{\Delta t}{2} \qquad (29)$$

where $\alpha^{(k)} = T^{(k)} + \dot{T}\,{}^{(k)}\,\frac{\Delta t}{2}$ (30)

By Equations 22 and 29

$$K_{j,1} \frac{\Delta t}{2} \hat{T}_{j-1}^{(k+1)} + (\bar{\rho}_j \, c\Delta \bar{V}_j + K_{j,2} \frac{\Delta t}{2}) \hat{T}_j^{(k+1)} + K_{j,3} \frac{\Delta t}{2} \hat{T}_{j+1}^{(k+1)}$$

$$= P_j^{(k+1)} + Q_j^{(k+1)} - \alpha_{j-1}^{(k)} K_{j,1} + \alpha_j^{(k)} K_{j,2} + \alpha_{j+1}^{(k)} K_{j,3} \qquad (31)$$

Let

$$S_{j,1} = K_{j,1} \frac{\Delta t}{2} \qquad (32)$$

$$S_{j,2} = \bar{\rho}_j c\Delta \bar{V}_j + K_{j,2} \frac{\Delta t}{2} \qquad (33)$$

$$S_{j,3} = K_{j,3} \frac{\Delta t}{2} \qquad (34)$$

$$F_j = P_j^{(k+1)} + Q_j^{(k+1)} - \alpha_{j-1} K_{j,1} + \alpha_j K_{j,2} + \alpha_{j+1} K_{j,3}{}^{(k)} \qquad (35)$$

Then Equation 31 becomes

$$S_{j,1} \hat{T}_{j-1}^{(k+1)} + S_{j,2} \hat{T}_j^{(k+1)} + S_{j,3} \hat{T}_{j+1}^{(k+1)} = F_j, \; j=1,2,---,N \qquad (36)$$

The system is a set of implicit equations and can be solved by the Thomas algorithm and transforms into an upper bidiagonal form. The coefficients of this new system designated by $S'_{j,1}$, $S'_{j,2}$, $S'_{j,3}$ and F'_j are as follows:

$$S'_{j,1} = 0, \quad j=2,3 \text{ -- } N \qquad (37)$$

$$S'_{j,2} = 1, \quad j=1,2,3 \text{ -- } N \qquad (38)$$

$$S'_{1,3} = S_{1,3}/S_{1,2}; \; F'_1 = F_1/S_{1,2} \qquad (39)$$

$$S'_{j+1,3} = \frac{S_{j+1,3}}{S_{j+1,2} - S_{j+1,1} \cdot S'_{j,3}} \tag{40}$$

$$F'_{j+1} = \frac{F_{j+1} - S_{j+1,1} F'_j}{S_{j+1,2} - S_{j+1,1} \cdot S'_{j,3}} \tag{41}$$

then $\dot{T}_N = F'_N$ (42)

and

$$\dot{T}_\ell = F'_\ell - S'_{\ell,3} \cdot \dot{T}_{\ell+1} \ , \ \ell = N-1, N-2, --, 2,1 \tag{43}$$

$$\bar{T}_j^{(k+1)} = \alpha_j^{(k)} + \dot{T}_j^{(k+1)} \cdot \frac{\Delta t}{2} \ , \ j=1,2, -- N \tag{44}$$

This is an implicit method of combining an explicit finite difference and an implicit finite difference scheme. It has advantage of unconditional stability at the cost of complexity of computation and longer computation time.

Verification

The model was verified on Fontana Reservoir for the period from February 20, 1966 to December 31, 1966.

Results of test run ---

Since the WRE model did not furnish the test run data, a set of input data for Fontana Reservoir was prepared in this study according to the WRE program. Based on the sensitivity analysis of Fontana Reservoir for the period from March 1, 1966 to December, 1966, the following effects on temperature stratification were observed.

(i) With Variation in Thickness of Horizontal Layer, Δz, Only --- WRE's report states that calculation with a constant thickness of one meter most closely matches the measured values of temperature. However, no details of the test runs are given. The results of our study show that the thickness of horizontal layer affects the thermal simulation greatly. This is undesirable. In general, our results indicate that in the warming period, Spring and early Summer, the larger the horizontal layer thickness the higher the temperature profile. A typical example can be seen in Figure 2. The temperature profile of Δz = 2m is 2°C to 3°C higher than that of Δz = 1m and the profile for Δz = 1.5m falls in between.

In the early fall, as the water body loses heat, the temperature profile predicted with the larger horizontal element followed the trend but at a more rapid rate at the water surface than at intermediate depths. Calculation with the larger vertical increments predicts a higher temperature than with the smaller vertical increments as indicated in Figure 3. During the period that the reservoir is isothermal, the profiles predicted are very similar for all thicknesses as shown in Figure 4.

The use of Δz = 0.6m probably violates the criterion that within the time period simulated the through flow must be less than the volume in that element. The temperature profile became isothermal in Fall as shown in Figure 3. Since no remedy is provided within the model and no warning is given if the situation exists, all simulation results should be examined very carefully.

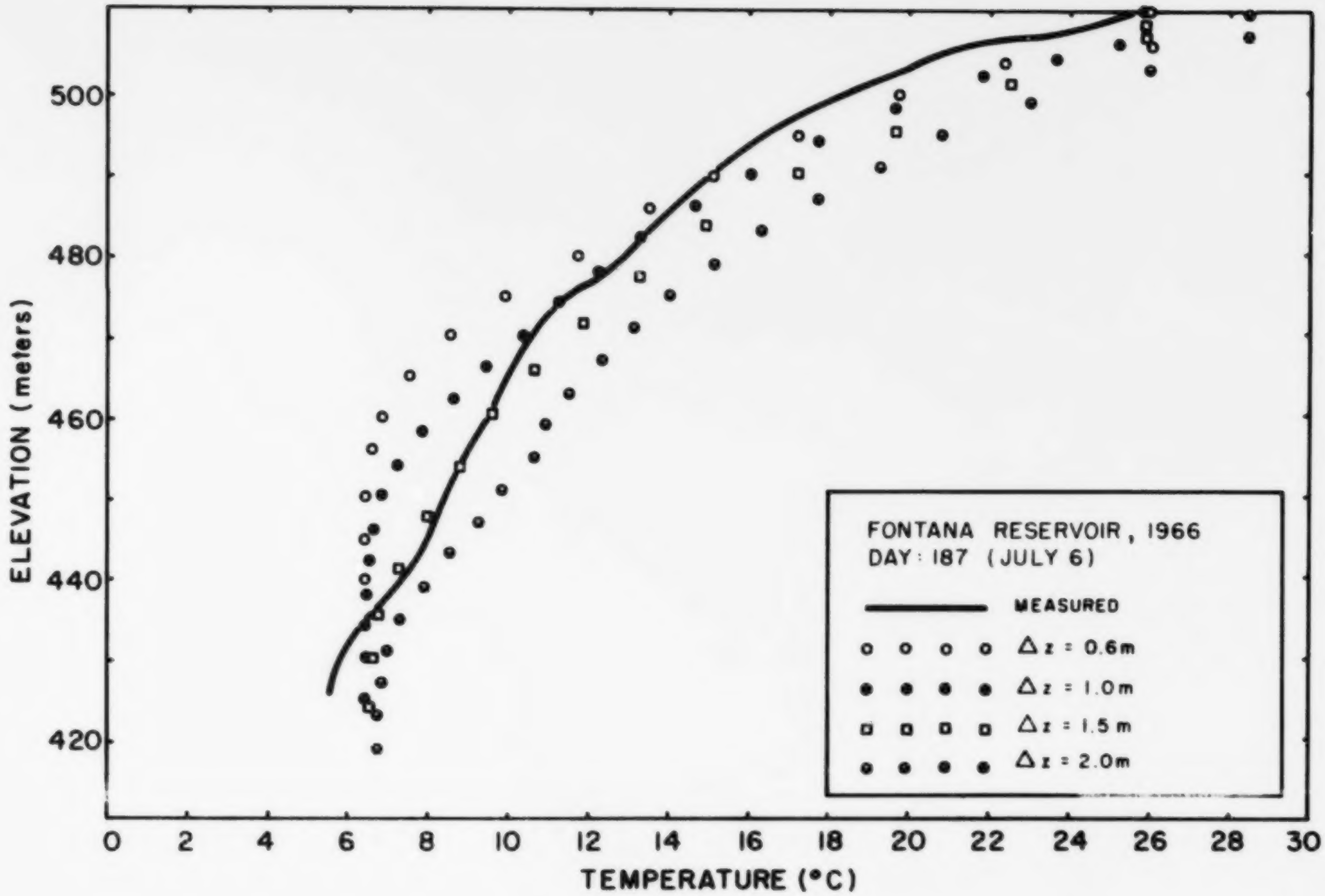

Figure 2. WRE model -- Effect of Thickness of Horizontal Layer (July 6)

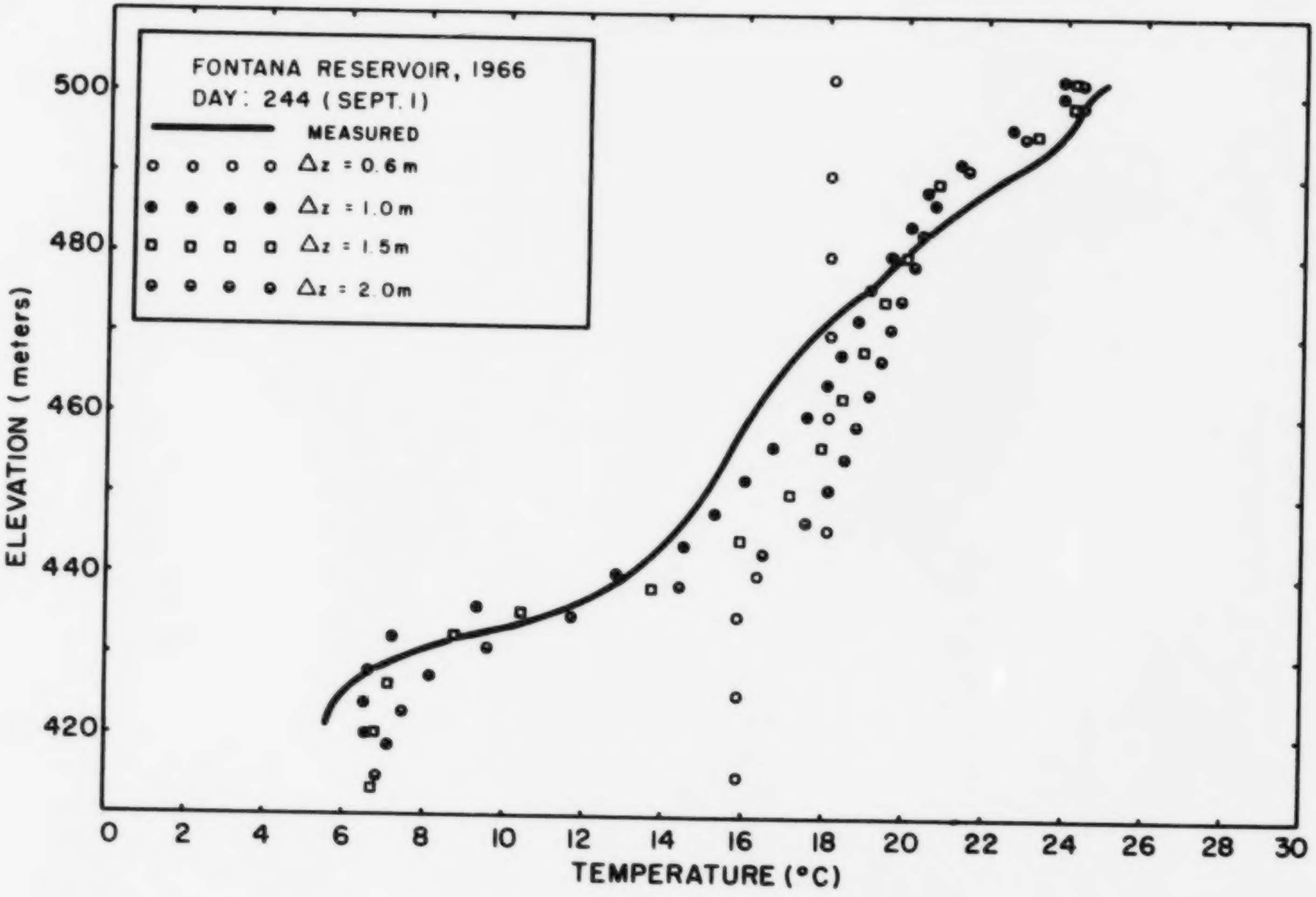

Figure 3. WRE model -- Effect of Thickness of Horizontal Layer (Sept. 1)

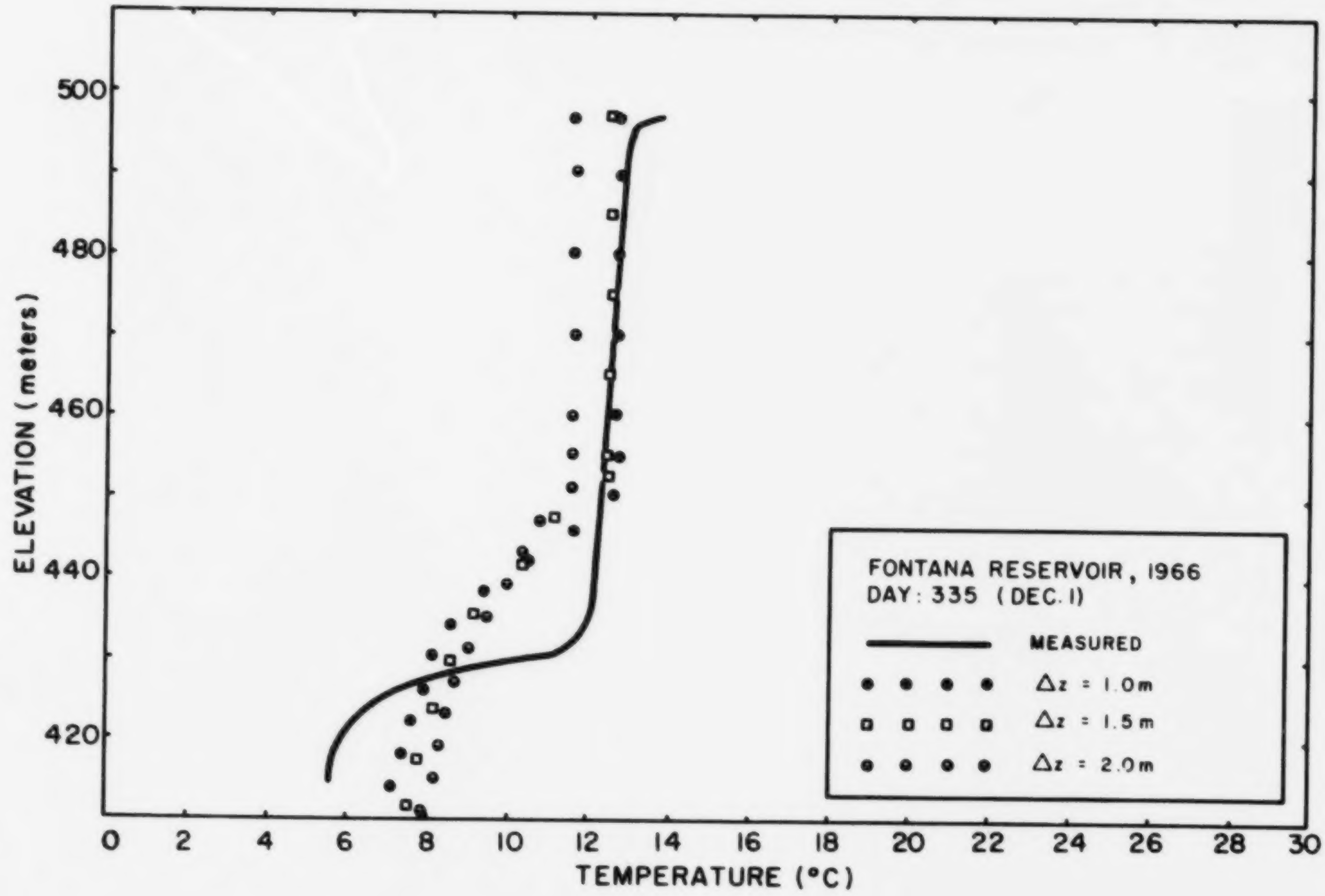

Figure 4. WRE model -- Effect of Thickness of Horizontal Layer (Dec. 1)

The use of a horizontal thickness of one meter in the Fontana Reservoir did simulate thermal profiles compatible with the measured field values. However, the extrapolation of this conclusion to other reservoirs may not be true. It is very likely that in some reservoirs a layer thickness other than one meter is necessary in order to satisfy the criterion mentioned above. In addition to the uncertainty of simulated results, the use of one meter instead of two meters or a larger thickness always means longer computation time.

The Fontana Reservoir is probably the best example for verification, since it is very deep, 100 meters, and has useful storage of more than one million acre-ft. It is concluded that large variations in temperature with changes in horizontal element thickness is a serious drawback of the WRE model.

(ii) With Variation in Diffusion Coefficient Only --- After the coding error in the diffusion term was corrected, the 'effective' diffusivity recommended by WRE is equivalent to:

$$D_c = 2.5 \times 10^{-7} \text{ m}^2/\text{sec}, \quad E<E_c \tag{45}$$

$$D_c = 1.5 \times 10^{-11} (E)^{-0.7} \text{ m}^2/\text{sec}, \quad E>E_c \tag{46}$$

where

$$E = \text{the stability of water}, = \frac{-1}{\rho} \frac{\partial \rho}{\partial z} \tag{47}$$

E_c = the critical stability parameter = $1.0 \times 10^{-6} \text{m}^{-1}$

which is of the same order as molecular diffusivity, 1.4×10^{-7} m^2/sec. Test runs using a diffusion coefficient one thousandth (1/1000) of the 'effective' diffusivity give almost identical results as runs using the 'effective' diffusivity (Equations 45 and 46). The comparison of the measured temperature profiles with those calculated with the diffusion coefficients listed in Equations 45 and 46, marked STAND, and diffusion coefficients 10 times as large are shown in Figures 5 through 7. For the early summer, Figure 5; late summer, Figure 6; and winter, isothermal, Figure 7; both diffusion coefficients give similar results and closely approximate the measured values.

MIT MODEL

The details of the development and testing of the thermal stratification model are shown in Reference 12. The current version has some modifications in the numerical scheme, selective withdrawal, etc., as pointed out in the "Foreward" of Reference 4. Most of the assumptions, factors considered in analysis and input data are similar to WRE's. The major differences between these two models are in the numerical scheme and the handling of inflows and outflows. The computer program is clear and easily followed. The inclusion of the test data on Fontana Reservoir in the report provided useful guidance to new users.

Principal Assumptions ---

(a) Thermal gradients exist in the vertical direction only, i.e., horizontal isotherms.

(b) The diffusion coefficient (molecular) is constant at all depths and at all times; mixing due to unstable density profile accounts for convection in the epilimnion.

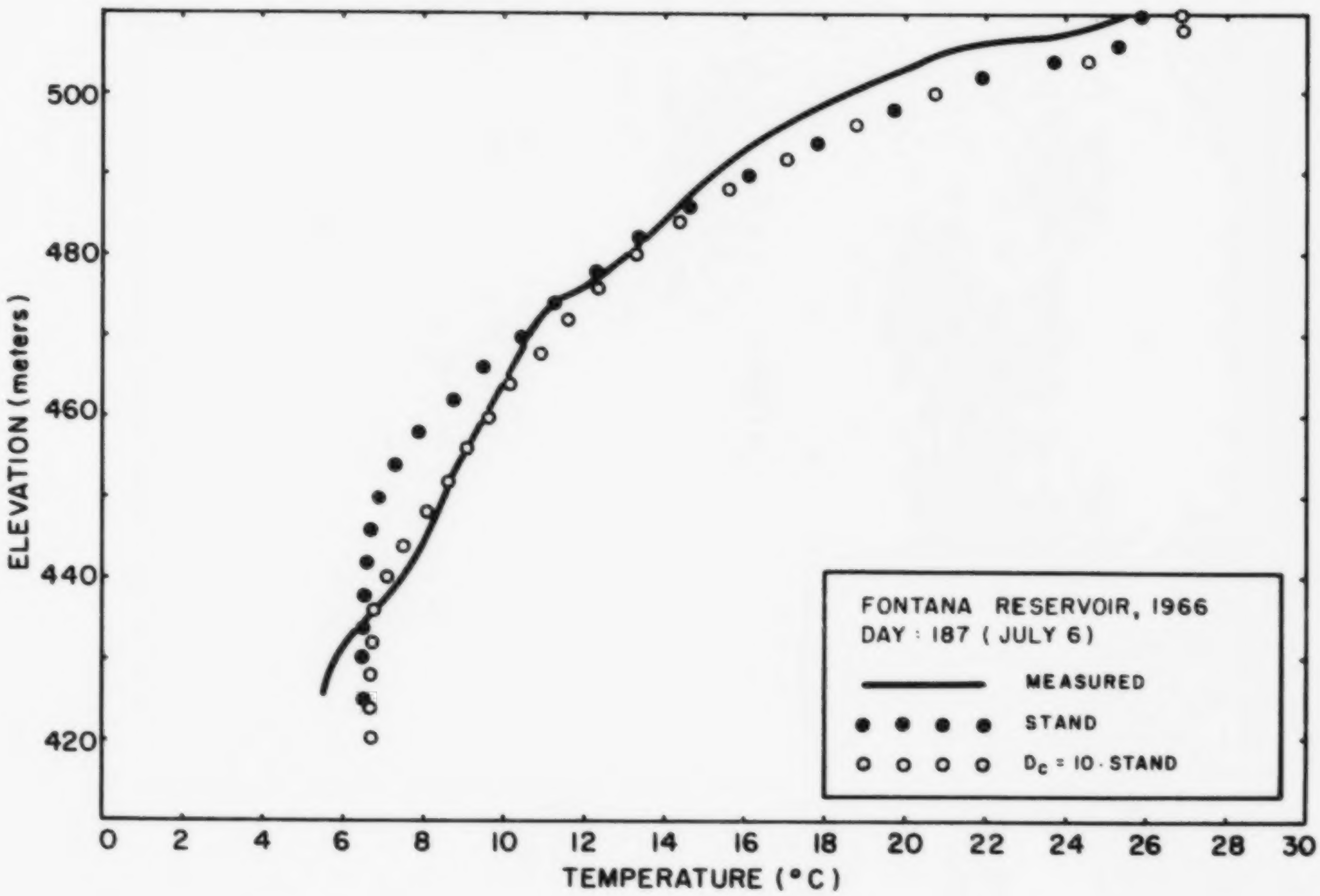

Figure 5. WRE model -- Effects of Diffusion Coefficient (July 6)

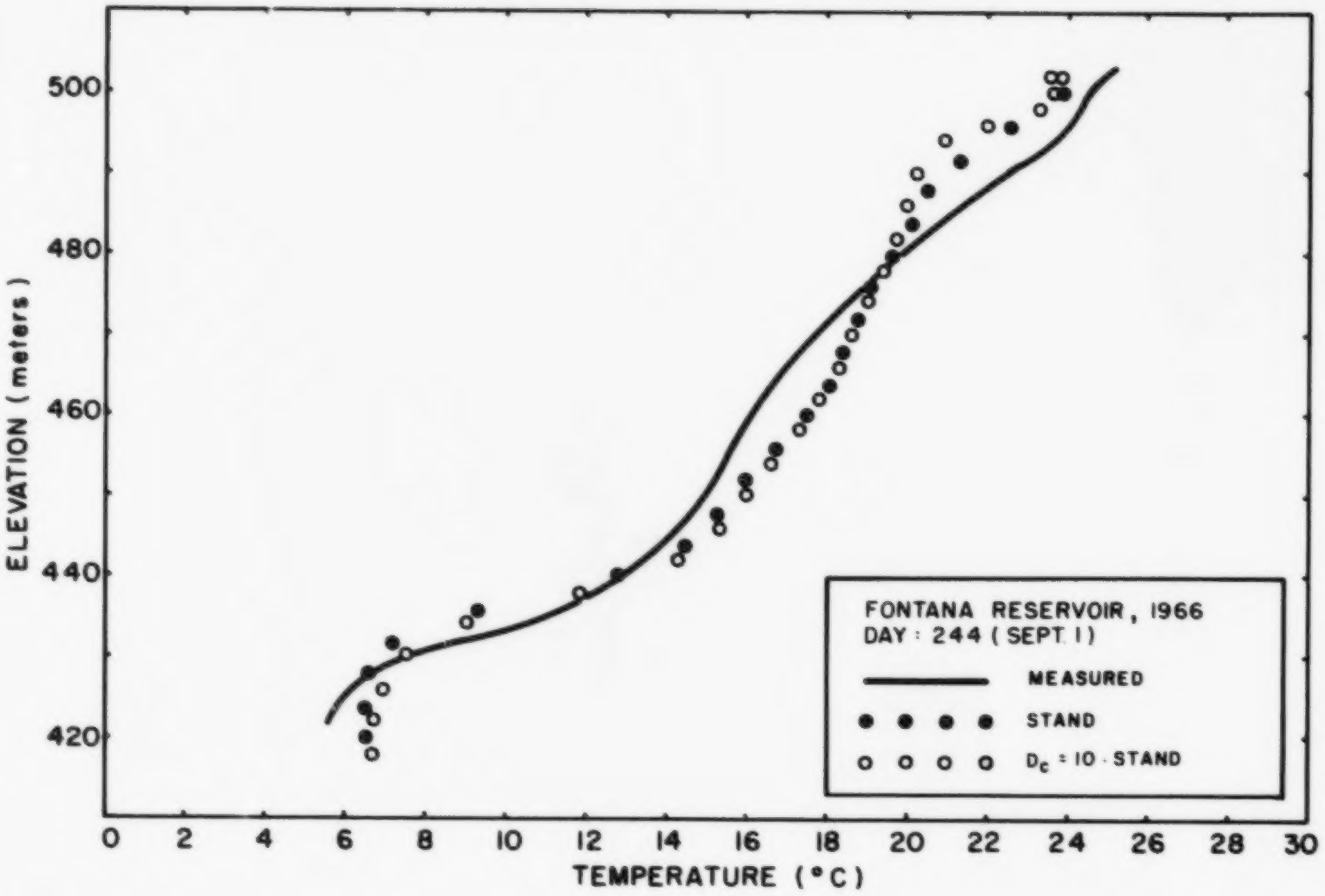

Figure 6. WRE model -- Effects of Diffusion Coefficient (Sept. 1)

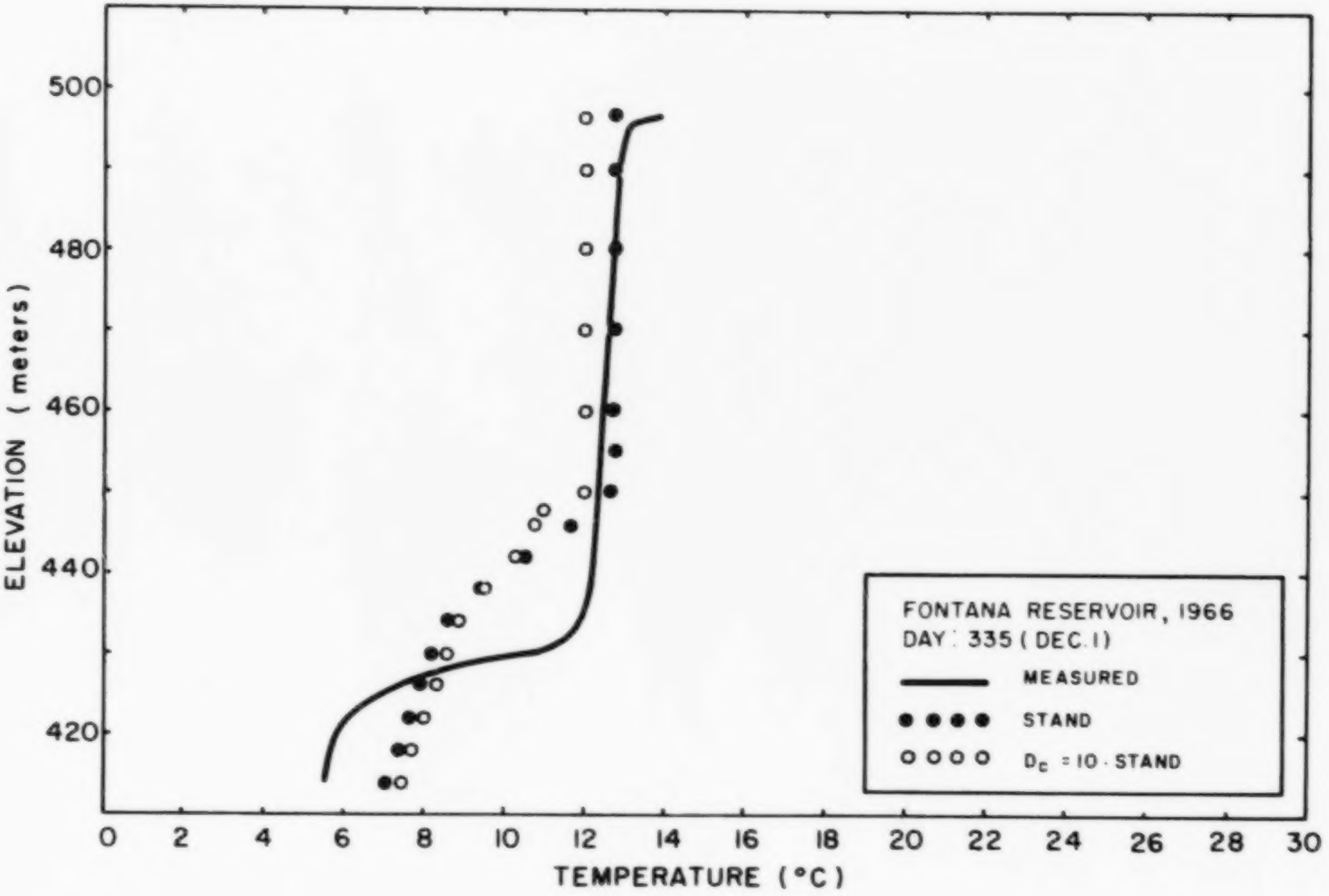

Figure 7. WRE model -- Effects of Diffusion Coefficient (Dec. 1)

(c) Solar radiation is transmitted in the vertical direction only and there is differential absorption of the incoming solar radiation below the water surface.

(d) The sides and bottom of the reservoir are insulated.

(e) The density and specific heat of water are constant.

Factors Considered and Basic Equations ---

(a) Variable area with depth

(b) Direct absorption

Transmission of radiation at elevation, y, is given by

$$\phi(y) = \phi_o(1-\beta)\ e^{-\eta\ (y_s-y)} \qquad (48)$$

where:

ϕ_o = net incident solar radiation

β = fraction of ϕ_o absorbed at the surface

η = light extinction coefficient

y_s = water surface elevation

(c) Inflow

(i) Inflow enters at the level at which its temperature, or the mixed inflow temperature if entrance mixing is allowed, matches the temperature in the reservoir.

(ii) An option to account for the travel or lag time of inflows within the reservoir is provided.

(iii) Entrance mixing could be included by providing an entrance mixing ratio; 100% is recommended for Fontana.

(iv) Inflow velocity profile is approximated by a Gaussian distribution, at elevation y

$$U_i\ (y) = U_{i_{max}}(t)e^{-\frac{\left((y-y_{in}(t)\right)^2}{2\sigma_i{}^2}} \tag{49}$$

where:

$U_{i_{max}}(t)$ = maximum value of the inflow velocity at time t,

is determined from:

$$Q_i(t) = \int_{y_b}^{y_s} B(y)\ U_i(y)\ dy \tag{50}$$

where:

$Q_i(t)$ = total inflow

y_s = surface elevation

y_b = bottom elevation

$B(y)$ = width of the reservoir at elevation y

$y_{in}(t)$ = elevation of inflow

σ_i = inflow standard deviation

(d) Outflow

(i) multiple outlets

(ii) outflows are centered at the outlet with a Gaussian velocity distribution:

$$U_o(y) = U_{o_{max}}(t)e^{-\frac{(y-y_{out})^2}{2\sigma_o^2}} \qquad (51)$$

where:

$U_{o_{max}}$ = maximum velocity or velocity at $y=y_{out}$

y_{out} = elevation of centerline of outlet

σ_o = the outflow standard deviation calculated on the basis that 95% of the outflow comes from the calculated withdrawal layer or:

$\sigma_o = \frac{\delta/2}{1.96}$

with $U_{o_{max}}$ evaluated from (52)

$$Q_o(t) = \int_{y_b}^{y_s} B(y)U_o(y)dy \qquad (53)$$

where:

$Q_o(t)$ is total outflow at the specified outlet

(iii) Withdrawal thickness calculated from modified Kao's equation(13) if the temperature gradient, $\frac{\partial T}{\partial y}$, at the outlet is greater than or equal to 0.01 °c/m.

$$\delta = 4.8 \left(\frac{q^2}{g\varepsilon}\right)^{1/4} \qquad (54)$$

where:

δ = thickness of withdrawal layer

q = outflow rate per unit width

ε = normalized density gradient $= -\frac{1}{\rho} \frac{\partial \rho}{\partial y}$ (55)

g = gravitational acceleration

If the temperature gradient at the outlet is smaller than the value specified above, the withdrawal layer is restricted by the thermocline. The built-in cut-off gradient is set at 0.05 ^{o}c/m.

(iv) The velocities from each outlet are superimposed on one another.

(e) Variable water surface elevation

The surface level is calculated from the initial surface level and the cumulative inflow and outflow. The measured elevations are used as reference only. The reservoir is schematized into a series of horizontal elements with constant thickness, Δy, except the bottom element, which is half as thick, and the surface element, which varies between $0.25\Delta y$ and $1.25\Delta y$ to account for the variation in the surface elevation.

(f) Governing Equations

The heat transport equation applied to each horizontal layer has the following form:

$$\frac{\partial T(y)}{\partial t} = \frac{DC}{A(y)} \frac{\partial}{\partial y} \left(A(y) \frac{\partial T(y)}{\partial y}\right) = \frac{1}{\rho c A(y)} \frac{\partial}{\partial y}(A(y)\phi(y)) - \tag{56}$$

$$\frac{1}{A(y)} \frac{\partial}{\partial y} (V(y)A(y)T(y)) + \frac{1}{A(y)} (U_i(y)B(y)T_i - U_o(y)B(y)T(y))$$

where:

$T(y)$ = temperature at elevation y

$V(y)$ = vertical velocity at elevation y

$U_i(y)$ = inflow velocity at elevation y

$U_o(y)$ = outflow velocity at elevation y

T_i = inflow temperature

$A(y)$ = area at elevation y

t = time

α = molecular diffusivity

$\phi(y)$ = transmission of radiation at elevation y

and the continuity equation can be written as

$$\frac{\partial}{\partial y}(V(y)A(y)) = B(y)\ (U_i(y)-U_o(y)) \tag{57}$$

The isothermal profile at the beginning of the Spring provided the initial condition and the two boundary conditions are given by the no heat flux through the reservoir bottom and the balance of heat input at the water surface.

The mathematical model used is an explicit finite difference scheme. The selection of layer thickness, Δy, is restricted by the stability criteria:

$$D\frac{\Delta t}{(\Delta y)^2} \leq \tfrac{1}{2} \tag{58}$$

$$V\frac{\Delta t}{\Delta y} \leq 1 \tag{59}$$

where:

D = diffusion coefficient

Δt = time increment

V = vertical advection velocity

Δy = depth increment

A routine check on the second criterion was built into the program to subdivide the time interval if the vertical velocity should become too large.

Verification

The model was verified on Fontana Reservoir for the same nine month period as the WRE model.

Sensitivity Analysis

The MIT model has been found to be the most satisfactory and has been most thoroughly evaluated. The evaluation results are shown in the Section II, Sensitivity Analyses.

CORNELL MODEL

The model was developed through an extension of a study on the physical effects of thermal discharge into Cayuga Lake(14). It is a one-dimensional model designed for deep stratified lakes. The surface elevation of the lake is assumed to be constant throughout the simulation period and the reservoir is divided into a number of horizontal layers of equal thickness. The geometry of the reservoir is not considered.

Heat flow from inflow, outflow, and vertical advection through each horizontal layer are not considered, nor is the differential adsorption of incoming solar radiation. Eddy diffusivity, which is related to wind induced turbulence and the buoyancy gradient is the primary factor of heat transfer within the reservoir.

Assumptions

(a) Horizontal homogeneity and constant cross-section area.

(b) Lake is deep and isothermal during the springtime.

(c) The lake is turbid and the incoming solar radiation is absorbed within a small layer near the surface.

(d) Eddy diffusivity accounts for all heat transfer within the lake except for the heat added by the power plant and pumping.

(e) The annual equilibrium temperature and wind speed over the lake can be expressed in a sinusoidal form.

Basic Equations

(a) Governing equations

The change in temperature with depth when the plant discharge surfaces is:

$$\frac{\partial T(z,t)}{\partial t} = \frac{\partial}{\partial z}\left(K_H \frac{\partial T(z,t)}{\partial z}\right) - w_p \frac{\partial T(z,t)}{\partial z} + S(z) \text{ for } z_d \leq z \leq z_i \qquad (60)$$

$$\frac{\partial T(z,t)}{\partial t} = \frac{\partial}{\partial z}\left(K_H \frac{\partial T(z,t)}{\partial z}\right) + S(z) \quad 0 \leq z < z_d \text{ or } z_i < z \leq z_m \qquad (61)$$

where:

T = temperature (^oC)

t = time (day)

z = depth below the water surface (ft)

K_H = thermal diffusivity (ft^2/day)

w_p = the specified pumping velocity (ft/day)

z_i, z_d = the specified intake and discharge depths (ft)

z_m = the depth of the lake (ft)

$S(z)$ = the explicit thermal discharge or heat input term (^oC/day)

$$S_z = \frac{2w_p\left[T(z_i) + \Delta T_p - T_s\right]}{a\sqrt{\pi}}\; e^{\frac{-(z-z_d)^2}{a^2}} \qquad (62)$$

where:

ΔT_p = temperature rise across condenser

T_s = surface temperature

w_p = pumping velocity

z = length scale

When the discharge temperature is less than the surface temperature, the effluent will remain submerged and S(z) is zero. The pumping speed is related to q_{pp}, the heat per unit area per unit time added by the power plant by the equation:

$$w_p = q_{pp}/\rho \cdot C_p \cdot \Delta T_p \qquad (63)$$

where:

$\rho \cdot C_p$ = heat capacity per cubic foot of water (112.32 BTU/^{o}C-ft^3)

ΔT_p = temperature difference produced by power plant

$$\Delta T_p = T(z_d) - T(z_i) \; (^{o}C) \qquad (64)$$

The thermal eddy diffusivity, K_H, has the form given by Rossby and Montgomery$^{(15)}$:

$$K_H = K_{Ho}(1 + \sigma R_i)^{-1} \qquad (65)$$

where:

K_{Ho} = $(C_1 + C_2 z)w^*$ = the eddy diffusivity of neutral stratification (ft^2/day)

σ = a dimensionless constant (=0.1 for preliminary study)

w^* = $\frac{\tau_s}{\rho} = B_1 + B_2 \sin (\frac{2\Pi}{365} t + \Psi)$, friction velocity (67)

The empirical relation of Munk and Anderson is suggested for determining wind speeds over lakes.

$$R_i = - (\frac{gz}{w^* 2})^{N-1} \alpha_v z \frac{\partial T}{\partial z}$$, Richardson Number (68)

$\alpha_v = A_1 + A_2 (T - 4^o) + A_3 (T - 4)^2$, Coefficient of volumetric expansion for water (69)

where:

N = a dimensionless constant (N=2)

τ_s = wind shear stress

$A_1, A_2, A_3, B_1, B_2, C_1, C_2$ = constants

(b) Initial condition

$$T(z,t_o) = T_o \quad (70)$$

(c) Boundary conditions

$$(\frac{\partial T}{\partial z})_{z=z_m} = 0 \quad (71)$$

$$-(\rho C_p K_H \frac{\partial T}{\partial z})_{z = 0} = K (T_E - T_s) \quad (72)$$

$T_E = \bar{T}_e + \delta T_e \sin (\frac{2\Pi}{365} t + \phi)$, the equilibrium temperature (73)

where:

T_s = temperature at water surface

t = time

Φ = phase angle

$\bar{T}_e$ = average value of equilibrium temperature over one annual cycle

δT_e = one half the annual variation

K = the heat transfer coefficient at the lake surface (BTU/ft^3-day-$^\circ$C)

An explicit finite difference scheme is used for numerical evaluation. At each time step, the thermal diffusivity is evaluated from the known temperature profile and its value is restricted to the range between the input maximum and minimum thermal diffusivities. The variable time increment, Δt, is then determined from the maximum value of the thermal diffusivity at this step by the following equation:

$$\Delta t_{k+1} = C_t \frac{(\Delta Z)^2}{(K_H)_{max}} \qquad (74)$$

where:

C_t = a nondimensional constant, $0 < C_t < 0.5$

ΔZ = spatial mesh size

Verification

The model has not been verified explicitly in any lake. The external parameters were chosen to correspond loosely with Cayuga Lake. The results of the model were in qualitative agreement with the measured values of the thermal profiles in Cayuga Lake.

Results of Test Run

A set of test data was prepared from Fontana Reservoir field data to evaluate the model. Several runs were made for different input conditions. Problems about the selection of input parameters were evident during the preparation of the data and during the running of the program. It became obvious that long computer times were required.

In the numerical example given by Cornell, the friction velocity, w^*, is taken to be the surface current velocity at 0.1 ft/sec. However, calculations according to Munk and Anderson's empirical relationship yield w^* at about one tenth of the value given in the example. The resultant eddy diffusivity, K_{HO}, is 4.96×10^3 ft^2/day compared to 7.98×10^2 ft^2/day used by the Cornell Aeronautical Laboratory. The eddy diffusivity affects both the thermal diffusivity and time step, and therefore the simulated thermal structure in reservoir. The current velocity at the surface in Fontana Reservoir is not available. If the suggested relation is used, the eddy diffusivity is of order of 5.0×10^3 ft^2/day and the computer time for a 300 day run will be about 90 minutes. Therefore, a maximum time limit of 15 minutes was set for all runs. Other parameters defined loosely are the dimensionless constant σ, in Equation 65, the length scale, 'a', in Equation 62, and the maximum and minimum thermal diffusivities.

In a lake of variable cross-sectional area with depth, the assumptions used in this model, constant cross-sectional area and horizontal homogeneity, imply a distortion of the vertical scale. Hence, the computed temperature profile has to be converted in some way before it can be compared with the measured value. Due to the nonlinearity of the diffusion coefficient with respect to depth and temperature gradient, the conversion will be very complicated. Since the model has not provided any method to account for vertical distortion and no available scheme is applicable to this situation, the values directly calculated are used for evaluation.

The profiles for typical times of the year are shown in Figures 8 through 10 for runs without inflow/outflow and with inflow/outflow converted to that corresponding to power plant cooling water. Both runs used a diffusion coefficient of 7.98×10^2 ft^2/day as in the Cornell example. As shown in Figure 8 for July 6th, the predicted values for both conditions are reasonable approximations of the measured values except at the surface where the difference is 6°C. In Figure 9, for September 1st, the predicted values vary greatly from the measured values, in some instances as much as 6°C. In Figure 10, December 1st, the predicted values are in better agreement with the measured values though differences as great as 4°C are noted. The predicted values for the inflow/outflow case are in much better agreement with the measured results than is the case without inflow/outflow. When higher diffusion coefficients were used, the time limit of 15 minutes was exceeded. The differences between computed and measured temperatures may be due to:

(i) distortion of the vertical scale of reservoir caused by use of a constant surface elevation and cross-section area.

(ii) neglect of inflow and outflow other than cooling water. Since in most of the reservoirs suitable for analysis of these models,

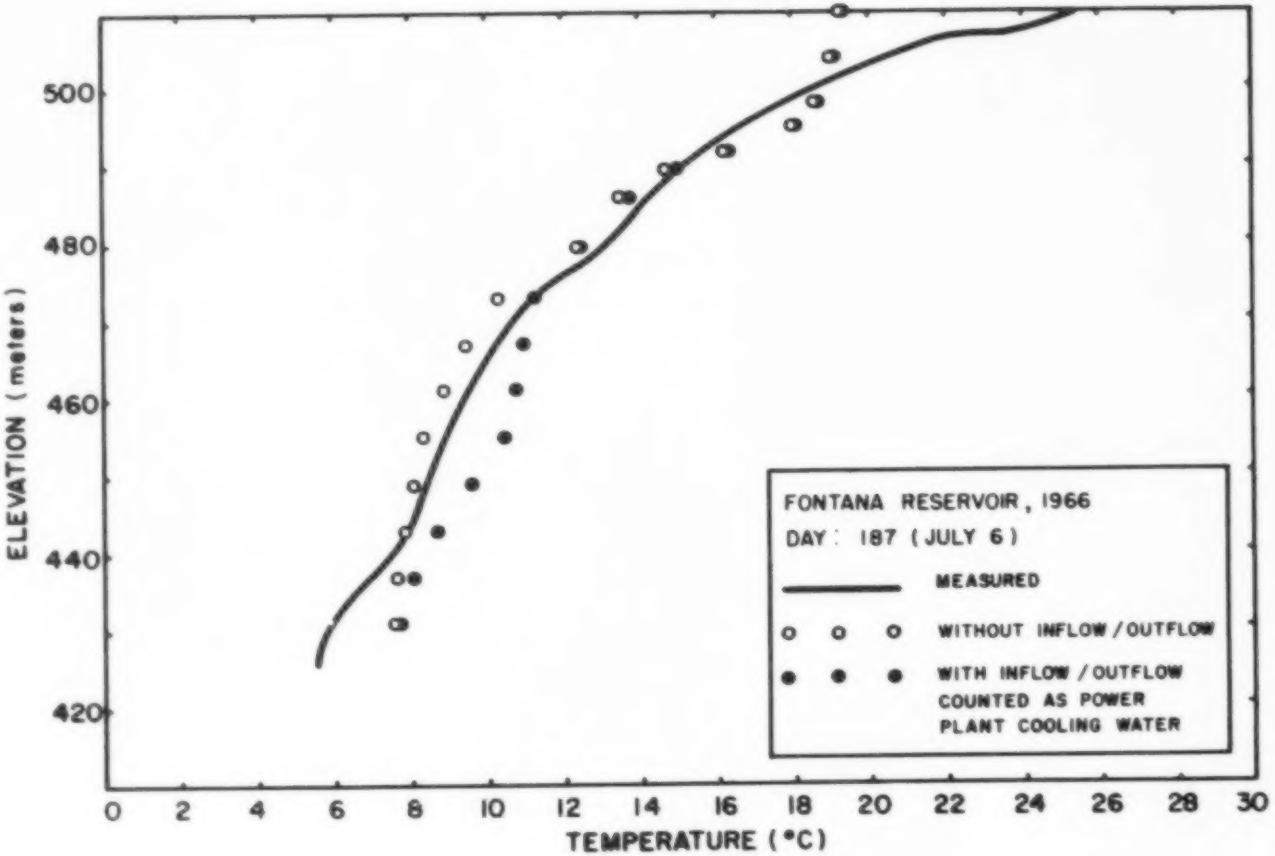

Figure 8. Cornell model test run results, July 6, 1966

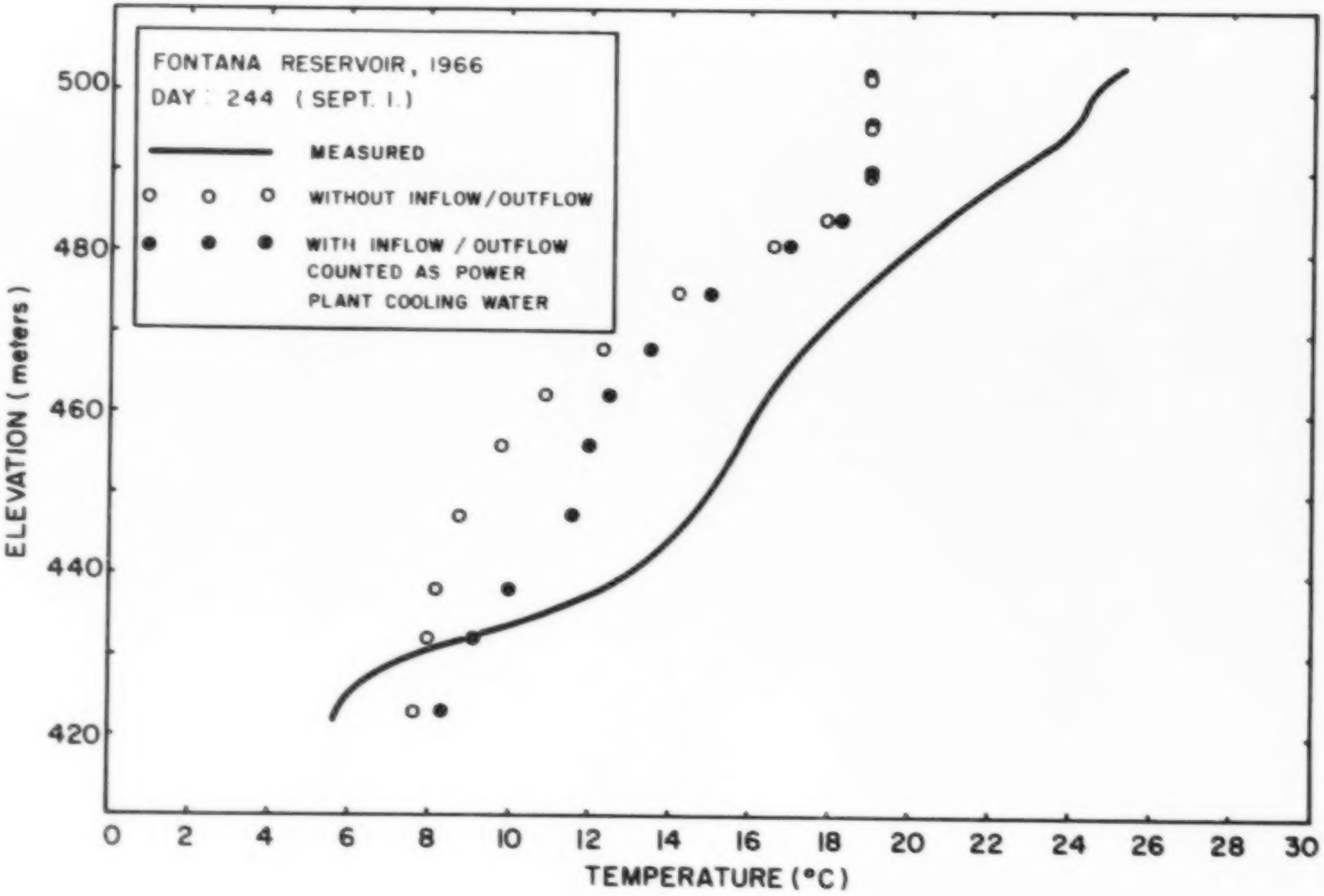

Figure 9. Cornell model test run results, September 1, 1966

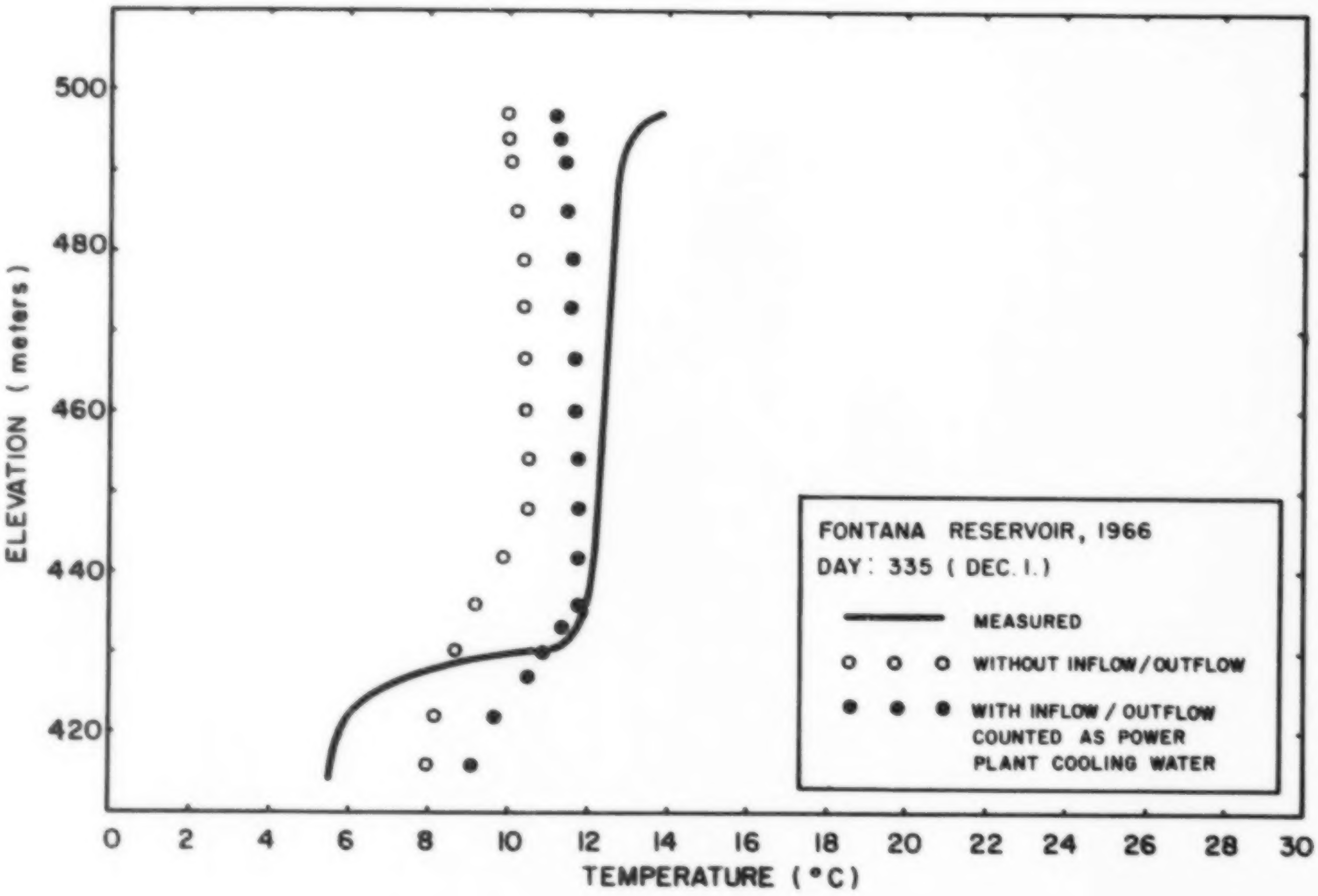

Figure 10. Cornell model test run results, December 1, 1966

average yearly flow is considerably greater than the volume of the reservoir, the inflow would bring in an amount of thermal energy which would not be negligible. The same, of course, would be true for the energy loss due to outflow. In addition, the inflow and withdrawal from hypolimnion would provide mixing which is not accounted for by eddy diffusion.

(iii) The eddy diffusivity depends too strongly on the wind conditions above the reservoir.

PROBLEMS WITH DEEP RESERVOIRS MODELS

All of the three models evaluated use temperature for the determination of the entrance level of inflow and for evaluation of whether an unstable condition prevails to enhance convection. Temperature is also used for the calculation of withdrawal thickness in the MIT model. However, the density of water is greatest at 4°C. Therefore, the models without modification, cannot be applied to a reservoir where the water temperature goes below 4°C. This oversight is probably due to the fact that the temperature of the Fontana Reservoir is higher than 4°C the year round. However, water of 4°C floating on the top of the colder water was discovered in the results from the test data supplied with Cornell model.

The calculation of water temperature at the surface layer is an important problem. With variable surface level, the volume of the surface layer also changes with time. The heat transport equation described earlier is derived for a fixed control volume with respect to time. Therefore, directly applying the heat transport equation to the surface layer, whose volume varies with time, will cause serious errors. To approximately account for the heat balance in the surface layer, one should calculate the total heat content of the surface layer at each time step. Suppose y_o, y_1, y_2 and y_3 are the surface elevations at the beginning of each day t_1, t_2, t_3, t_4, etc., as shown in Figure 11. A linear variation of water surface is assumed. The mean elevation, $\bar{y}_1$, $\bar{y}_2$, and $\bar{y}_3$, should be used at each time step, t_1, t_2, t_3 for calculating the thickness of the surface layer water surface area and the absorption of the solar radiation at different levels below the water surface. The heat balance equation of the surface layer can then be written as:

$$c\rho T^{(k+1)}V_s = c\rho T^{(k)}V_{so} + (c\rho T_{in}q_{in} - c\rho T_{out}q_{out} + Q_{av} + Q_d + Q_h)\cdot\Delta t \qquad (75)$$

$$\text{with } V_s = V_{so} + \frac{dV}{dt}\Delta t \qquad (76)$$

where:

V_{so} = volume in the element corresponding to the present surface

V_s = volume of surface layer at the end of the current time step

k = time step

ρ = density of water

q_{in} = inflow rate

q_{out} = outflow rate

Q_d = heat transport due to diffusion

Q_h = heat transport due to absorption of radiation

Q_{av} = heat transport due to vertical advection

Another approximate method could also be derived. The surface elevations are assumed to be discrete, instead of continuous, as indicated by the solid line in the Figure 11. At each step the surface elevation is held constant and equal to its mean value $\bar{y}_1$, $\bar{y}_2$, $\bar{y}_3$. The heat transport and continuity equations for internal elements are the same as usual. However, the same heat transport equation can be applied to the surface layer only by modifying the continuity equation. The assumption of a constant surface elevation at each time interval implies that a volume of water with a temperature equal to that of the surface layer has been added to that layer if the surface elevation is rising, or is subtracted from the surface layer if the surface elevation is falling. The volume of water added or subtracted is equal to the vertical advection through the interface of the surface layer and is the most immediate underlying layer. The continuity equation for the surface layer is then written in the MIT model notation as:

$$u_i B\Delta y + V'_{jm} A = u_o B\Delta y \tag{77}$$

The V'_{jm} is different from V_{jm} which when multiplied by the area between the surface layer and the immediate underlying layer is the sum of the inflow and outflow for all elements below the surface layer, or

$$V_{jm} = \frac{1}{A} \left(\sum_{i=1}^{jm-1} (u_i B(y)\Delta y - u_o B(y)\Delta y) \right) \tag{78}$$

These two terms are related to ΔV_s as shown in Equation 79:

$$V_{jm} - V'_{jm} = \frac{\Delta V_s}{\Delta t} \cdot \frac{1}{A} \tag{79}$$

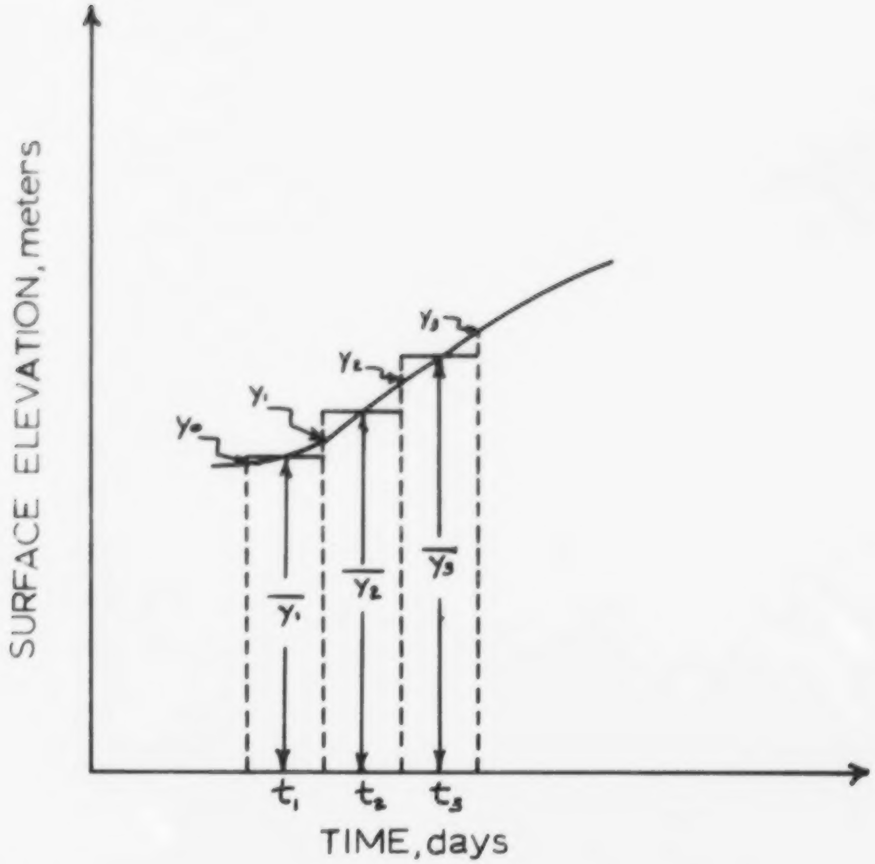
SURFACE ELEVATION, meters
TIME, days
y_0
y_1
y_2
y_3
$\overline{y_1}$
$\overline{y_2}$
$\overline{y_3}$
t_1
t_2
t_3

Figure 11. Surface layer schematic

The heat transport terms due to inflow, outflow and vertical advection are:

i) $V_{jm} > 0$

$$\Delta T \cdot V_s = V'_{jm} \cdot A \cdot T_{jm-i}\,\Delta t + \Delta V_s\,(T_{jm-i} - T_{jm}) + u_i\,B\Delta y T_i \cdot \Delta t - u_o \cdot B \cdot \Delta y \cdot T_{jm} \cdot \Delta t \qquad (80)$$

Substituting Equations 77 and 79:

$$\Delta T \cdot V_s = V_{jm} \cdot A \cdot (T_{jm-i} - T_{jm})\,\Delta t + u_i\,B\Delta y\,(T_i - T_{jm})\Delta t \qquad (81)$$

(ii) $V_{jm} < 0$

$$\Delta T \cdot V_s = V'_{jm} \cdot A \cdot T_{jm}\,\Delta t + u_i\,B\Delta y \cdot T_i \cdot \Delta t - u_o B_{jm} \Delta y T_{jm} \cdot \Delta t \qquad (82)$$

By Equation 77:

$$\Delta T \cdot V_s = u_i B\Delta y(T_i - T_{jm})\,\Delta t \qquad (83)$$

The MIT model uses the second approximate method. The final results, Equations 3.20 and 3.22 in Reference 4 are correct, although the continuity equation for surface layer, Equation 3.14 appears to be wrong. Equation 3.14 implies that total inflow and outflow are always equal, which is not always the case. The approximation has proved to be satisfactory as determined by verification on seven TVA reservoirs when compared to the results from the first approximate method which was incorporated into the MIT model in TVA's study$^{(17,18)}$.

The WRE model also uses an approximate method in which the same heat transport and continuity equations used for internal elements are applied to the surface layer. It is modified only when the vertical advection, q_{av}, is positive. The quantity $(q_{av} \cdot T_s)$ is then deducted from the total surface layer heat. No modification is necessary when the advection is negative. The WRE model for the surface layer appears to be incorrect. It may have contributed to the wide variation in predicted temperatures when the layer thickness was varied.

In the Cornell model, a constant surface elevation is assumed.

SECTION V

SENSITIVITY ANALYSIS

Based on results from the test runs on Fontana Reservoir, the three models were evaluated. Only the MIT model was chosen for further sensitivity analysis of input parameters on seven TVA reservoirs. The Cornell model, though it has some attractive theoretical features, lacks means of inputing inflow, outflow, and the variation of surface elevation. The model, therefore, does not approximate the most typical cases. The running time for the model is considerably greater than for the other two models. In addition, the test run results are poor compared to the measured field data.

The Water Resources Engineers' Model has also been found to be inappropirate due to the complex structure of the program, the longer computer run times for the program and because of inadequate documentation of the model. In addition, a drastic change in the predicted temperature in response to variation in the layer thickness was observed.

The MIT model is, in our opinion, the most easily used. We have applied the model to seven TVA reservoirs, having widely different flow through times, volumes and depths. We have varied the height of the vertical increments, Δy, the fraction of radiation absorbed in the top meter of water in the reservoir, β, and the average absorption coefficient of water, η, and the vertical diffusion coefficient. Transmission of the radiation below the water surface is related to β and η as shown in Equation 48.

$$\phi_Y = \phi_o (1 - \beta) e^{-\eta Y} \tag{48}$$

where:

ϕ_Y = the quantity of radiation arriving at a horizontal plane (Y meters below the water surface) in kilocalories

β = the fraction of radiation absorbed by the top meter of water in the reservoir

ϕ_o = total incoming radiation in kilocalories

η = the average absorption coefficient of the water (meter^{-1}), and

Y = depth below the water surface in meters

The degree of variation of the parameters is shown in Table 5. We have tried to cover the range of values to be expected: from average flow through times of 0.01 to 0.85 years; absorption coefficients suitable to distilled water and to highly turbid water; diffusion coefficients from molecular diffusion to 1000 times molecular diffusion; depth increments from 1 to 3 meters; and fraction of radiation absorbed in the top meter of water from 0.2 to 0.5.

Parameters not included in the sensitivity analysis were held constant throughout the study. The original time step input of one day was used, since all the meteorological and hydrological inputs were daily averages measured on a daily basis. Inflow travel time within reservoirs is neglected and a mixing ratio of 1.0 and four grid spaces are used for entrance mixing. Entrance mixing is simply a way to represent the mechanisms not accounted for by the mathematical model and is considered unsatisfactory as pointed out by the authors of the model.

Table 5.

PARAMETERS VARIED IN SENSITIVITY ANALYSIS

Units	Average Values	Low Values	High Values
Vertical Increments, m	2	1	3
Fraction of Radiation Absorbed in Top Meter of Water	0.50	0.20	0.40*
Average Absorption Coefficient of Water, m^{-1}	0.75	0.05	1.40
Vertical Diffusion Coefficient	Molecular Diffusion	30 Times Molecular Diffusion	1000 Times Molecular Diffusion

*Not the high value

Atmospheric radiation was calculated by the model. If measured solar radiation is not available, the routine described in TVA Report 14[19] was used for computation.

We used the original program unless we found programming or logic errors. For this study several modifications were made:

(i) In Function 'FLXOUT(N)' the statement:

```
RAD = 1.13587 E - 6* ( (TS + 273.16)** 4 - 0.937 E - 5* (TAIR + 273.16)**
      6* (1.0 + 0.017* CC**2)
```

was replaced by the following two statements

```
AR  = 0.937 E - 5* 1.13587 E - 6* (TAIR + 273.16)**6* (1.0 + 0.17*
      CC**2)
RAD = 1.13587 E - 6* (TS + 273.16)** 4 - AR
```

This is done in order to correct the error in the coefficient and make a proper transfer of the parameter back to the main program.

(ii) In SUBROUTINE'SPEED(N)' the statement:

`IF (EPSIL.LT.0.0) EPSIL = - EPSIL` was inserted into the program after statement No. 15.

This is necessary only in Douglas Reservoir where a negative temperature gradient was formed.

(iii) In SUBROUTINE 'SPEED(N)' the cut-off gradient was put into the routine for calculating withdrawal layer thickness when using Kao's or Koh's formulae. The original program applied the cut-off gradient only when the temperature gradient at the outlet was less than 0.01 and Kao's and Koh's formulae are not used in that case. This results in withdrawal of a large amount of surface water such as occurred in Norris Reservoir.

(iv) In addition, the program was modified to call a subroutine TPLOT to plot the simulated temperature profiles for chosen dates and to store the results in the computer disc. A routine was also written to read and plot the results of the sensitivity analysis.

One of the important parameters is the amount of evaporation. There are a number of empirical formulas available. The MIT model uses two different evaporation formulas.

Kohler's $E_m = 0.000180\, W\rho\, (e_s - \Psi e_a)$ (84)

and Rohwer's $E_m = (0.000\,308 + 0.000185W)\, \rho(e_s - \Psi e_a)$ (85)

where:

E_m = mass flux in kg/day-m^2

ρ = density of water in kg/m^3

W = windspeed in m/sec

e_s = saturation vapor pressure of the air at the temperature of water surface in mm Hg

e_a = saturation vapor pressure of the air at temperature Ta (air temperature) in mm Hg

Ψ = relative humidity expressed as a fraction

The major difference in the two formulations is that Kohler's shows no evaporation at zero windspeed while Rohwer's does indicate evaporation at zero windspeed. We have found no apriori means of deciding which is most appropriate. However, the test runs indicate Rohwer's equation yields better results only in Fontana Reservoir; both give about equal results in South Holston Reservoir and Kohler's shows more favorable results in the rest of the reservoirs tested. Whichever evaporation formula more nearly predicted the measured values was subsequently used in all of the sensitivity analyses for that particular reservoir. The frequency analysis of wind speeds shown in Table 6, seems to indicate that Kohler's formula yields better results in the reservoir where the wind speeds are mostly higher than 2 mph.

The results of the sensitivity analysis are shown in Figures 12-201. The legend for these figures is shown in Table 7.

FONTANA RESERVOIR

Figure 12 shows the measured Fontana Reservoir Temperature data with depth for selected days. Figure 13 shows the computed temperature data for the same days using the corrected MIT model. As can be seen from the figures and from Tables 8 and 9, the predicted and measured values for the outlet water temperature and the surface water temperature have standard errors of estimate of 1.2 and 1.7 degrees C respectively. Such good agreement might have been expected, since the model coefficients were adjusted to fit the measured values of this reservoir for this year. We were interested in how well the model would fit the measured temperatures for other reservoirs and other years.

The closeness of the estimate of the outflow temperature using the Rohwer evaporation formula to the measured outflow temperature is shown on Figure 14. The effects of the variation of the layer thickness, fraction of solar radiation absorption at the water surface, radiation absorption coefficient, and the diffusion coefficient for selected days are shown on Figures 15-21, 22-28, 29-35 and 36-42 respectively. It

Table 6.

FREQUENCY ANALYSIS OF THE WIND SPEED

		1	2	3	4	5	6	7	8	9	10	11
Wind Speed		0.0	2.0	4.0	6.0	8.0	10.0	12.0	14.0	16.0	18.0	>20.0
(MPH)		2.0	4.0	6.0	8.0	10.0	12.0	14.0	16.0	18.0	20.0	
Fontana	No	18.0	117.0	100.0	39.0	18.0	10.0	3.0	1.0	0.0	0.0	0.0
	%	5.9	38.2	32.7	12.7	5.9	3.3	1.0	0.3	0.0	0.0	0.0
Douglas	No	4.0	162.0	128.0	46.0	20.0	3.0	2.0	0.0	0.0	0.0	0.0
	%	1.1	44.4	35.1	12.6	5.5	0.8	0.5	0.0	0.0	0.0	0.0
Cherokee	No	3.0	49.0	112.0	103.0	48.0	31.0	13.0	2.0	3.0	1.0	0.0
	%	0.8	13.4	30.7	28.2	13.2	8.5	3.6	0.5	0.8	0.3	0.0
Norris	No	0.0	31.0	128.0	87.0	58.0	31.0	16.0	9.0	2.0	3.0	0.0
	%	0.0	8.5	35.1	23.8	15.9	8.5	4.4	2.5	0.5	0.8	0.0
South Holston	No	22.0	91.0	94.0	48.0	33.0	12.0	2.0	4.0	0.0	0.0	0.0
	%	7.2	29.7	30.7	15.7	10.8	3.9	0.7	1.3	0.0	0.0	0.0
Hiwassee	No	1.0	20.0	128.0	91.0	71.0	33.0	8.0	7.0	2.0	3.0	1.0
	%	0.3	5.5	35.1	24.9	19.5	9.0	2.2	1.9	0.5	0.8	0.3
Fort Loudoun	No	0.0	31.0	128.0	87.0	58.0	31.0	16.0	9.0	2.0	3.0	0.0
	%	0.0	8.5	35.1	23.8	15.9	8.5	4.4	2.5	0.5	0.8	0.0

Table 7.

LEGEND FOR FIGURES 12-201

	Layer Thickness ΔY(m)	Fraction of Solar Radiation Absorbed at The Water Surface β	Radiation Absorption Coefficient $\eta(m^{-1})$	Diffusion Coefficient $D(m^2/day)$
STAND	2.0	0.50	0.75	Dm*
DELZ 1	1.0	0.50	0.75	Dm
DELZ 2	3.0	0.50	0.75	Dm
BETA 1	2.0	0.40	0.75	Dm
BETA 2	2.0	0.20	0.75	Dm
ETA 1	2.0	0.50	0.05	Dm
ETA 2	2.0	0.50	1.40	Dm
ETA 3	2.0	0.50	0.40	Dm
DIFF 1	2.0	0.50	0.75	30 Dm
DIFF 3	2.0	0.50	0.75	100 Dm

*Dm = molecular diffusion

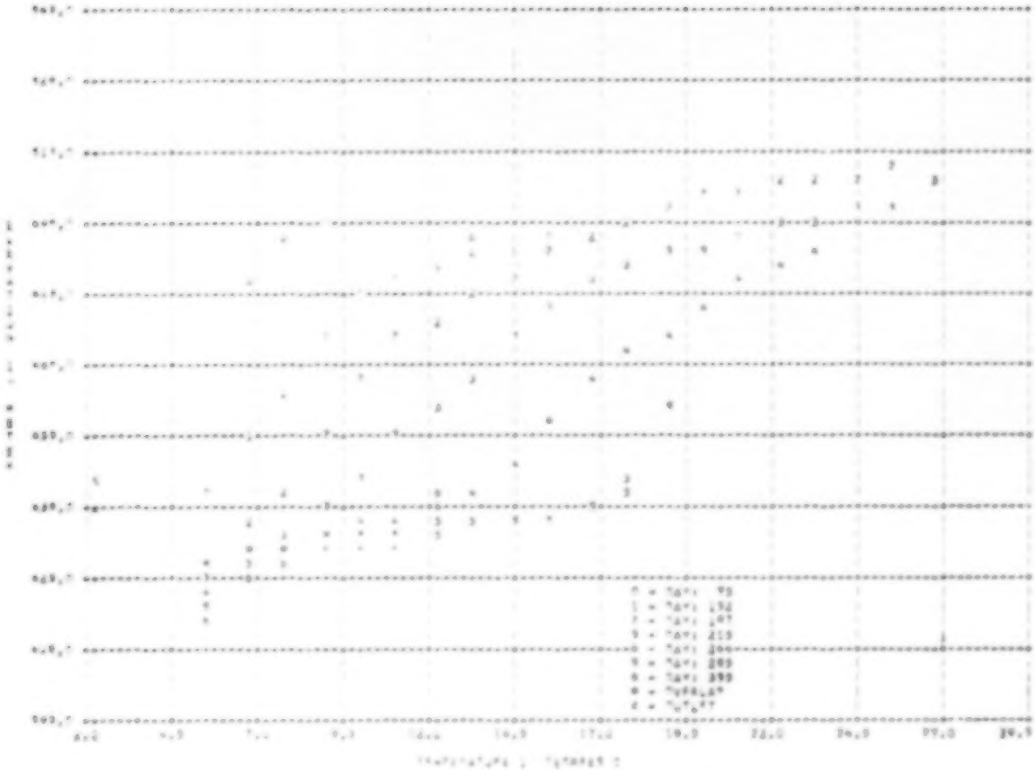

FIGURE 11 [illegible] TEMPERATURE PROFILES

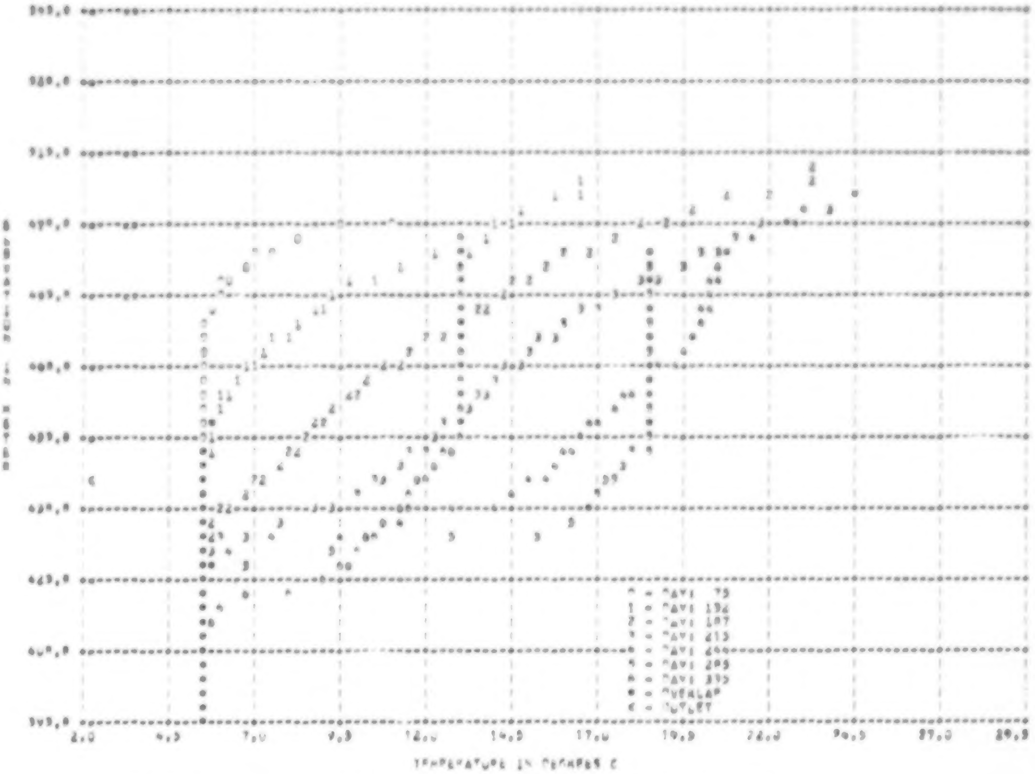

FIGURE 11 [illegible] COMPUTED TEMPERATURE PROFILES

Table 8.

STATISTICAL ANALYSIS FOR THE PREDICTED
WATER TEMPERATURE AT OUTLET LEVEL

Reservoir/Year: Fontana/1966

Time Period Covered: 120th - 330th Julian Day

File Name	Std. error of estimate (°C)	Correlation Coefficient
STAND	1.19	0.96
DELZ 1	1.25	0.96
DELZ 2	1.16	0.97
BETA 1	1.19	0.96
BETA 2	1.22	0.96
ETA 1	2.88	0.77
ETA 2	1.21	0.96
ETA 3	1.27	0.96
DIFF 1	1.15	0.97
DIFF 3	1.25	0.96

Table 9.

STATISTICAL ANALYSIS FOR THE PREDICTED SURFACE WATER TEMPERATURE

Reservoir/Year: Fontana/1966

Time Period Covered: 60th - 360th Julian Day

File Name	Std. error of estimate (°C)	Correlation Coefficient
STAND	1.74	0.95
DELZ 1	1.75	0.95
DELZ 2	1.70	0.96
BETA 1	1.74	0.95
BETA 2	1.70	0.96
ETA 1	2.20	0.92
ETA 2	1.74	0.95
ETA 3	1.75	0.95
DIFF 1	1.76	0.95
DIFF 3	1.81	0.95

can be seen in Figures 15-21, that the variation in the thickness of the horizontal layers from 1 meter to 3 meters had virtually no effect on the predicted temperatures. The standard errors of estimate for the temperature when varying the depth confirm this.

It can be seen in Figures 22-28 that the variation from 0.2 to 0.5 in the fraction of the solar radiation absorbed at the surface made little difference in the predicted temperature. This is also confirmed in Tables 8 and 9.

It can be seen in Figures 29-35 that the variation of the radiation absorption coefficient from 0.05 to 1.40 made a great difference but the variation from 1.40 to 0.75 made little difference. The use of a coefficient of 0.05, however, made a large difference between the predicted and measured temperatures. This is also confirmed in Tables 8 and 9.

It can be seen in Figures 30-42 that a variation in the diffusion coefficient from molecular diffusion to 100 times molecular diffusion resulted in a great difference between the predicted temperature and the measured temperature for the greater diffusion coefficient. This difference was most pronounced during the warmer part of the year as shown in Figures 38-40 and as indicated in Tables 8 and 9.

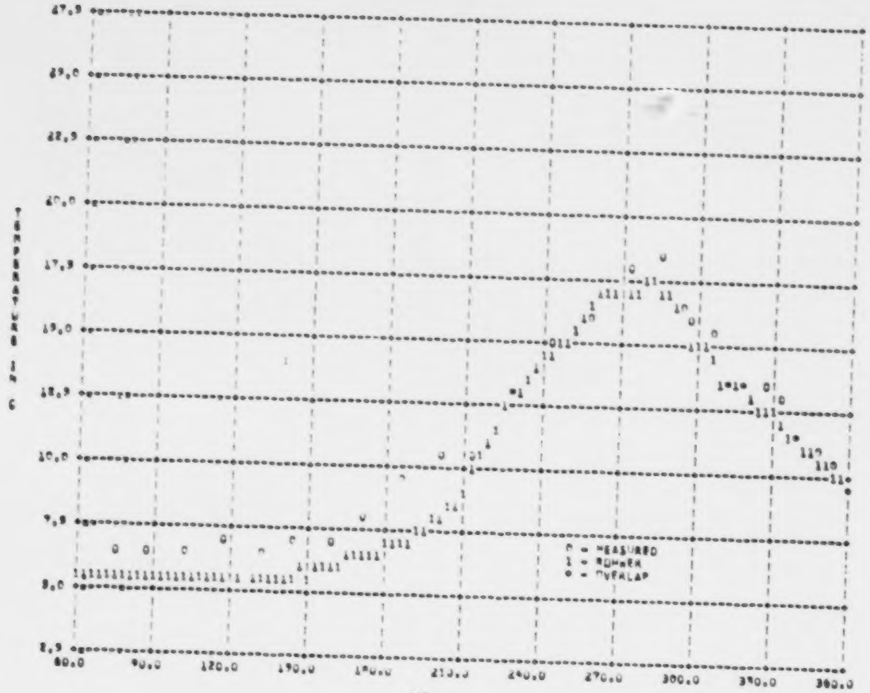

Figure 14 MIT MODEL 1 FONTANA RESERVOIR 1986--COMPUTED OUTFLOW TEMPERATURE--

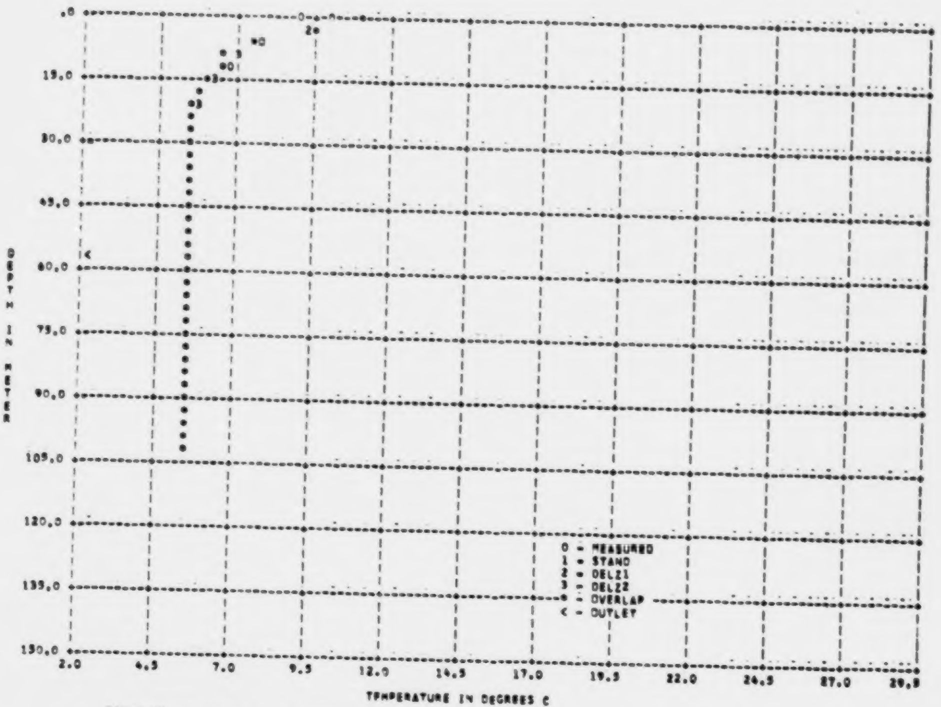

Figure 15 MIT MODEL * FONTANA RESERVOIR 1986--DAY: 75 --SURFACE ELEV: 500.3 M

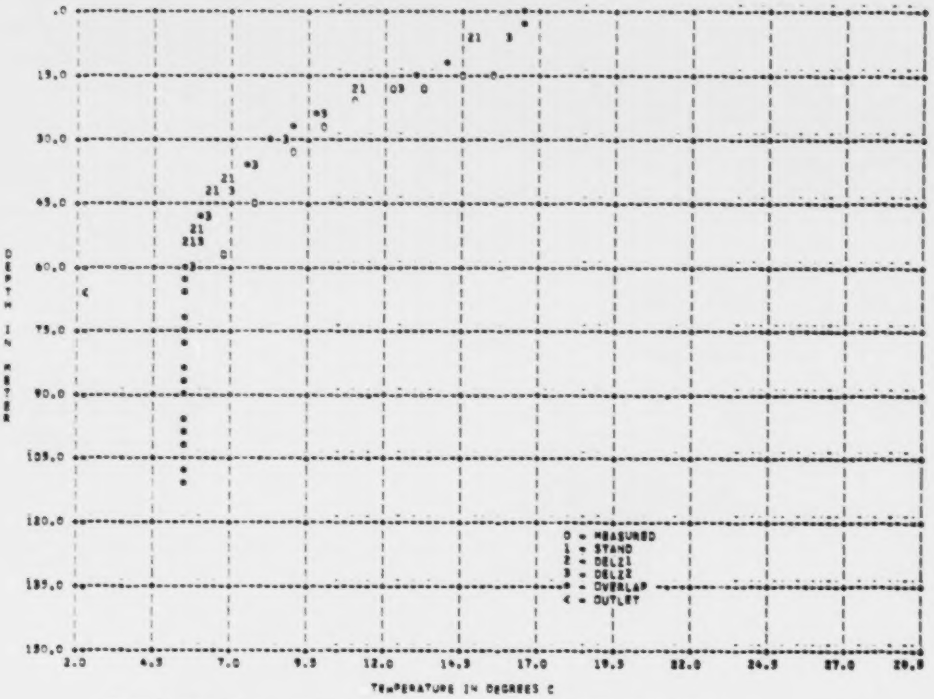

Figure 16 MIT MODEL * FONTANA RESERVOIR 1966--DAY:132 --SURFACE ELEV: 308.4 M

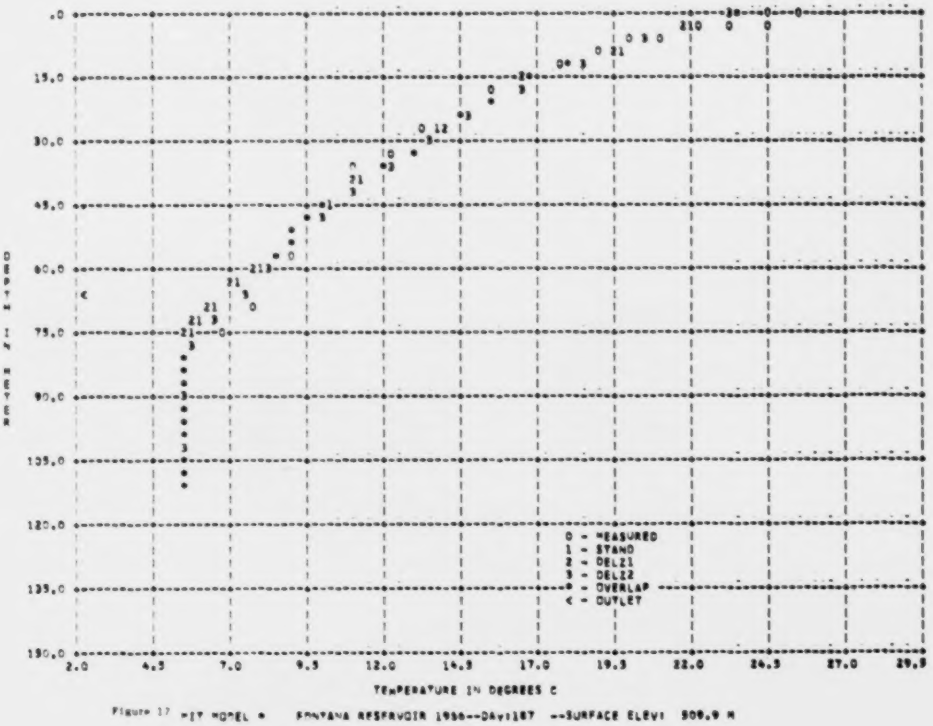

Figure 17 MIT MODEL * FONTANA RESERVOIR 1966--DAY:187 --SURFACE ELEV: 309.9 M

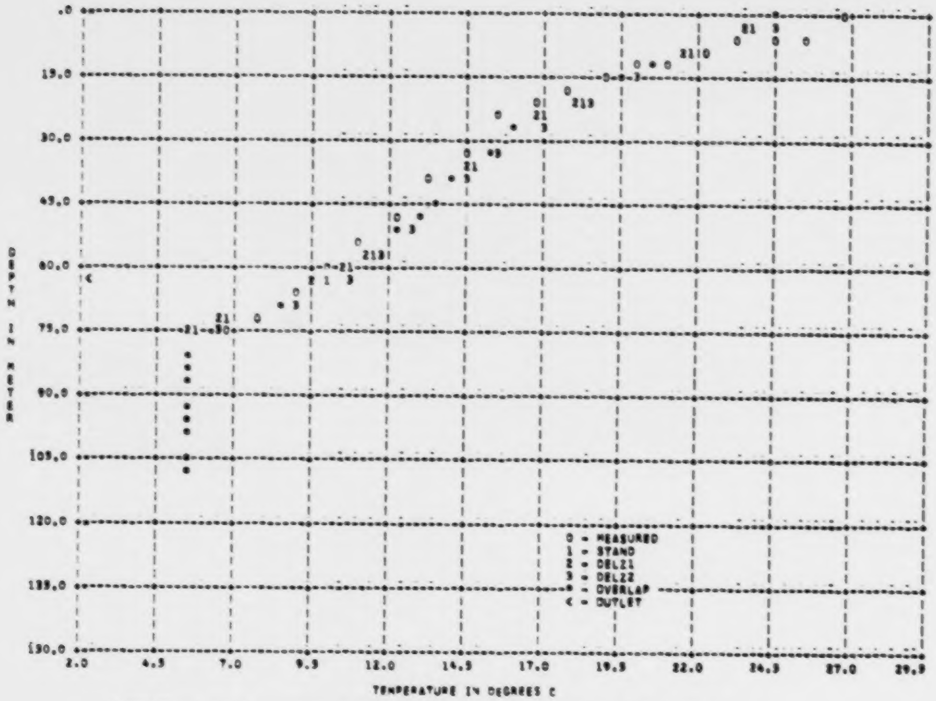

Figure 18 MIT MODEL * FONTANA RESERVOIR 1966--DAY:215 --SURFACE ELEV: 303.9 M

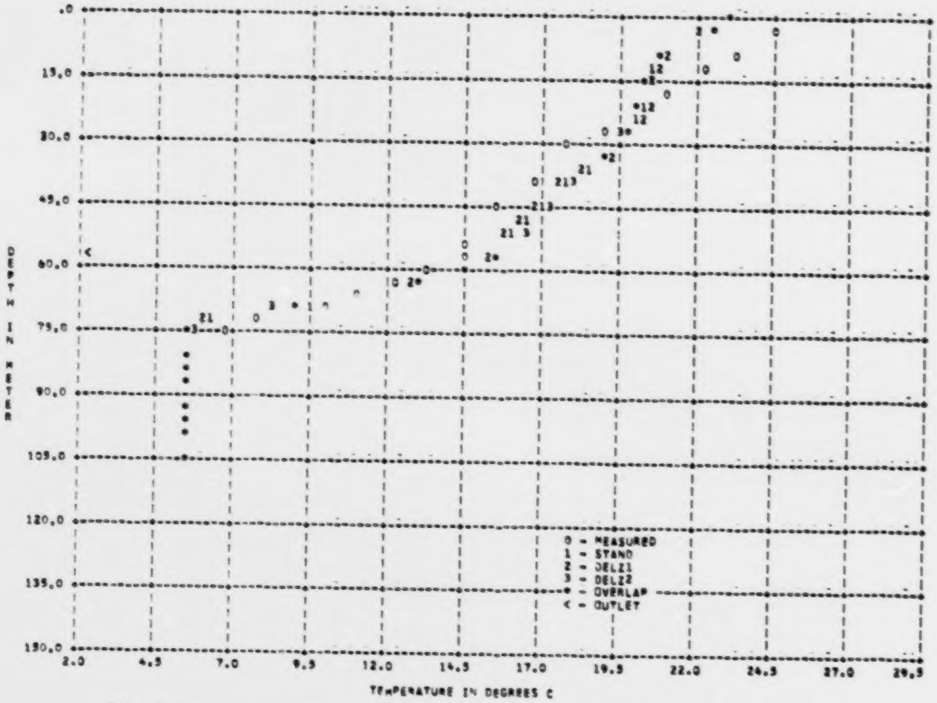

Figure 19 MIT MODEL * FONTANA RESERVOIR 1966--DAY:244 --SURFACE ELEV: 301.9 M

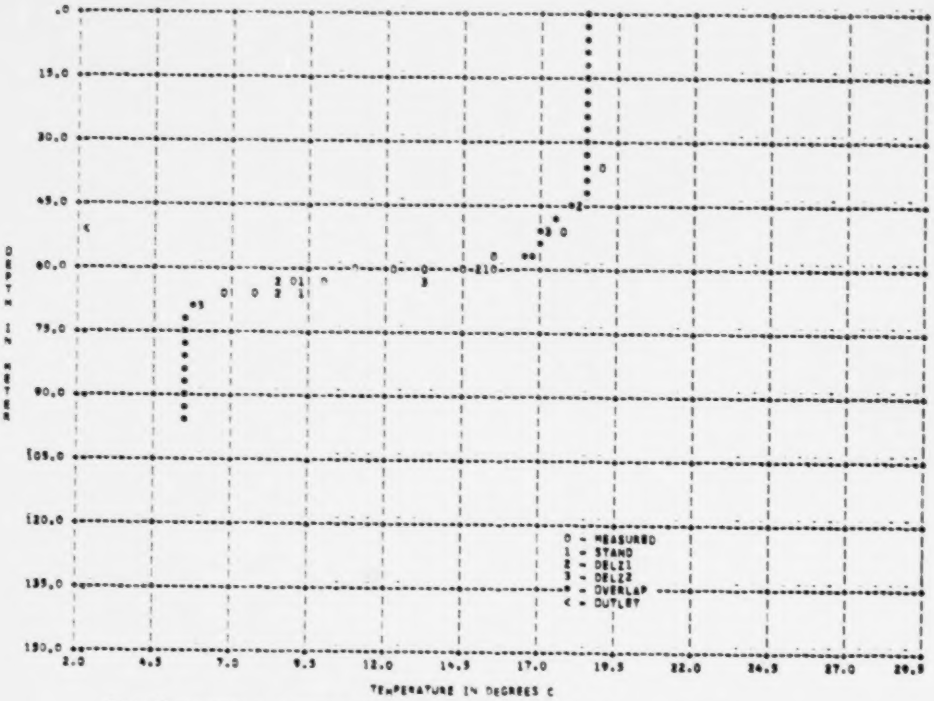

Figure 20 MIT MODEL * FONTANA RESERVOIR 1966--DAY:285 --SURFACE ELEV: 494.3 M

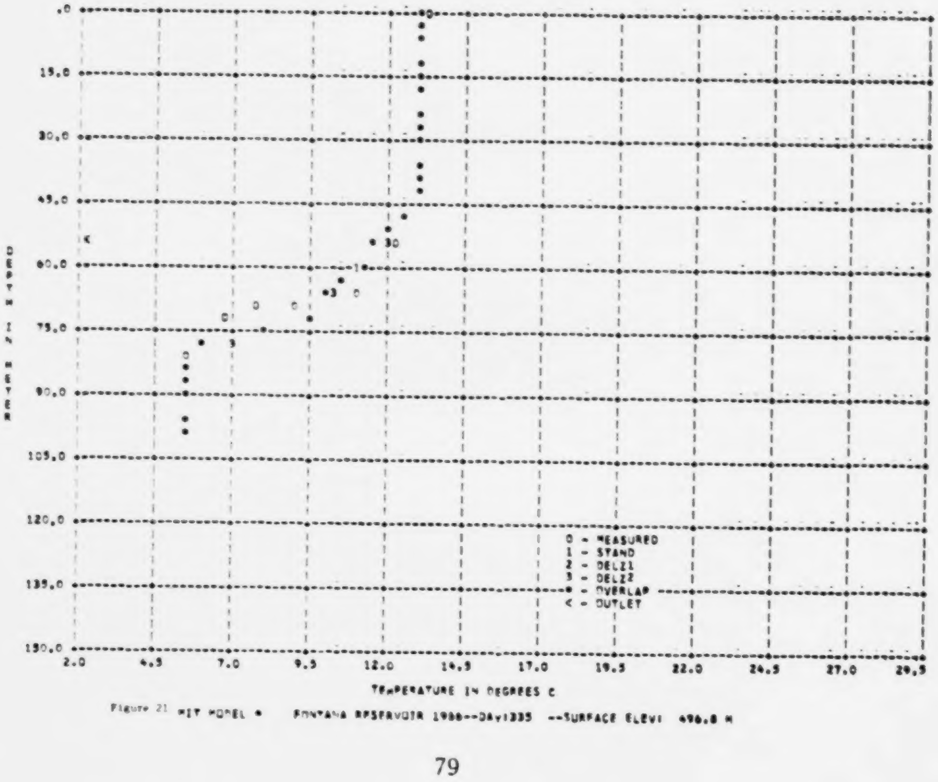

Figure 21 MIT MODEL * FONTANA RESERVOIR 1966--DAY:335 --SURFACE ELEV: 496.8 M

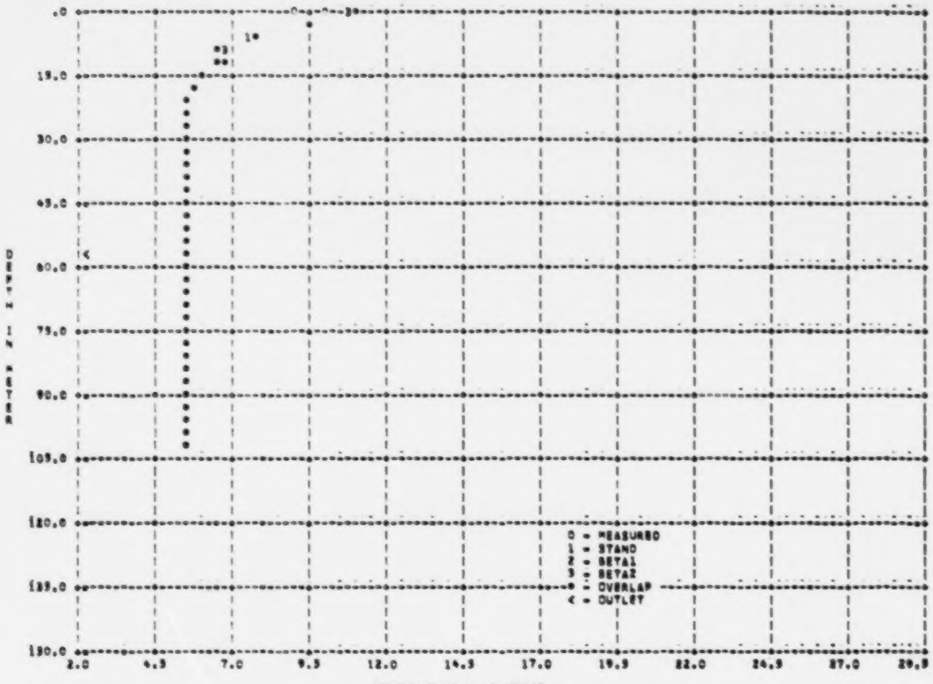

Figure 22 MIT MODEL * FONTANA RESERVOIR 1966--DAY: 75 --SURFACE ELEV: 500.3 M

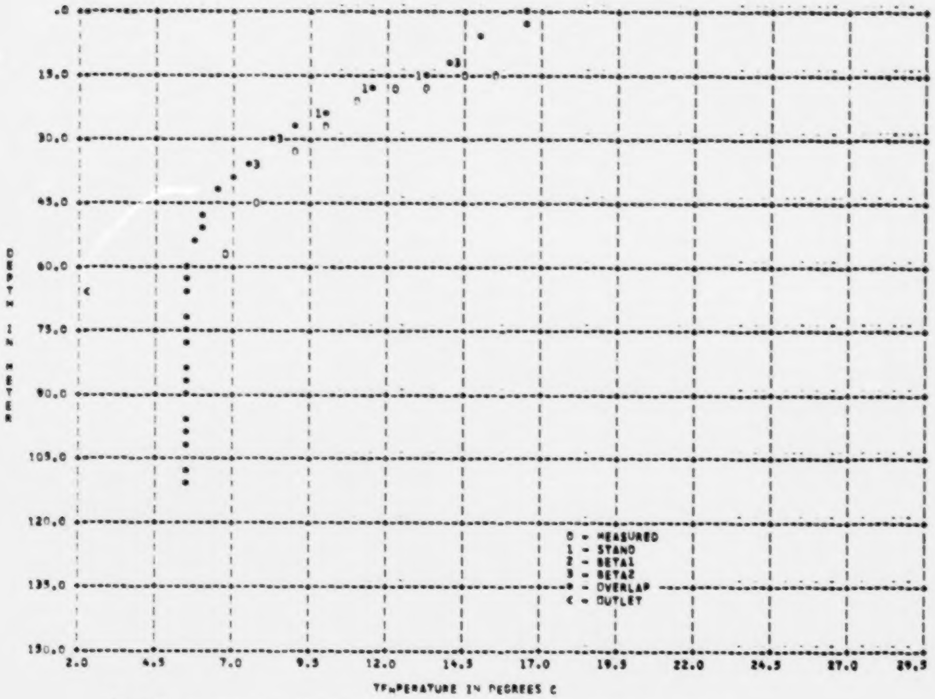

Figure 23 MIT MODEL * FONTANA RESERVOIR 1966--DAY:132 --SURFACE ELEV: 508.4 M

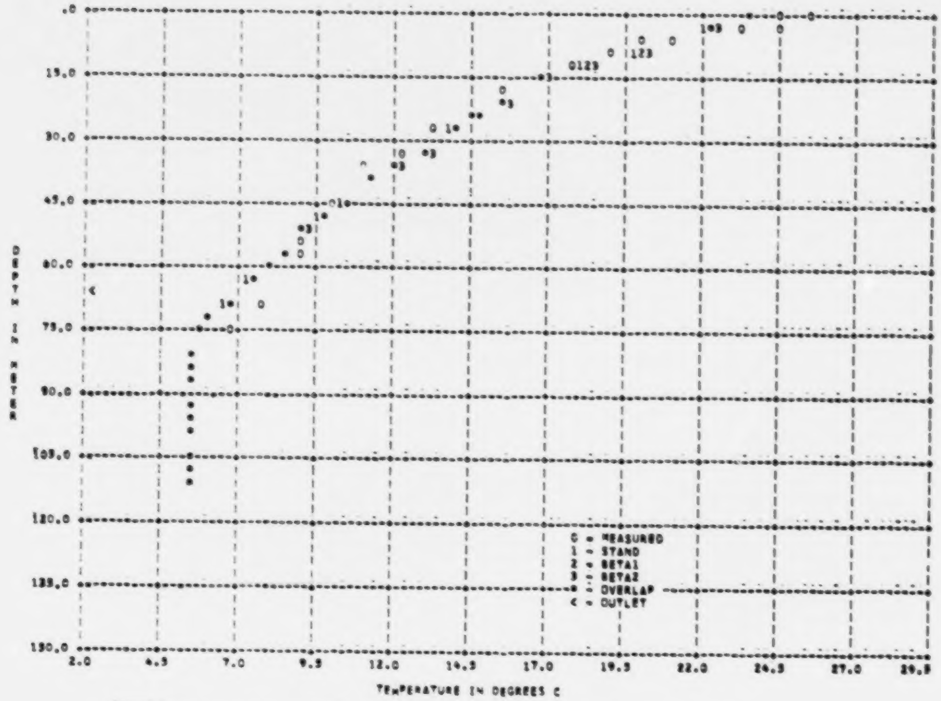

Figure 24 MIT MODEL * FONTANA RESERVOIR 1966--DAY:187 --SURFACE ELEV: 509.9 M

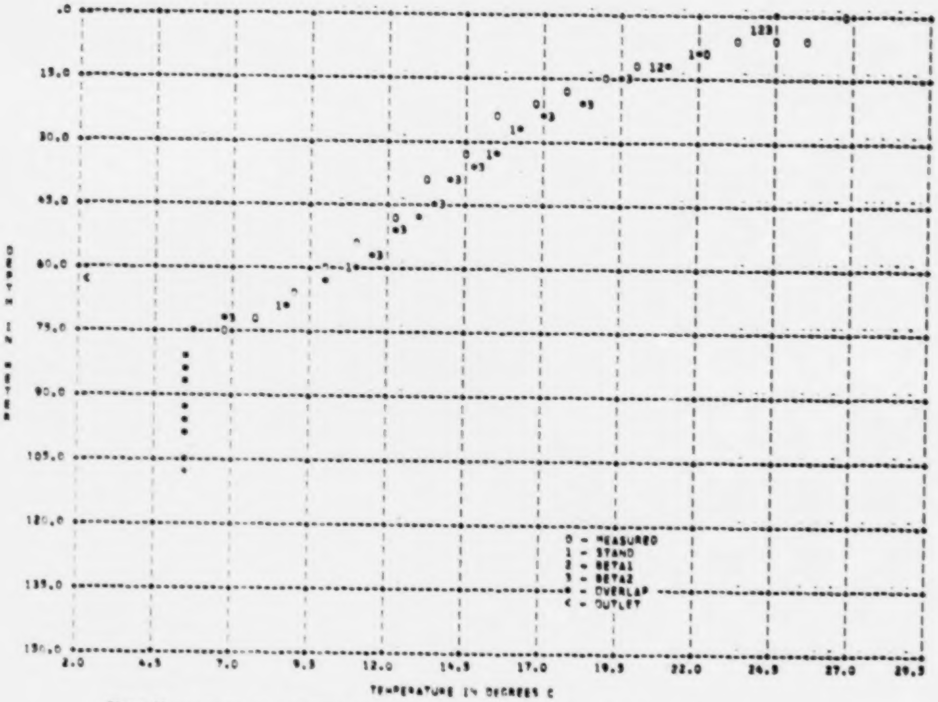

Figure 25 MIT MODEL * FONTANA RESERVOIR 1966--DAY:215 --SURFACE ELEV: 508.9 M

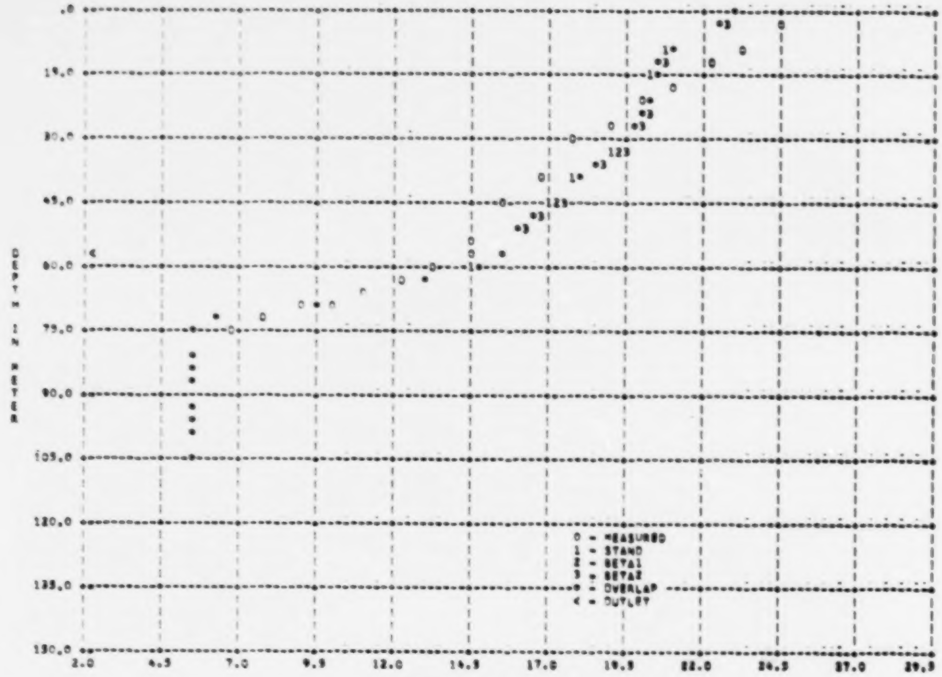

Figure 26 MIT MODEL * FONTANA RESERVOIR 1966--DAY:244 --SURFACE ELEV: 501.9 M

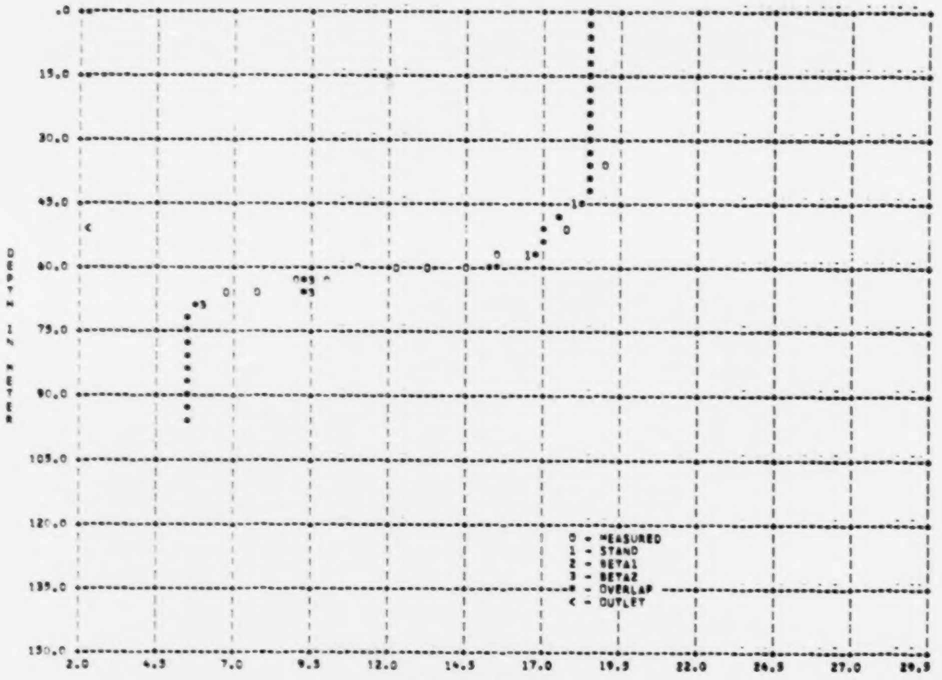

Figure 27 MIT MODEL * FONTANA RESERVOIR 1966--DAY:285 --SURFACE ELEV: 496.3 M

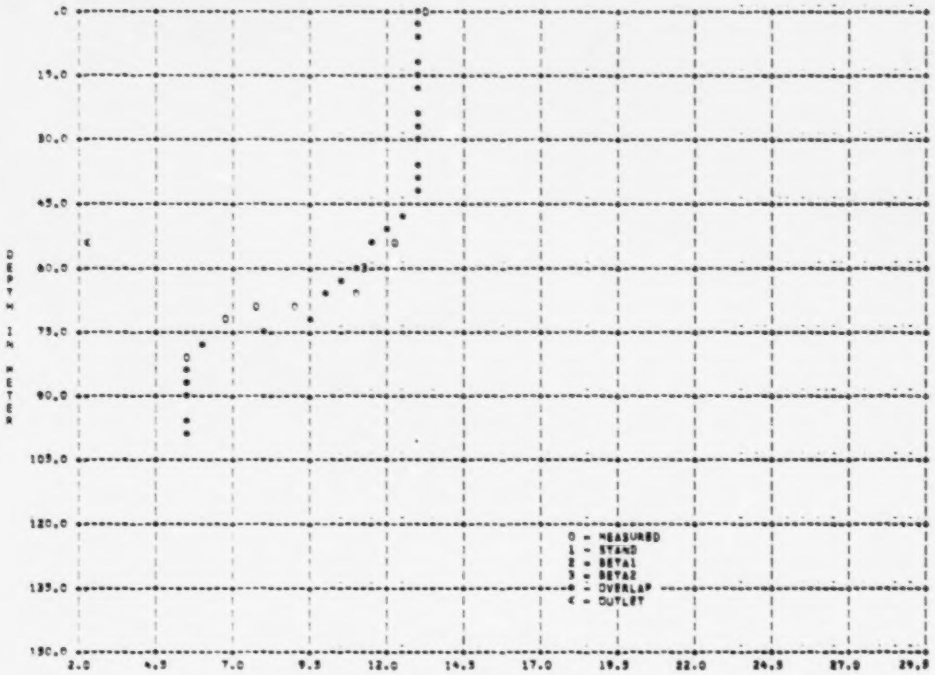

Figure 28 MIT MODEL * FONTANA RESERVOIR 1966--DAY:335 --SURFACE ELEV: 496.8 M

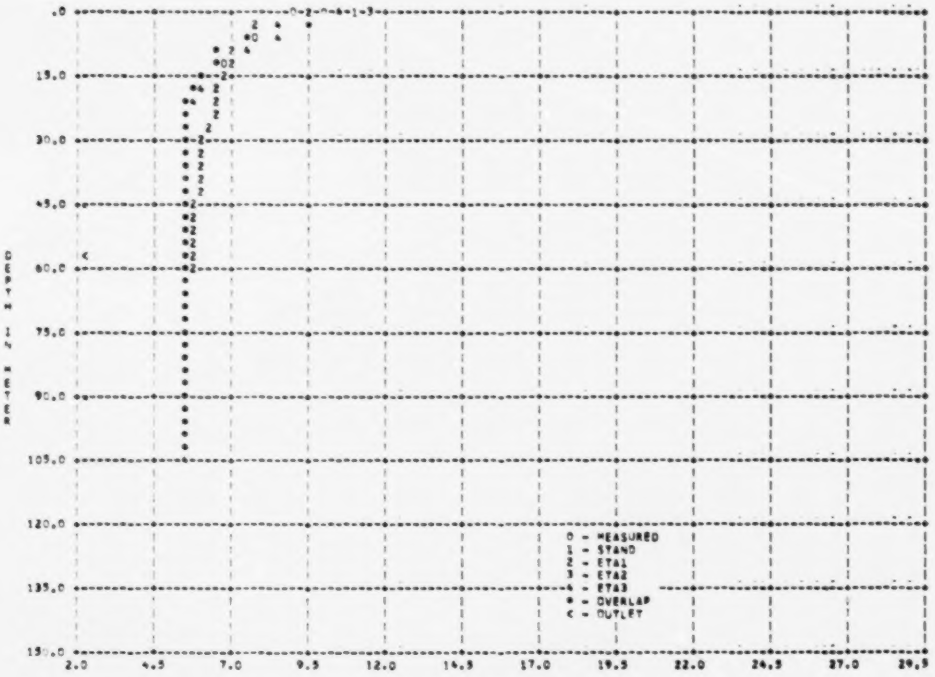

Figure 29 MIT MODEL * FONTANA RESERVOIR 1966--DAY: 75 --SURFACE ELEV: 500.3 M

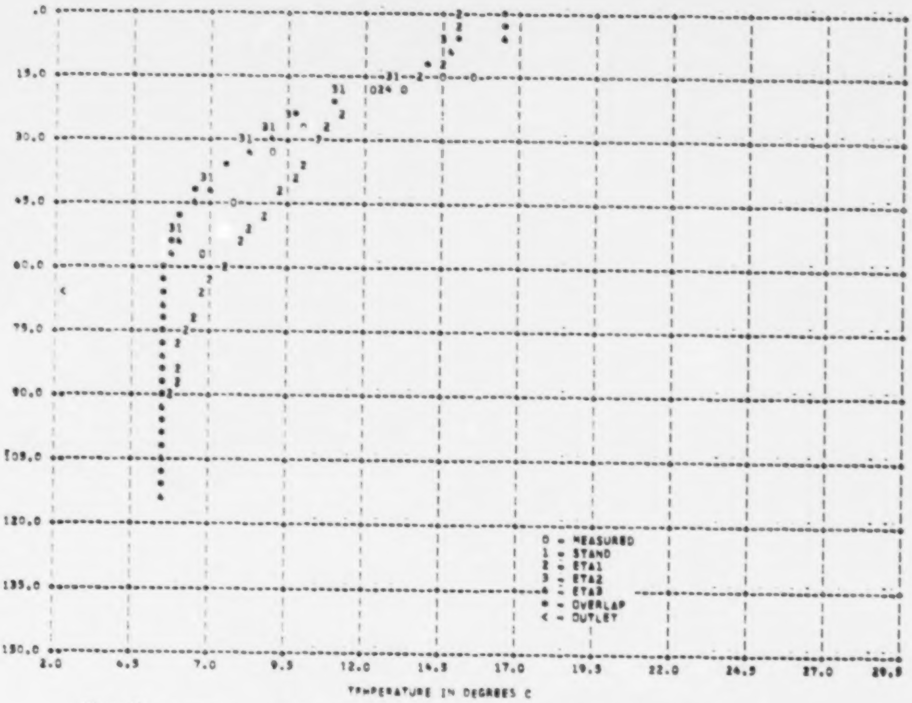

Figure 30 MIT MODEL * FONTANA RESERVOIR 1966--DAY:182 --SURFACE ELEV: 308.4 M

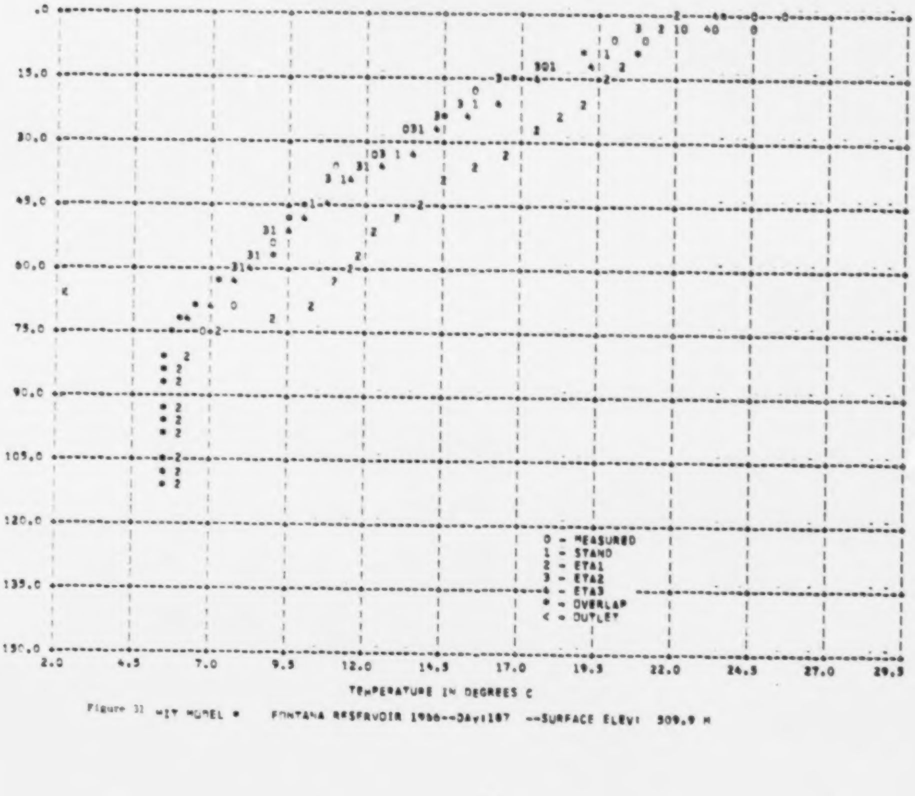

Figure 31 MIT MODEL * FONTANA RESERVOIR 1966--DAY:187 --SURFACE ELEV: 309.9 M

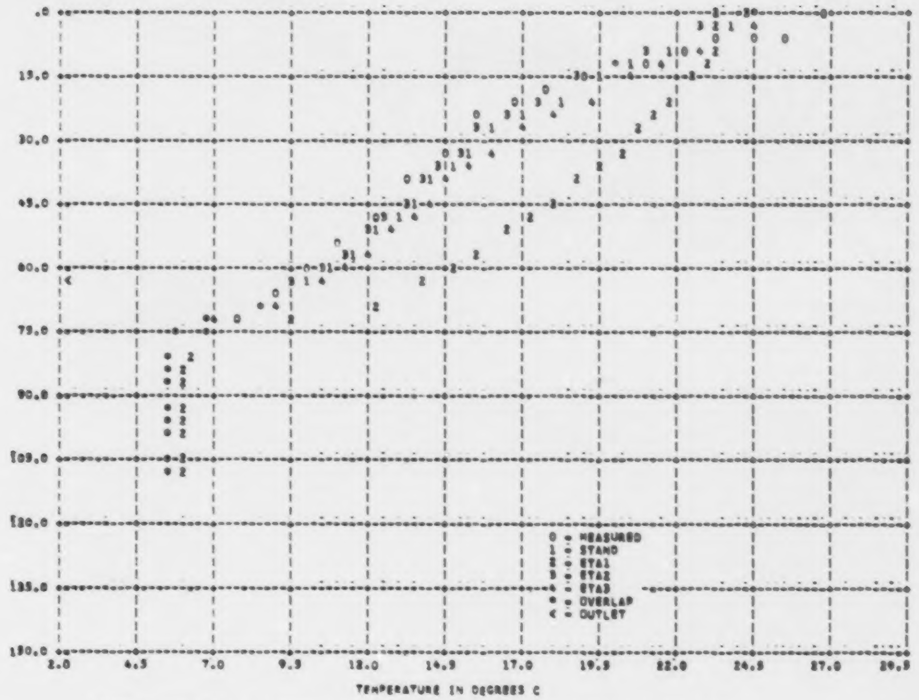

Figure 32 MIT MODEL * FONTANA RESERVOIR 1966--DAY:215 --SURFACE ELEV: 305.9 M

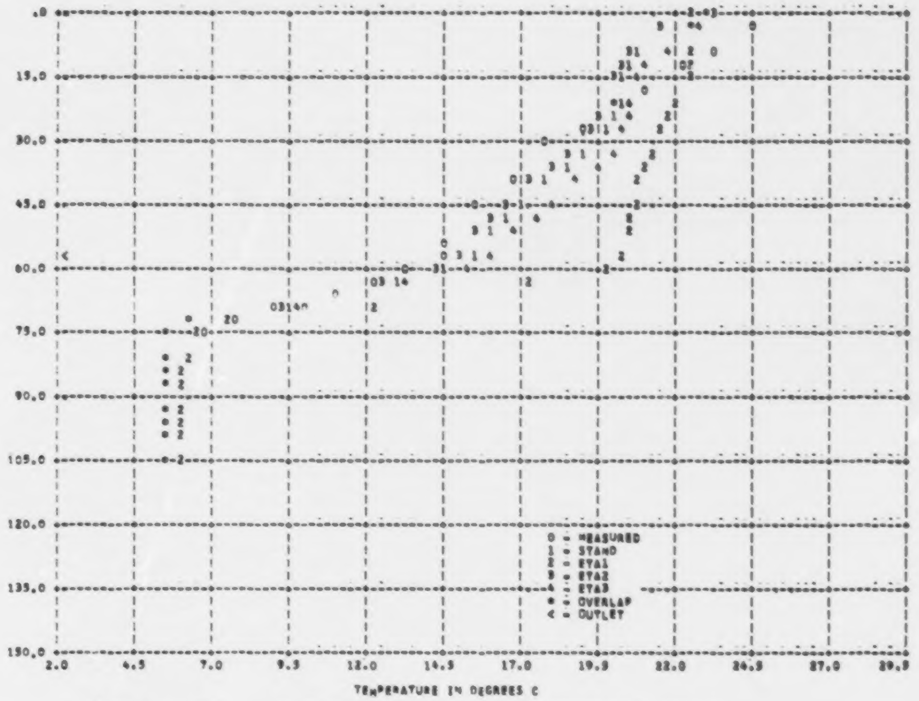

Figure 33 MIT MODEL * FONTANA RESERVOIR 1966--DAY:244 --SURFACE ELEV: 301.9 M

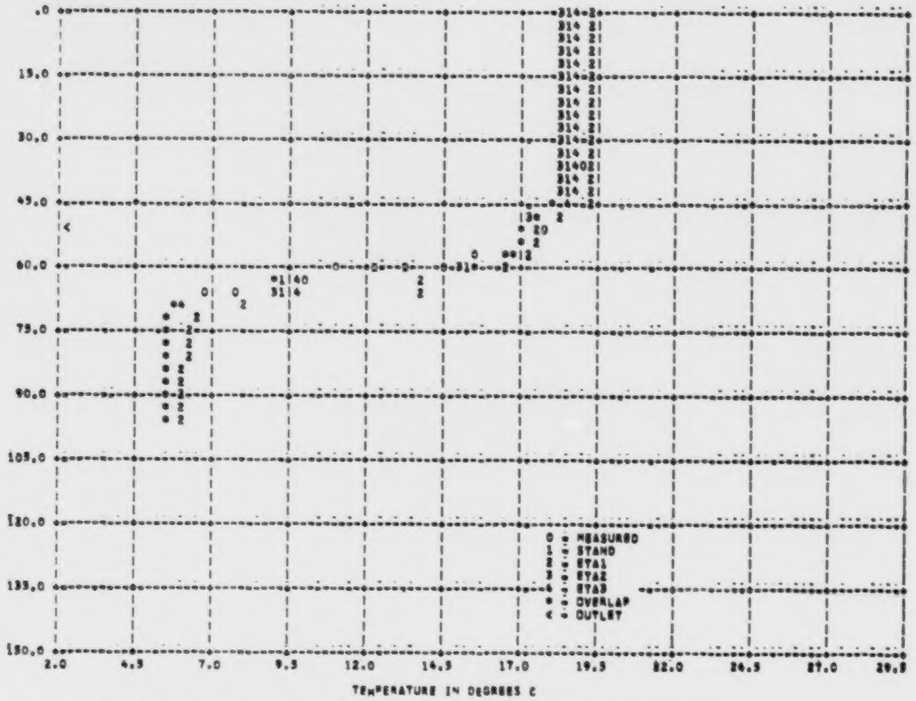

Figure 34 MIT MODEL * FONTANA RESERVOIR 1966--DAY:285 --SURFACE ELEV: 494.3 M

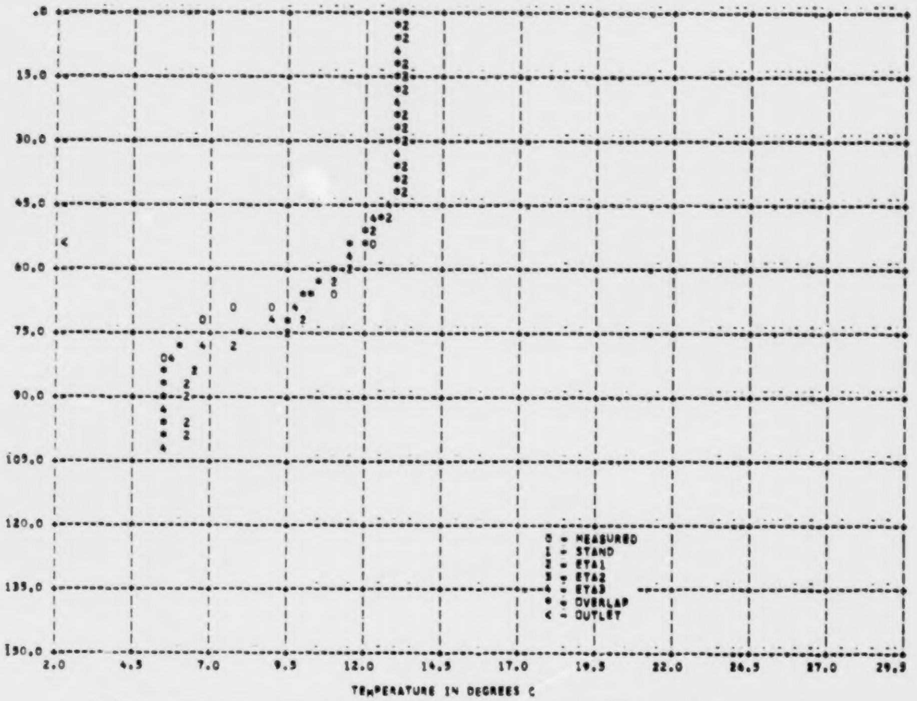

Figure 35 MIT MODEL * FONTANA RESERVOIR 1966--DAY:335 --SURFACE ELEV: 496.8 M

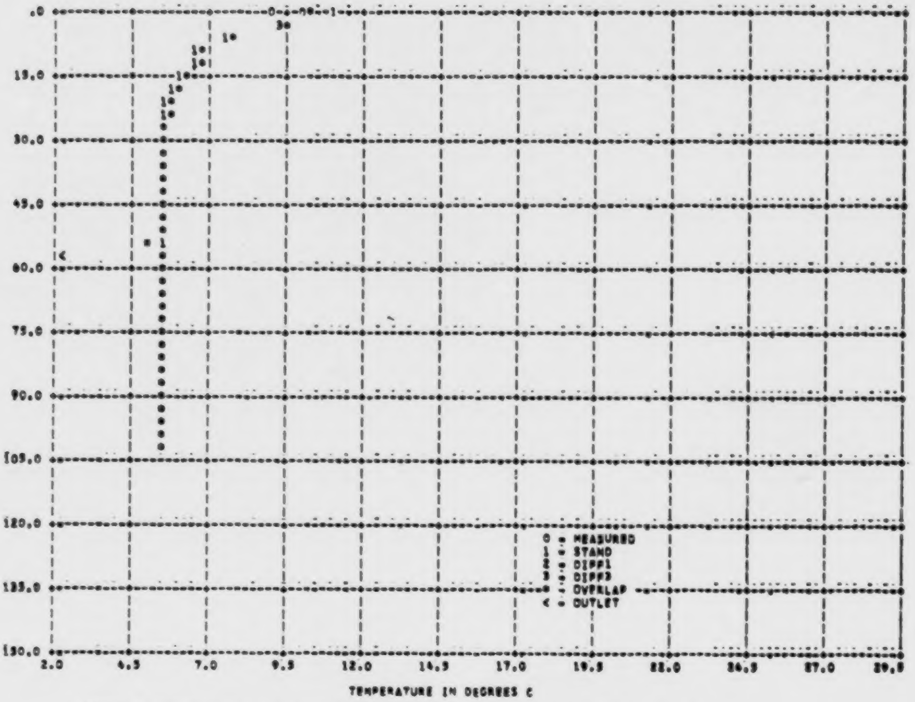

Figure 36 MIT MODEL * FONTANA RESERVOIR 1966--DAY: 75 *--SURFACE ELEV: 500.3 M

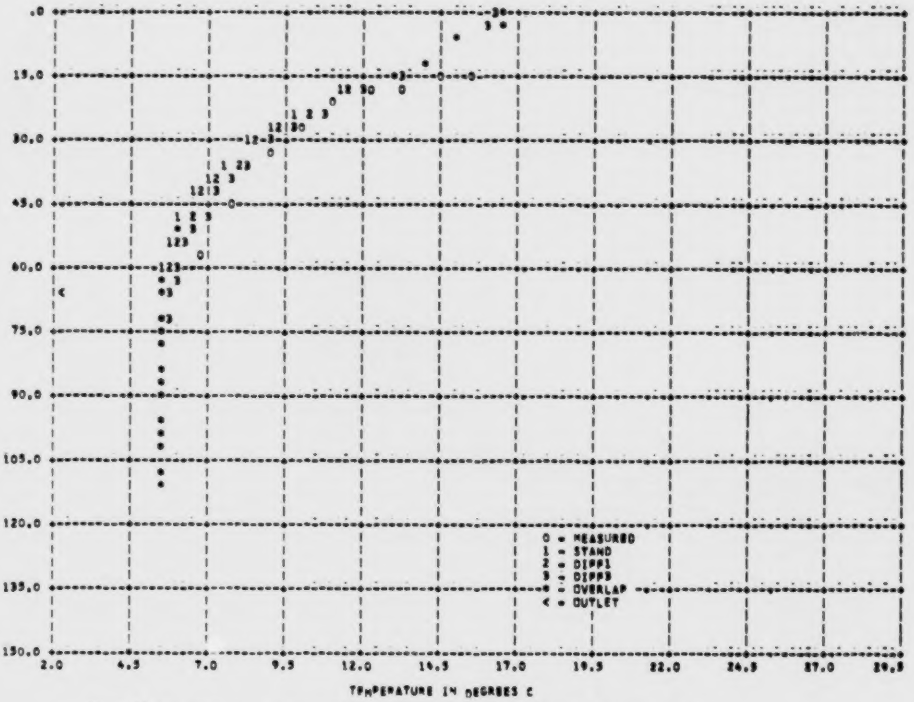

Figure 37 MIT MODEL * FONTANA RESERVOIR 1966--DAY:152 *--SURFACE ELEV: 508.4 M

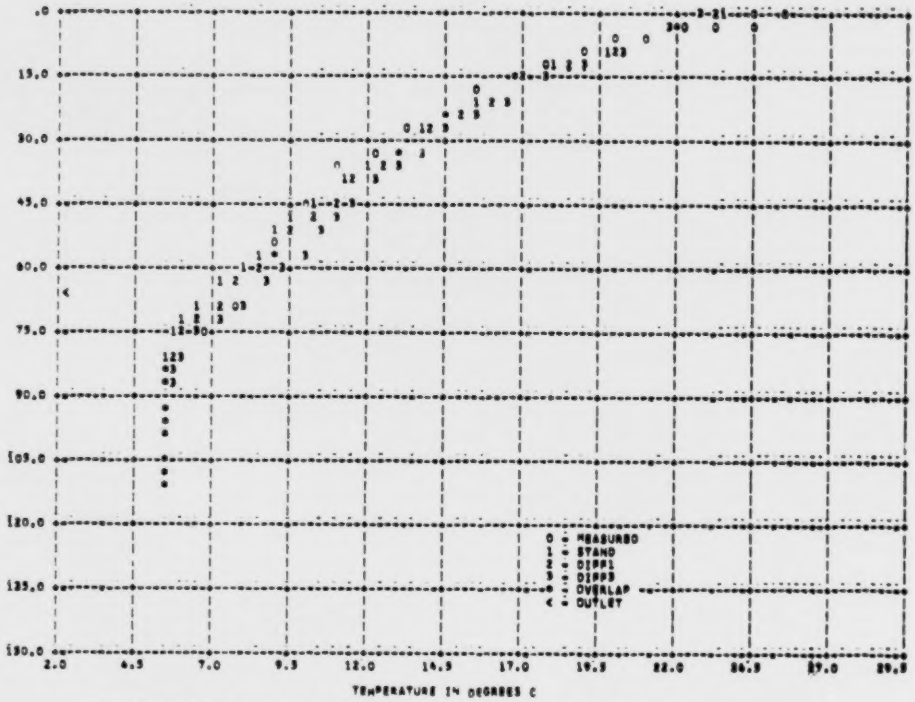

Figure 38 MIT MODEL * FONTANA RESERVOIR 1966--DAY:187 *--SURFACE ELEV: 509.9 M

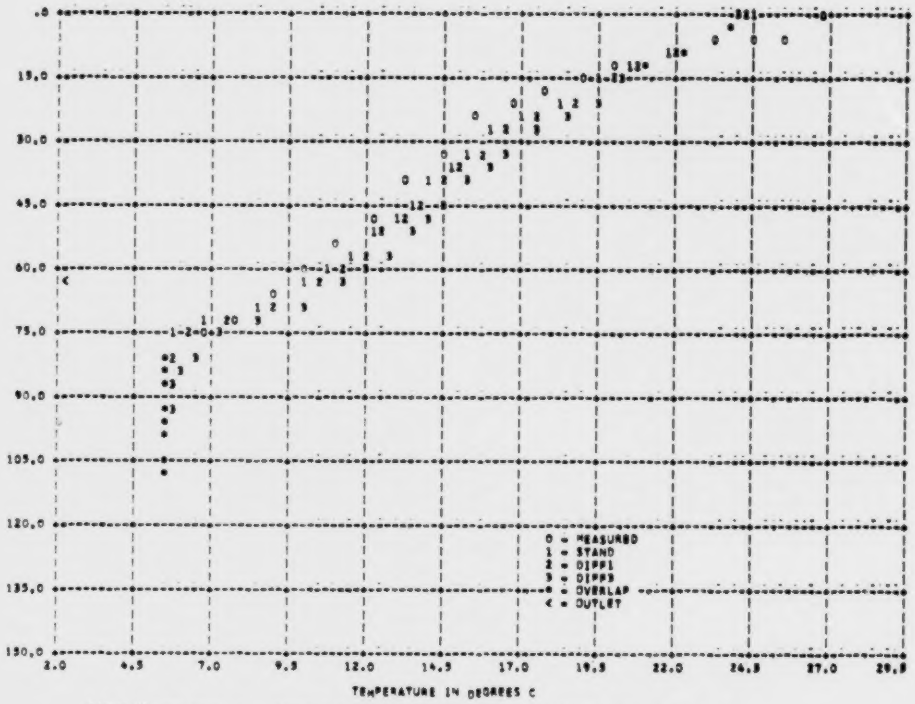

Figure 39 MIT MODEL * FONTANA RESERVOIR 1966--DAY:215 *--SURFACE ELEV: 505.9 M

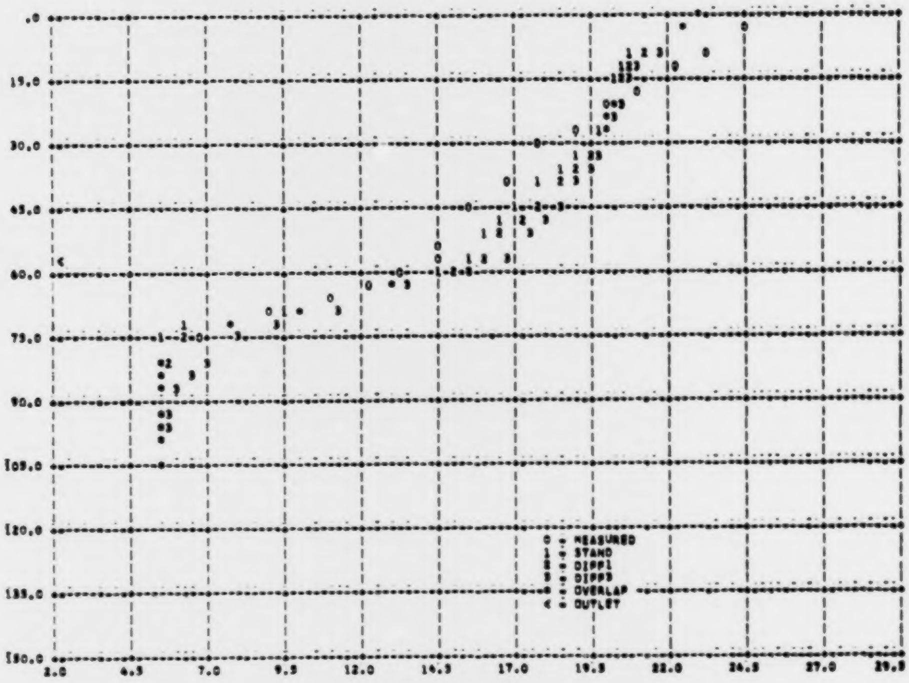

Figure 40 MIT MODEL * FONTANA RESERVOIR 1966--DAY:244 *--SURFACE ELEV: 501.9 M

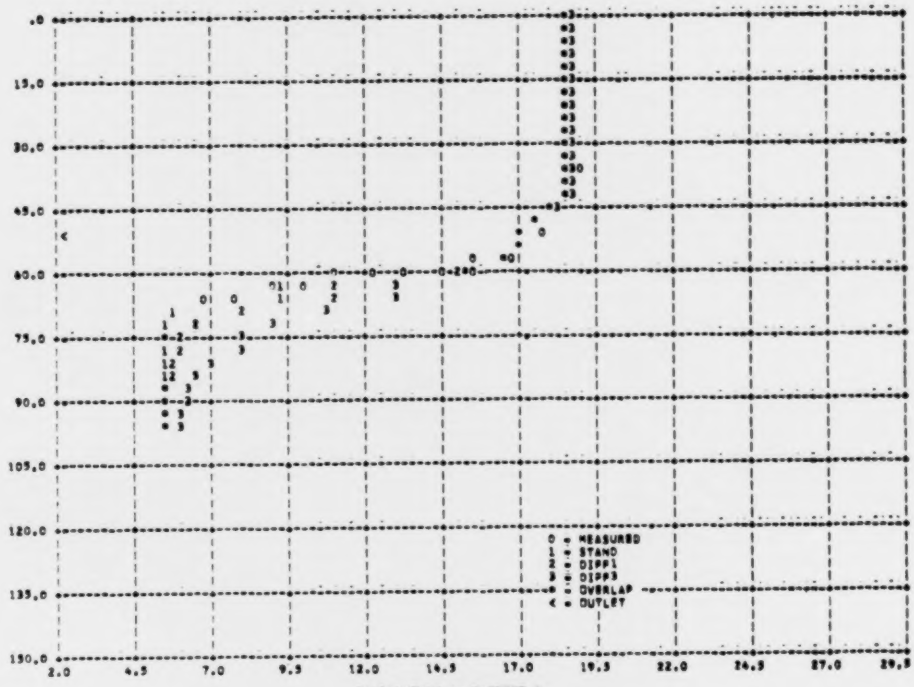

Figure 41 MIT MODEL * FONTANA RESERVOIR 1966--DAY:285 *--SURFACE ELEV: 494.3 M

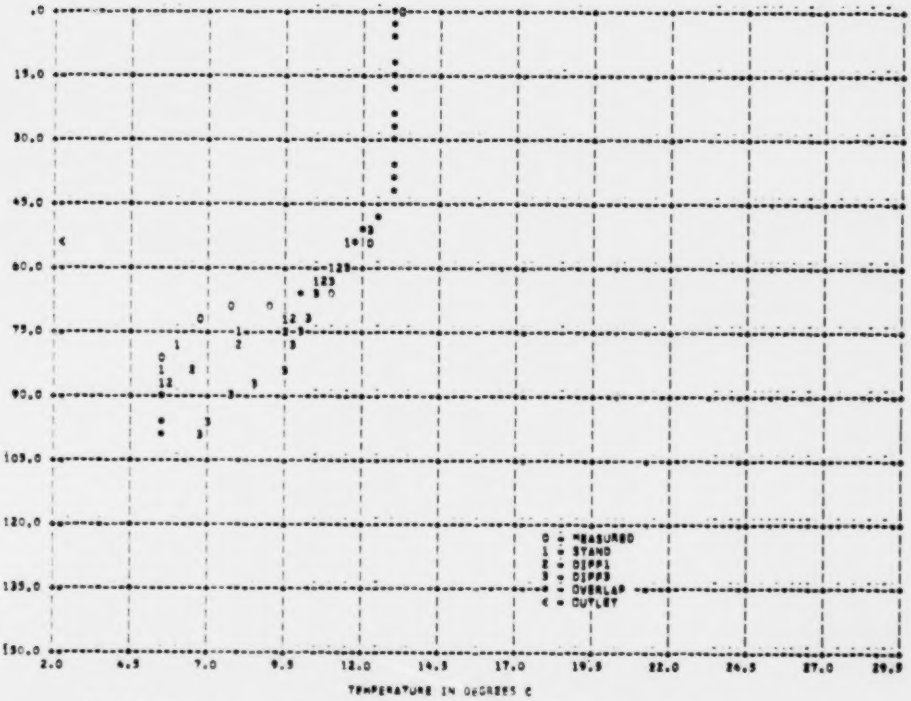

Figure 42 MIT MODEL * FONTANA RESERVOIR 1966--DAY:335 --SURFACE ELEV: 496.8 M

Douglas Reservoir

Figures 43 and 44 show the computed temperature data for Douglas Reservoir for 1969 at various depths and the computed outflow temperature. These can be compared with the measured data as shown in Figures 45 through 50. It can be seen from the Figures and as shown in Tables 10 and 11 that the predicted results, standard errors of estimate of 2.1° and 2.0° for outlet water temperatures and surface water temperature, respectively, are not as good as they were for Fontana Reservoir. In Figures 45 to 50 it can also be seen that, the variation in the horizontal increments from 1 to 3 meters makes a random difference in the predicted results, with 3 meters giving better results on day 121 and 1 meter giving better results on day 186. Overall, as shown in the statistical analysis in Tables 10 and 11, the change in thickness in the horizontal segments makes little difference. In Figures 51 to 56 the effect of a change in β, the fraction of solar radiation absorbed at the water surface, from 0.20 to 0.5 has a negligible effect on the predicted temperature. As shown in the discussion on the variation of the horizontal segments, the predicted values vary randomly both greater and less than the measured values. Over the whole year, however, the variation in the predicted values do not differ markedly from the standard errors of estimate as shown in Tables 10 and 11.

In Figures 57 to 62, the effect of a variation in η, the radiation absorption coefficient from 0.05 to 1.40 is shown. While there are slight differences from each other in the predicted temperatures when η of 0.75 and 1.40 are used, there is a very large difference from the other predicted temperature and the measured temperature when an η of 0.05 is used. This is also verified by the statistical analysis reported in Tables 10 and 11, where the standard error of estimate for an η of 0.05 is twice the standard error of estimate for the water temperature at the outlet level for the other eta values.

In Figures 63 to 68 the effects of a variation in the diffusion coefficient from molecular diffusion to 100 times molecular diffusion is shown. It can be seen that 100 times molecular diffusion generally gives poor results and only on day 121 does 30 times molecular diffusion give predicted temperature results closer to the measured values than does molecular diffusion. It can be seen from Table 10 and 11 that overall 30 times molecular diffusion predicts similar temperatures to those predicted using molecular diffusion and that using 100 times molecular diffusion gives measurably worse results.

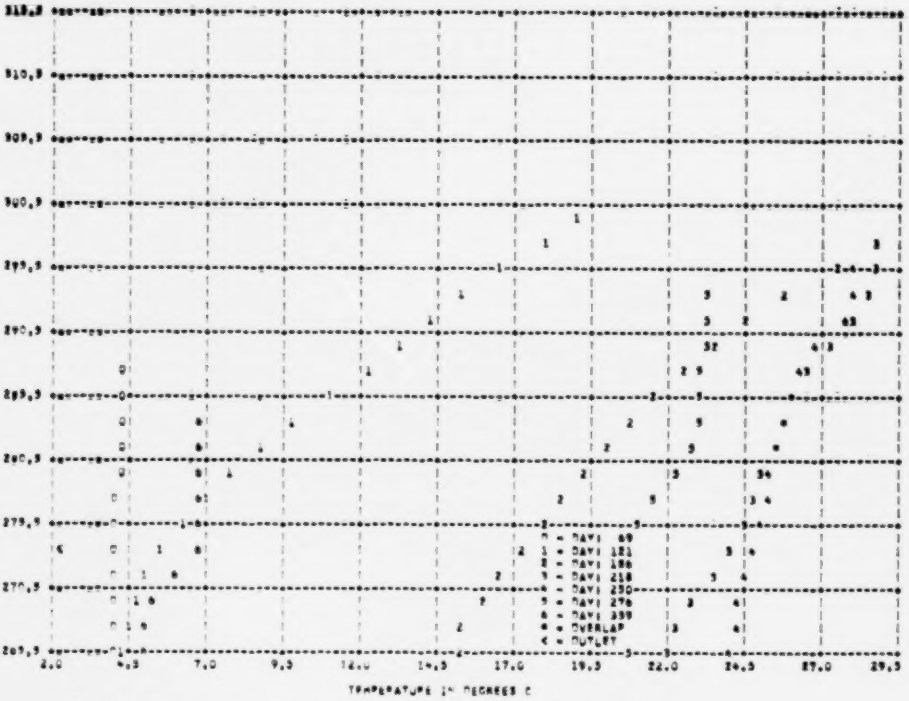

Figure 43 MIT MODEL * DOUGLAS RESERVOIR 1969--COMPUTED TEMPERATURE PROFILE--

TABLE 10

STATISTICAL ANALYSIS FOR THE PREDICTED WATER TEMPERATURE AT OUTLET LEVEL

Reservoir/Year: Douglas/1969

Time period covered: 120th - 330th Julian Day

File Name	Std. error of estimate (°c)	Correlation coefficient
STAND	2.11	0.95
DELZ 1	2.23	0.94
DELZ 2	2.07	0.95
BETA 1	2.11	0.94
BETA 2	2.15	0.95
ETA 1	5.73	0.28
ETA 2	2.28	0.94
ETA 3	2.12	0.94
DIFF 1	2.09	0.94
DIFF 3	4.97	0.63

TABLE 11

STATISTICAL ANALYSIS FOR THE PREDICTED SURFACE WATER TEMPERATURE

Reservoir/Year: Douglas/1969

Time Period Covered: 60th - 360 Julian Day

File Name	Std. error of estimate (°C)	Correlation Coefficient
STAND	2.03	0.98
DELZ 1	2.05	0.98
DELZ 2	2.07	0.98
BETA 1	1.97	0.98
BETA 2	1.88	0.98
ETA 1	2.26	0.97
ETA 2	2.22	0.97
ETA 3	2.13	0.98
DIFF 1	1.98	0.98
DIFF 3	blows up	

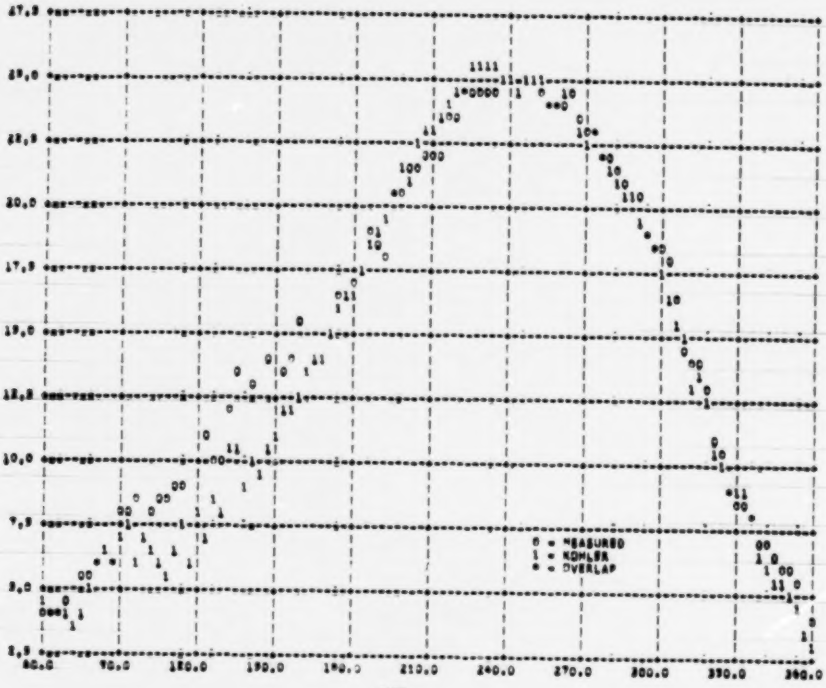

Figure 44 MIT MODEL I DOUGLAS RESERVOIR 1969--COMPUTED OUTFLOW TEMPERATURE--

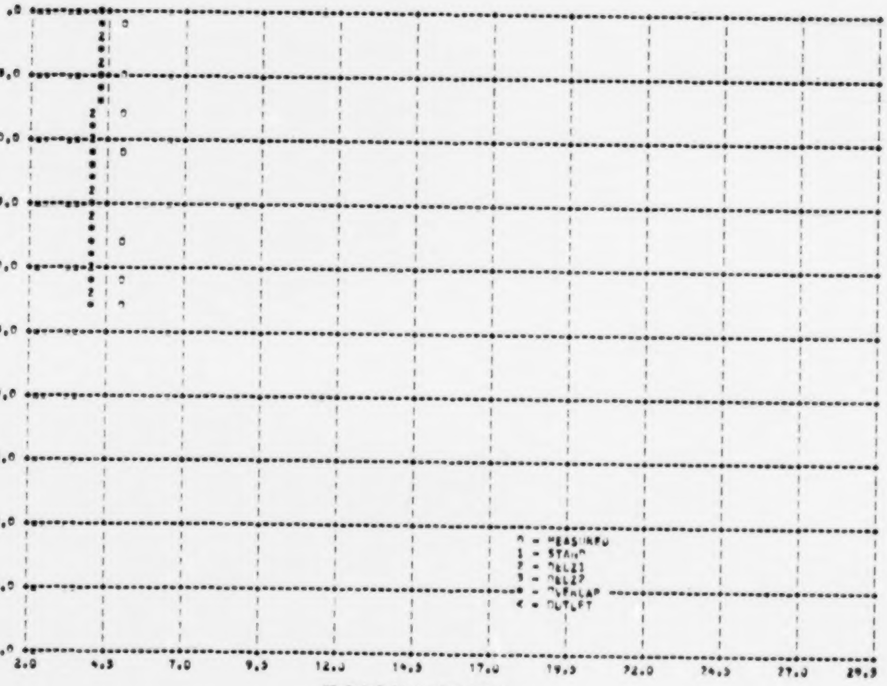

Figure 45 MIT MODEL II DOUGLAS RESERVOIR 1969--DAY: 89 --SURFACE ELEV

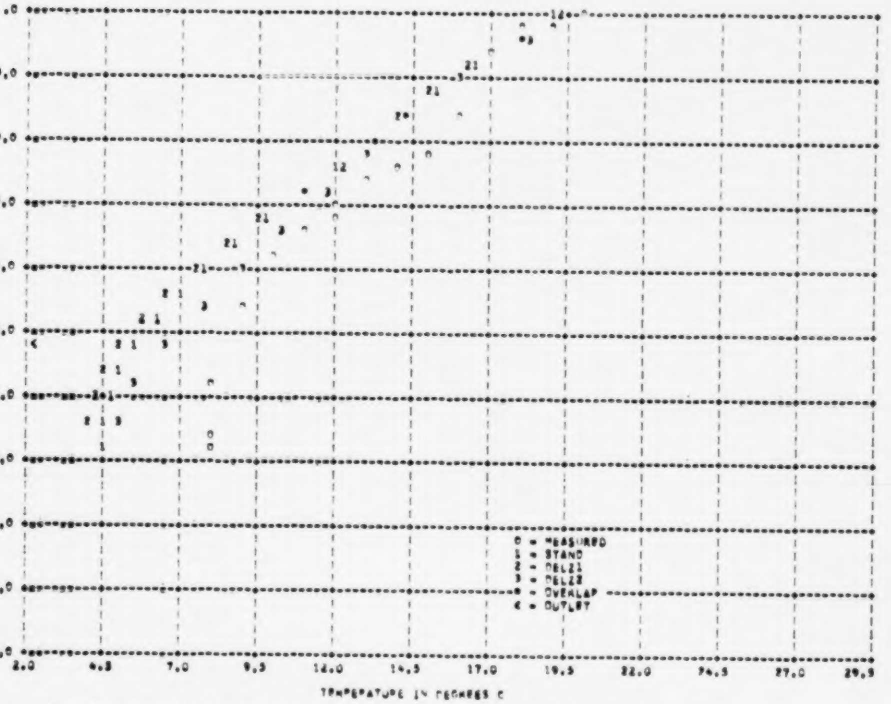

Figure 46 MIT MODEL * DWORSHAK RESERVOIR 1959--DAY:171 --SURFACE ELEV: 299.0 M

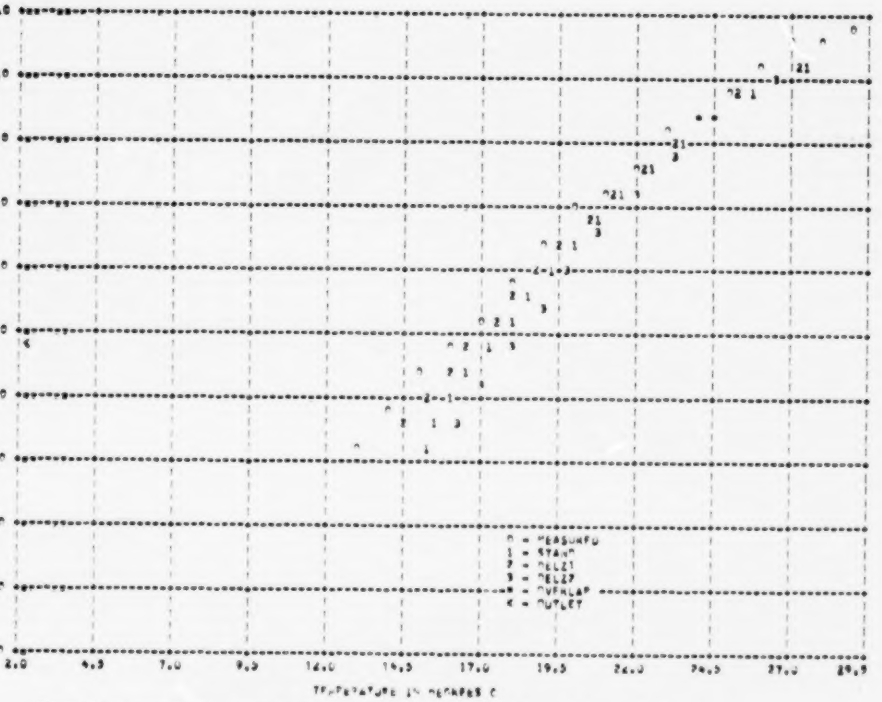

Figure 47 MIT MODEL * DWORSHAK RESERVOIR 1959--DAY:186 --SURFACE ELEV: 293.9 M

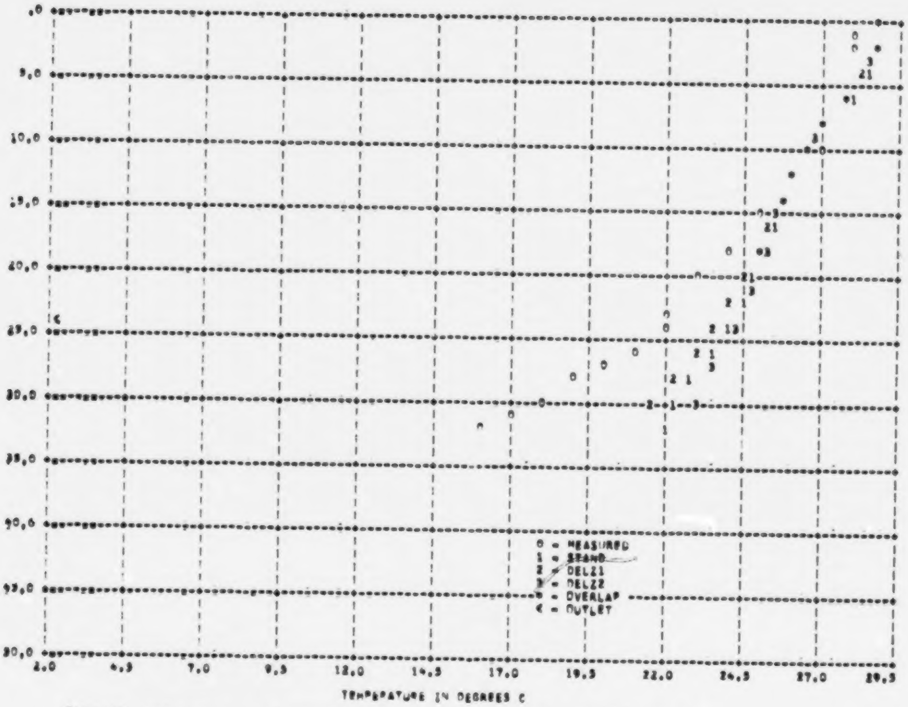

Figure 48 MIT MODEL * DOUGLAS RESERVOIR 1969--DAY1216 --SURFACE ELEV: 297.7 M

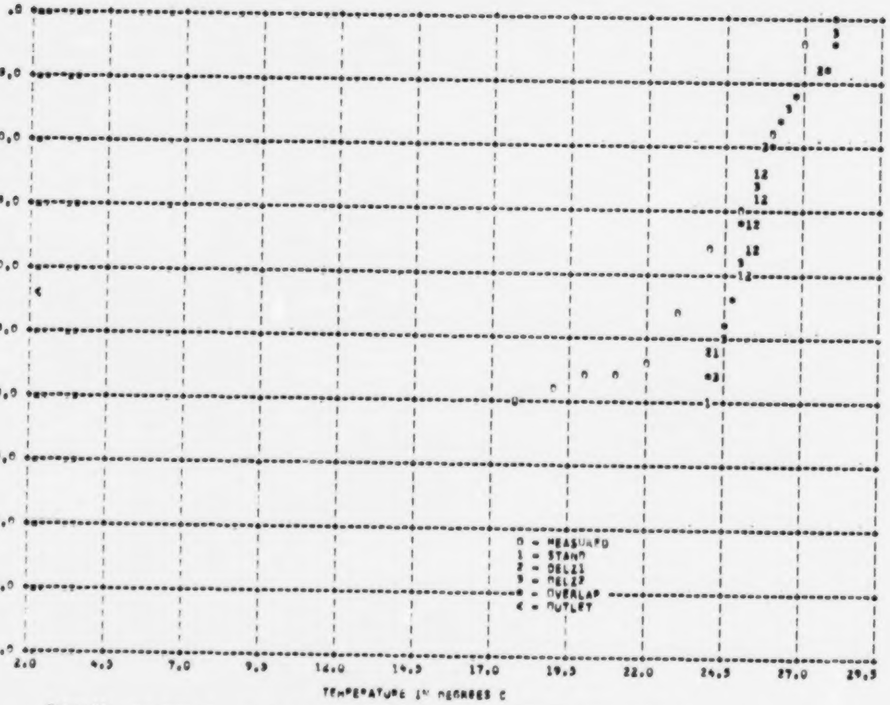

Figure 49 MIT MODEL * DOUGLAS RESERVOIR 1969--DAY1230 --SURFACE ELEV: 295.8 M

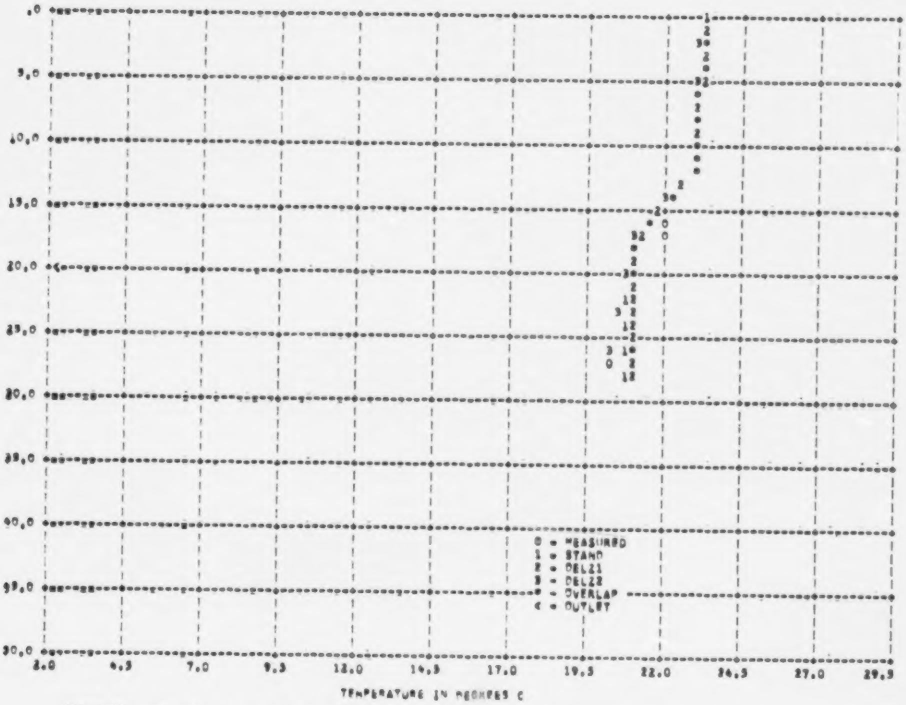

Figure 50 MIT MODEL • DOUGLAS RESERVOIR 1969--DAY: 276 --SURFACE ELEV: 293.3 M

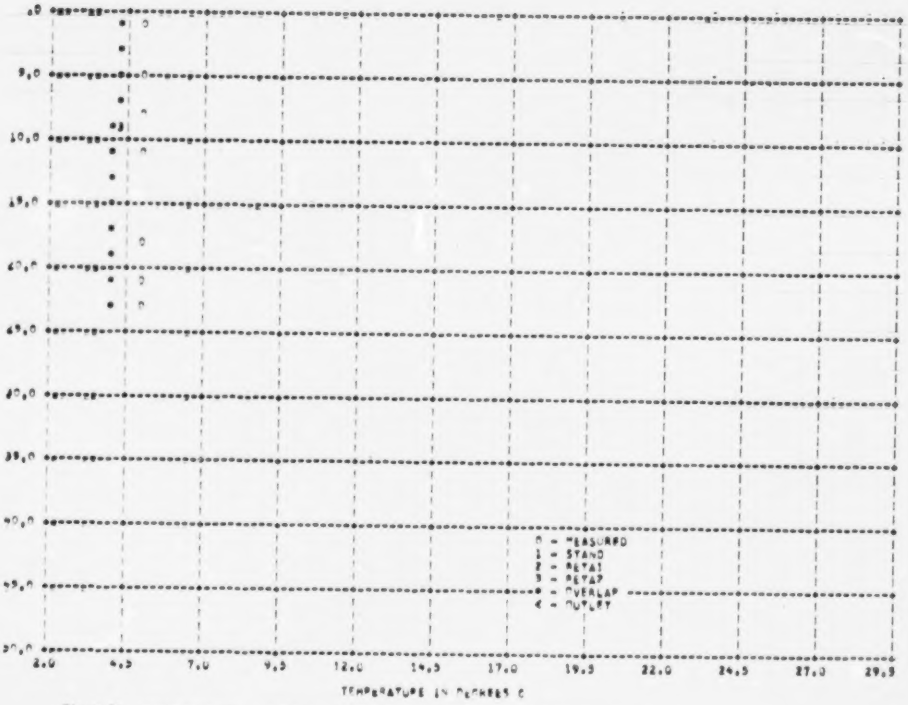

Figure 51 MIT MODEL • DOUGLAS RESERVOIR 1969--DAY: 89 --SURFACE ELEV:

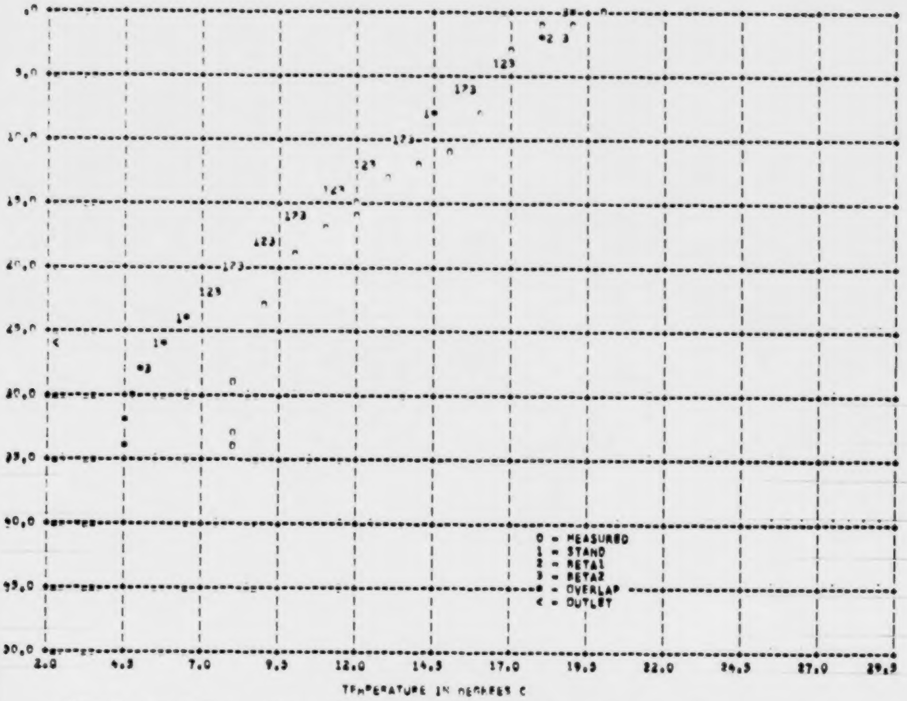

Figure 52 MIT MODEL * DOUGLAS RESERVOIR 1959--DAY121 --SURFACE ELEV: 299.8 M

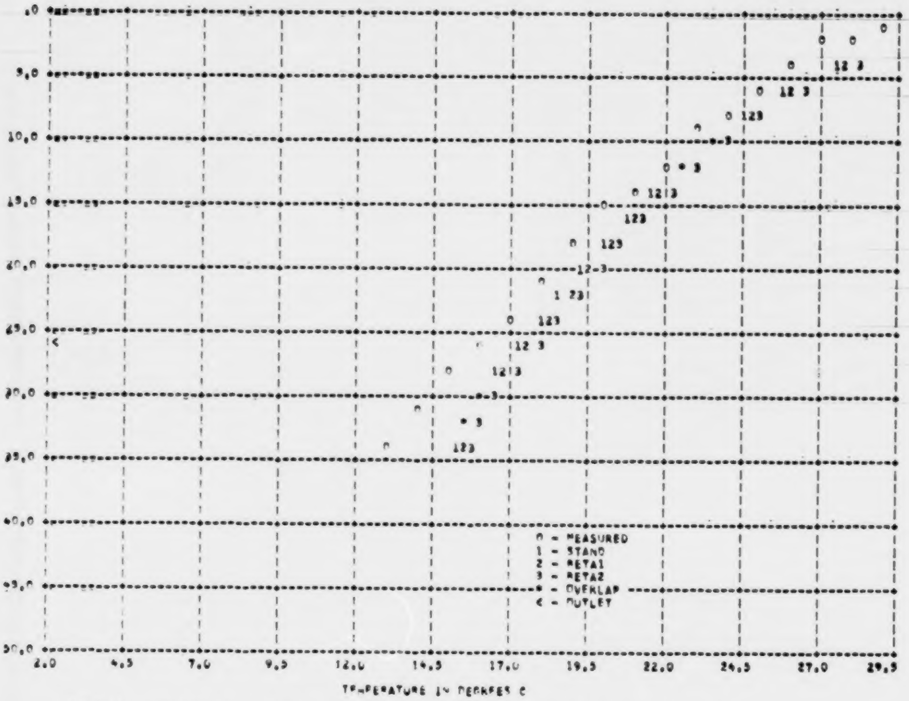

Figure 53 MIT MODEL * DOUGLAS RESERVOIR 1959--DAY186 --SURFACE ELEV: 299.9 M

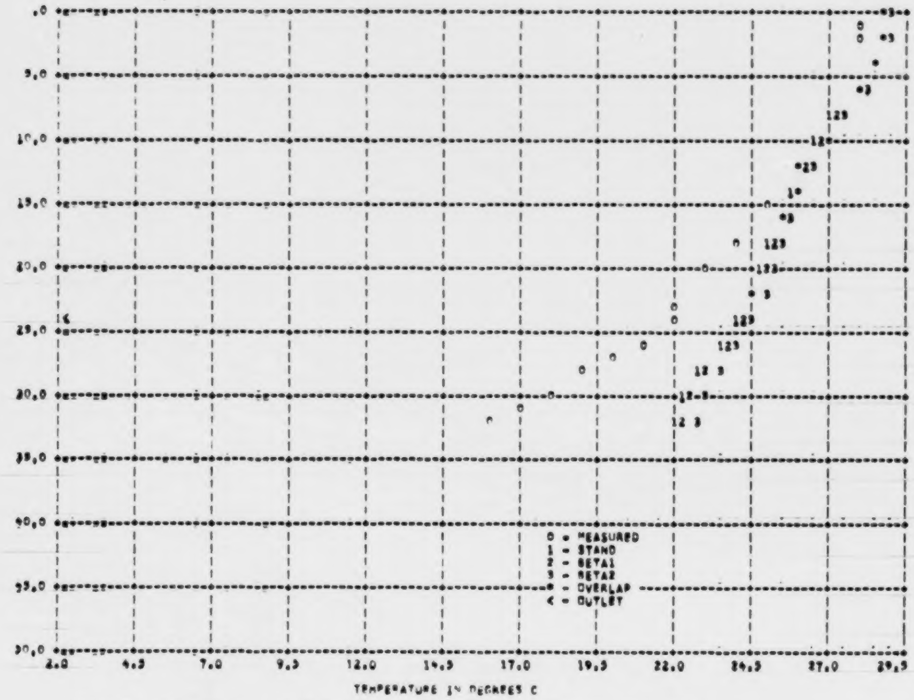

Figure 54 MIT MODEL * DOUGLAS RESERVOIR 1969--DAY:218 --SURFACE ELEV: 297.7 M

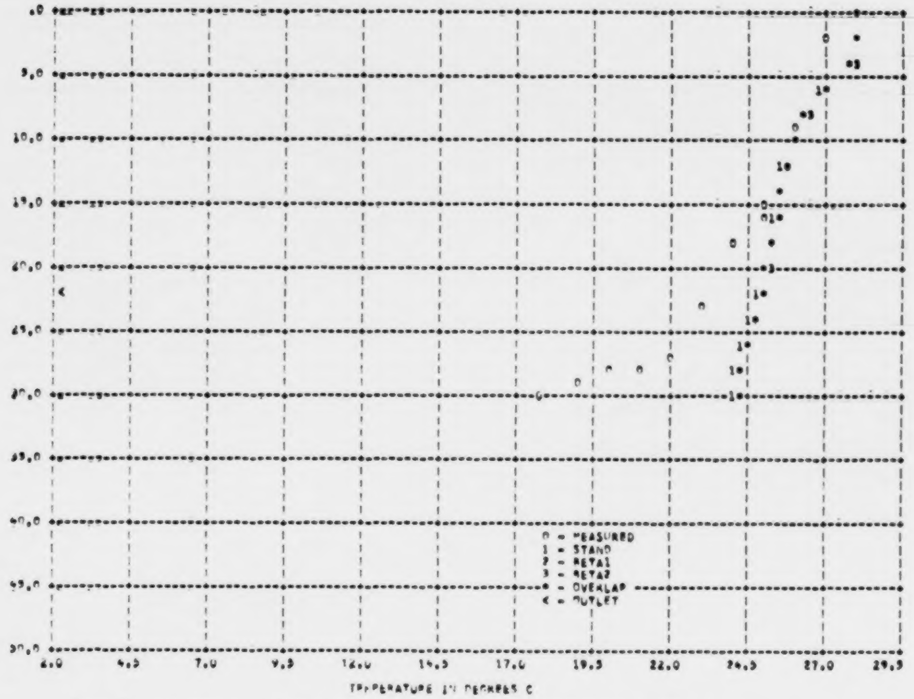

Figure 55 MIT MODEL * DOUGLAS RESERVOIR 1969--DAY:250 --SURFACE ELEV: 295.6 M

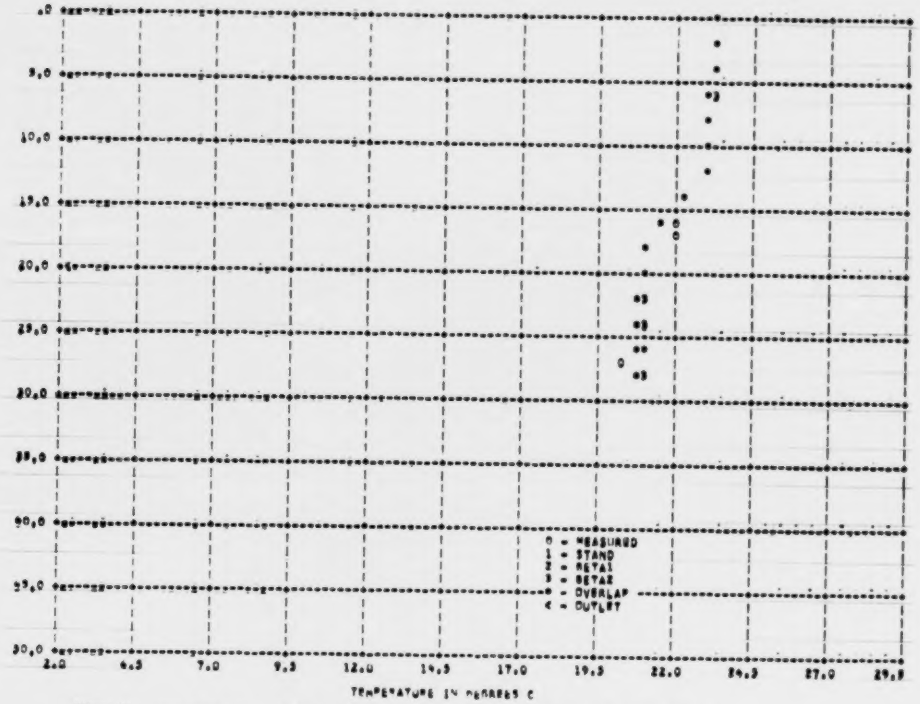

Figure 56 MIT MODEL — DOUGLAS RESERVOIR 1969--DAY 276 --SURFACE ELEV: 293.3 M

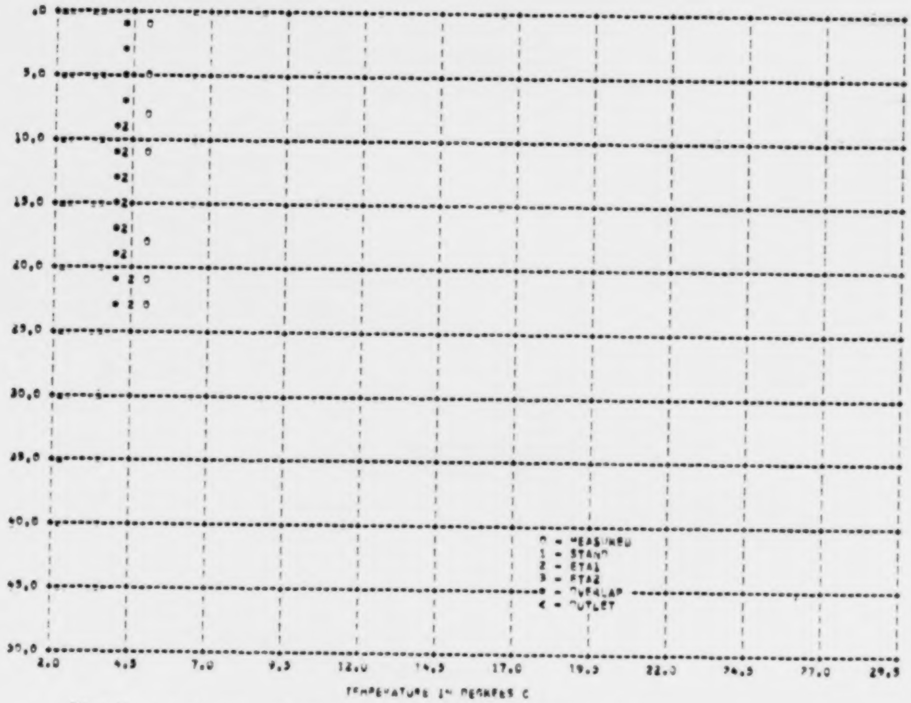

Figure 57 MIT MODEL — DOUGLAS RESERVOIR 1969--DAY [illegible] --SURFACE ELEV:

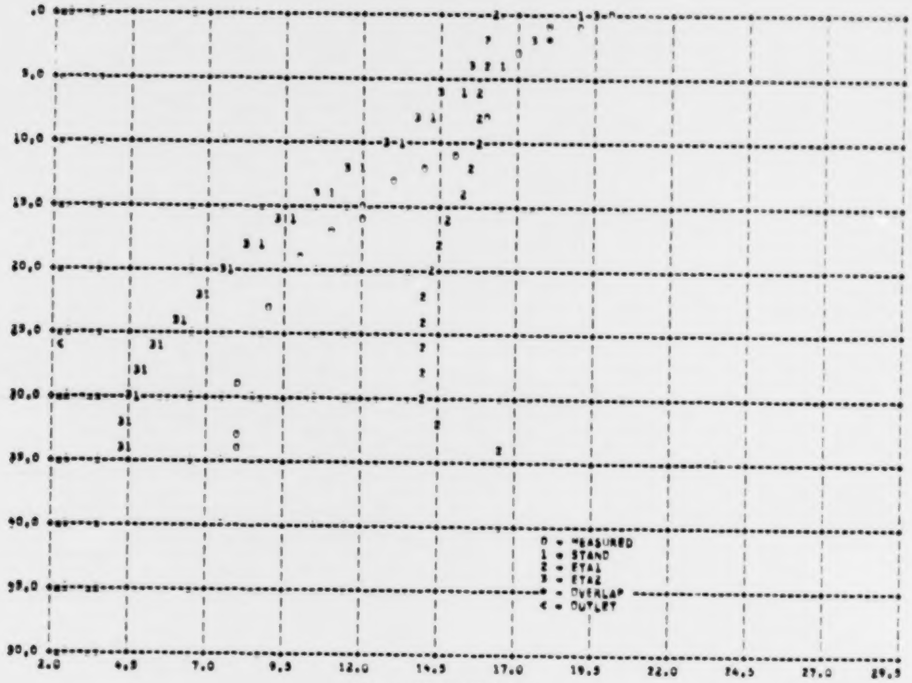

Figure 58 MIT MODEL - DWORSHAK RESERVOIR 1979--DAY121 --SURFACE ELEV 489.8 M

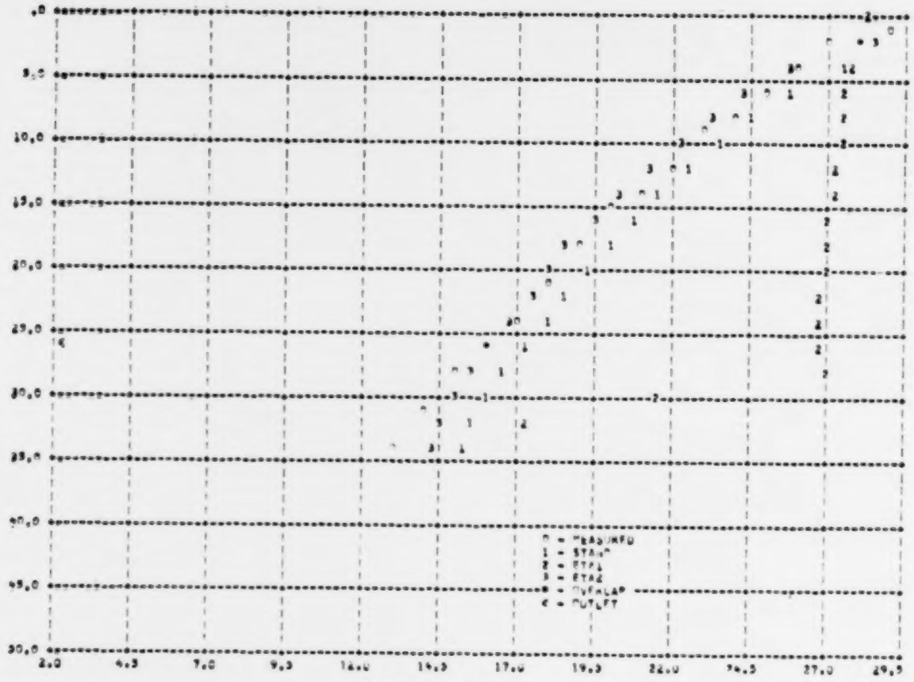

Figure 59 MIT MODEL - DWORSHAK RESERVOIR 1979--DAY128 --SURFACE ELEV 489.9 M

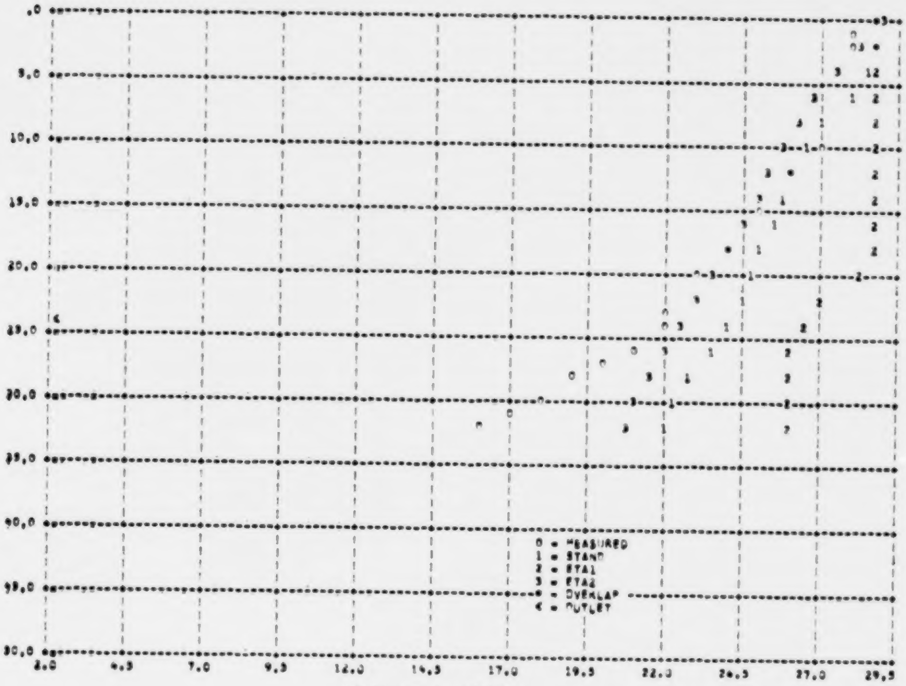

Figure 60 MIT MODEL • DOUGLAS RESERVOIR 1959--DAY 218 --SURFACE ELEV: 297.7 M

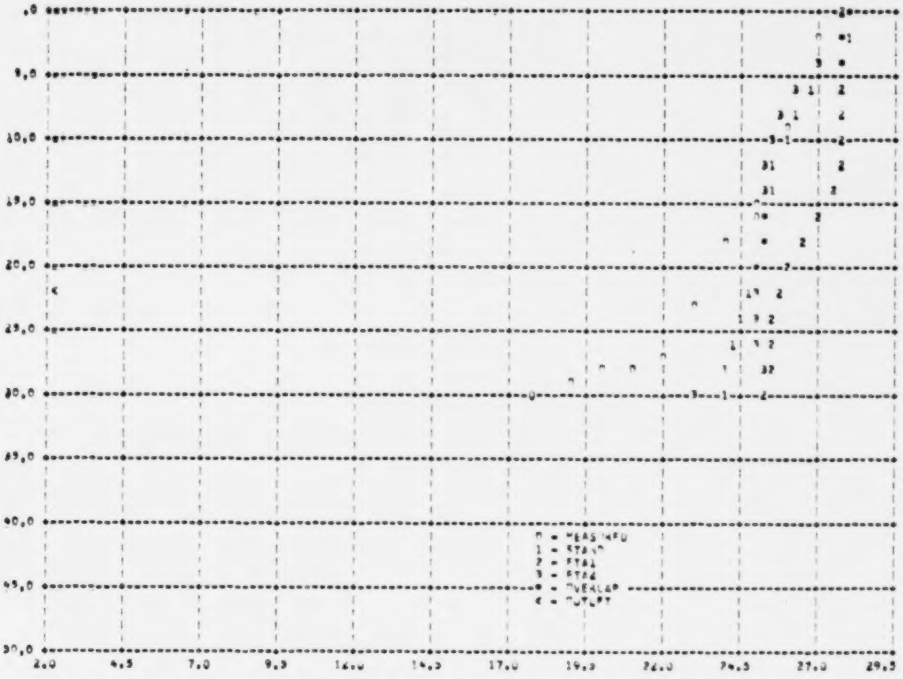

Figure 61 MIT MODEL • DOUGLAS RESERVOIR 1959--DAY 250 --SURFACE ELEV: 295.8 M

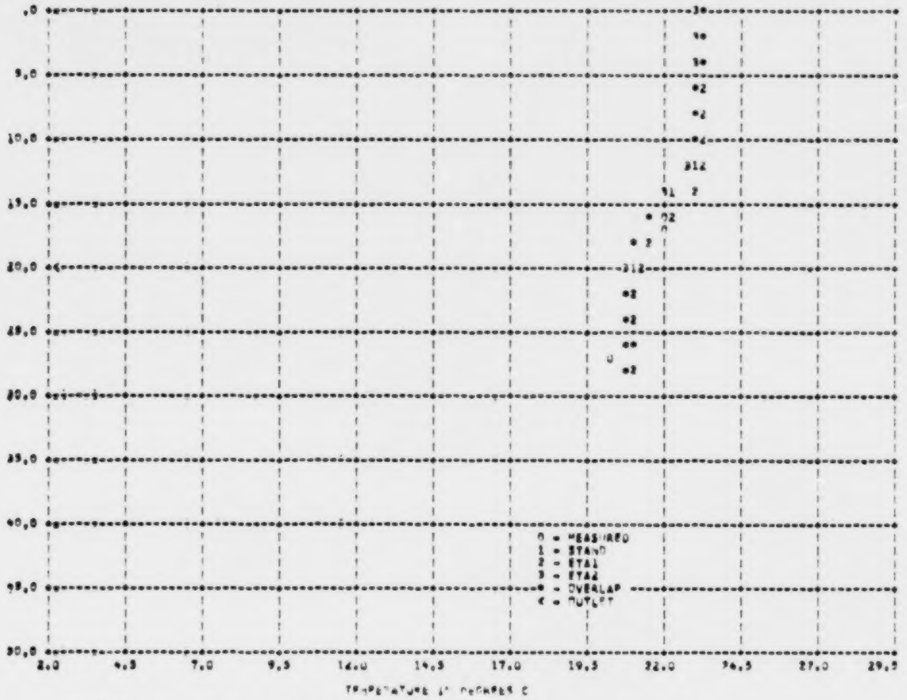

Figure 62 MIT MODEL * [illegible] 1979--JULY 27 --SURFACE ELEV. 203.3 m

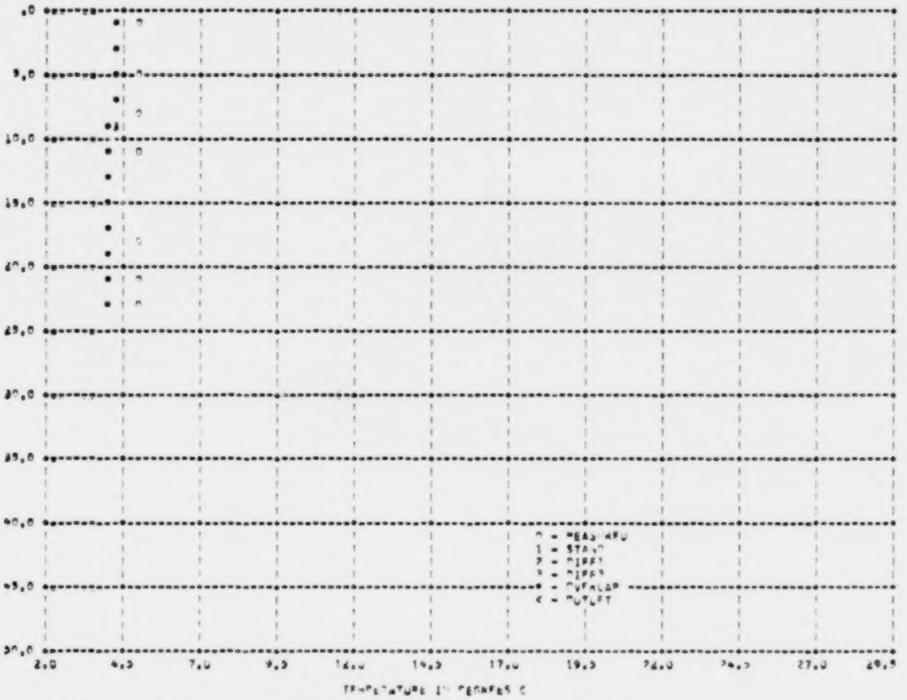

Figure 61 MIT MODEL * [illegible] 1979--[illegible] --SURFACE ELEV.

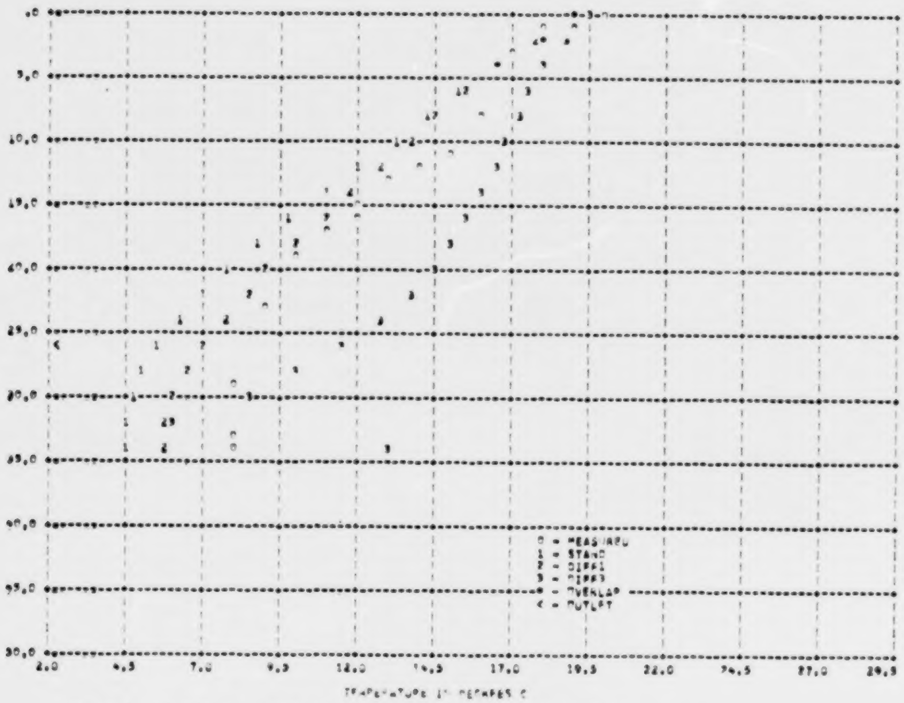

Figure 64 MIT MODEL • [illegible] RESERVOIR 1959--[illegible] --SURFACE ELEV: [illegible]

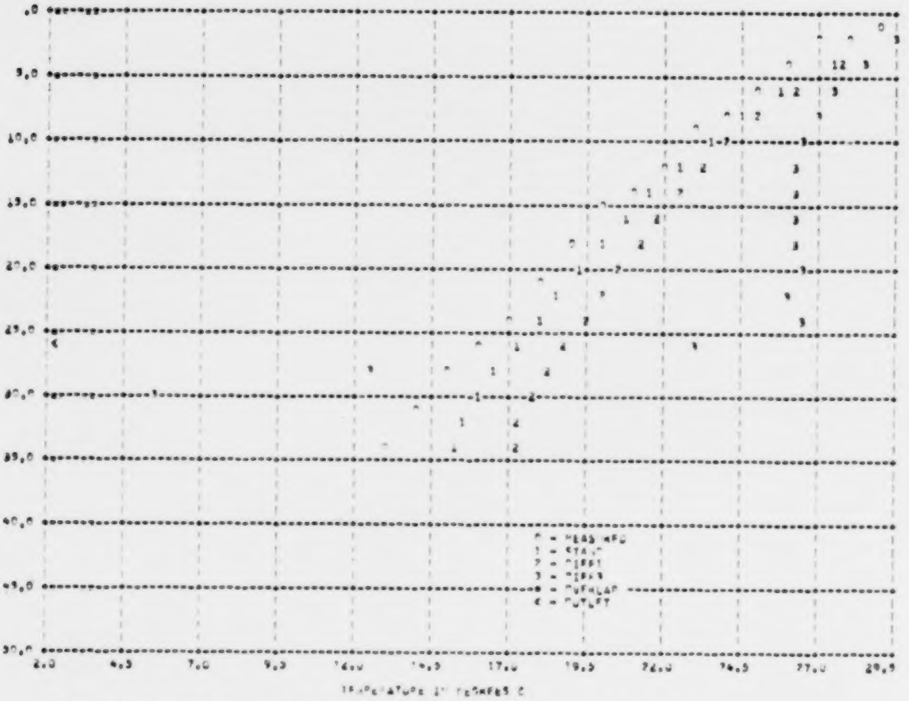

Figure 65 MIT MODEL • [illegible] RESERVOIR 1959--[illegible] --SURFACE ELEV: [illegible]

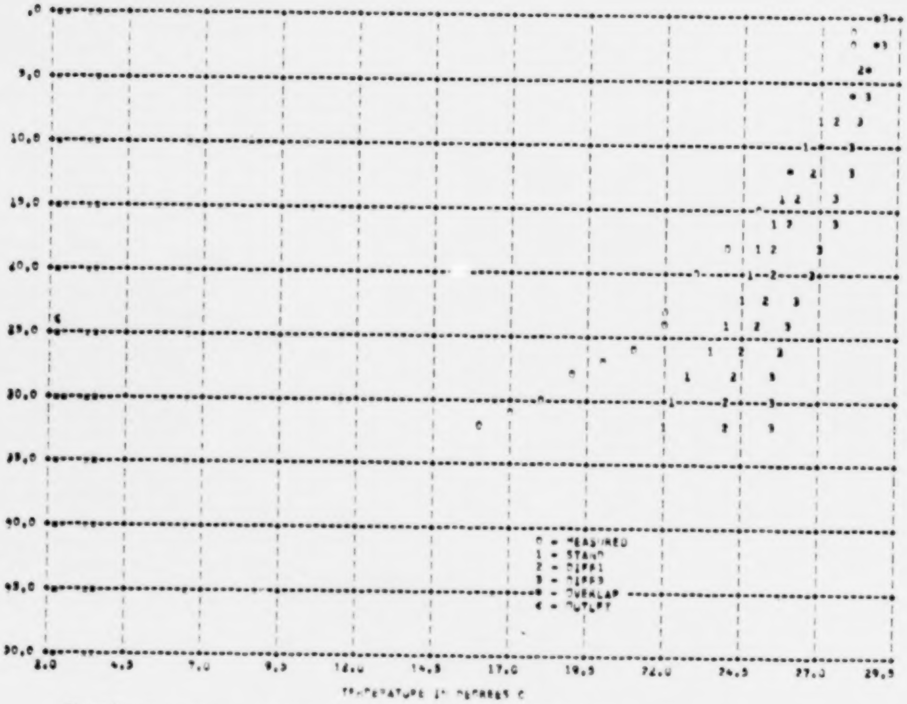

Figure 66 MIT MODEL - DWORSHAK RESERVOIR 1959--DAY 218 --SURFACE ELEV 487.7 M

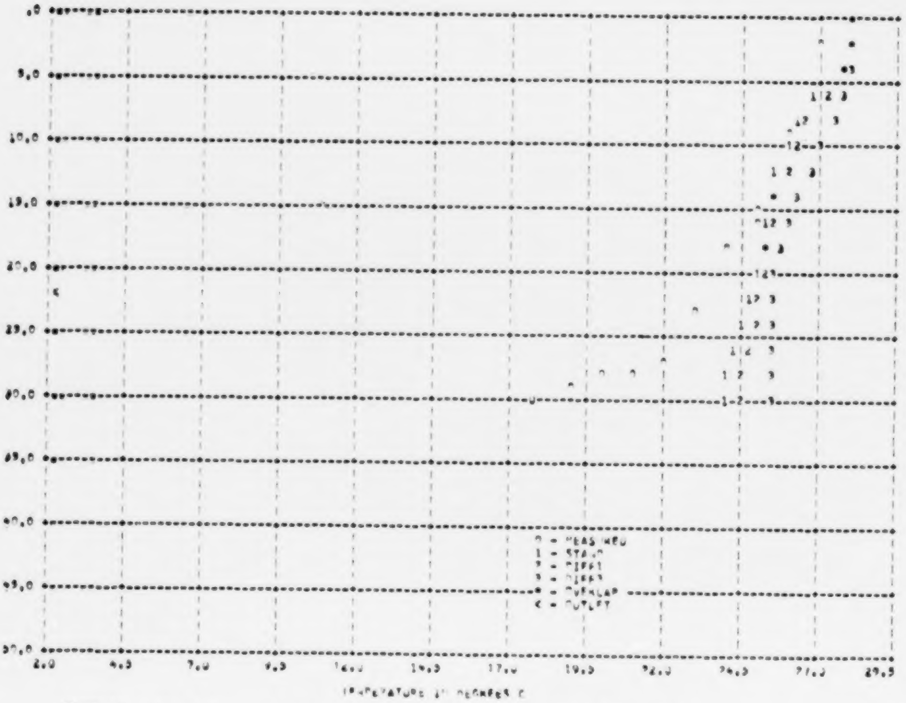

Figure 67 MIT MODEL - DWORSHAK RESERVOIR 1959--DAY 250 --SURFACE ELEV 485.0 M

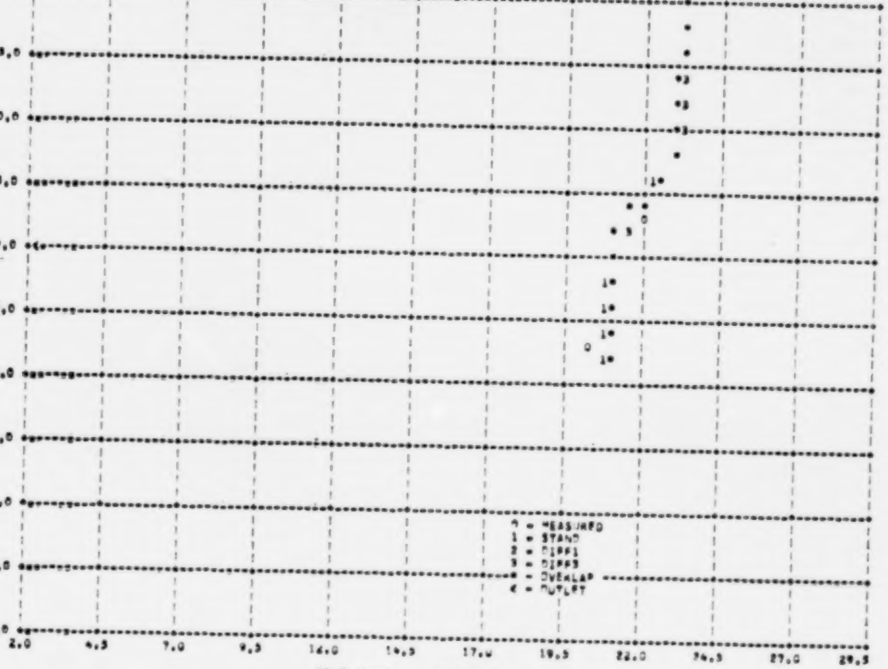

Figure 68 MIT MODEL - DOUGLAS RESERVOIR 1979--DAY127B --SURFACE ELEV: 293.3 M

CHEROKEE RESERVOIR

Figures 69 and 70 show the computed reservoir temperatures and the computed outflow temperature at Cherokee Reservoir respectively, for 1967. These can be compared with the measured data as shown in Figures 71 to 76. It can be seen from the Figures and as shown in Table 12 and 13 that the predicted temperatures at the outlet and at the surface have larger standard errors of estimate, 2.7° and 2.1° respectively, than the results for Fontana Reservoir. It can also be seen from Figures 71 to 76 that the variation in thickness of the horizontal segments from 1 to 3 meters makes minor differences in the predicted results with the measured temperature than does the 2 meter thickness. This is also evident in Tables 12 and 13.

It can be seen from Figures 77 to 82 that a variation in β, the fraction of solar radiation absorbed at the water surface, from 0.2 to 0.5 makes little difference in the predicted temperatures. This is also evident from Tables 12 and 13.

In Figures 83 to 88 the effect of a change in η, the radiation absorption coefficient, from 0.05 to 1.40 is shown. It is also shown that the use of a sorption coefficient of 0.05 predicts the temperature very poorly and that in general the value of 0.4 gives the best predictions. This is verified in Tables 12 and 13 where the standard error of estimate is 2.3° and 1.9°C for the outlet temperature and the surface water temperature, respectively.

In Figures 89 to 94, the effects of varying the diffusion coefficient from molecular to 100 times molecular diffusion are shown.

Table 12

STATISTICAL ANALYSIS FOR THE PREDICTED WATER TEMPERATURE AT OUTLET LEVEL

Reservoir/Year: Cherokee/1967

Time Period Covered: 120th - 330th Julian Day

File Name	Std. error of estimate (°C)	Correlation Coefficient
STAND	2.70	0.83
DELZ 1	2.99	0.80
DELZ 2	2.22	0.88
BETA 1	2.62	0.85
BETA 2	2.54	0.86
ETA 1	5.52	0.00
ETA 2	2.97	0.78
ETA 3	2.29	0.89
DIFF 1	1.80	0.92
DIFF 3	2.08	0.88

Table 13

STATISTICAL ANALYSIS FOR THE PREDICTED SURFACE WATER TEMPERATURE

Reservoir/Year: Cherokee/1967

Time Period Covered: 60th - 300th Julian Day

File Name	Std. error of estimate (°C)	Correlation Coefficient
STAND	2.07	0.95
DELZ 1	2.09	0.92
DELZ 2	2.11	0.95
BETA 1	2.06	0.95
BETA 2	2.01	0.96
ETA 1	1.49	0.98
ETA 2	2.25	0.95
ETA 3	1.88	0.96
DIFF 1	1.90	0.96
DIFF 3	1.72	0.97

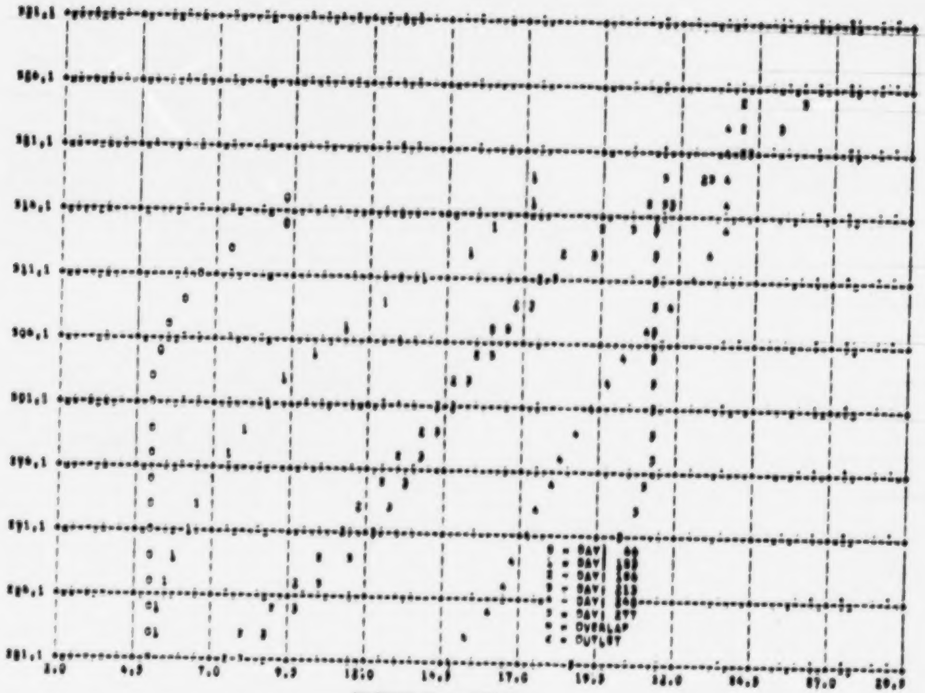

Figure [illegible] MIT MODEL - CHEROKEE RESERVOIR 1967--COMPUTED TEMPERATURE PROFILE--

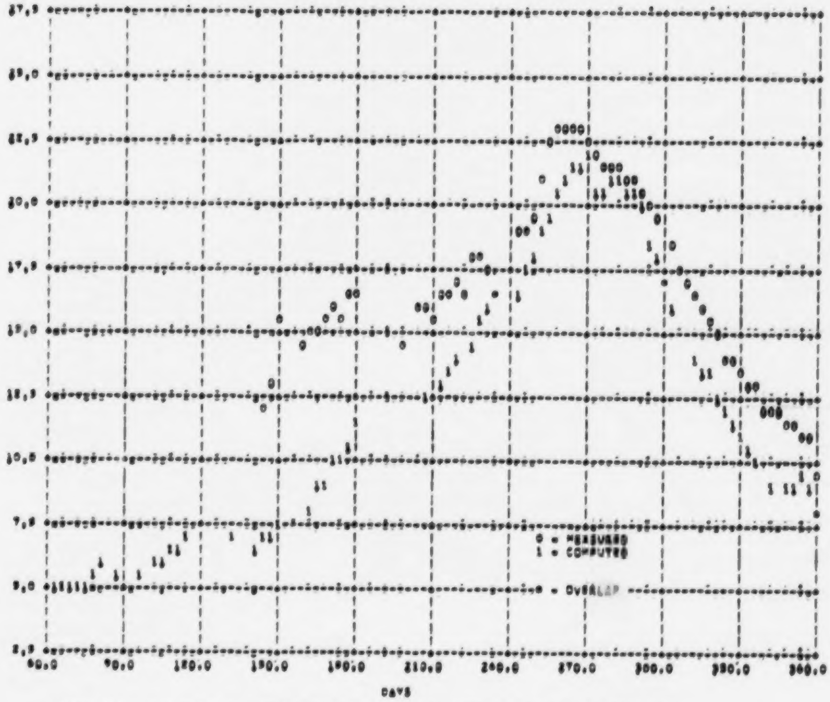

Figure 70 MIT MODEL I CHEROKEE RESERVOIR 1967--COMPUTED OUTFLOW TEMPERATURE--

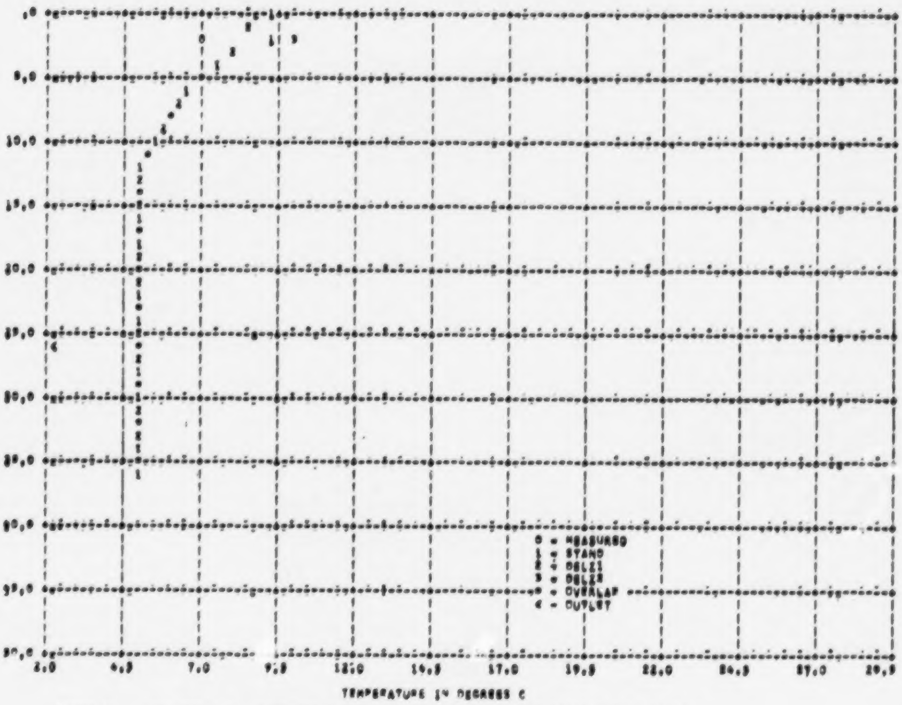

Figure 71 MIT MODEL I CHEROKEE RESERVOIR 1967--DAY: 60 --SURFACE ELEV: 316.9 M

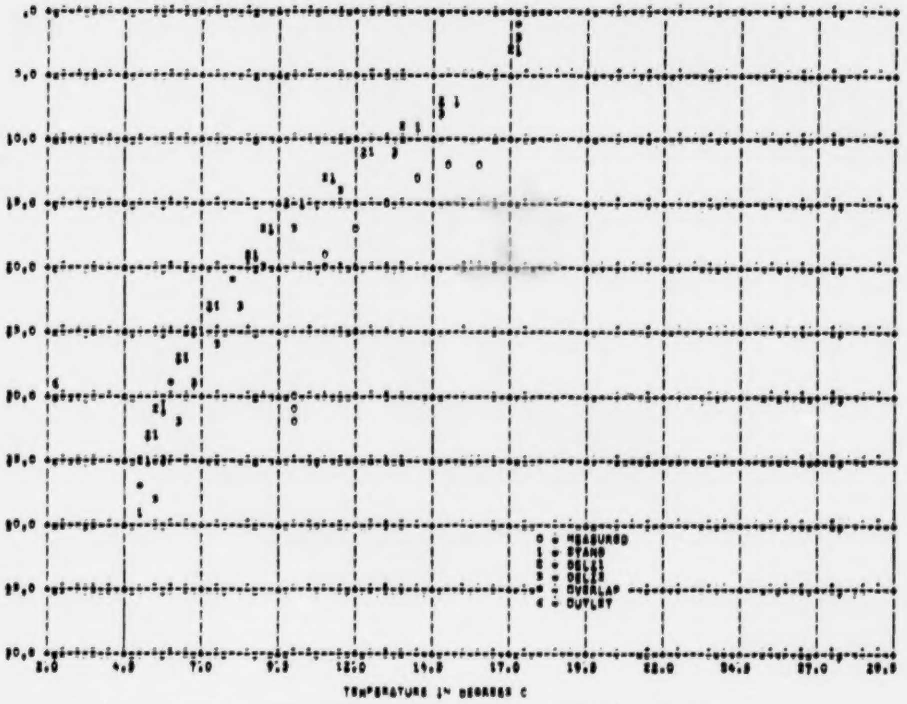

Figure 72 MIT MODEL * CHEROKEE RESERVOIR 1967--DAY:123 **SURFACE ELEV: 320.0 M

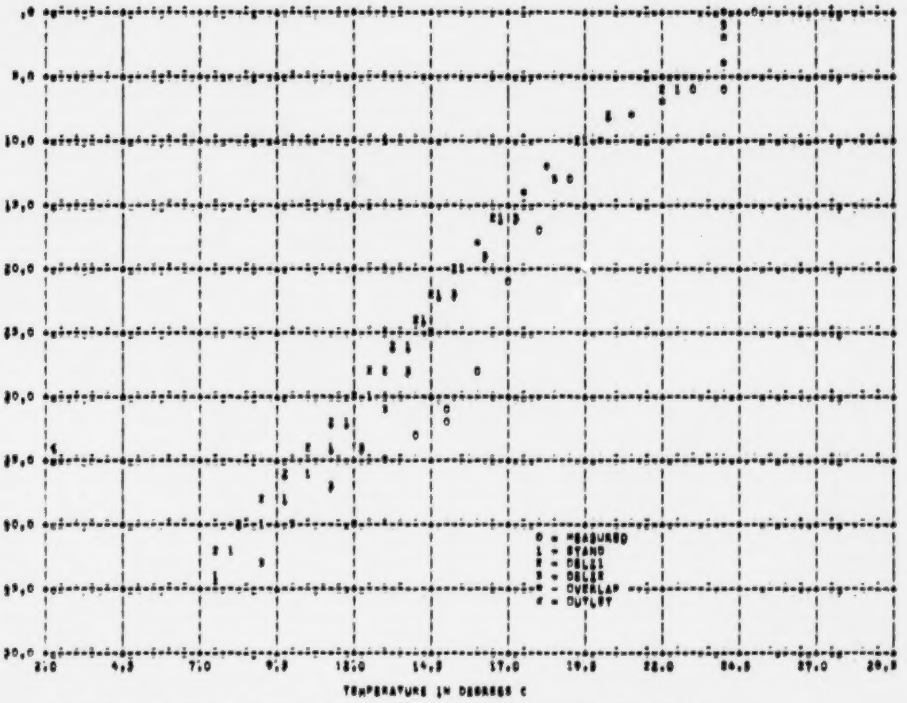

Figure 73 MIT MODEL * CHEROKEE RESERVOIR 1967--DAY:186 **SURFACE ELEV: 325.1 M

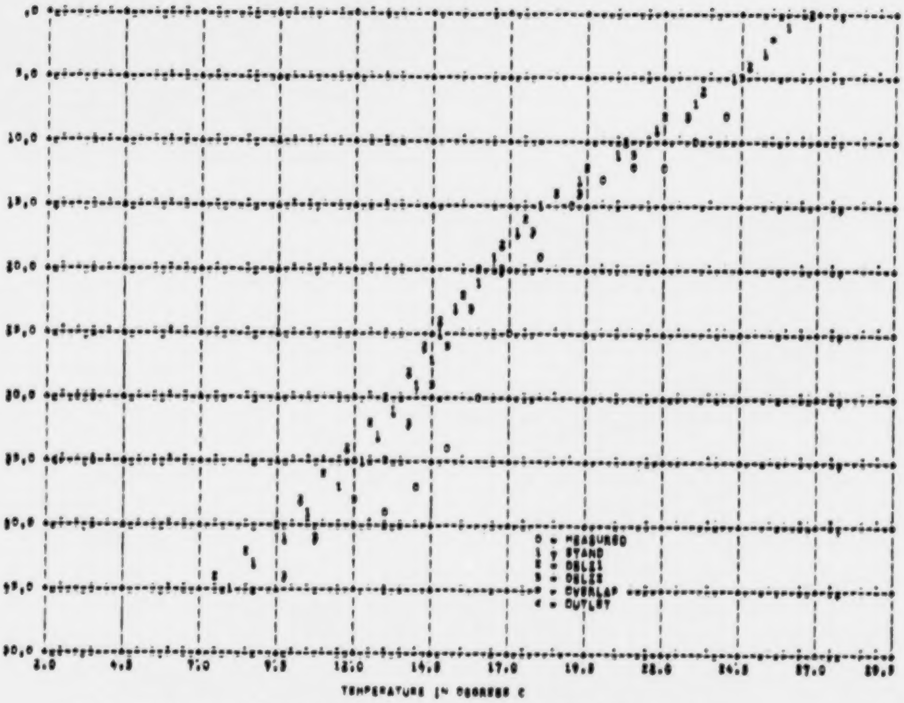

Figure 74 MIT MODEL * CHEROKEE RESERVOIR 1975-DAY 213 **SURFACE ELEV: 326.4 M

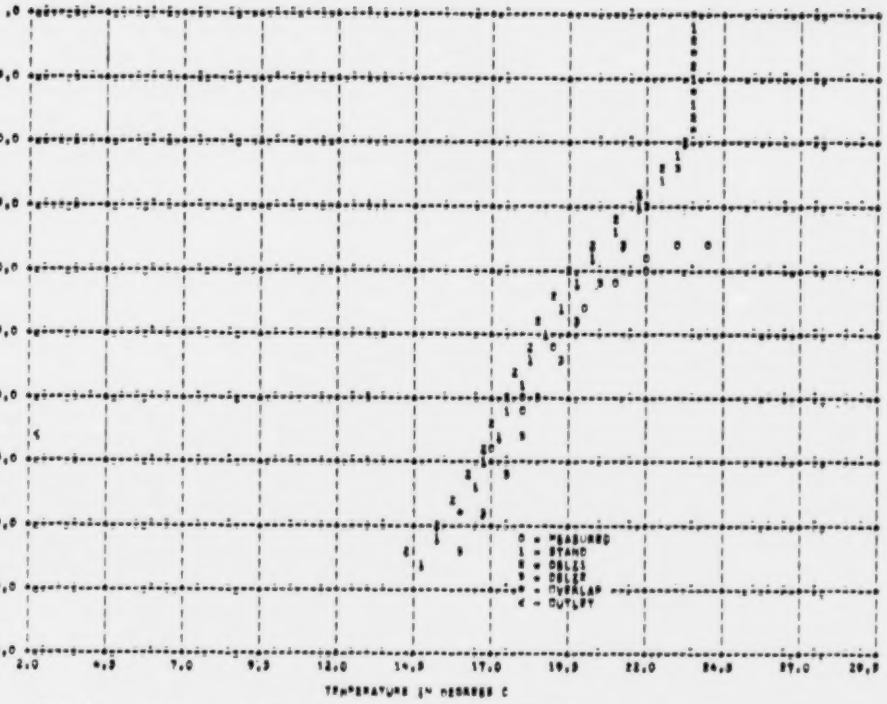

Figure 75 MIT MODEL * CHEROKEE RESERVOIR 1975-DAY 248 **SURFACE ELEV: 324.1 M

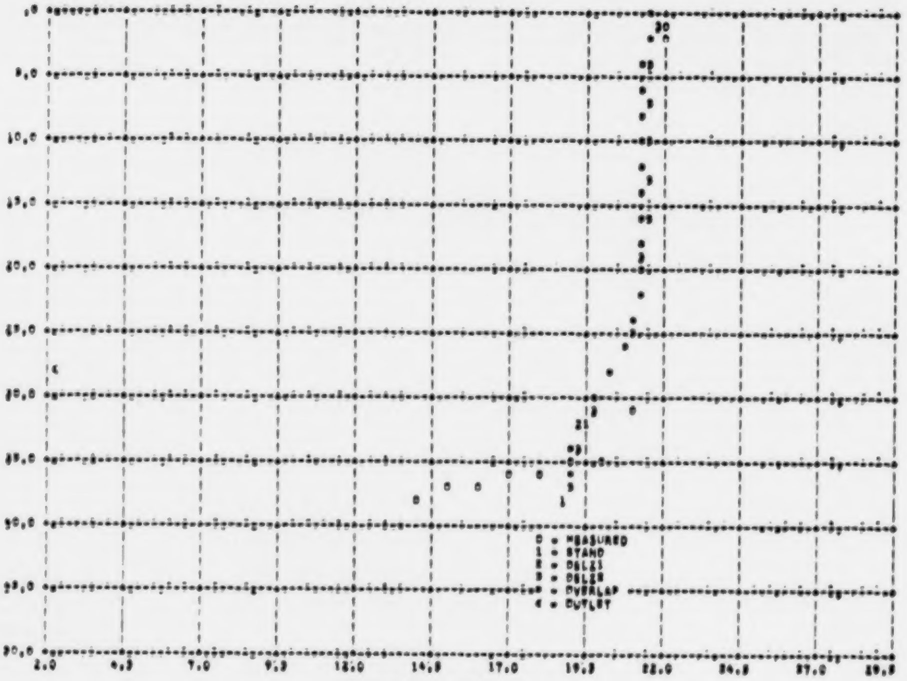

Figure 76 MIT MODEL - CHEROKEE RESERVOIR 1967--DAY:277 --SURFACE ELEV: 319.1 M

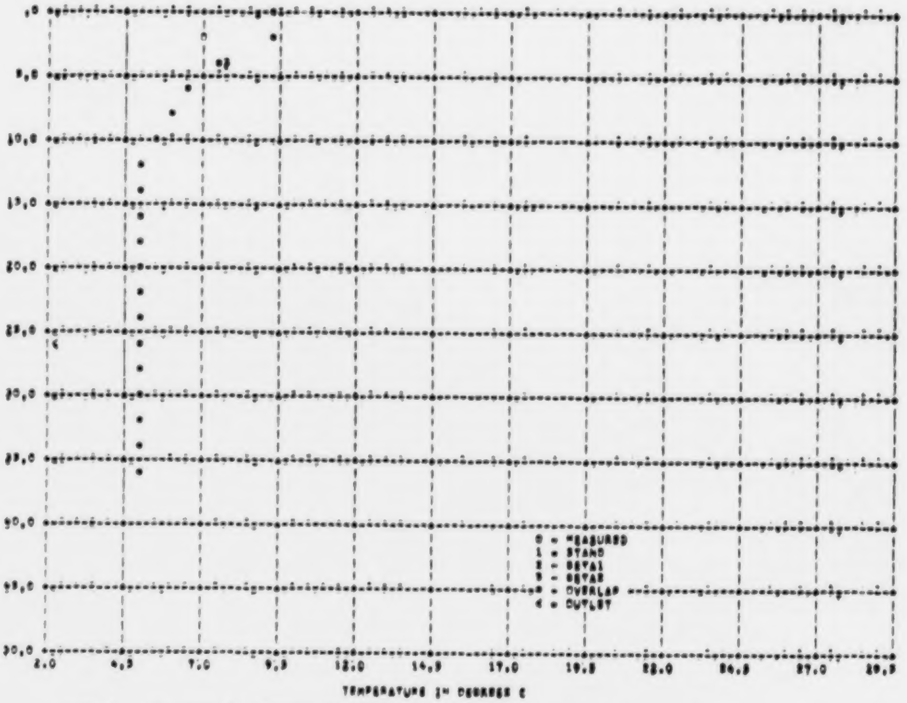

Figure 77 MIT MODEL - CHEROKEE RESERVOIR 1967--DAY: 66 --SURFACE ELEV: 316.9 M

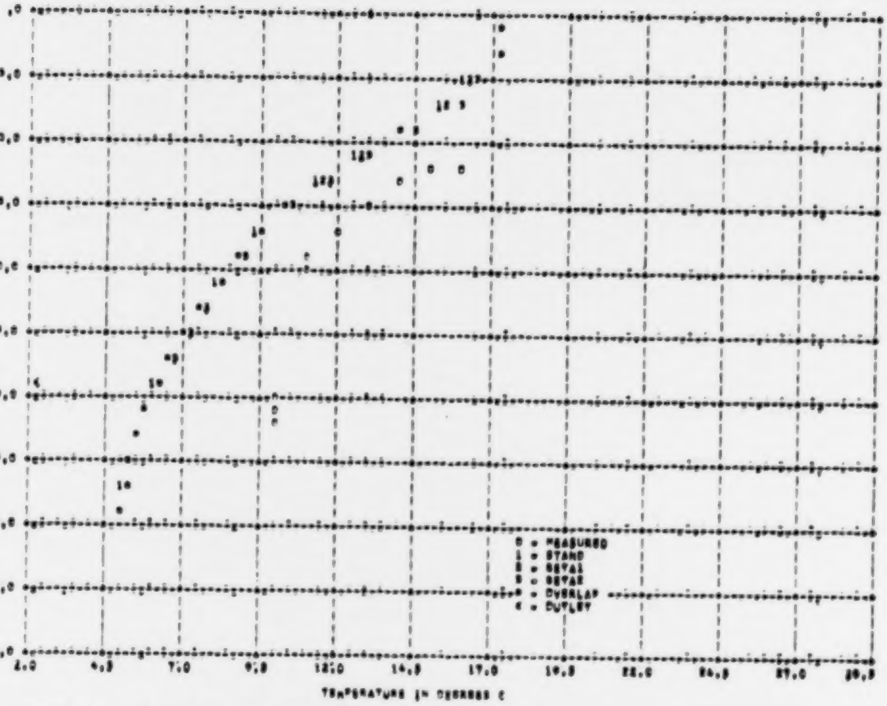

Figure 78 MIT MODEL - CHEROKEE RESERVOIR 1967--DAY 123 **SURFACE ELEV: 320.0 M

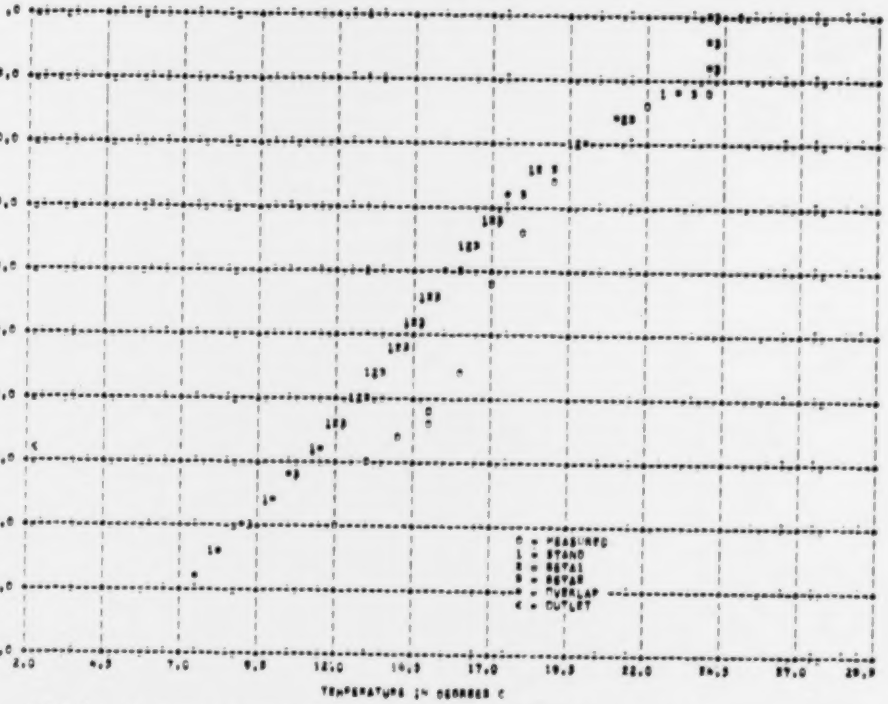

Figure 79 MIT MODEL - CHEROKEE RESERVOIR 1967--DAY 186 **SURFACE ELEV: 323.1 M

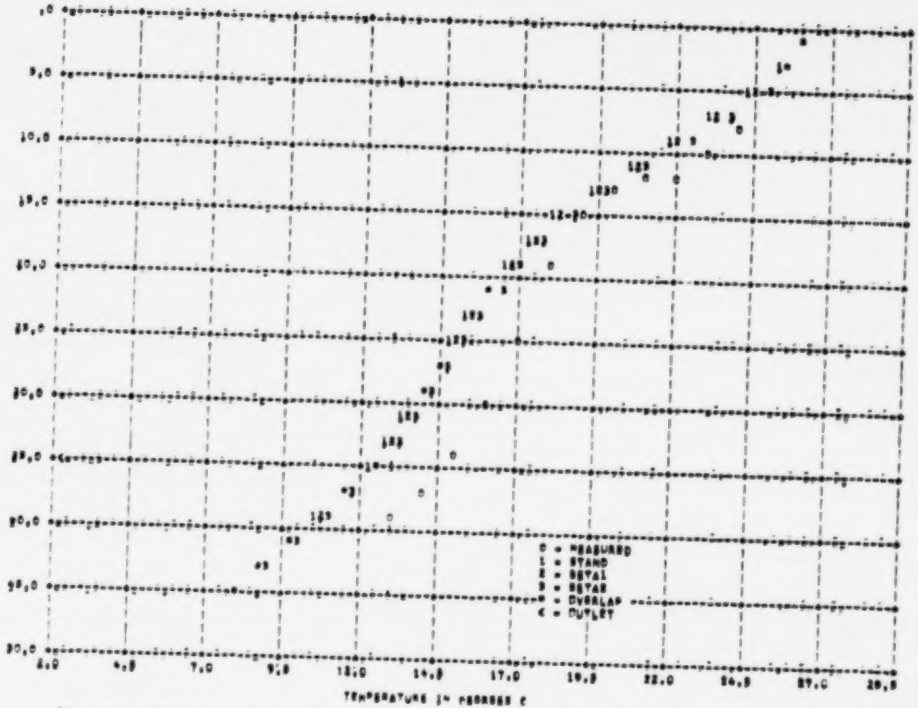

Figure [illegible] MIT MODEL - CHEROKEE RESERVOIR 1967--DAY:213 --SURFACE ELEV: 326.4 M

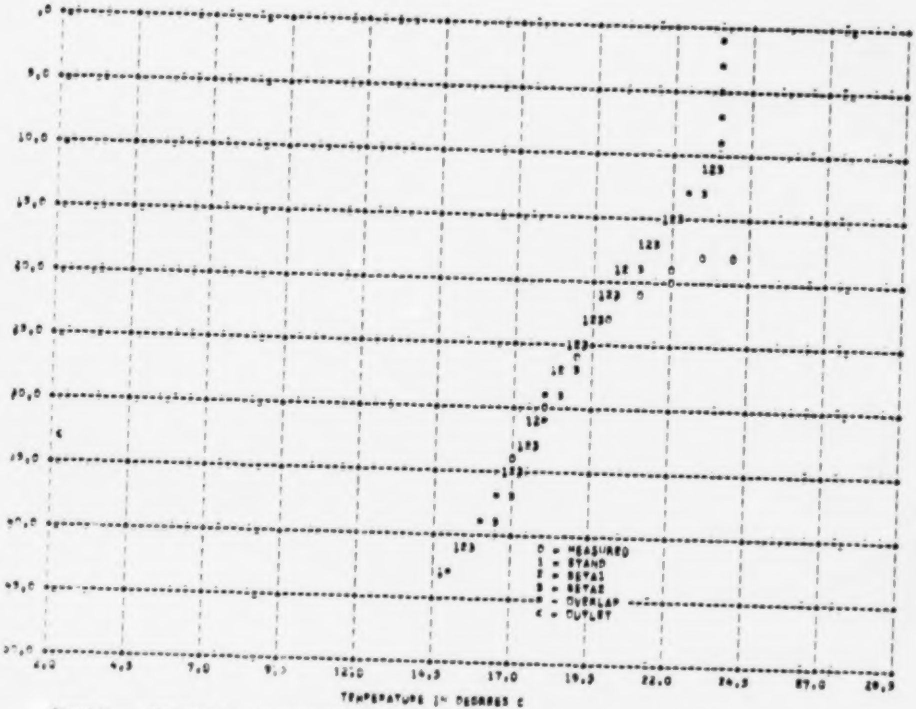

Figure [illegible] MIT MODEL - CHEROKEE RESERVOIR 1967--DAY:248 --SURFACE ELEV: 324.1 M

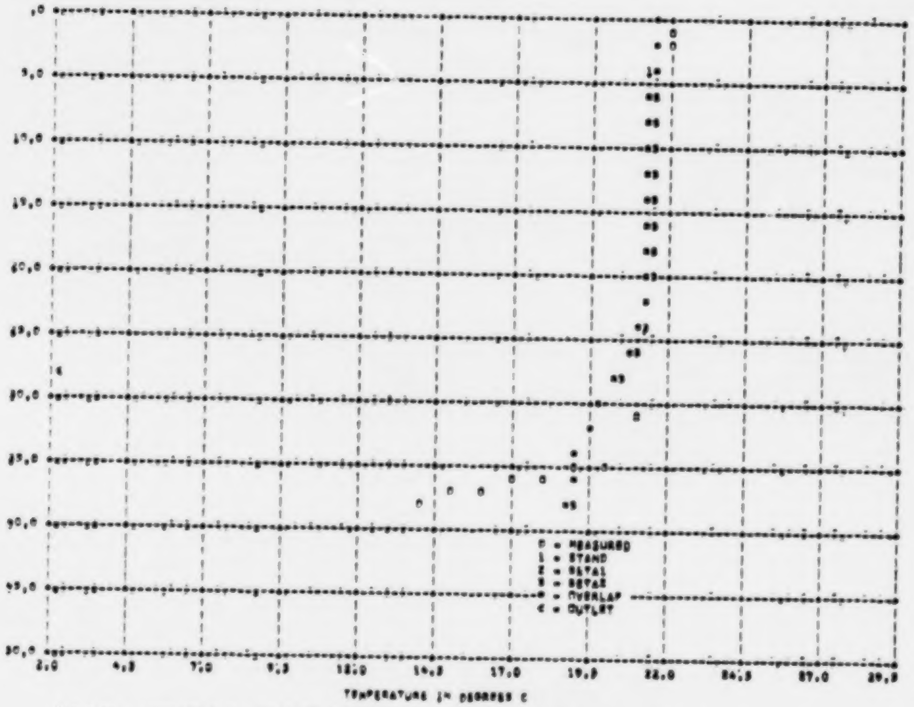

Figure 82 MIT MODEL - CHEROKEE RESERVOIR 1967--DAY:277 --SURFACE ELEV: 319.1 M

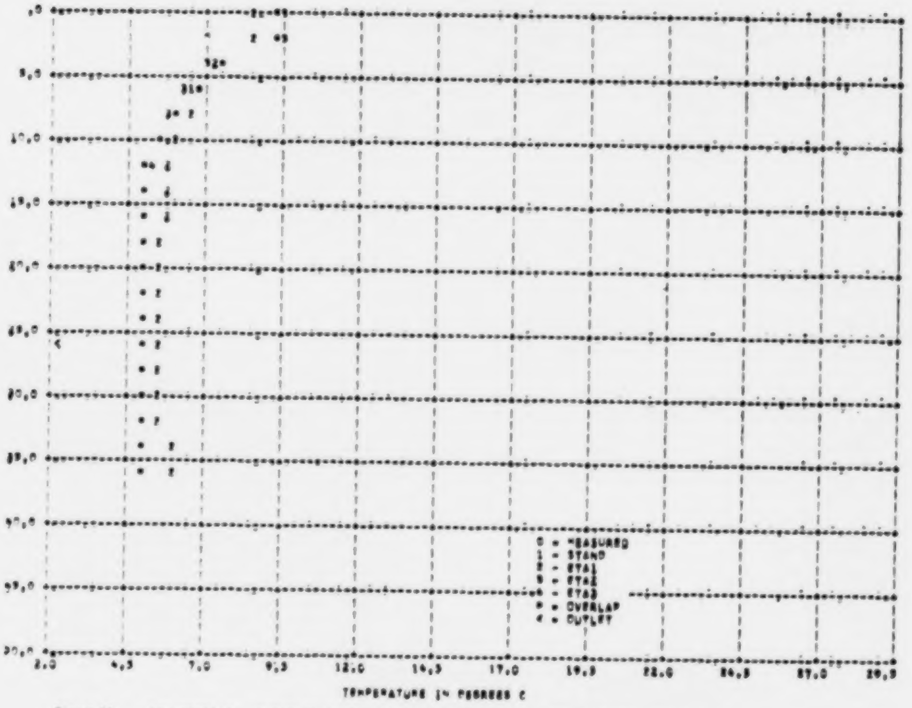

Figure 83 MIT MODEL - CHEROKEE RESERVOIR 1967--DAY: 88 --SURFACE ELEV: 316.9 M

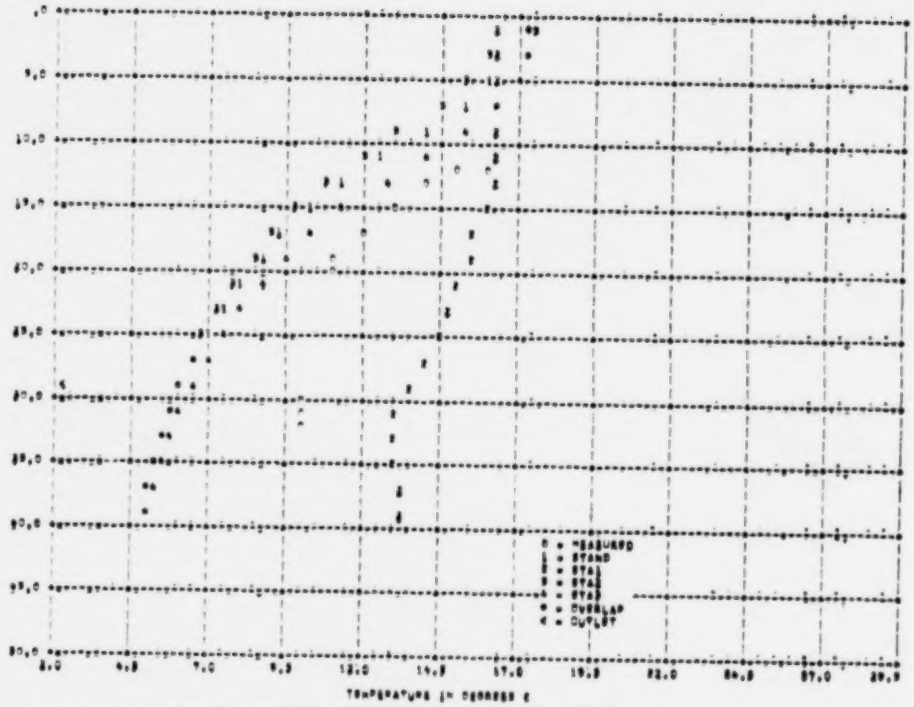

Figure [illegible]. MIT MODEL - CHEROKEE RESERVOIR 1967--DAY[illegible] --SURFACE ELEV: [illegible] M

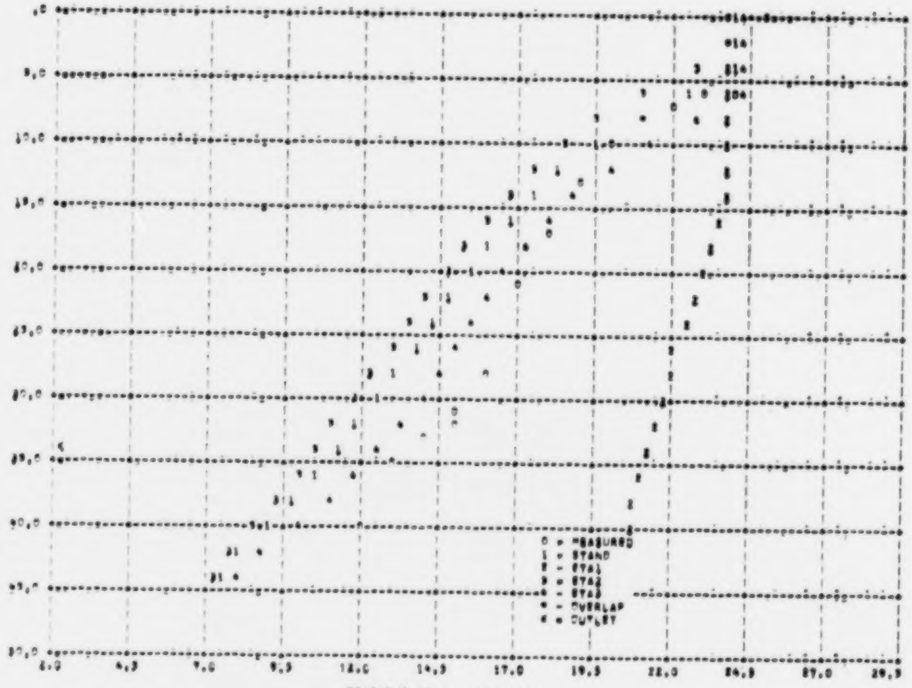

Figure [illegible]. MIT MODEL - CHEROKEE RESERVOIR 1967--DAY[illegible] --SURFACE ELEV: [illegible] M

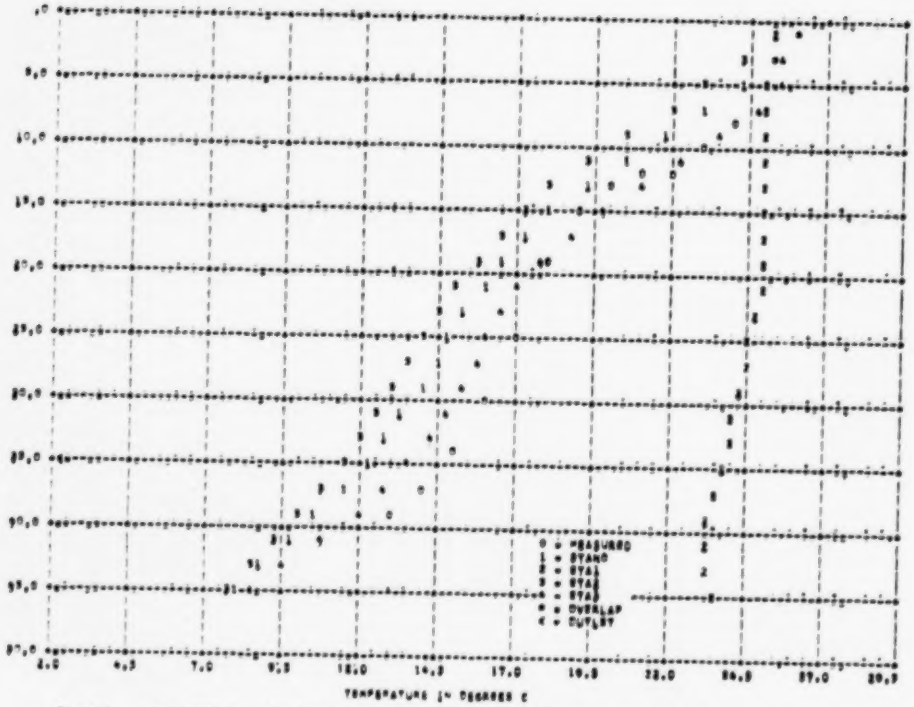

Figure 80. MIT MODEL - CHEROKEE RESERVOIR 1967--DAY 213 --SURFACE ELEV: 326.4 M

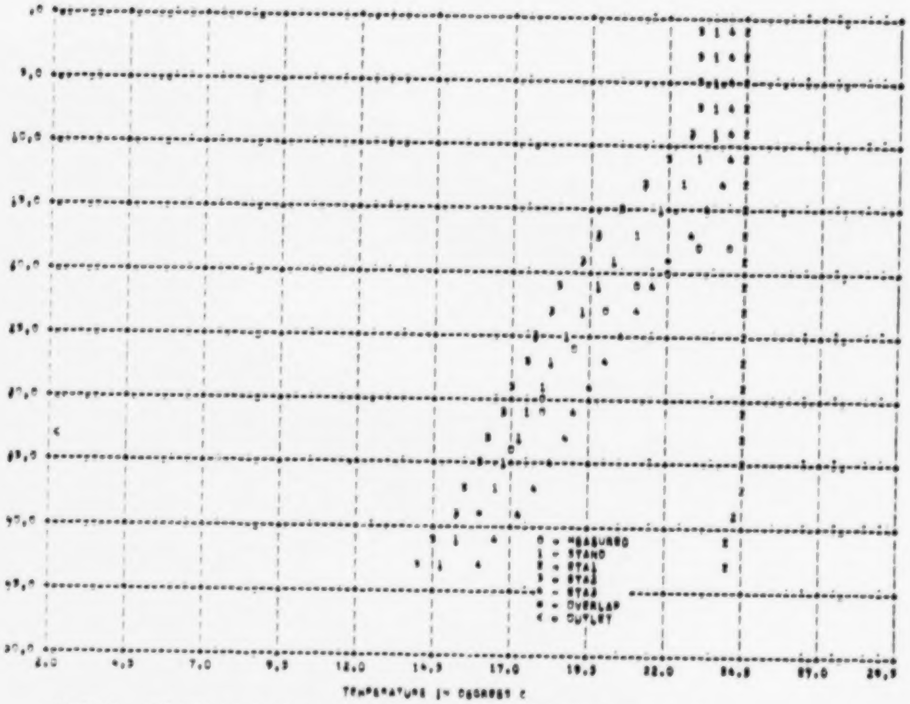

Figure 81. MIT MODEL - CHEROKEE RESERVOIR 1967--DAY 248 --SURFACE ELEV: 326.1 M

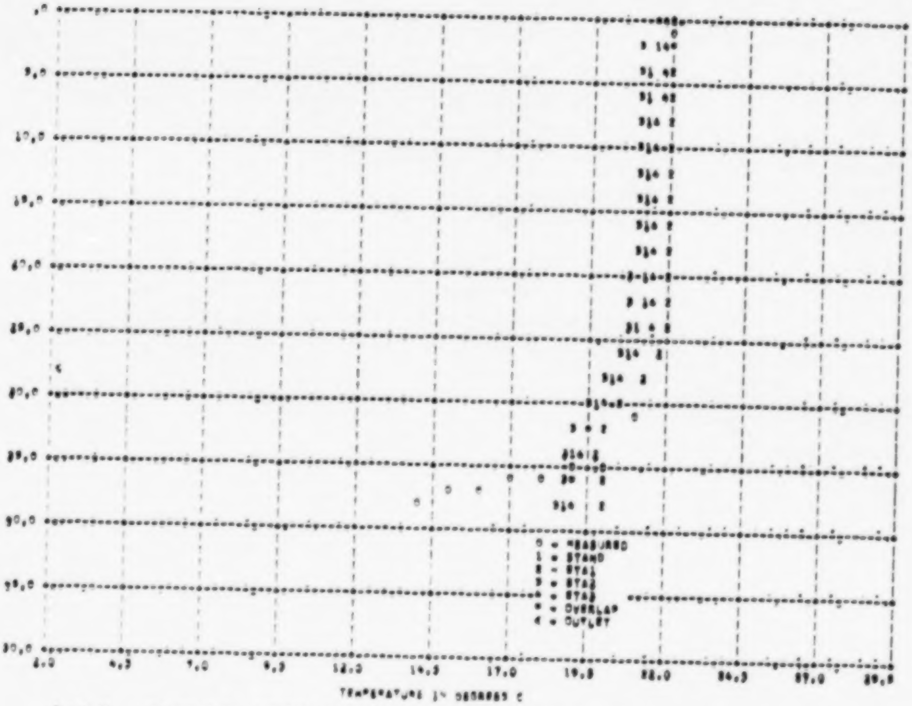

Figure 86. MIT MODEL 4 CHEROKEE RESERVOIR 1967--DAY 177 --SURFACE ELEV: 319.1 M

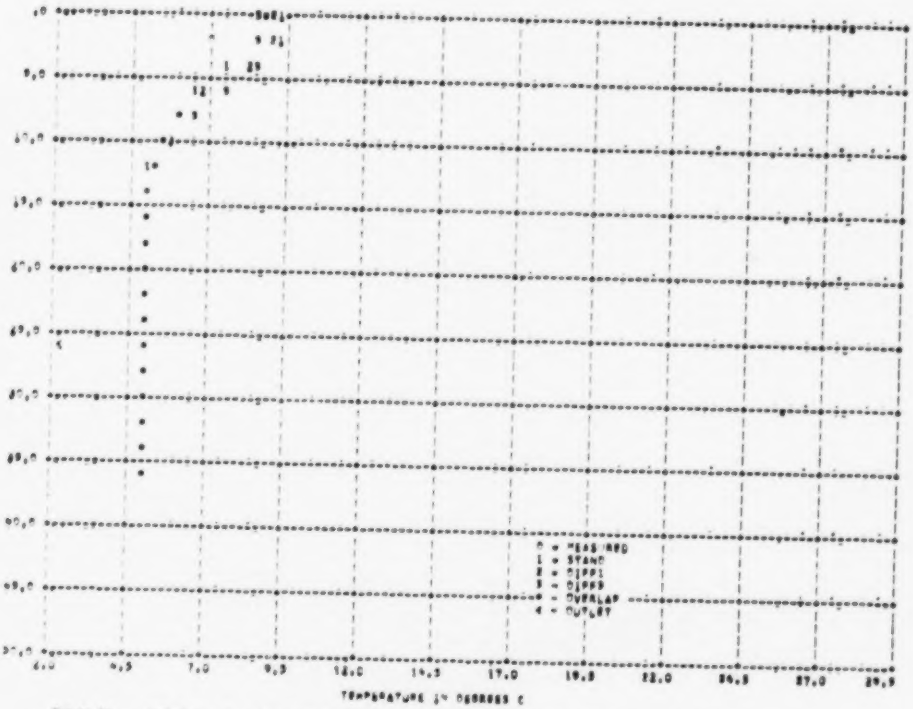

Figure 87. MIT MODEL 4 CHEROKEE RESERVOIR 1967--DAY 88 --SURFACE ELEV: 316.9 M

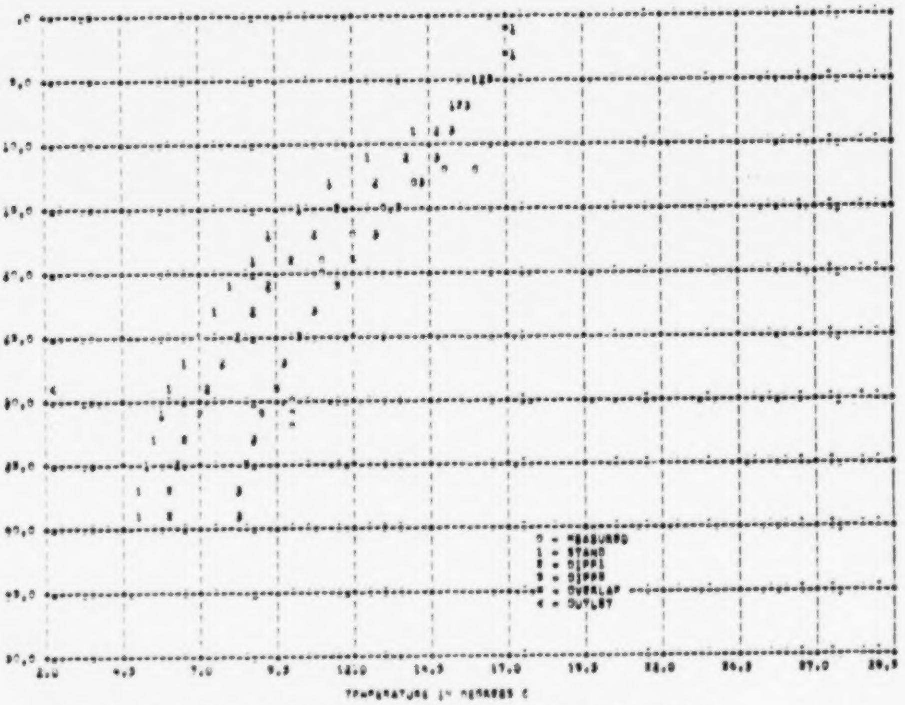

Figure [illegible] MIT MODEL - CHEROKEE RESERVOIR 1967--DAY123 --SURFACE ELEV: 320.0 M

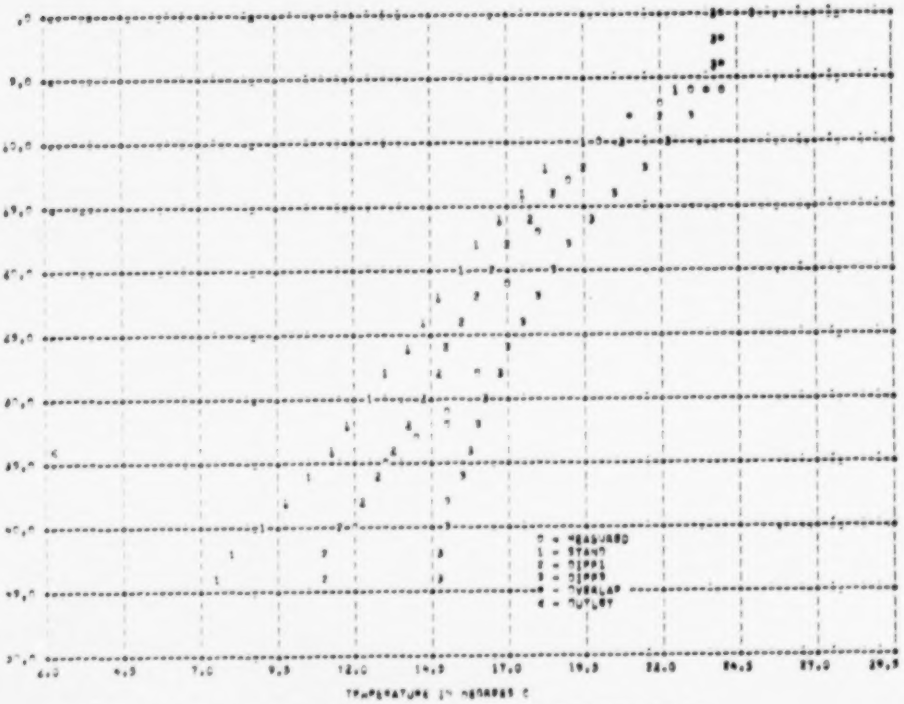

Figure [illegible] MIT MODEL - CHEROKEE RESERVOIR 1967--DAY130 --SURFACE ELEV: 323.1 M

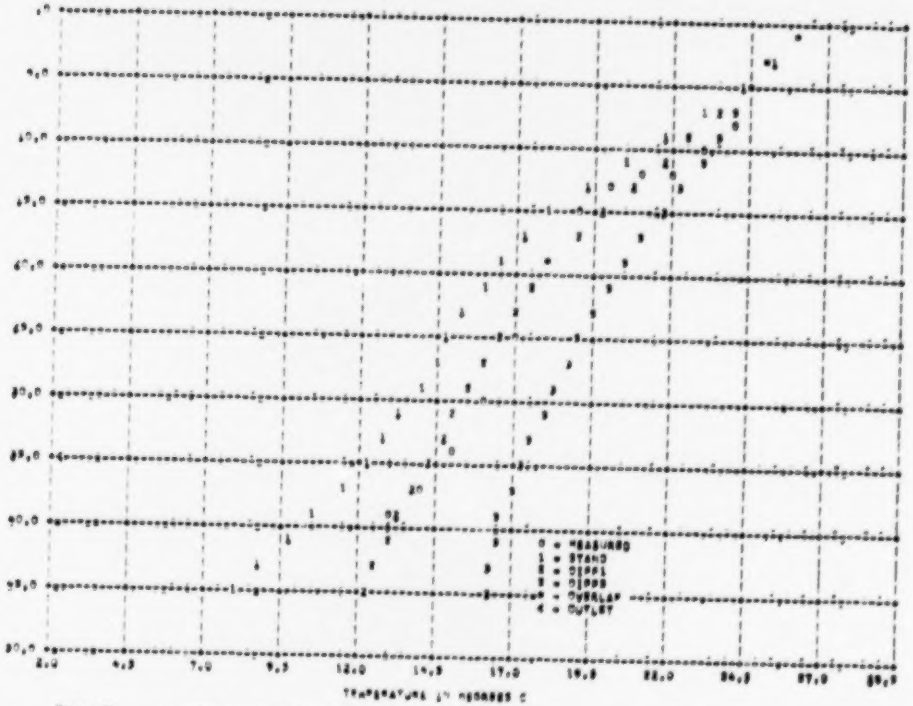

Figure 92   MIT MODEL — CHEROKEE RESERVOIR 1987--DAY:213 --SURFACE ELEV: 328.4 M

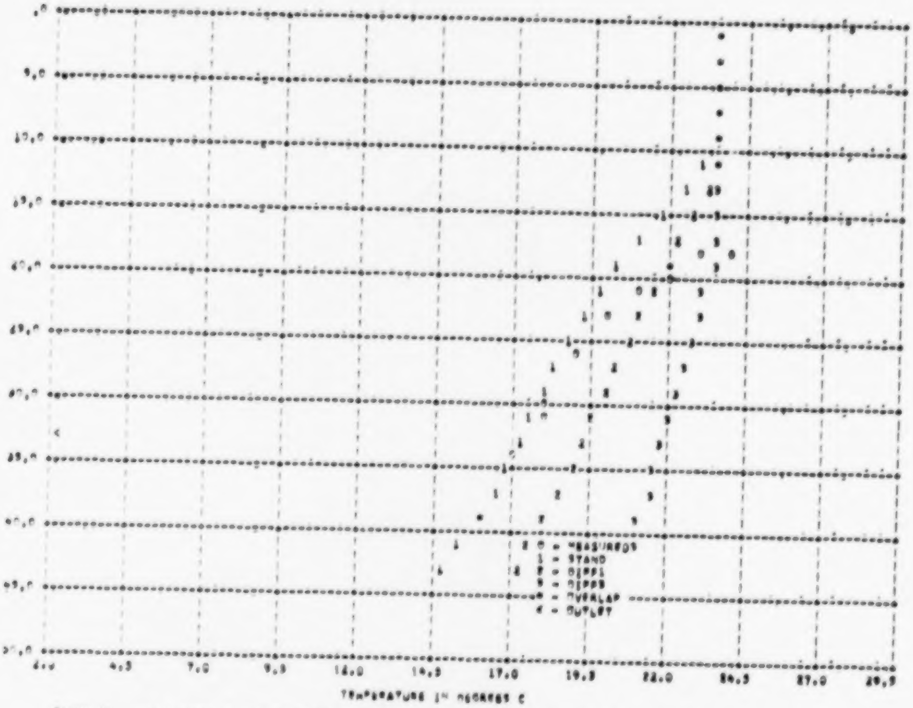

Figure 93   MIT MODEL — CHEROKEE RESERVOIR 1987--DAY:248 --SURFACE ELEV: 324.1 M

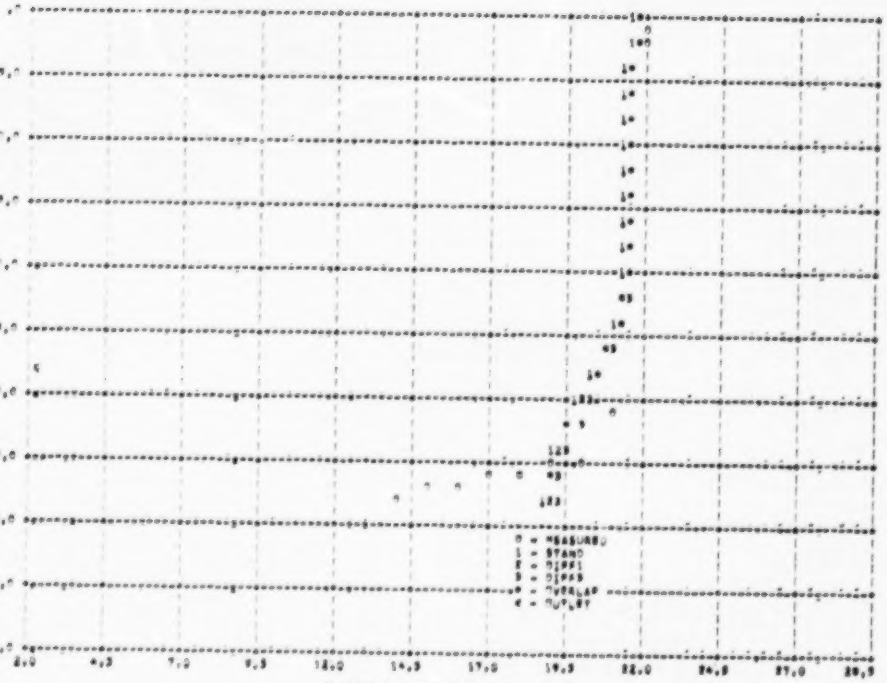

[illegible] SURFACE ELEV: 319.1 M

NORRIS RESERVOIR

Figures 95 and 96 show the computed reservoir temperatures and the computed outflow temperatures respectively, at Norris Reservoir for 1971. These can be compared with the measured temperatures as shown in Figures 97 to 101. It can be seen from the Figures and in Table 14 that the predicted temperatures have larger standard errors of estimate than do the predicted temperatues for Fontana Reservoir.

In Figures 97 to 102 it can be seen that the variation in thickness of the horizontal segments from 1 to 3 meters makes minor differences though the use of the 3 meter segment does lead to a larger error as shown in Table 14.

It can also be seen from Figures 102 to 106 that a variation from 0.2 to 0.5 in β, the fraction of solar radiation absorbed at the water surface, makes little difference in the predicted temperatures. This is varified in Table 14, where the standard errors of estimate of temperature are essentially the same for all three βs tested.

It can be seen from Figures 107 to 111 that a change from 0.05 to 1.40 per meter in η, the radiation absorption coefficient, predicts the temperature poorly when the absorption coefficient of 0.05 is used. The error is as great as 12°C in some instances. This is verified in Table 14, where the standard error of estimate of the temperature is 1°C greater with the use of the lowest absorption coefficient.

In Figures 112 to 116, the effect of varying the diffusion coefficient from molecular to 100 times molecular diffusion is shown. It can be seen that in general the use of 30 times molecular diffusion yields the best prediction of temperature with the use of 100 times molecular yielding the worst.

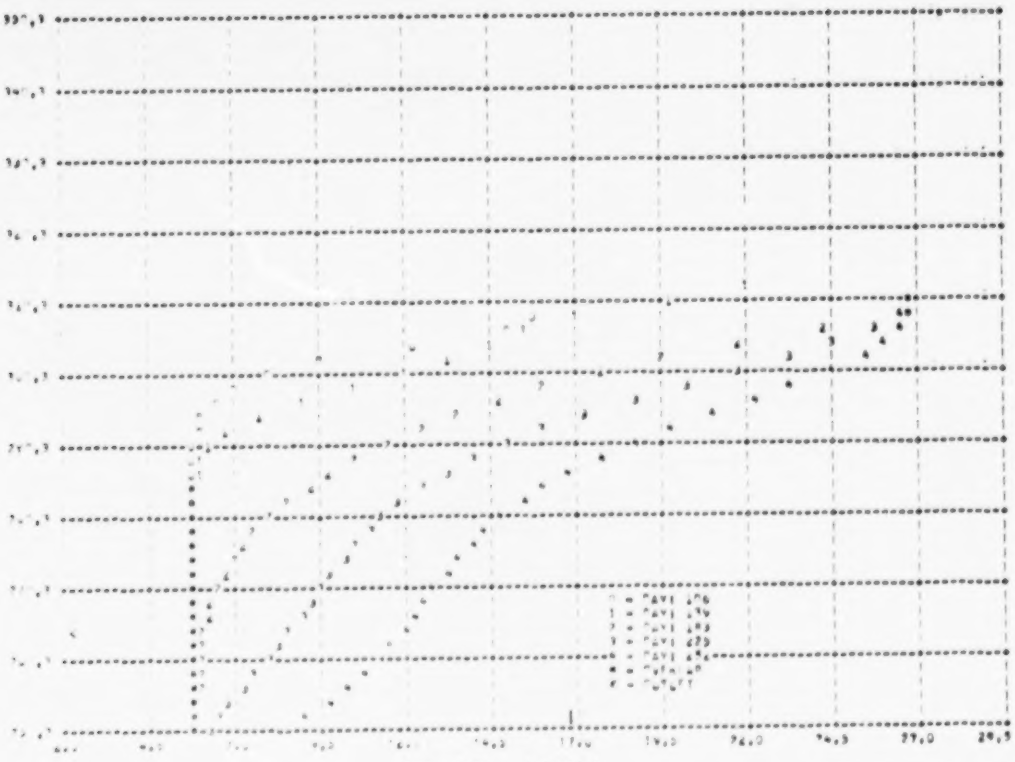

Figure [illegible]

Reproduced from best available copy.

Table 14

STATISTICAL ANALYSIS FOR THE PREDICTED SURFACE WATER TEMPERATURE

Reservoir/Year: Norris/1972

Time Period Covered: 60th - 360th Julian Day

File Name	Std. error of estimate (^oC)	Correlation Coefficient
STAND	2.31	0.94
DELZ 1	2.29	0.94
DELZ 2	3.16	0.92
BETA 1	2.32	0.94
BETA 2	2.28	0.94
ETA 1	3.21	0.89
ETA 2	2.36	0.93
ETA 3	2.39	0.94
DIFF 1	2.46	0.93
DIFF 3	2.64	0.92

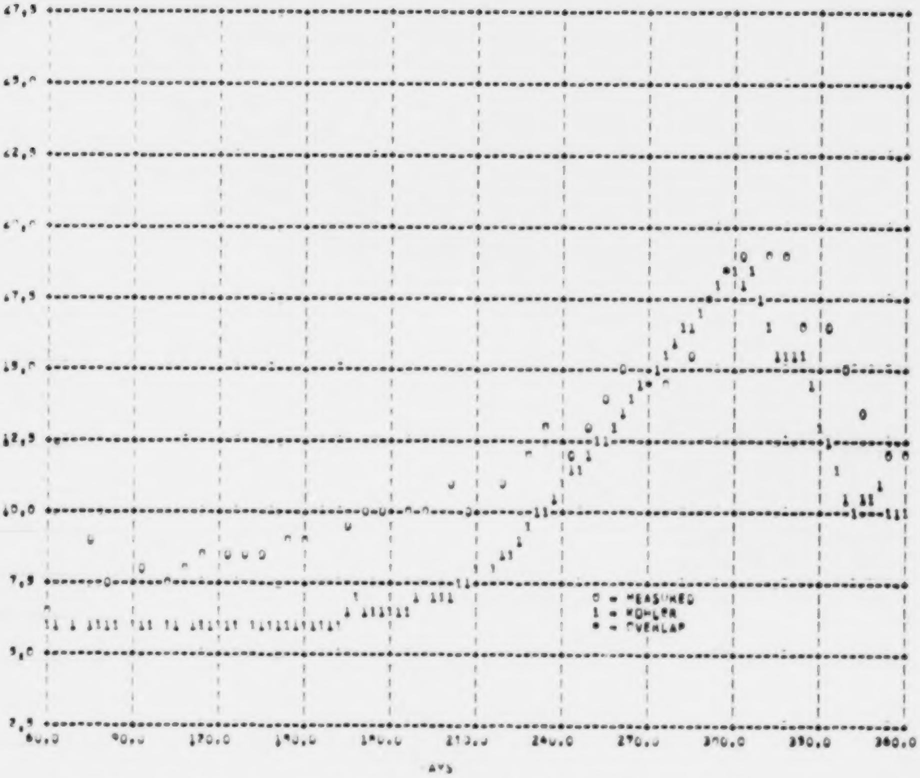

Figure 96 [illegible] 1971 --COMPUTED OUTFLOW TEMPERATURE--

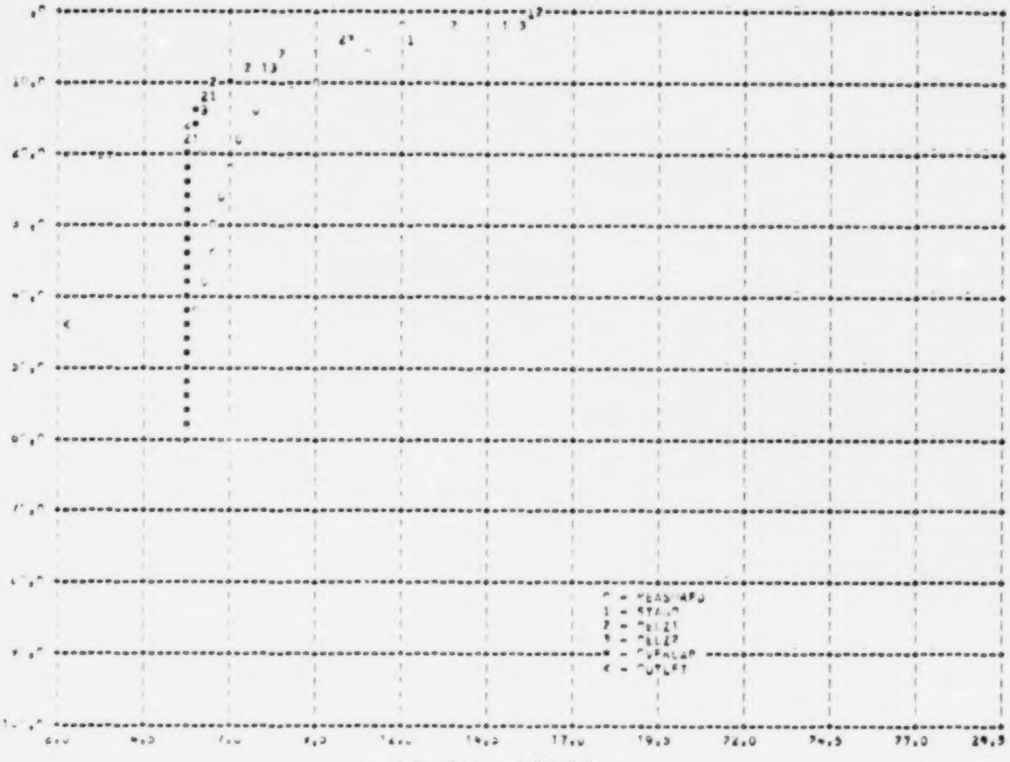

Figure 97 [illegible] 1971--[illegible] --SURFACE ELEV: [illegible] M

Reproduced from best available copy.

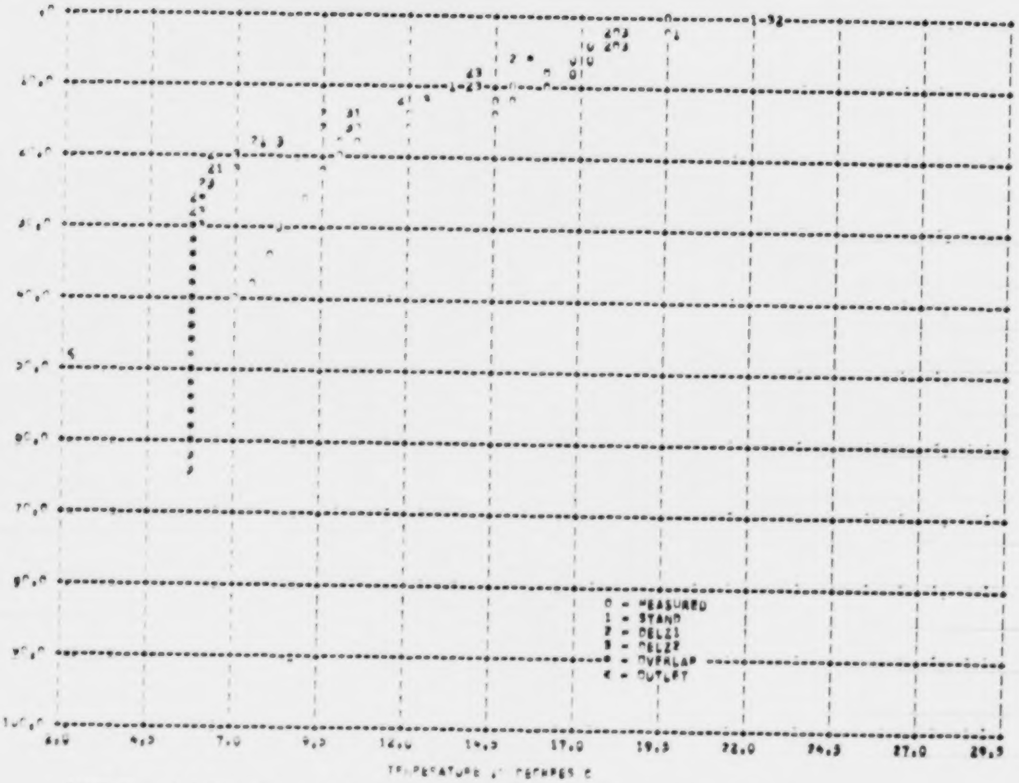

Figure 98 [illegible] 1971--DAY139 --SURFACE ELEV 312.6 M

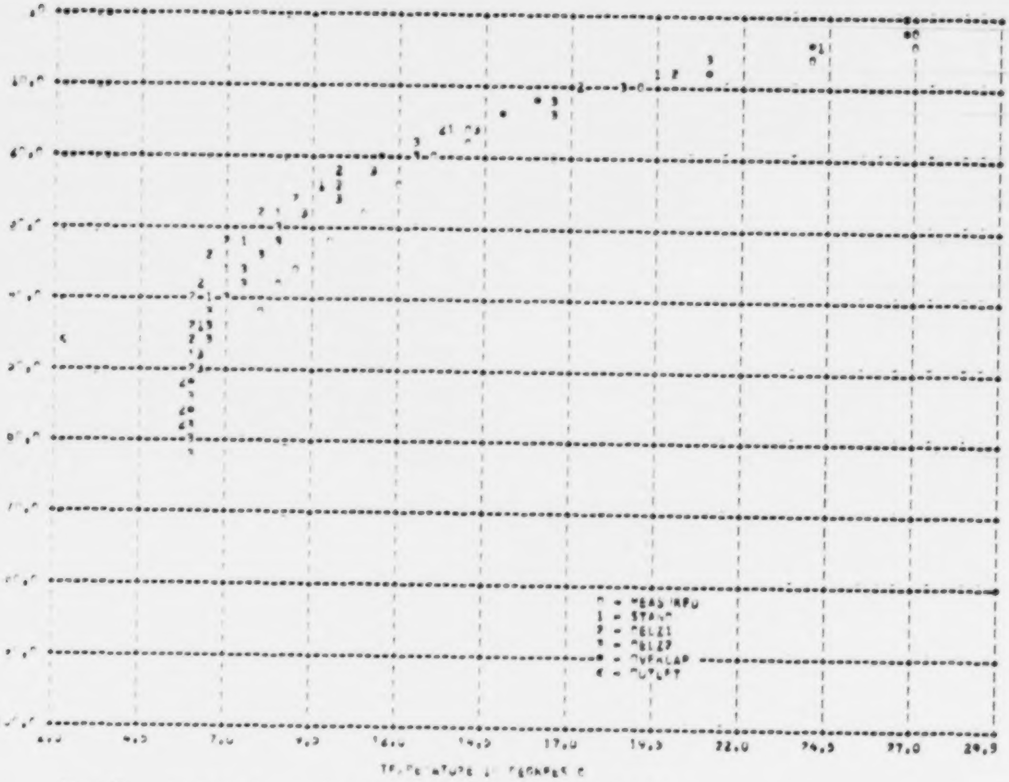

Figure 99 [illegible] 1971--DAY [illegible] --SURFACE ELEV 310.3 M

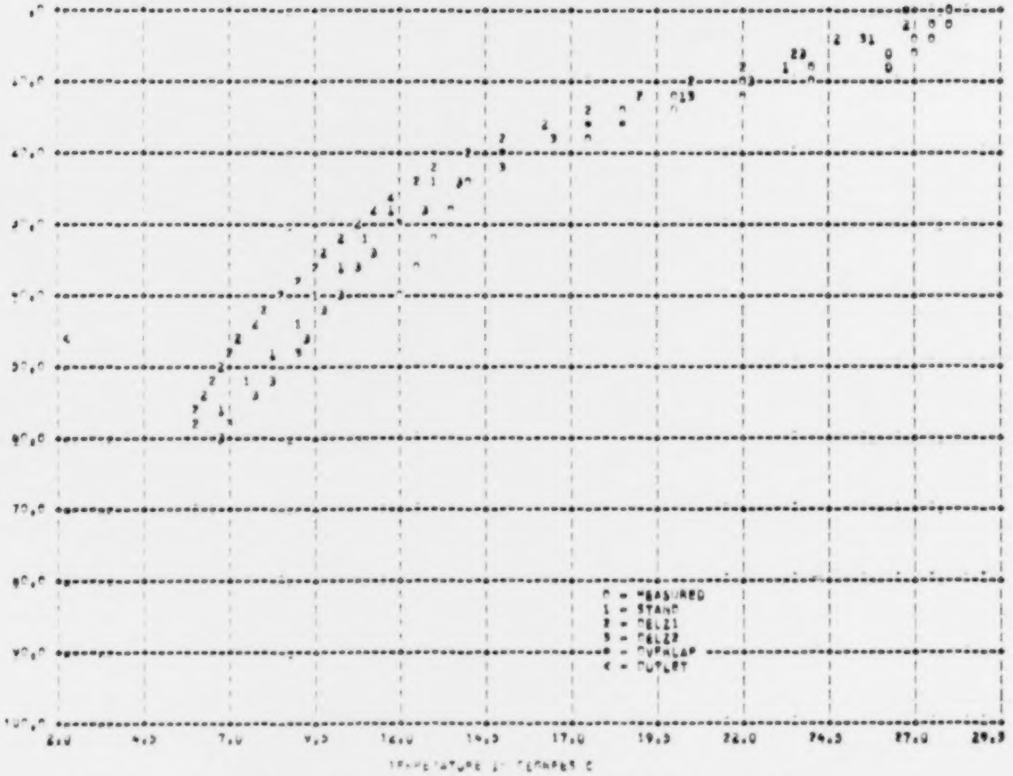

Figure 100 [illegible] --SURFACE ELEV 310.1 M

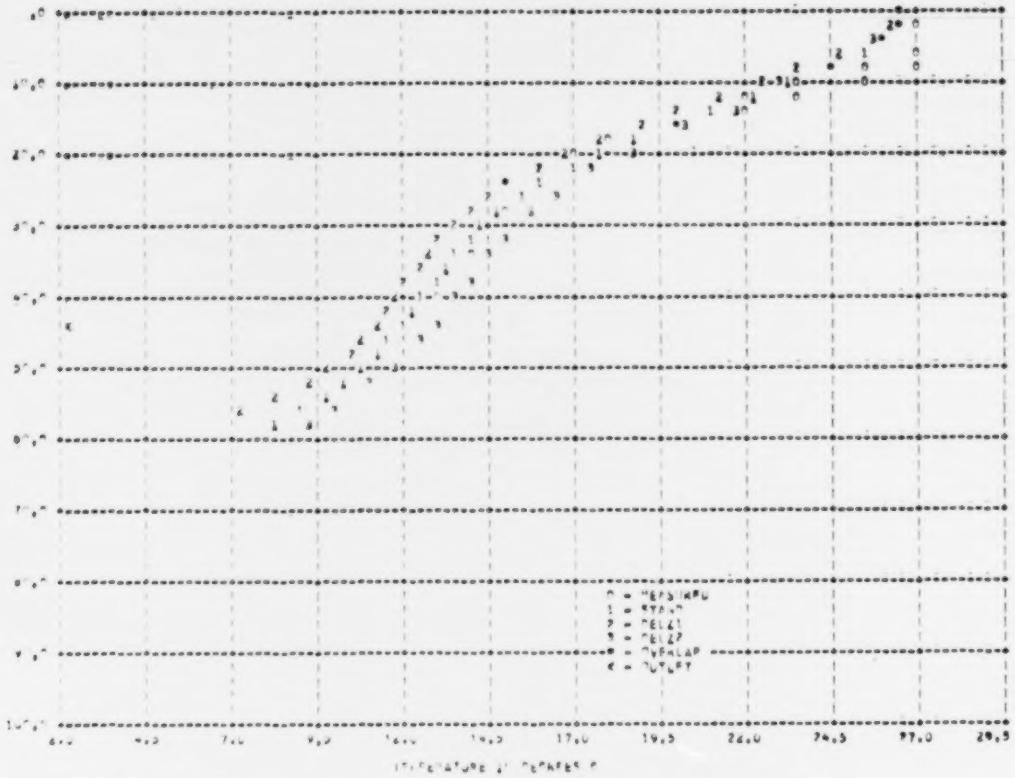

Figure 101 [illegible] --SURFACE ELEV 307.9 M

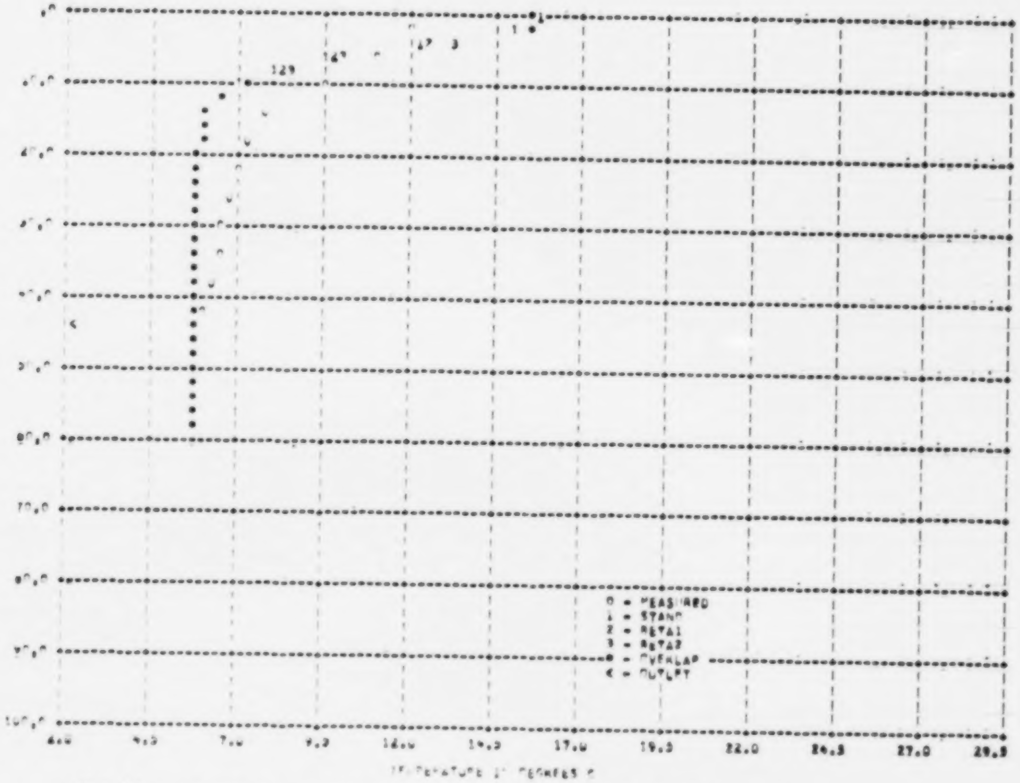

Figure 102 [illegible] --SURFACE ELEV: [illegible] M

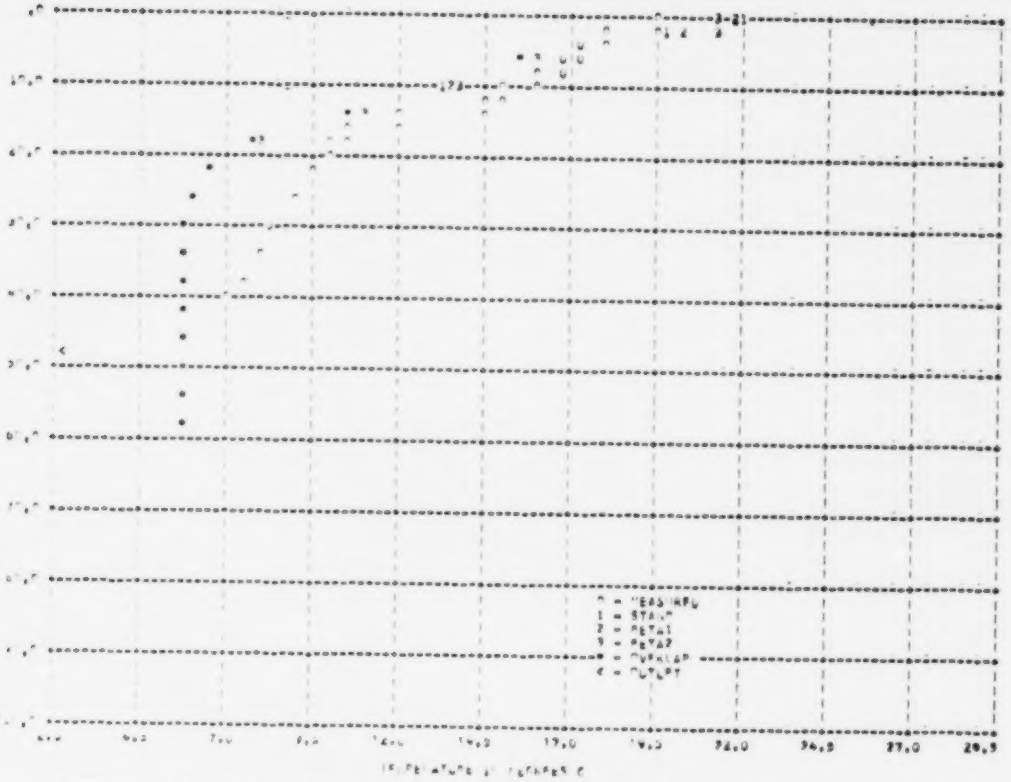

Figure 103 [illegible] --SURFACE ELEV: 312.2 M

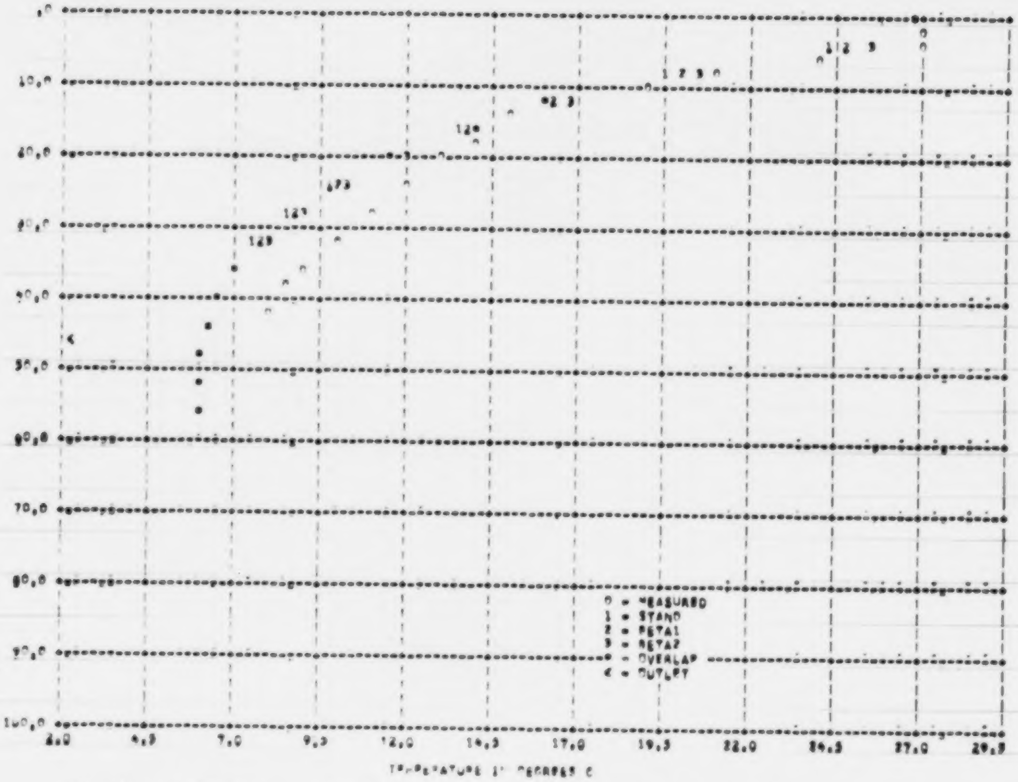

Figure 104 [illegible] [illegible] 1971--[illegible] --SURFACE ELEV 310.3 M

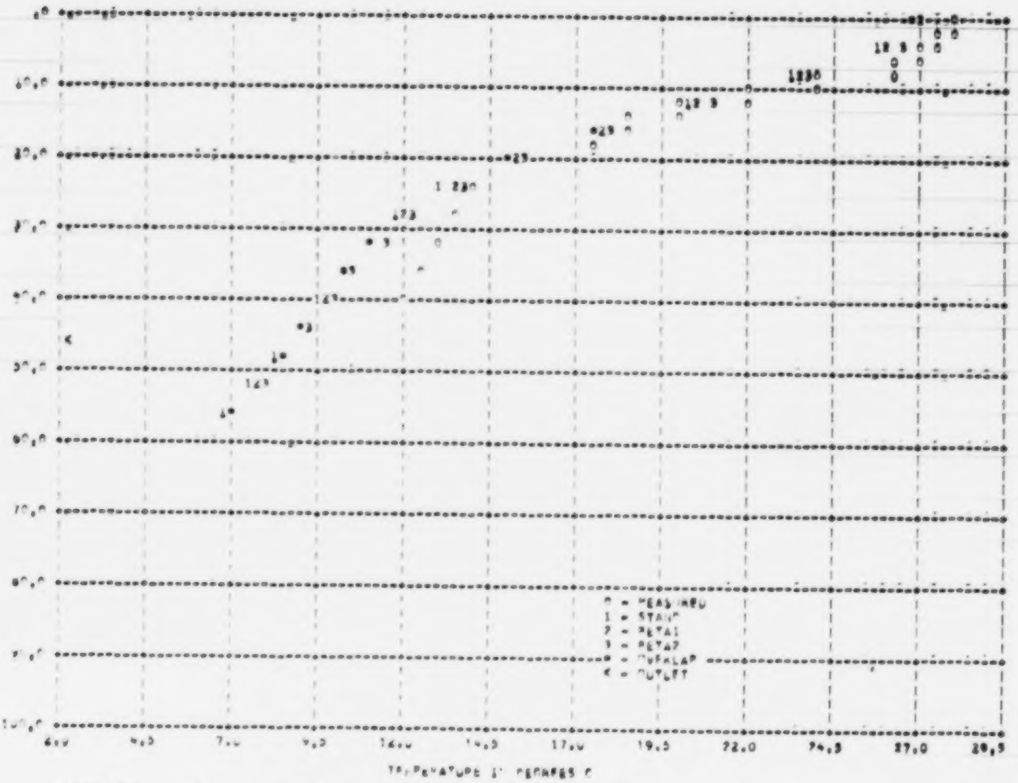

Figure 105 [illegible] [illegible] 1971--[illegible] --SURFACE ELEV 310.1 M

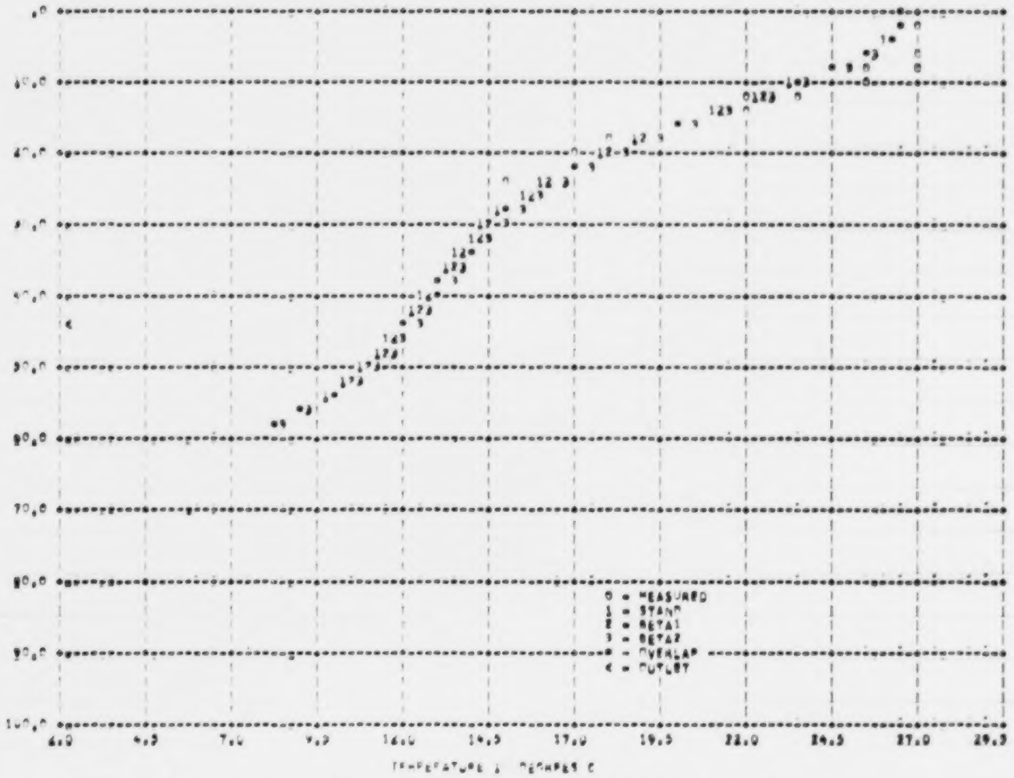

Figure 106 [illegible] 207.0 M

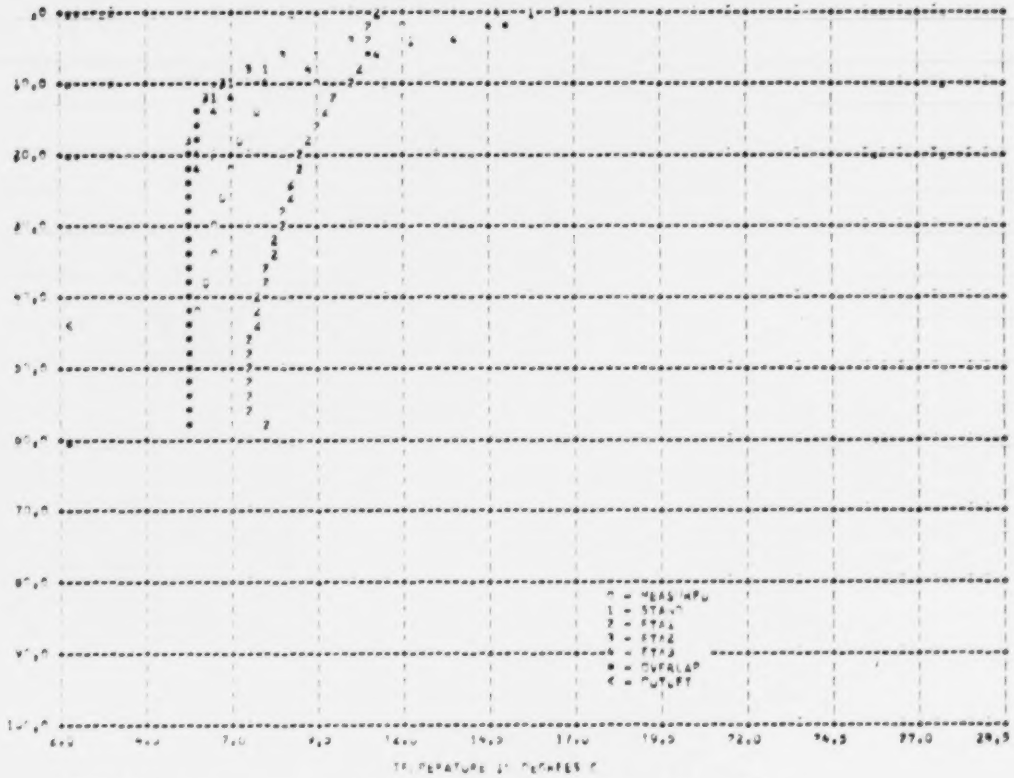

Figure 107 [illegible]

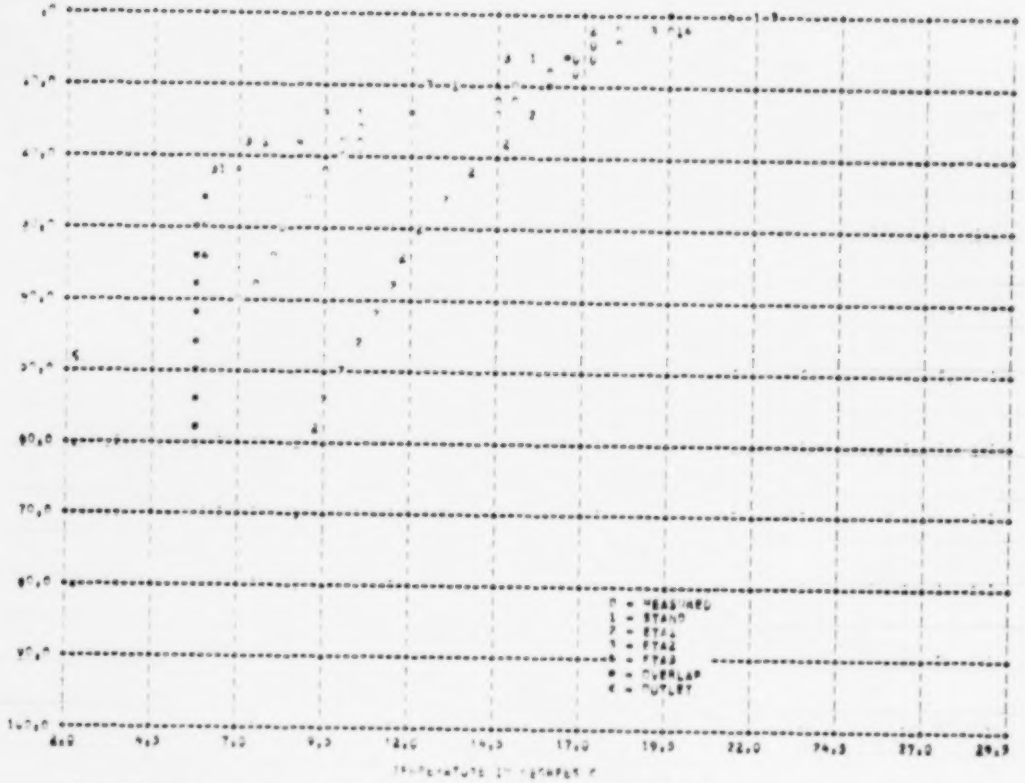

Figure 108 [illegible]

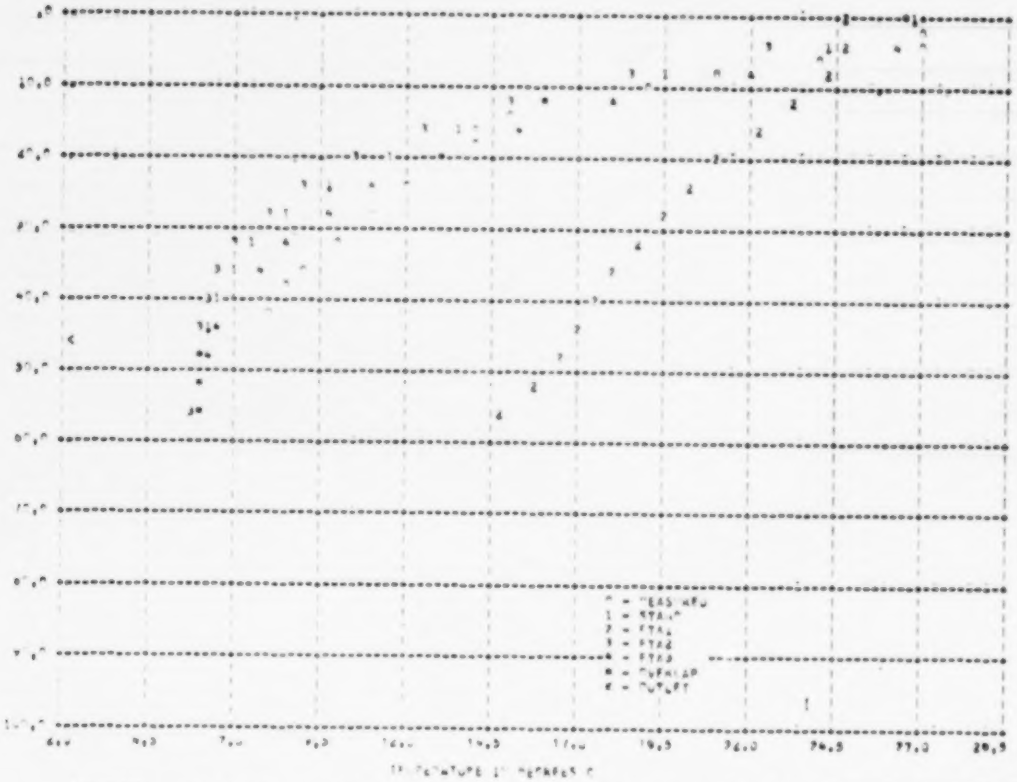

Figure 109 [illegible]

Reproduced from
best available copy.

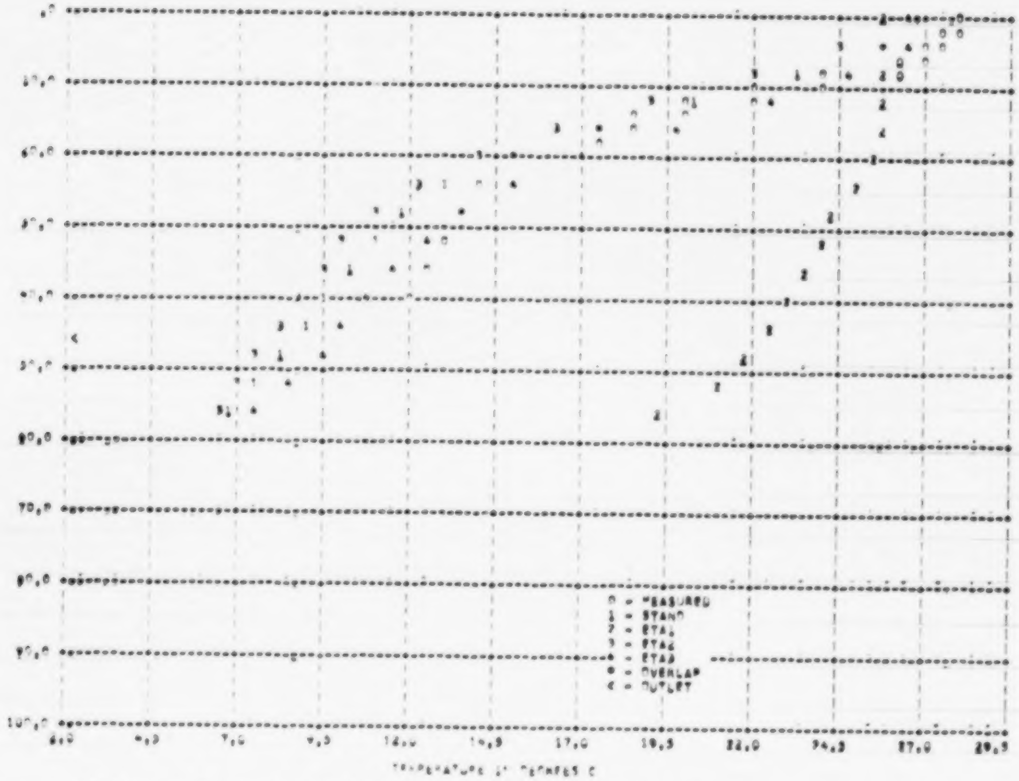

Figure 110 [illegible] 1971 [illegible] --SURFACE ELEV. 310.1 M

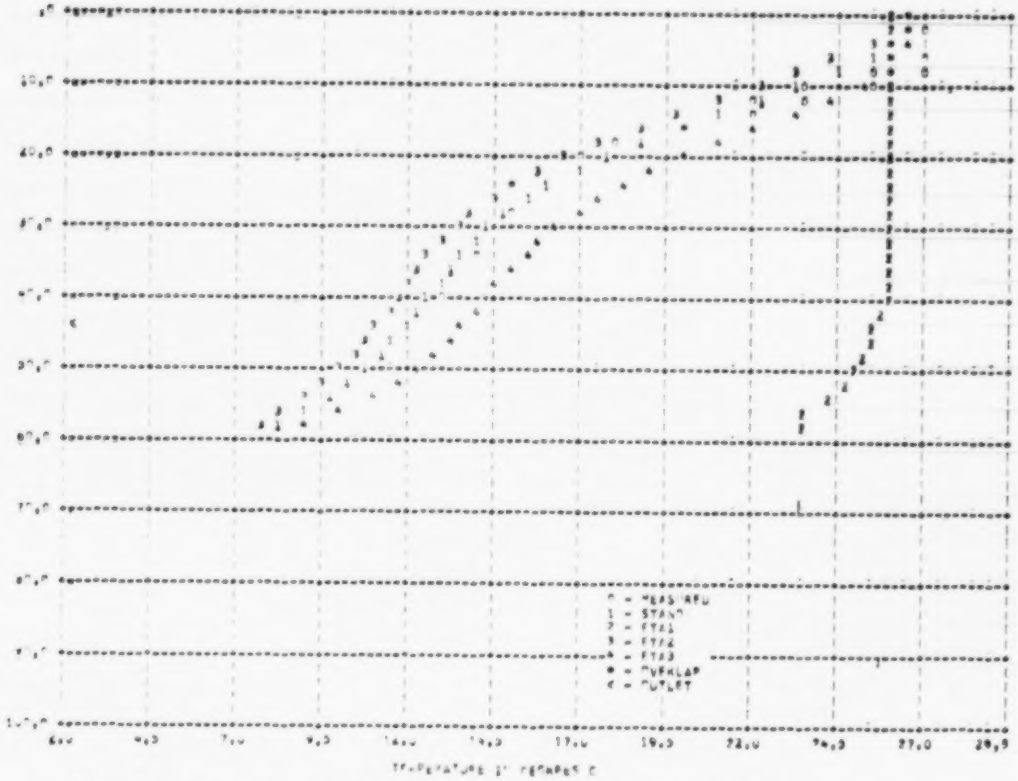

Figure 111 [illegible] 1971 [illegible] --SURFACE ELEV. 307.9 M

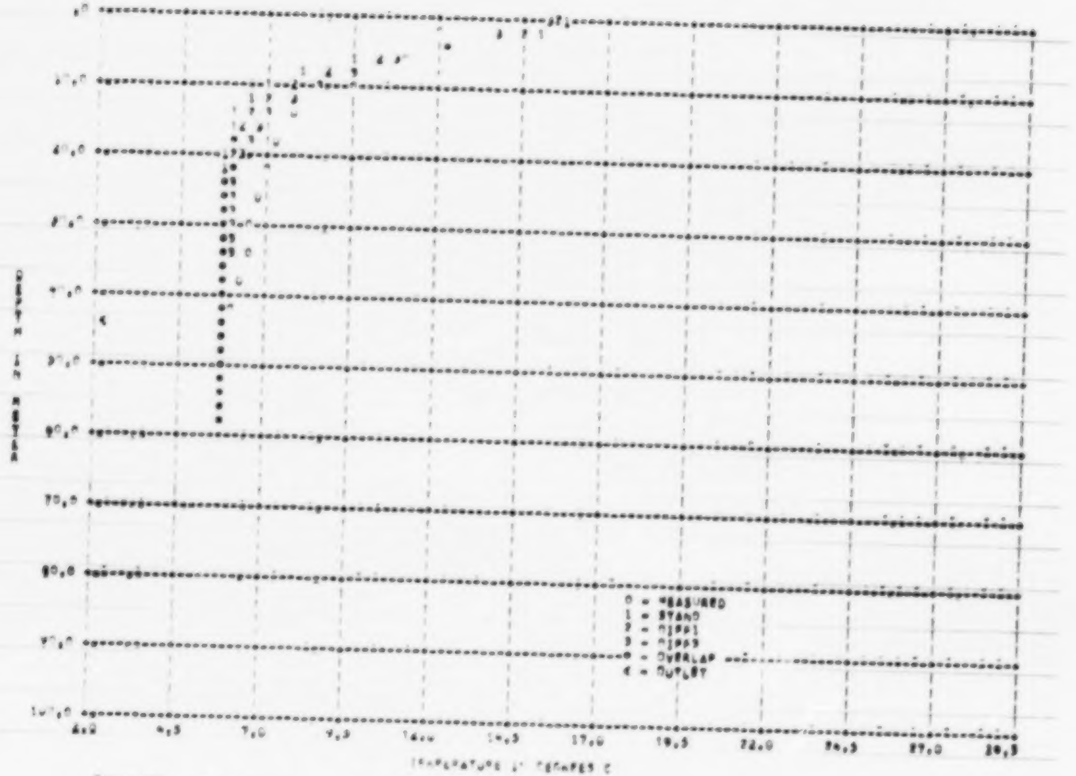

Figure 112 [illegible] SURFACE ELEV: 308.1 M

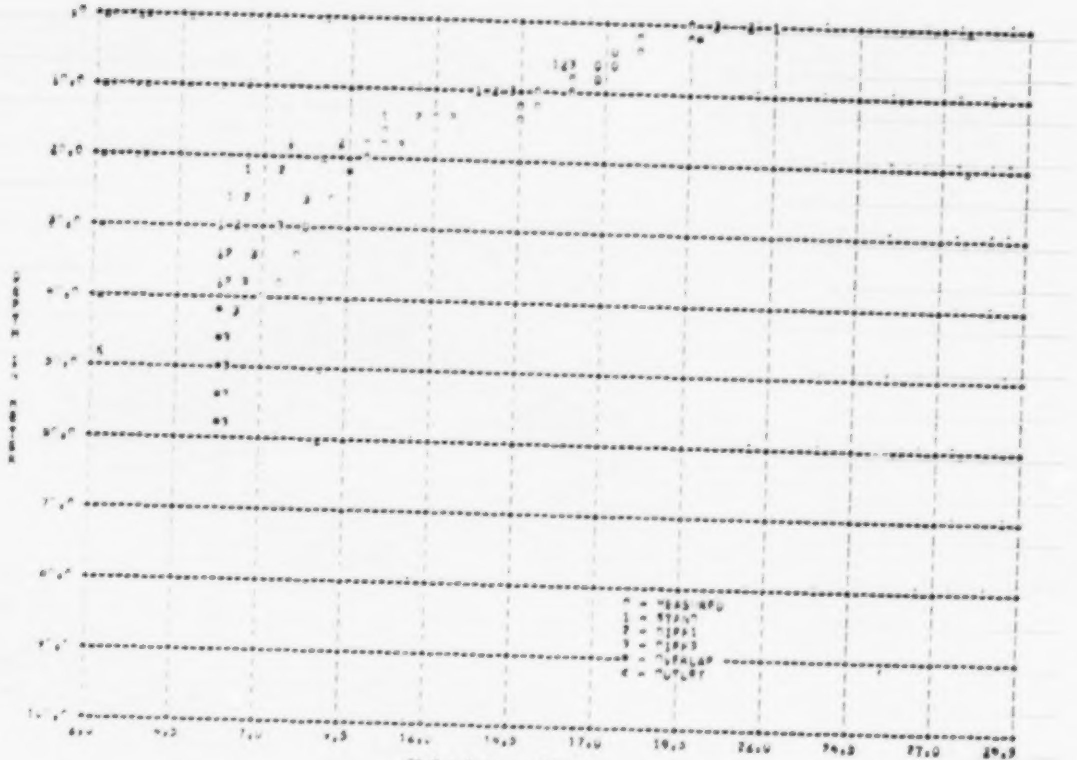

Figure 113 [illegible] SURFACE ELEV: 312.2 M

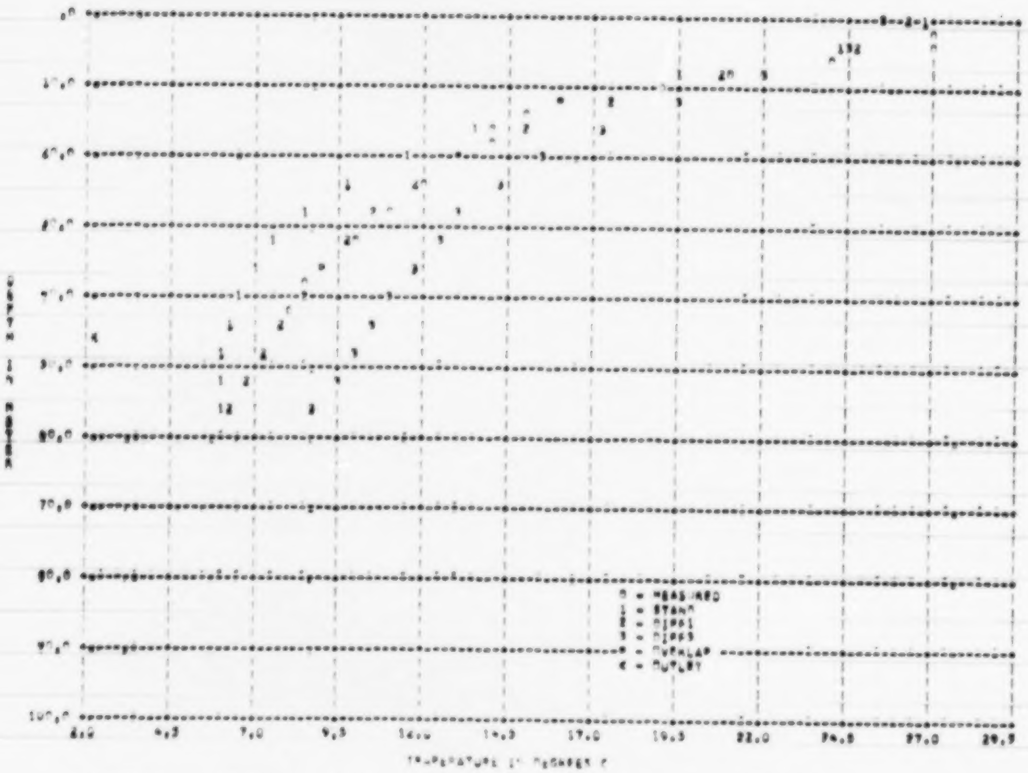

Figure 114 [illegible] SURFACE ELEV. [illegible]

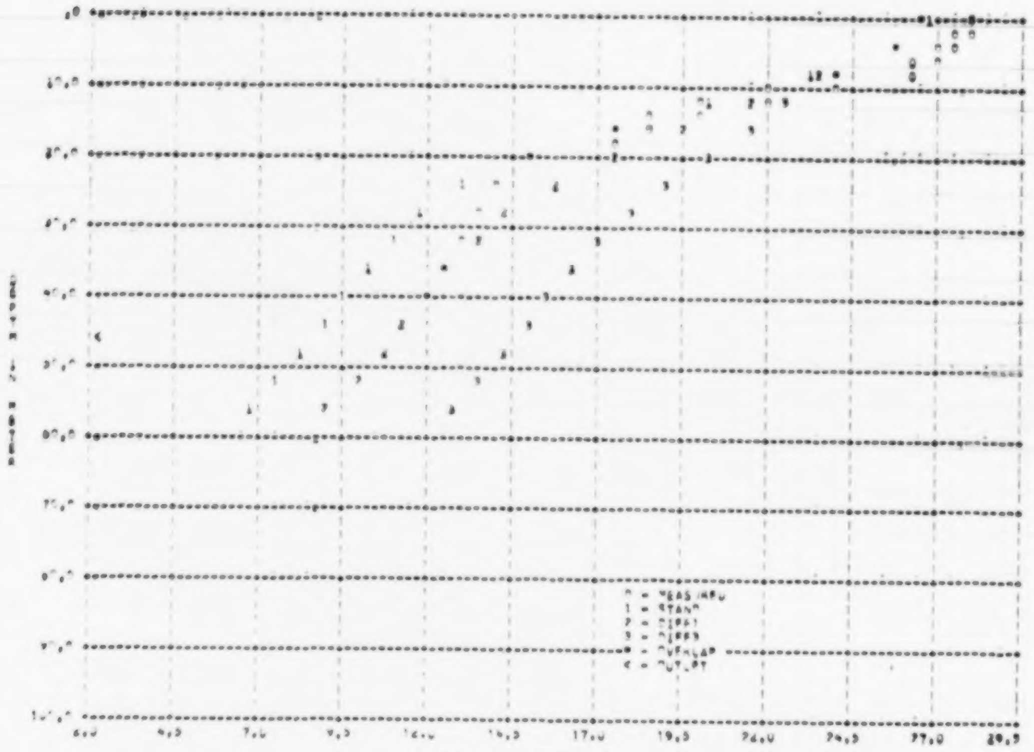

Figure 115 [illegible] SURFACE ELEV. [illegible]

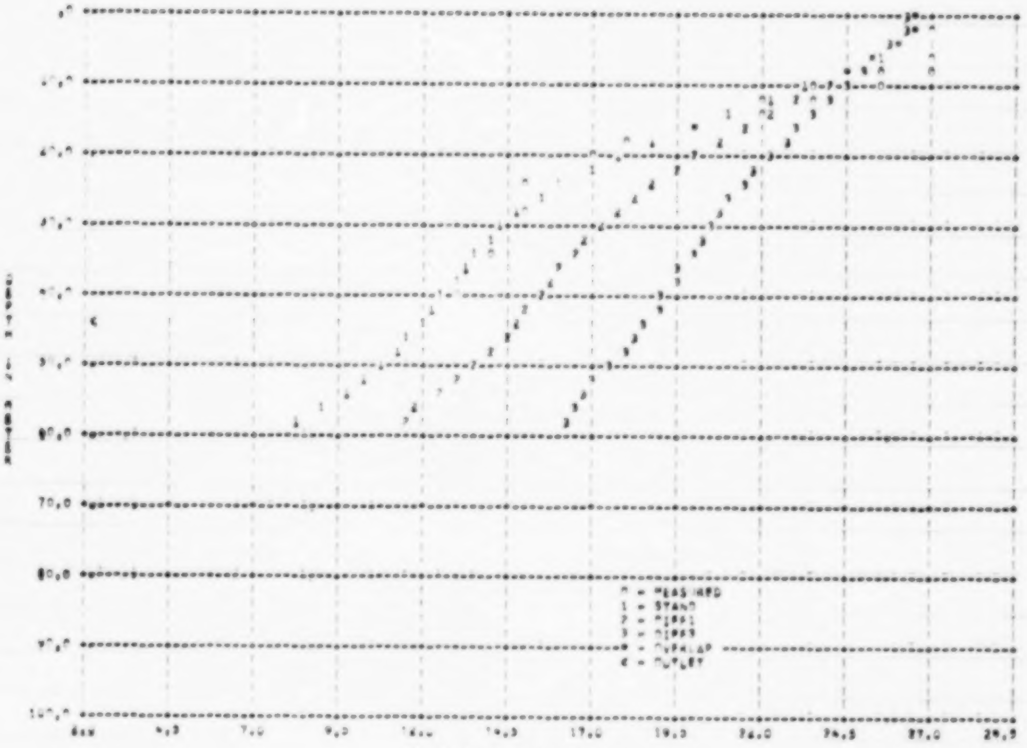

Figure 116 [illegible]

STOP [illegible]

SOUTH HOLSTON RESERVOIR

Figures 117 and 118 show the computed and measured temperature profiles for South Holston Reservoir for 1953. It can be seen that the computed temperatures do compare, in general, reasonably well with the measured temperatures. However, some of the predicted temperatures are quite different from the measured values and account for the fairly large standard errors of estimate for outlet level and surface water temperatures, as shown in Tables 15 and 16, 2.4° and 2.9° respectively. The computed outflow temperature using the Kohler evaporation formula is shown in Figure 119. In Figures 120 and 125 it is shown that the effect of the variation in thickness of the horizontal segments from 1 to 3 meters makes only minor differences in the predicted temperatures. This is verified in Tables 15 and 16 where the standard errors of estimate are similar to those predicted by using the standard thickness of 2 meters.

In Figures 126 to 131 the effect of the variation of β, the fraction of solar radiation abosrbed at the water surface, from 0.2 to 0.5 on the predicted temperature is shown to be negligible. This is verified in Tables 15 and 16 where the standard errors of estimate are shown to be similar to those obtained for the standard β of 0.5.

In Figures 132 to 137 is shown the effect of variation in η, the radiation absorption coefficient, from 0.05 to 1.40. It can be seen that the use of the 0.05 coefficient predicts temperatures quite different from the measured values and quite different from the predicted values using other absorption coefficients. This is verified in Tables 15 and 16, where the standard errors of estimate are one half and twice those predicted with the standard absorption coefficient, 0.75.

In Figures 138 to 143 are shown the effects of varying the diffusion coefficient from molecular to 100 times molecular diffusion on the temperatures. It can be seen that, in general, the use of the molecular diffusion coefficient predicts the temperatures most closely and that the use of 100 times molecular diffusion predicts the temperature most poorly as indicated in Tables 15 and 16.

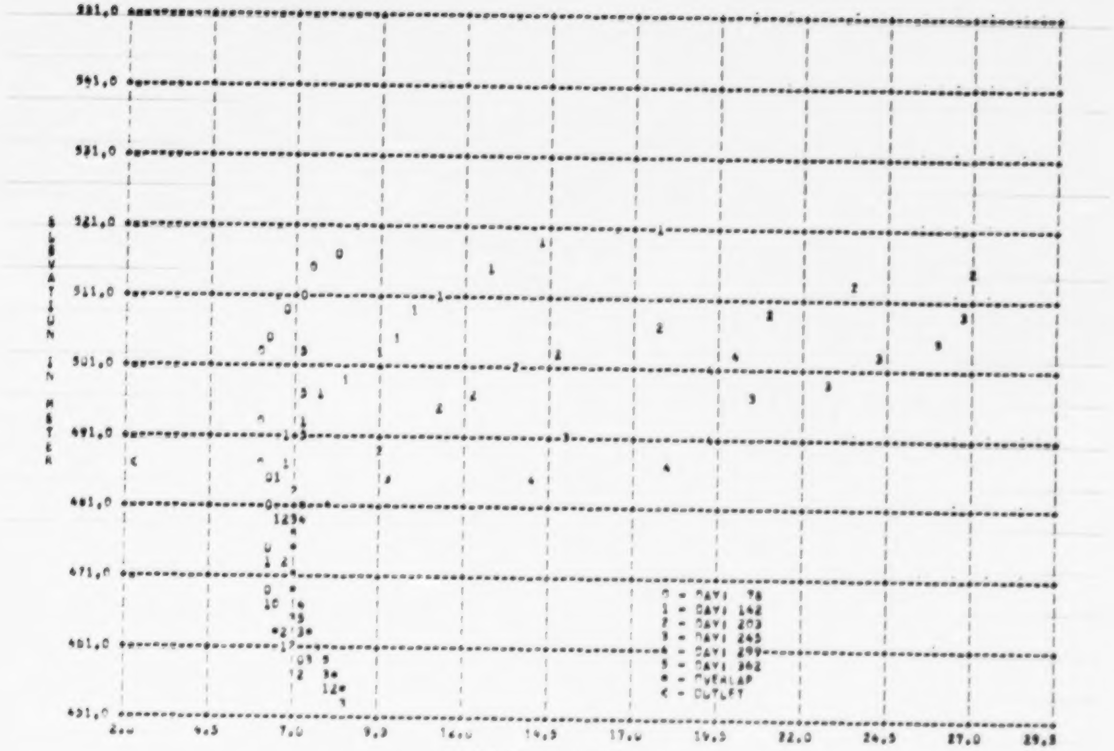

Figure 117 [illegible] SOUTH INLET [illegible] TEMPERATURE PROFILE

STOP 0

Table 15

STATISTICAL ANALYSIS FOR THE PREDICTED WATER TEMPERATURE AT OUTLET LEVEL

Reservoir/Year: South Holston/1953

Time Period Covered: 120th - 330th Julian Day

File Name	Std. error of estimate (°C)	Correlation Coefficient
STAND	2.88	0.87
DELZ 1	2.72	0.89
DELZ 2	3.02	0.86
BETA 1	2.95	0.87
BETA 2	3.08	0.86
ETA 1	7.07	0.00
ETA 2	2.49	0.90
ETA 3	----	----
DIFF 1	3.21	0.83
DIFF 3	4.19	0.66

Table 16

STATISTICAL ANALYSIS FOR THE PREDICTED SURFACE WATER TEMPERATURE

Reservoir/Year: South Holston/1953

Time Period Covered: 60th - 360th Julian Day

File Name	Std. error of estimate (°C)	Correlation Coefficient
STAND	2.44	0.96
DELZ 1	2.53	0.96
DELZ 2	3.09	0.94
BETA 1	2.32	0.96
BETA 2	2.29	0.96
ETA 1	1.05	0.99
ETA 2	2.82	0.95
ETA 3	----	----
DIFF 1	2.18	0.97
DIFF 3	1.75	0.98

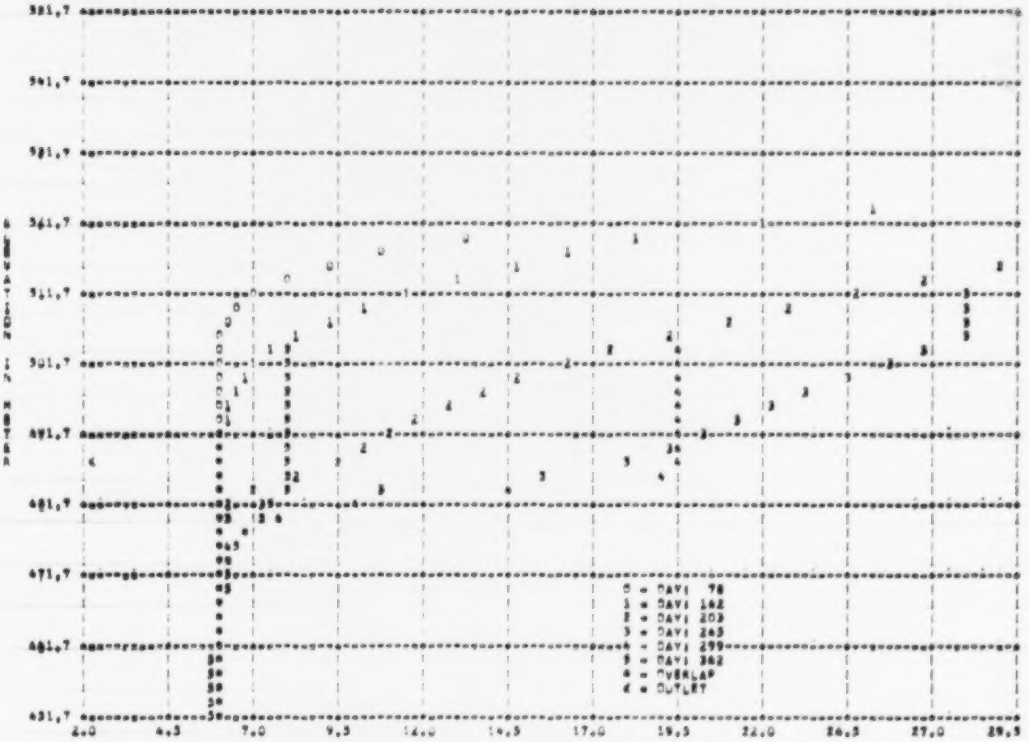

Figure 118 [illegible] COMPUTED TEMPERATURE PROFILES

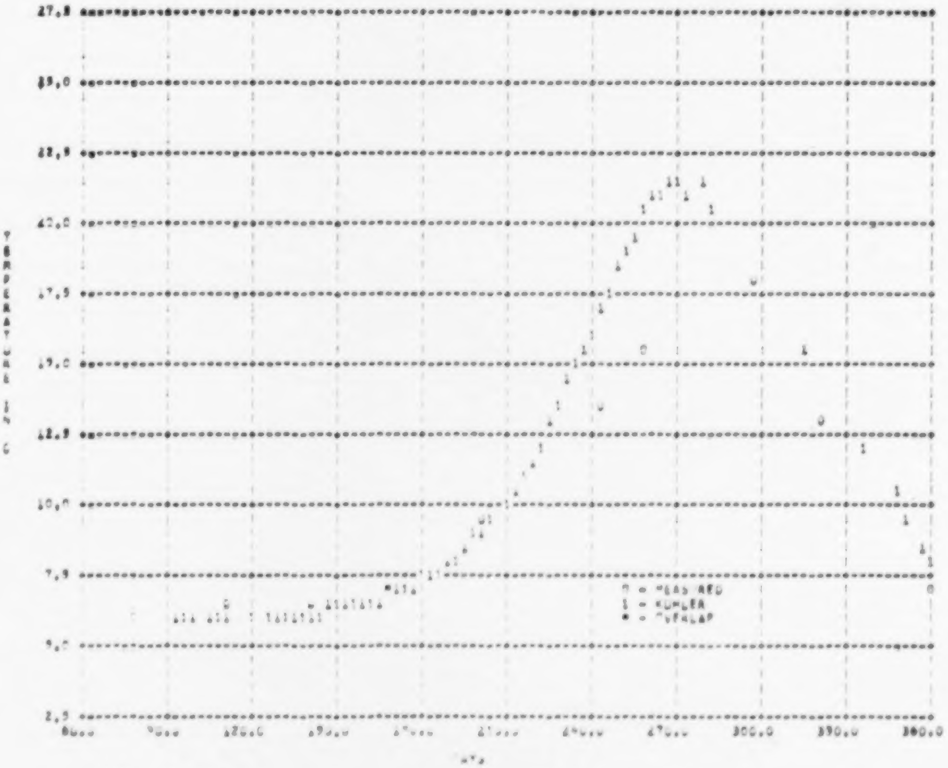

Figure 119 [illegible] COMPUTED OUTFLOW TEMPERATURES

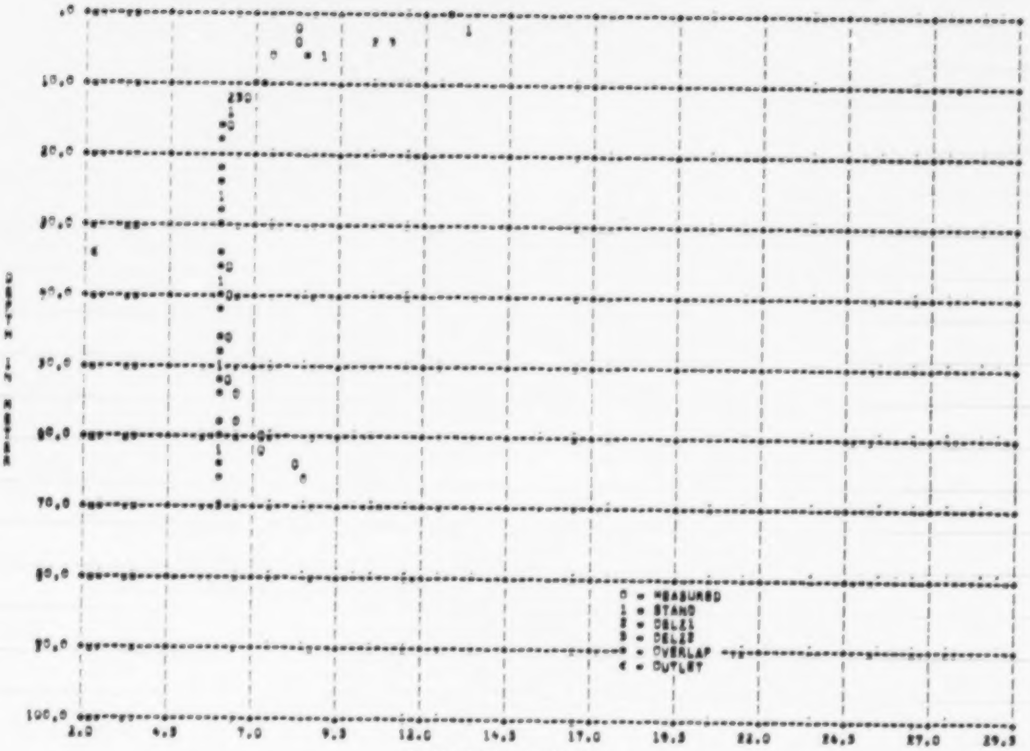

Figure 120. MIT MODEL * SOUTH HOLSTON 1959--DAY 78 --SURFACE ELEV: 520.9 M

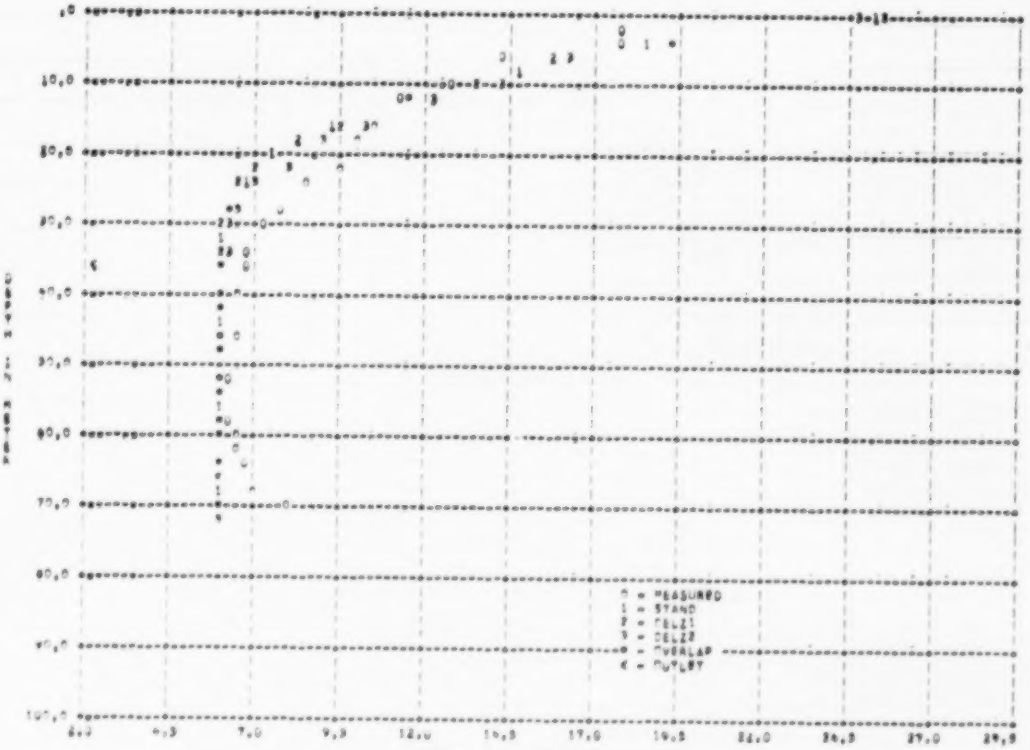

Figure 121. MIT MODEL * SOUTH HOLSTON 1959--DAY 142 --SURFACE ELEV: 524.2 M

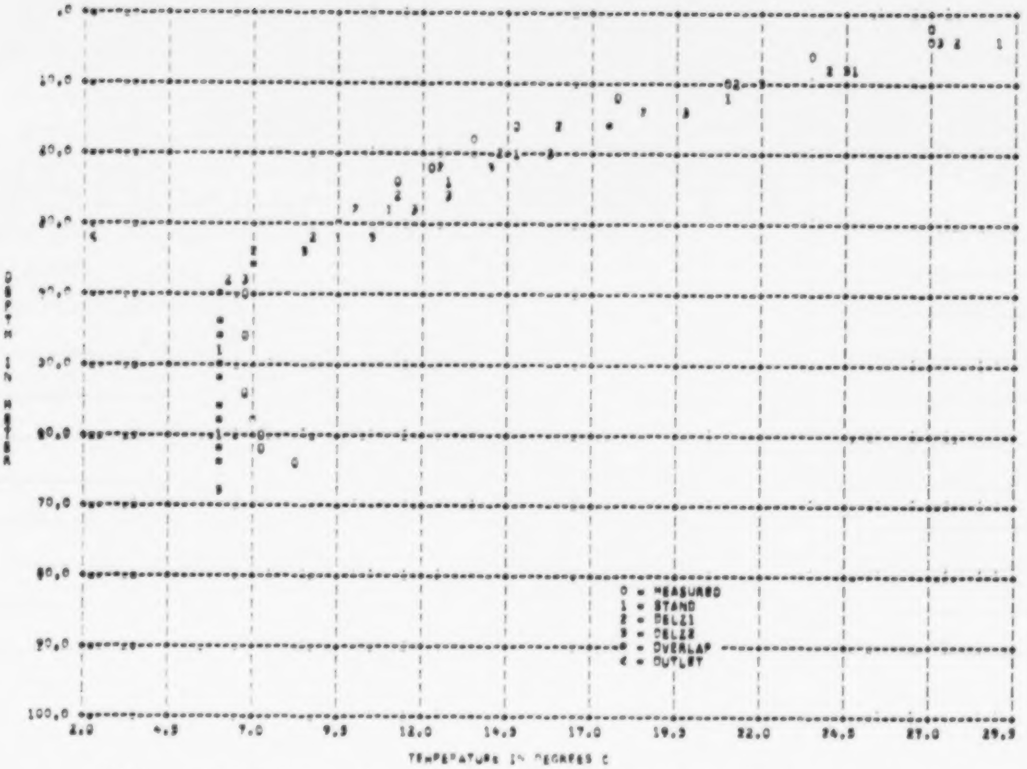

Figure 122 MIT MODEL * SOUTH HOLSTON 1959--DAY=203 --SURFACE ELEV: 518.8 M

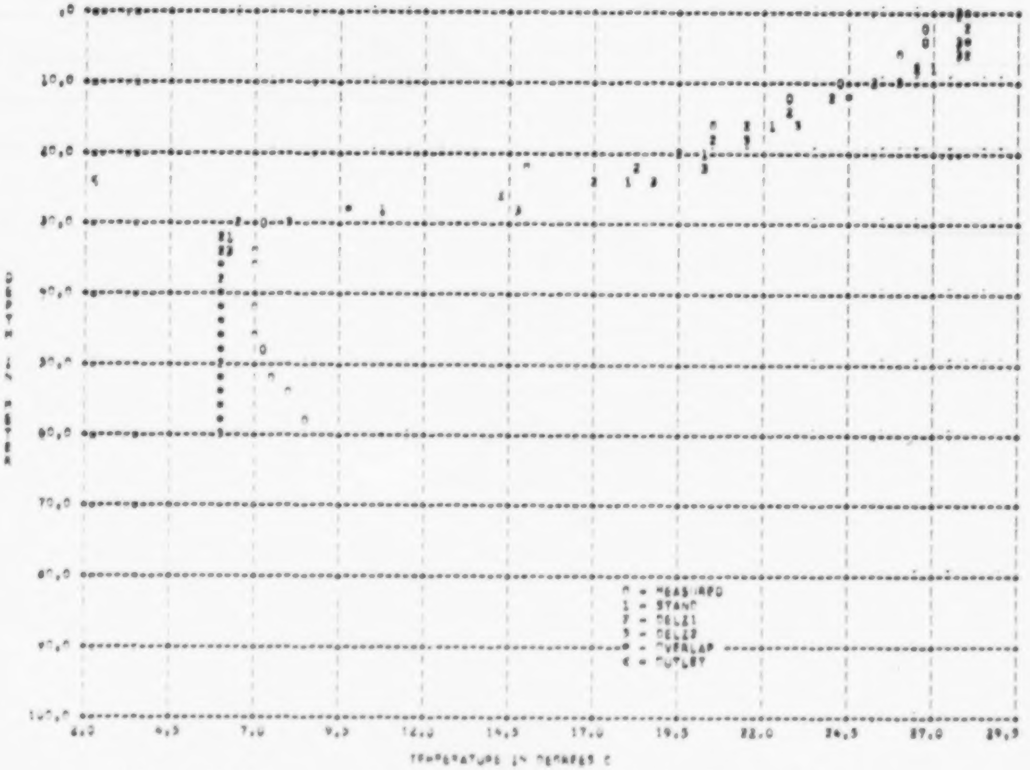

Figure 123 MIT MODEL * SOUTH HOLSTON 1959--DAY=249 --SURFACE ELEV: 511.8 M

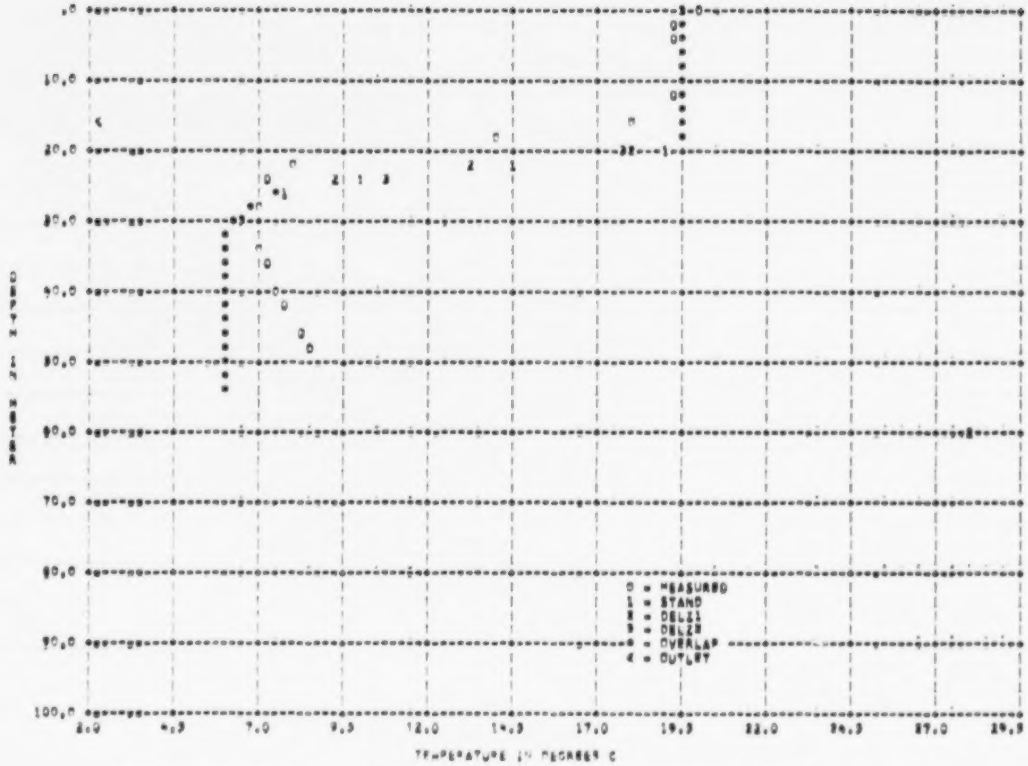

FIGURE 126. MIT MODEL 4 SOUTH HOLSTON 1989--DAY129 --SURFACE ELEV: 503.1 M

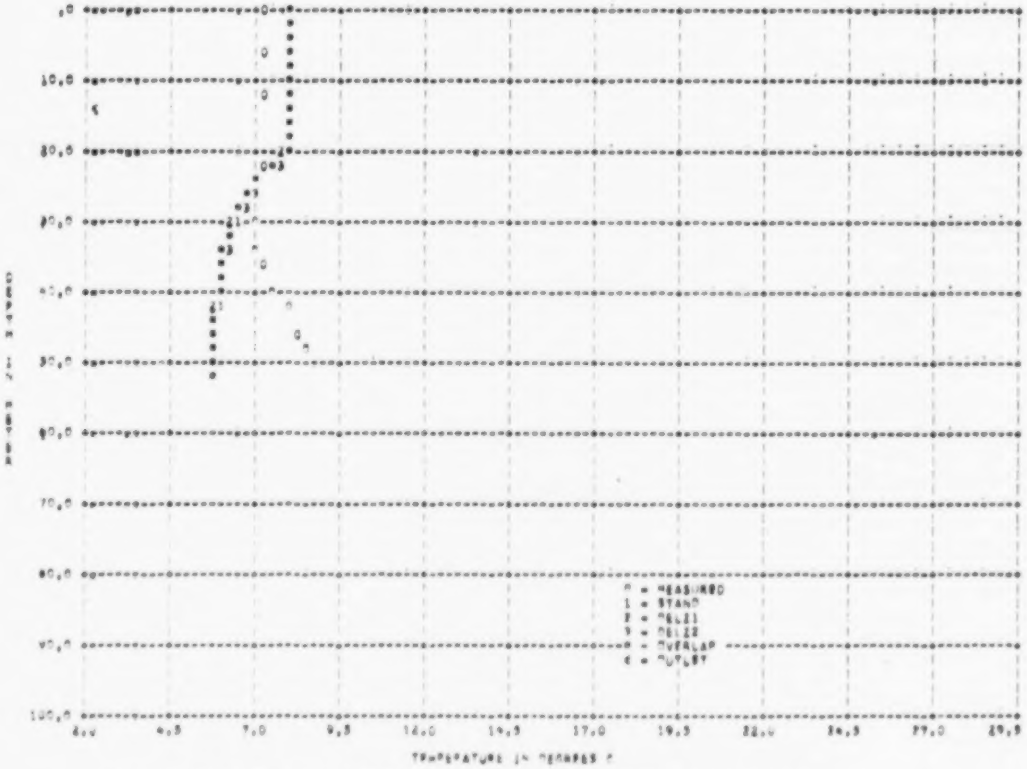

FIGURE 127. MIT MODEL 4 SOUTH HOLSTON 1989--DAY134 --SURFACE ELEV: 502.8 M

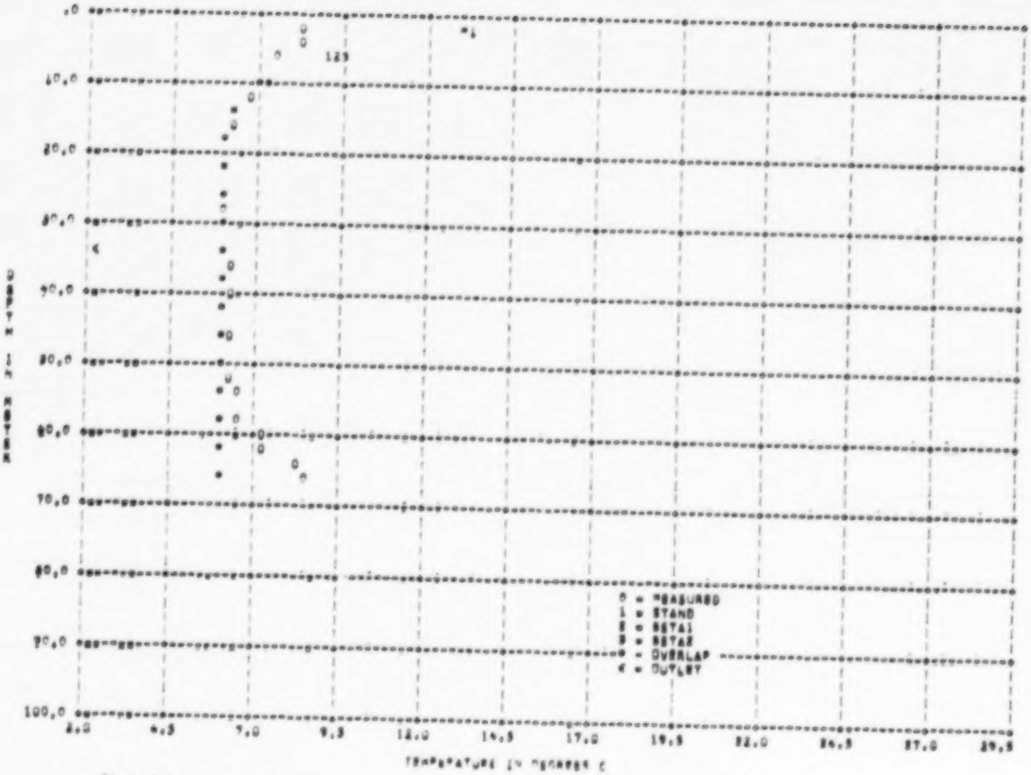

Figure 126 MIT MODEL - SOUTH HOLSTON 1959--DAY178 --SURFACE ELEV: 520.9 M

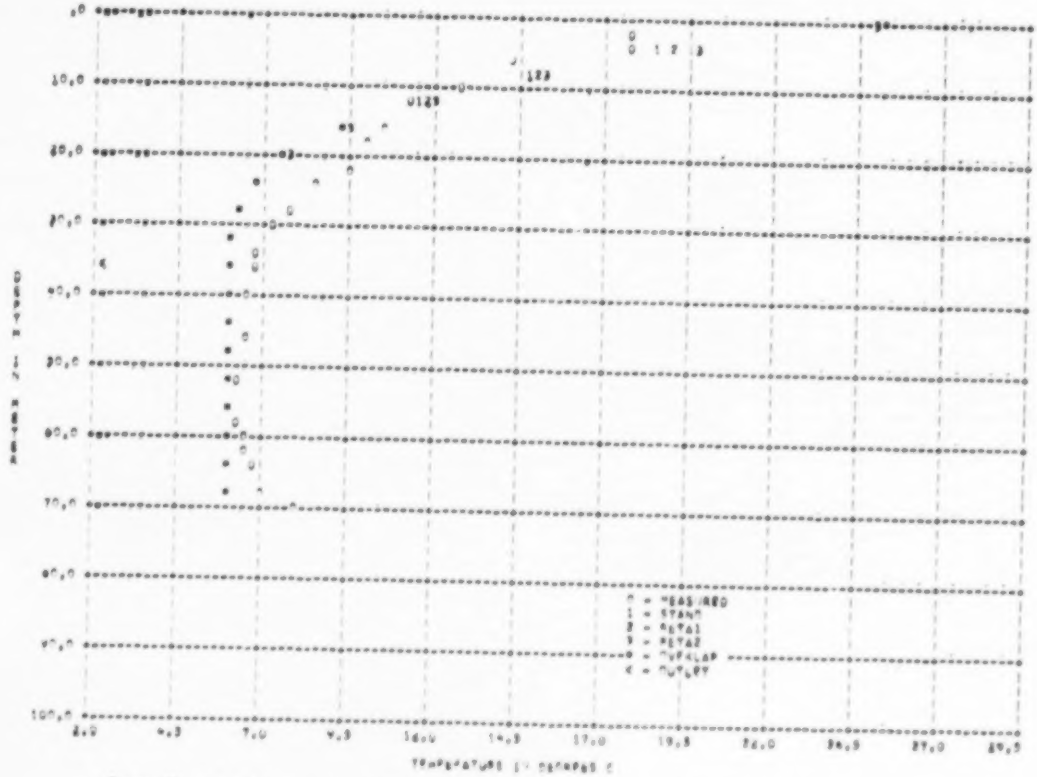

Figure 127 MIT MODEL - SOUTH HOLSTON 1959--DAY184 --SURFACE ELEV: 524.4 M

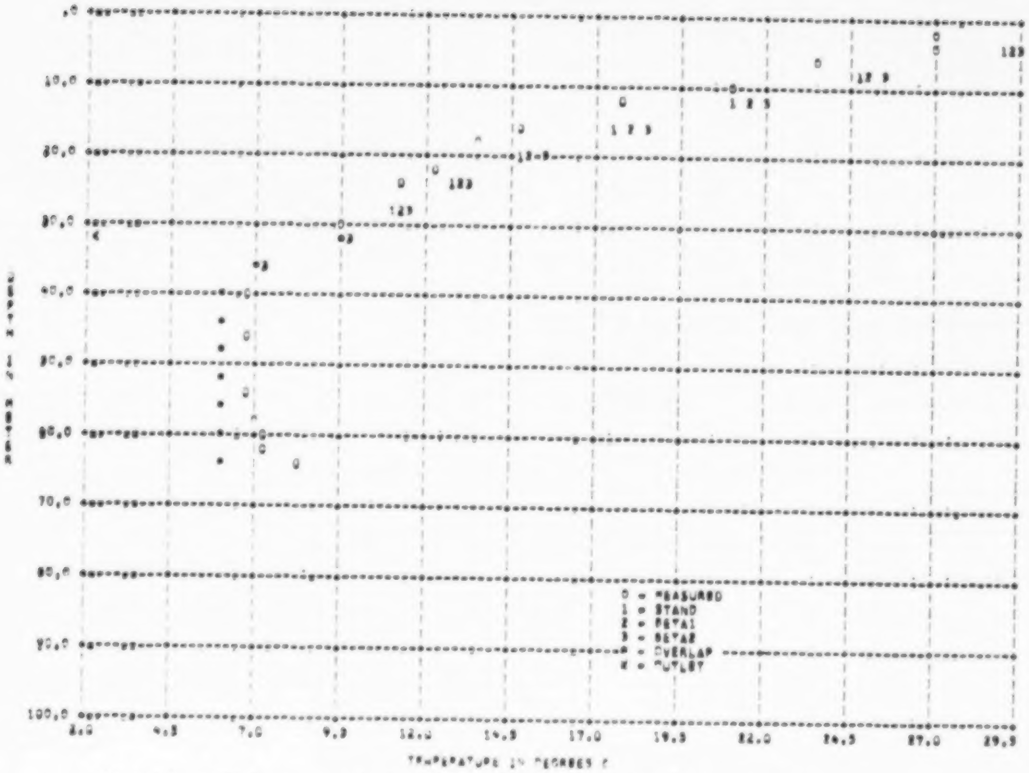

Figure [illegible]. MIX MODEL ● SOUTH HOLSTON 1953--DAY1263 --SURFACE ELEV: 516.8

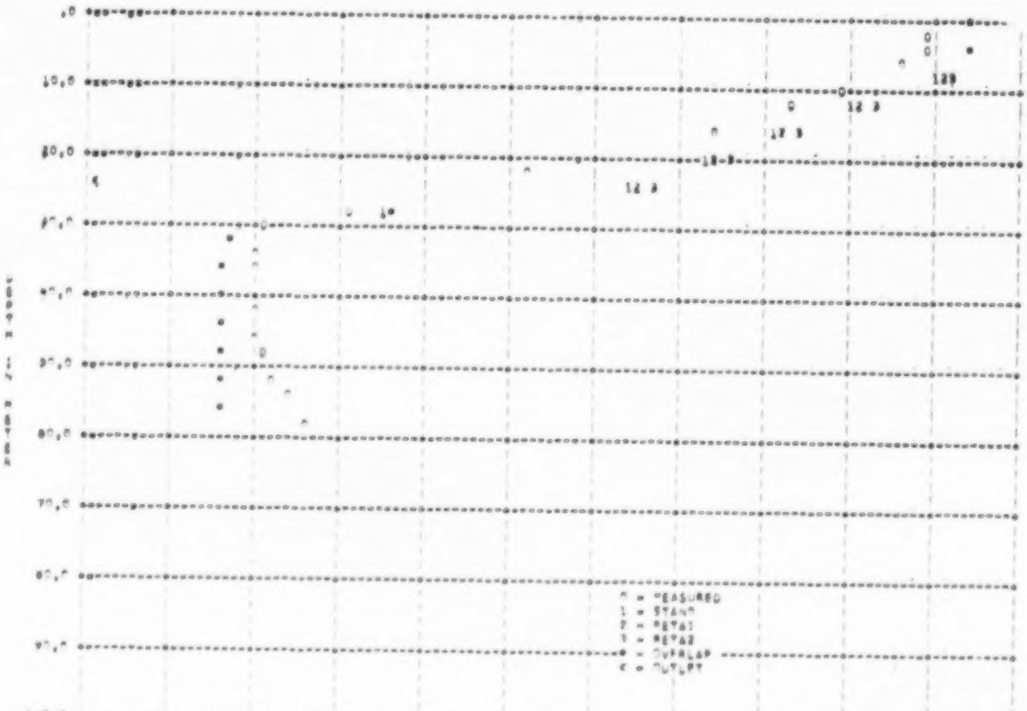

Figure [illegible]. MIX MODEL ● SOUTH HOLSTON 1953--DAY1265 --SURFACE ELEV: 511.6 M

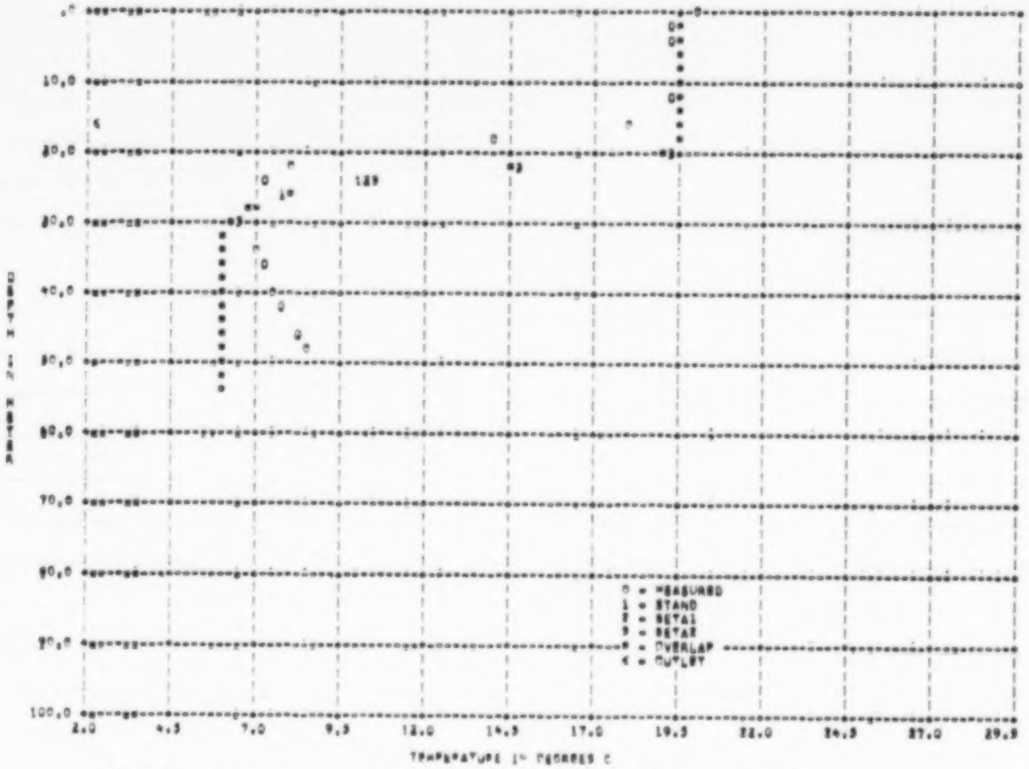

Figure 130 . HIT MODEL # SOUTH HOLSTON 1989--DAY1299 --SURFACE ELEV: 503.1 M

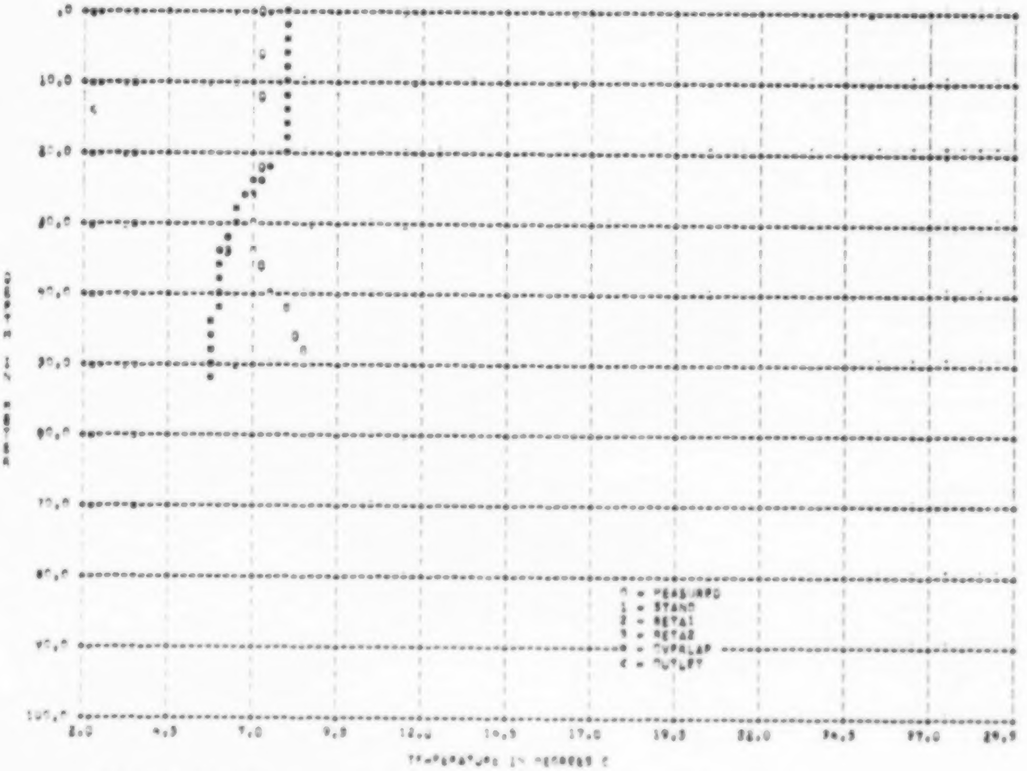

Figure 131 . HIT MODEL # SOUTH HOLSTON 1989--DAY1302 --SURFACE ELEV: 502.2 M

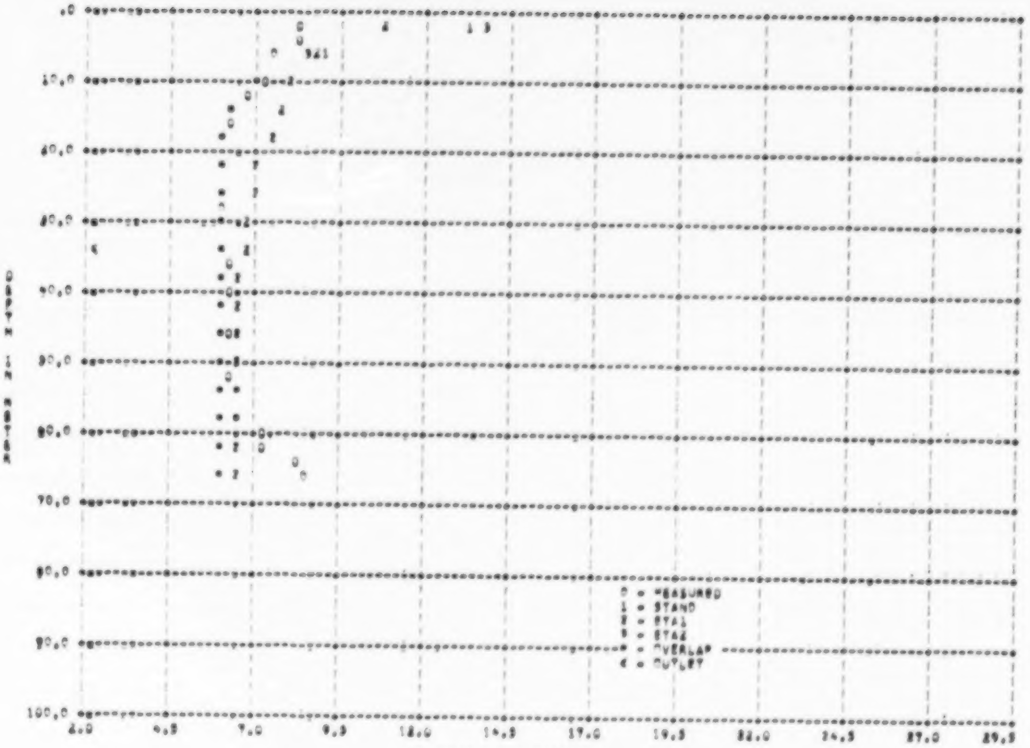

Figure [illegible] [illegible] SOUTH HOLSTON 1979—[illegible] —SURFACE ELEV: [illegible] M

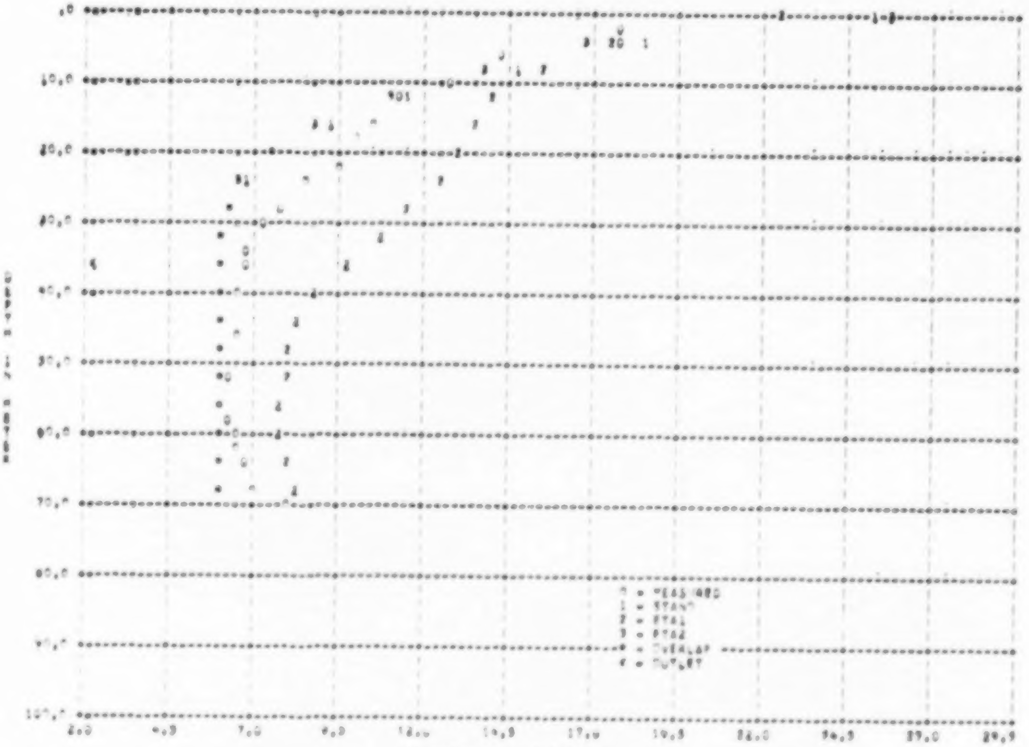

Figure [illegible] [illegible] SOUTH HOLSTON 1979—[illegible] —SURFACE ELEV: [illegible] M

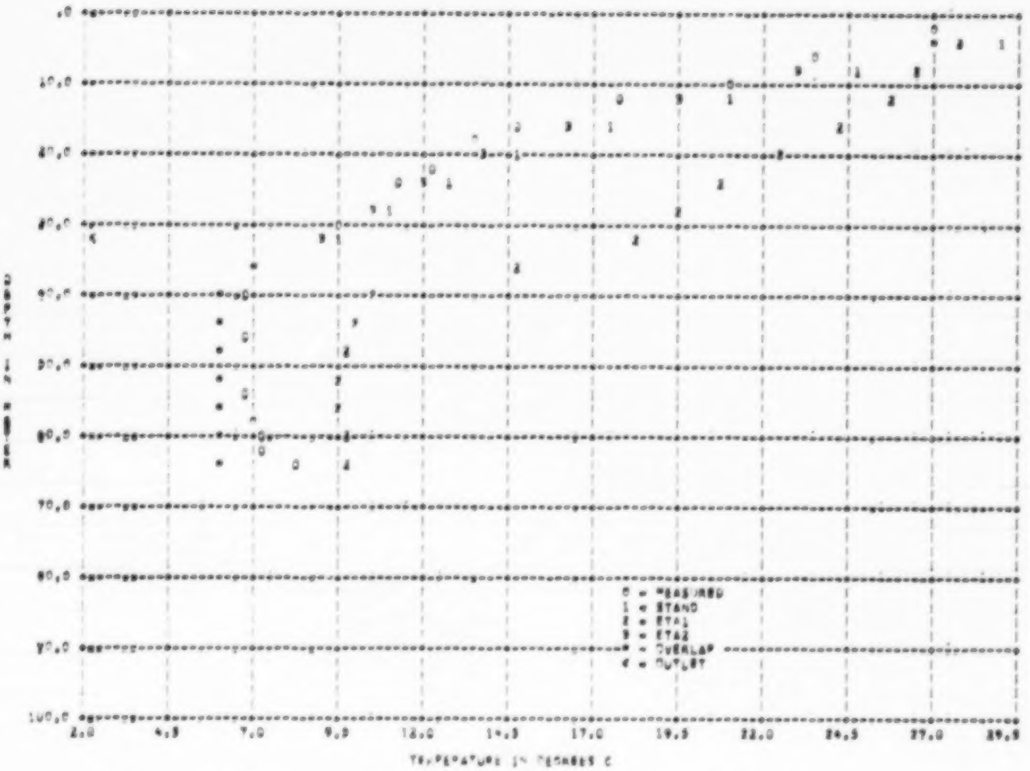

Figure 110. MIT MODEL [illegible] SOUTH HOLSTON 1959--DAY [illegible] --SURFACE ELEV: 518.8 M

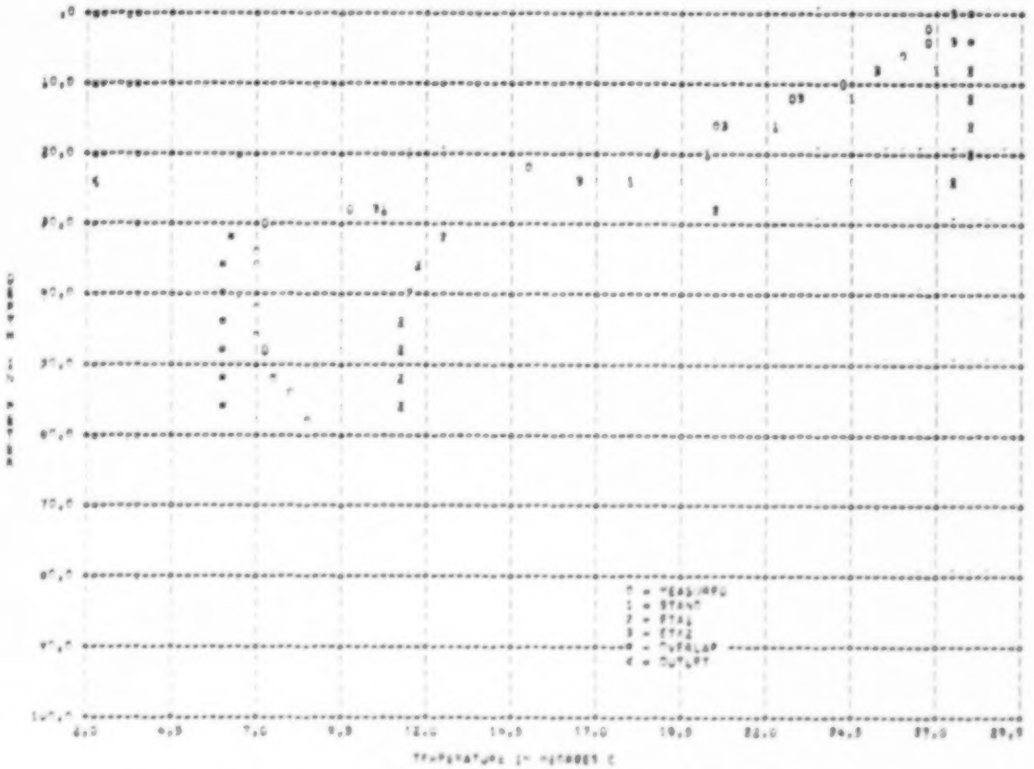

Figure 111. MIT MODEL [illegible] SOUTH HOLSTON 1959--DAY [illegible] --SURFACE ELEV: 511.0 M

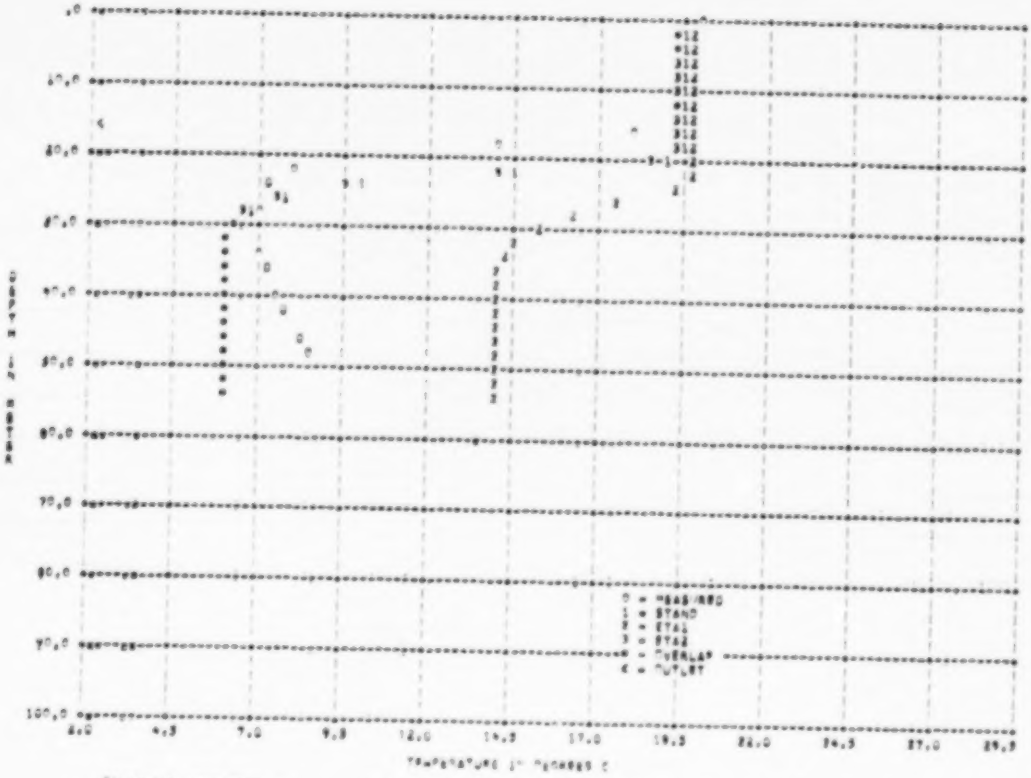
DEPTH IN METERS
TEMPERATURE IN DEGREES C
.0
10.0
20.0
30.0
40.0
50.0
60.0
70.0
80.0
90.0
100.0
2.0
4.5
7.0
9.5
12.0
14.5
17.0
19.5
22.0
24.5
27.0
29.5
0 = MEASURED
1 = STAND
2 = ETA1
3 = ETA2
* = OVERLAP
4 = OUTLET

[illegible]

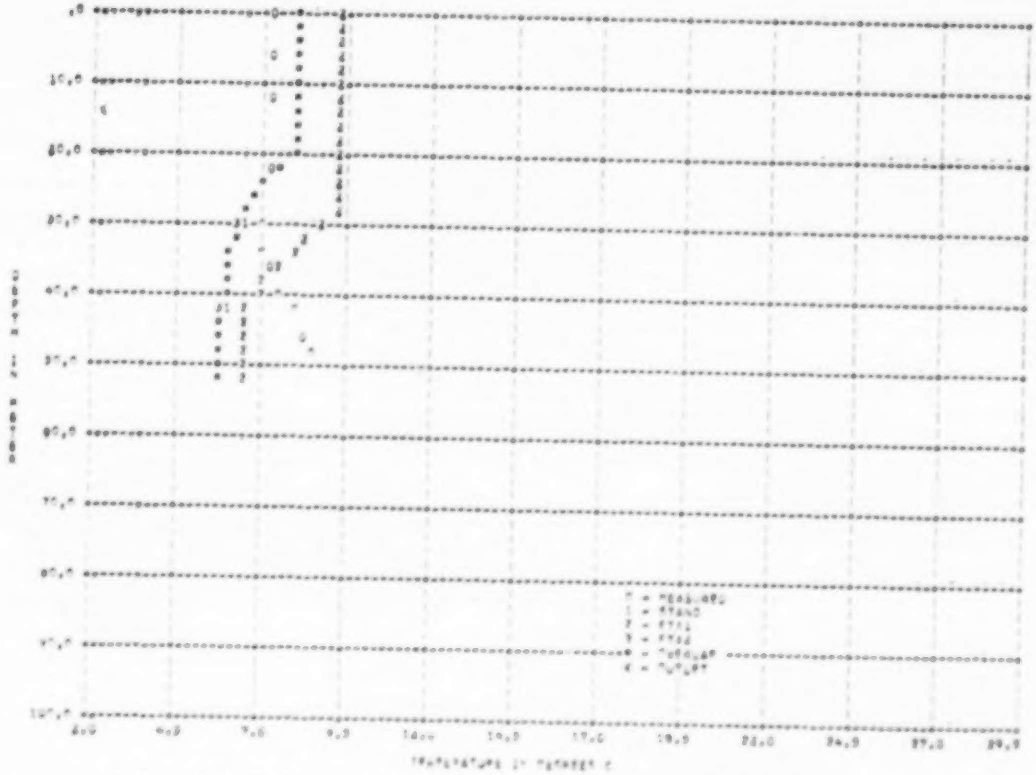
DEPTH IN METERS
TEMPERATURE IN DEGREES C
.0
10.0
20.0
30.0
40.0
50.0
60.0
70.0
80.0
90.0
100.0
2.0
4.5
7.0
9.5
12.0
14.5
17.0
19.5
22.0
24.5
27.0
29.5
0 = MEASURED
1 = STAND
2 = ETA1
3 = ETA2
* = OVERLAP
4 = OUTLET

[illegible]

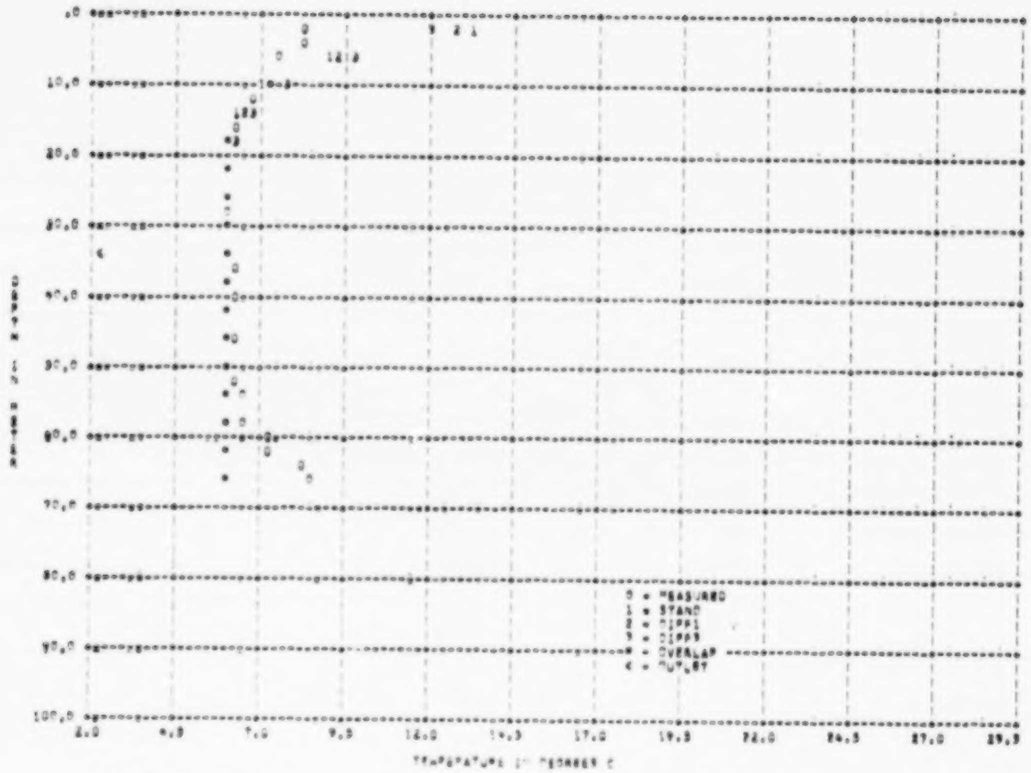

Figure [illegible] [illegible] 320.0 m

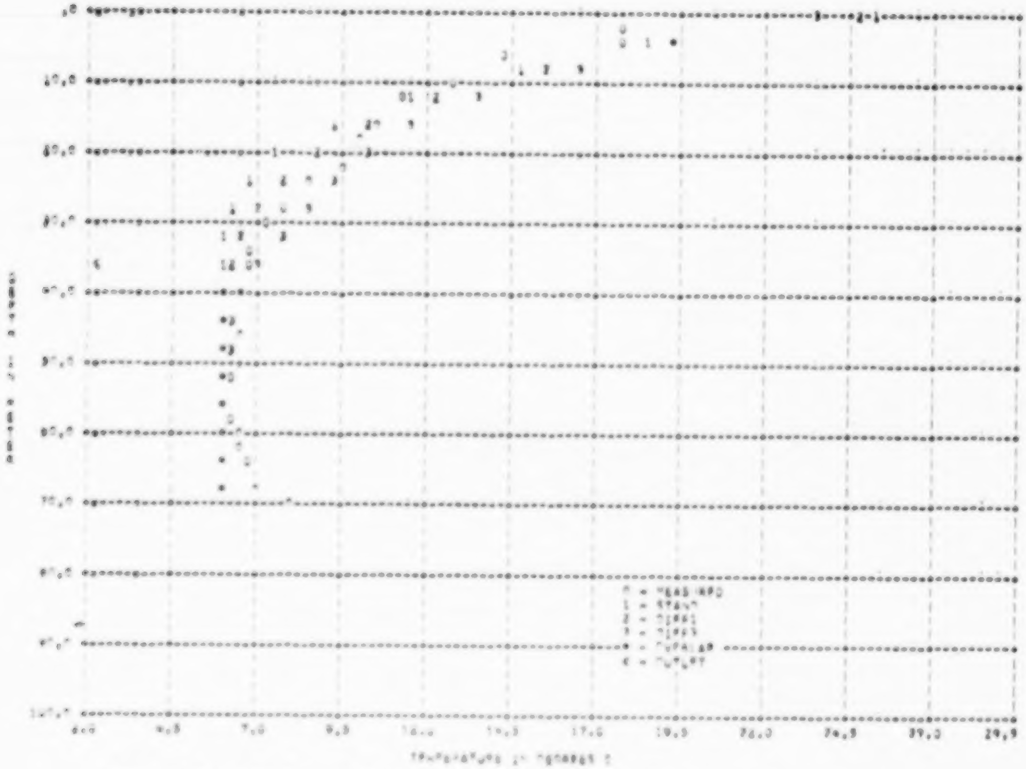

Figure [illegible] [illegible]

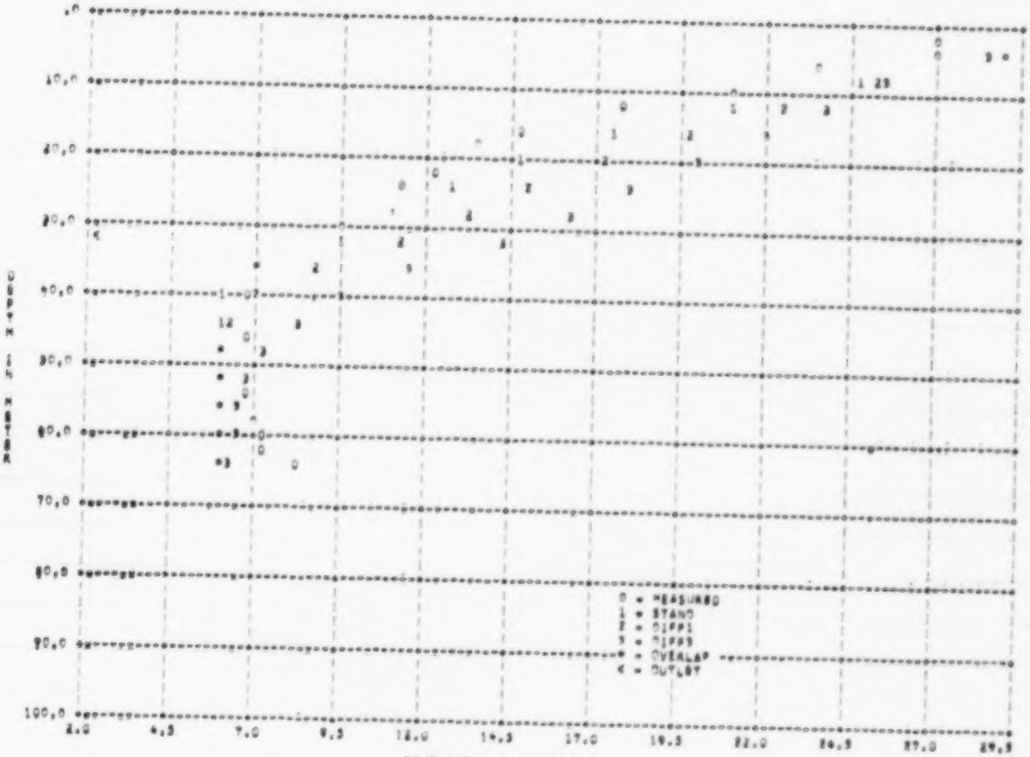

Figure 140 MIT MODEL * SOUTH HOLSTON 1959--DAY=233 --SURFACE ELEV: 510.8 M

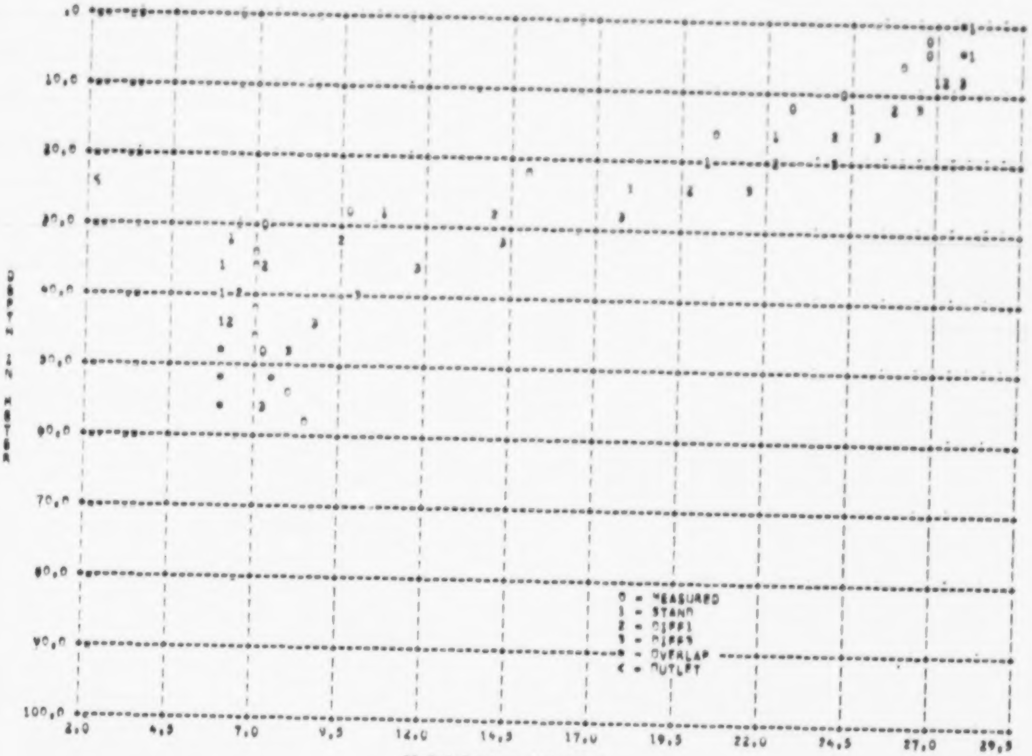

Figure 141 MIT MODEL * SOUTH HOLSTON 1959--DAY=240 --SURFACE ELEV: 511.0 M

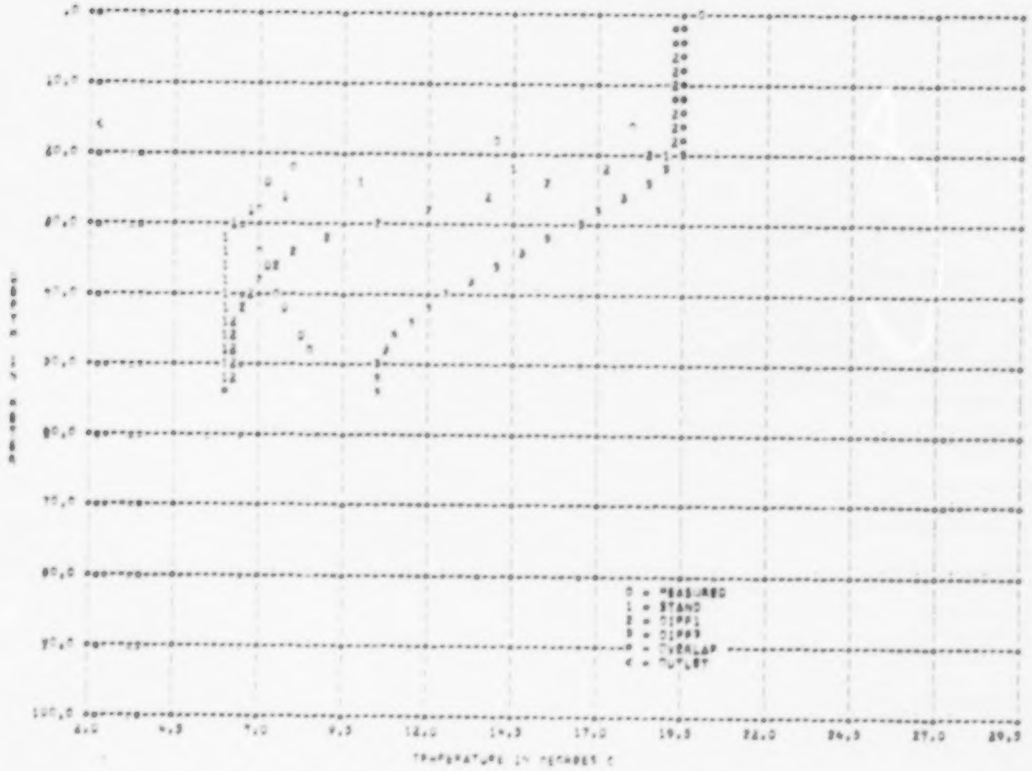

FIGURE [illegible] MIT MODEL • SOUTH HOLSTON 1959--DAY 299 --SURFACE ELEV: 508.1 M

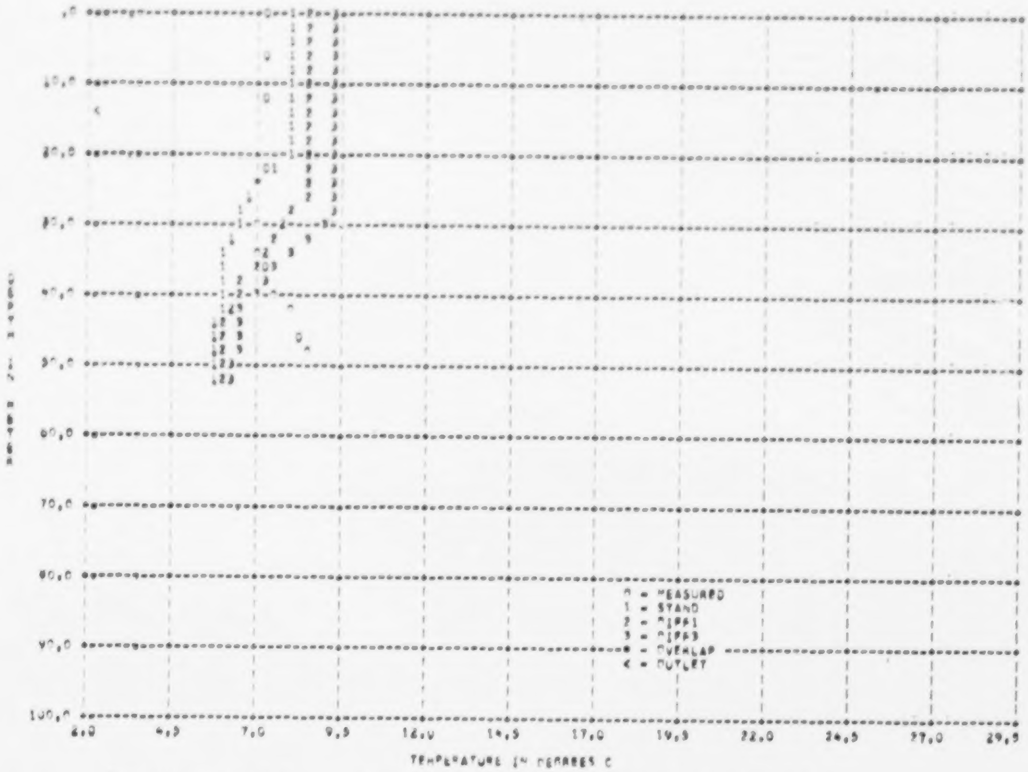

FIGURE [illegible] MIT MODEL • SOUTH HOLSTON 1959--DAY 342 --SURFACE ELEV: 502.2 M

HIWASSEE RESERVOIR

Figures 144 and 145 show the computed and measured temperature profiles for Hiwassee Reservoir for 1947 It can be seen that the computed temperatures do compare, in general, reasonably well with the measured temperatures. This can also be seen in Tables 17 and 18 where the standard errors of estimate are quite small, 1.0° and 1.4° for the outlet and surface water temperatures, respectively. The computed outflow temperature is compared with the measured outflow temperature in Figure 146 and is found to predict the temperatures very closely as is shown in Table 17. In Figures 147 to 152, is shown the effect of the variation in the thickness of the horizontal segments from 1 to 3 meters. The change causes only minor differences in the predicted temperature. This is verified in Tables 17 and 18 where the standard errors of estimate are only slightly different from those calculated using a 2 meter segment.

In Figures 153 to 158 the effect of the variation of β, the fraction of the solar radiation absorbed at the water surface, from 0.2 to 0.5 on the predicted temperature is shown to be negligible. This is verified in Tables 17 and 18, where the standard errors of estimate are shown to be similar to those obtained with the standard β of 0.5.

In Figures 159 to 164 is shown the effect of variation in η, the radiation absorption coefficient, from 0.05 to 1.40 per meter. It can be seen that the use of an absorption coefficient as low as 0.05 per meter gives very different results on day 209 in Figure 161 and similar results during most of the rest of the year. This is verified in Tables

17 and 18 where the standard error of estimate of temperature at the outlet level is almost 4 times the error for the standard case.

In Figures 165 to 170 are shown the effects in predicting temperatures of varying the diffusion coefficient from molecular to 100 times molecular diffusion. It can be seen that, in general, the use of molecular and 30 times molecular diffusion coefficients predicts the temperatures more closely to the measured values than does the use of the 100 times molecular diffusion coefficient. This is also indicated in Tables 17 and 18.

Table 17

STATISTICAL ANALYSIS FOR THE PREDICTED WATER TEMPERATURE AT OUTLET LEVEL

Reservoir/Year: Hiwassee/1947

Time Period Covered: 120th - 330th Julian Day

File Name	Std. error of estimate (°C)	Correlation Coefficient
STAND	1.01	0.98
DELZ 1	0.96	0.98
DELZ 2	1.03	0.98
BETA 1	1.03	0.98
BETA 2	1.06	0.98
ETA 1	3.95	0.79
ETA 2	1.08	0.98
ETA 3	----	----
DIFF 1	1.06	0.98
DIFF 3	1.44	0.97

Table 18

STATISTICAL ANALYSIS FOR THE PREDICTED SURFACE WATER TEMPERATURE

Reservoir/Year: Hiwassee/1947

Time Period Covered: 120th - 330th Julian Day

File Name	Std. error of estimate (°C)	Correlation Coefficient
STAND	1.38	0.99
DELZ 1	1.53	0.98
DELZ 2	1.34	0.99
BETA 1	1.38	0.99
BETA 2	1.37	0.99
ETA 1	1.44	0.98
ETA 2	1.40	0.99
ETA 3	----	----
DIFF 1	1.30	0.99
DIFF 3	1.26	0.99

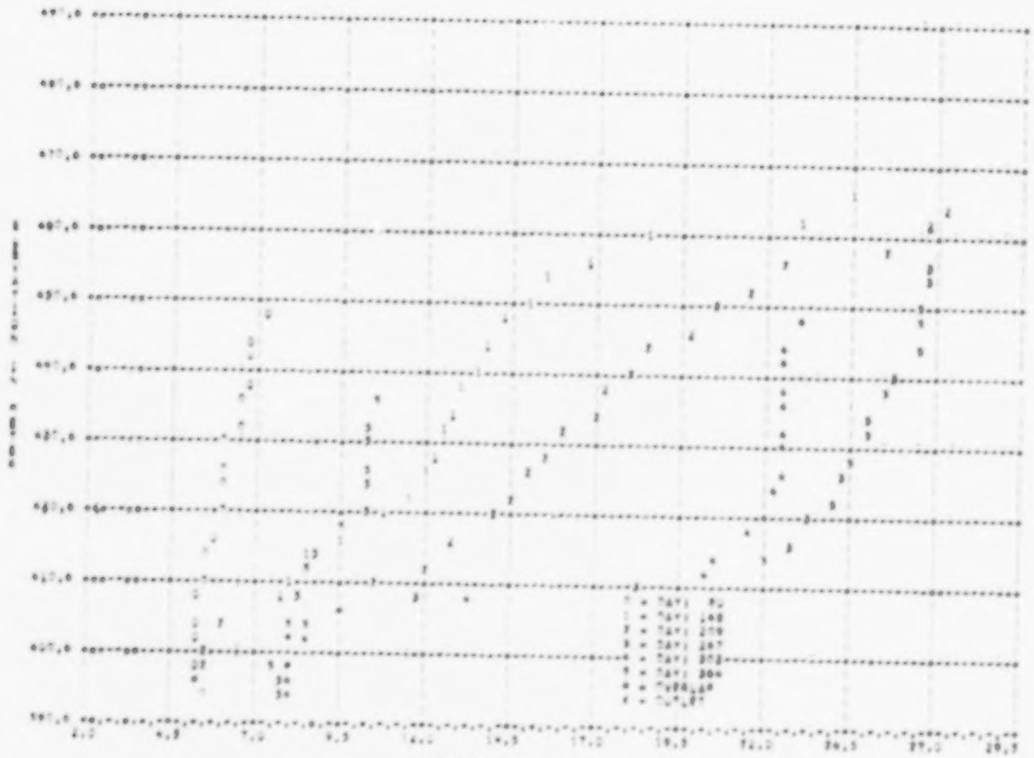

Figure [illegible]

MIT MODEL - HIWASSEE RESERVOIR 1967--MEASURED TEMPERATURE PROFILE--

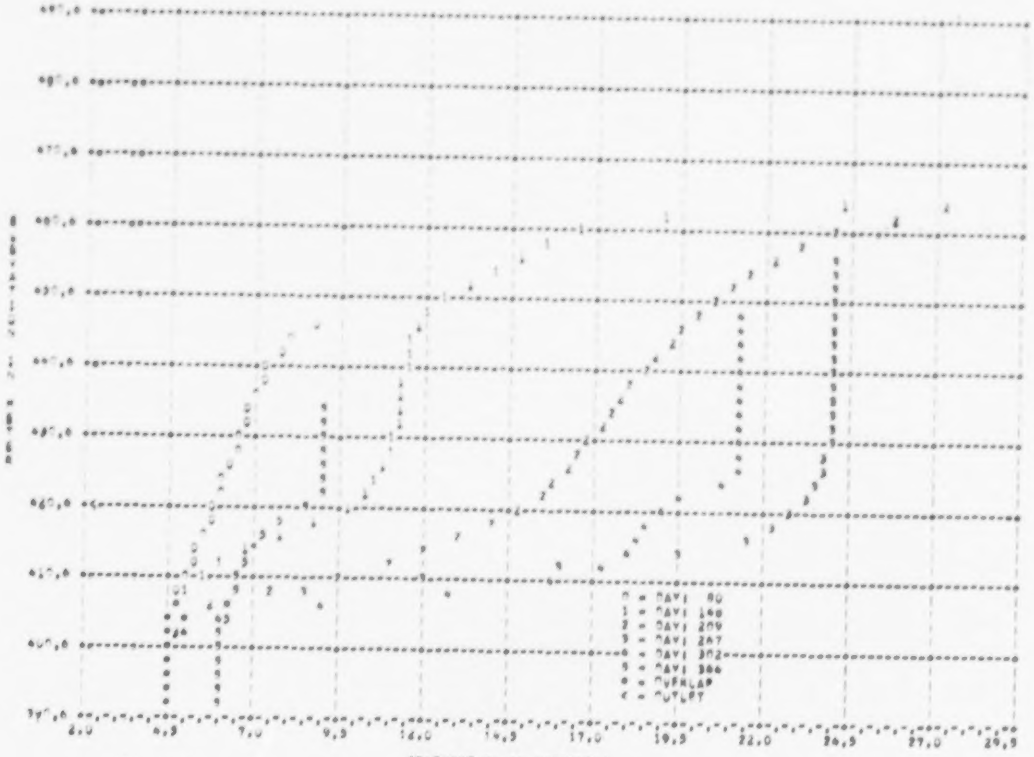

Figure [illegible]

MIT MODEL - HIWASSEE RESERVOIR 1967--COMPUTED TEMPERATURE PROFILE--

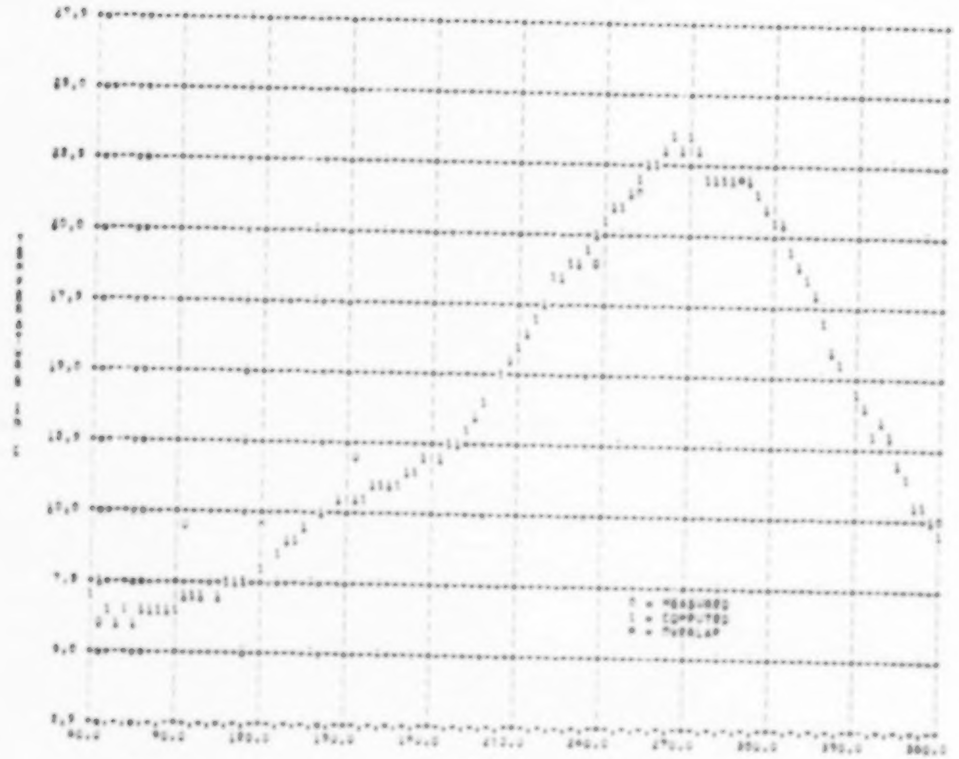

Figure 146

MIT MODEL I HIWASSEE RESERVOIR 1967--COMPUTED OUTFLOW TEMPERATURE--

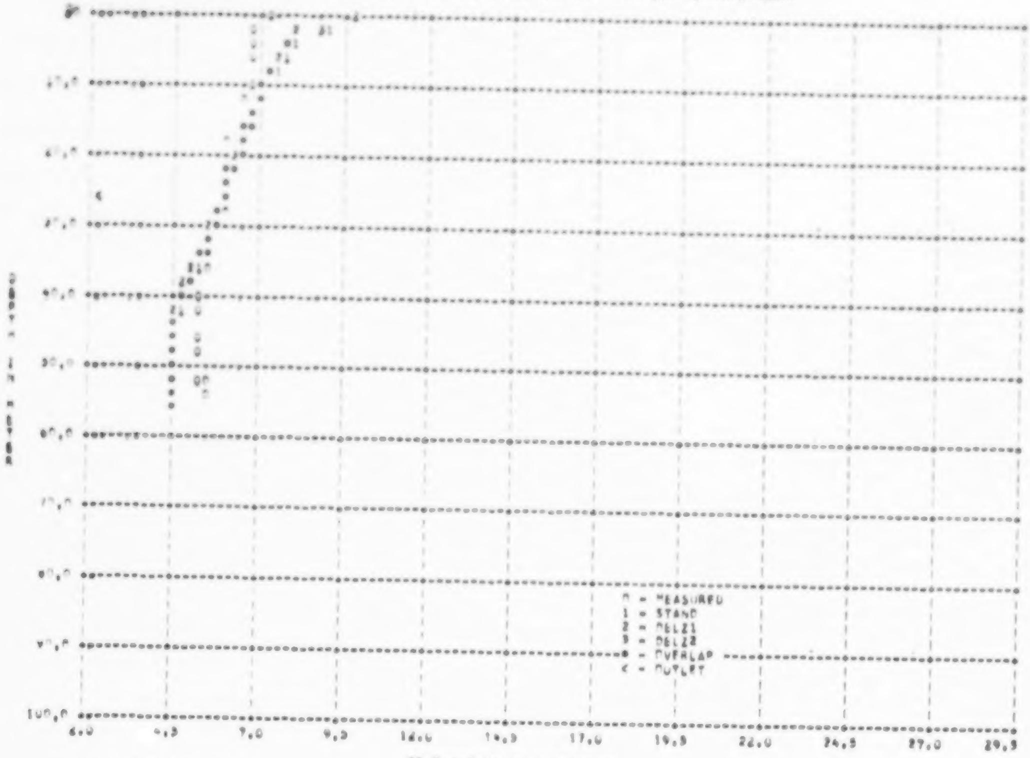

Figure 147

MIT MODEL * HIWASSEE RESERVOIR 1967--DAY [illegible] --SURFACE ELEV 466.0 M

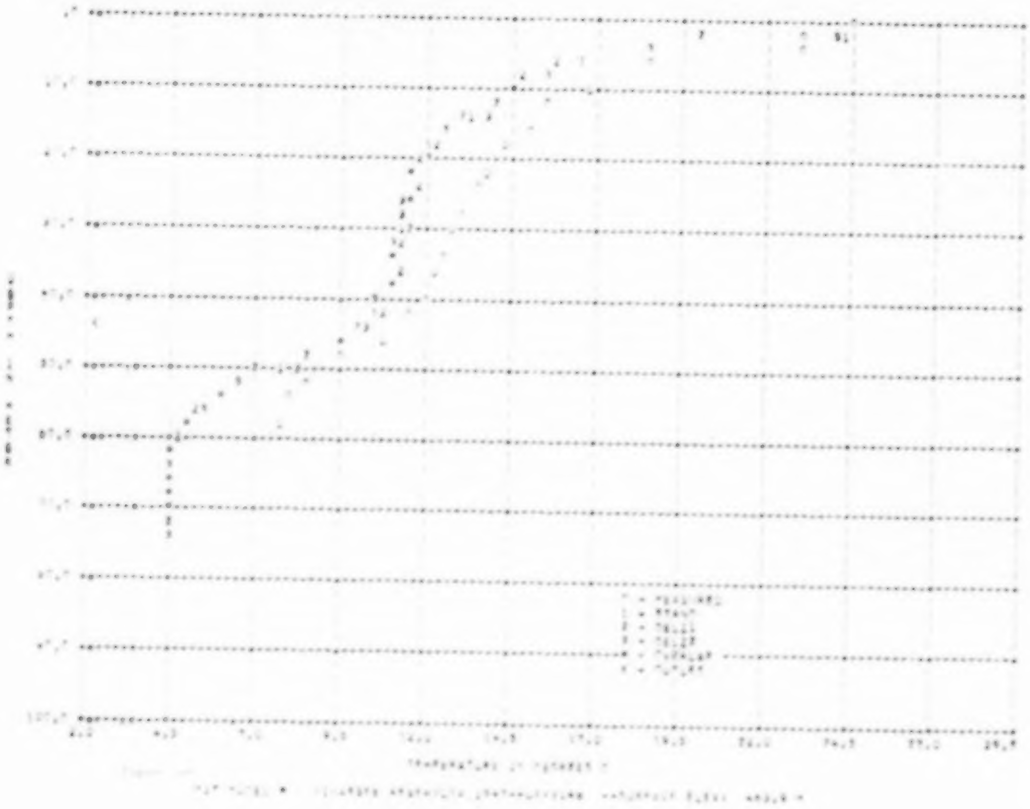
2.0
4.5
7.0
9.5
12.0
14.5
17.0
19.5
22.0
24.5
27.0
29.5
TEMPERATURE IN DEGREES C
0 = MEASURED
2 = DELZ1
3 = DELZ2
* = OVERLAP

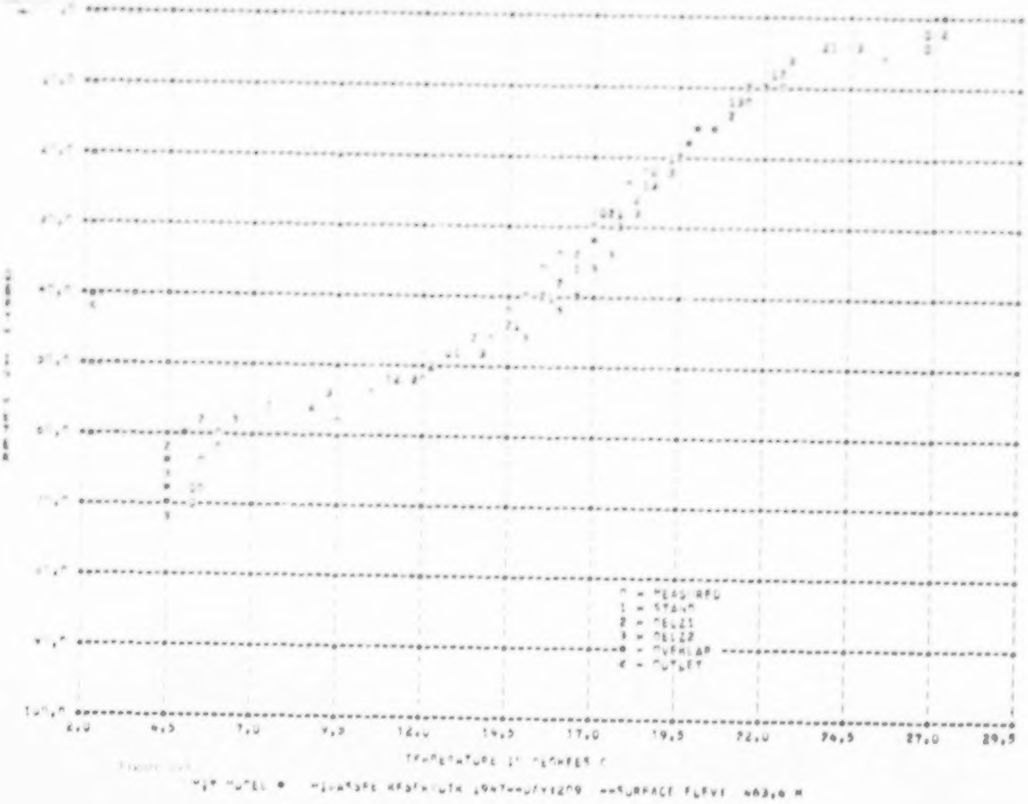
2.0
4.5
7.0
9.5
12.0
14.5
17.0
19.5
22.0
24.5
27.0
29.5
TEMPERATURE IN DEGREES C
0 = MEASURED
1 = STAND
2 = DELZ1
3 = DELZ2
* = OVERLAP
SURFACE ELEV. 463.6 M

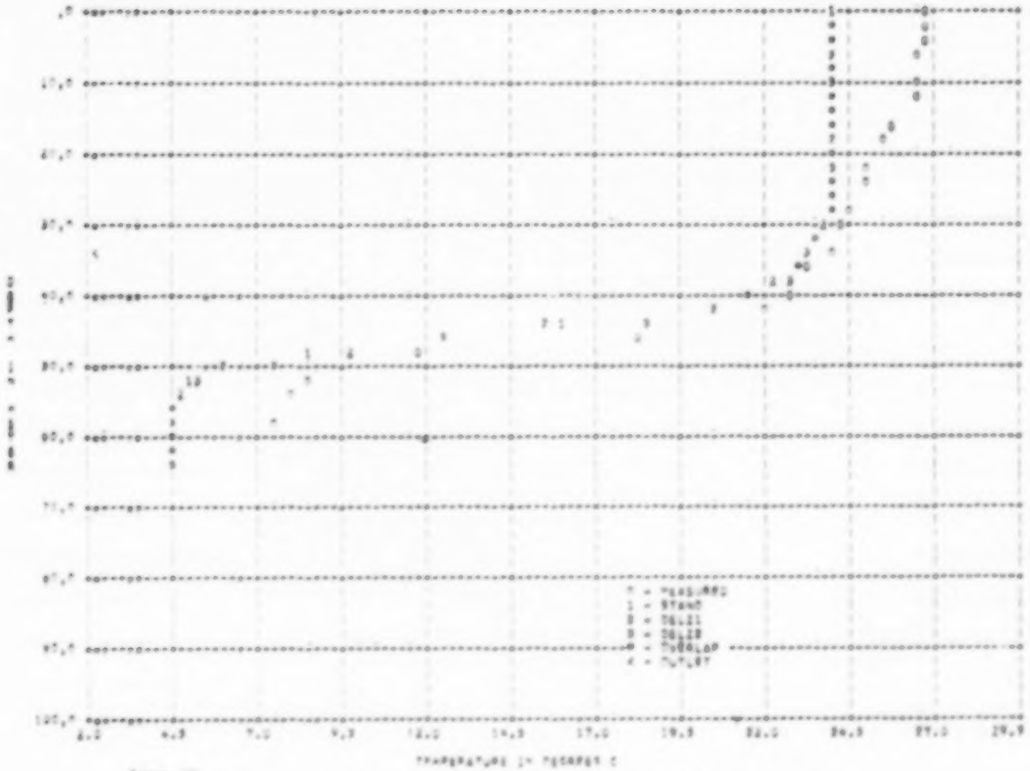

Figure 150

MIT MODEL 8 HIWASSEE RESERVOIR 1967--DAY=1307 --SURFACE ELEV= 464.8 M

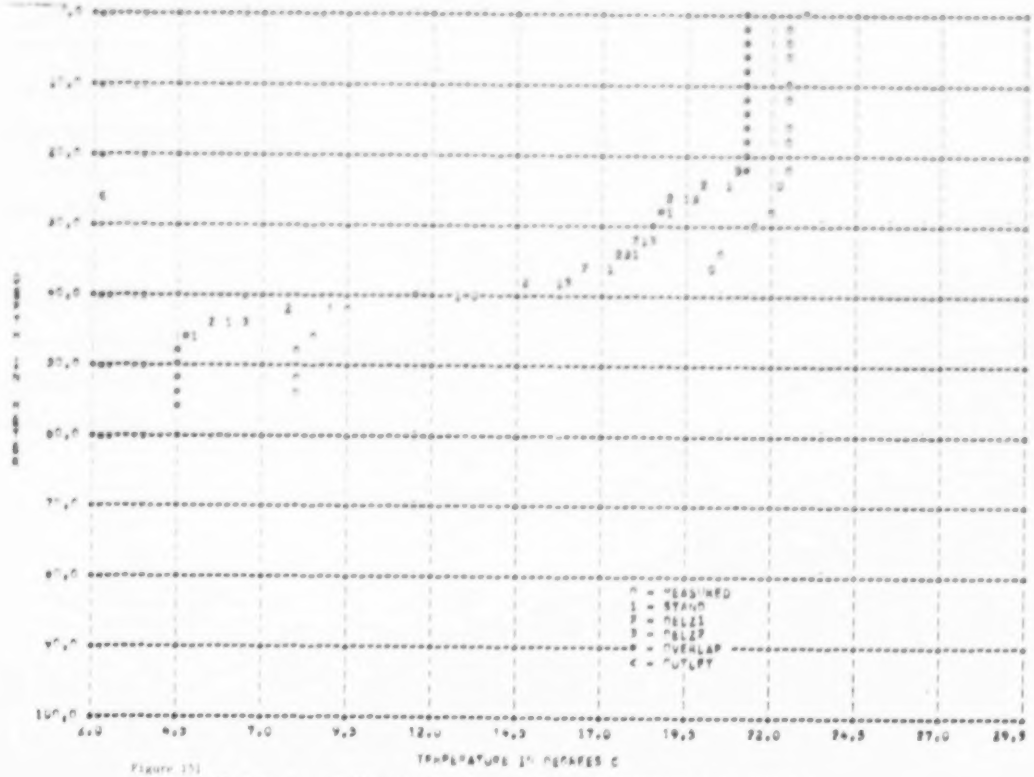

Figure 151

MIT MODEL 8 HIWASSEE RESERVOIR 1967--DAY=1304 --SURFACE ELEV= 466.3 M

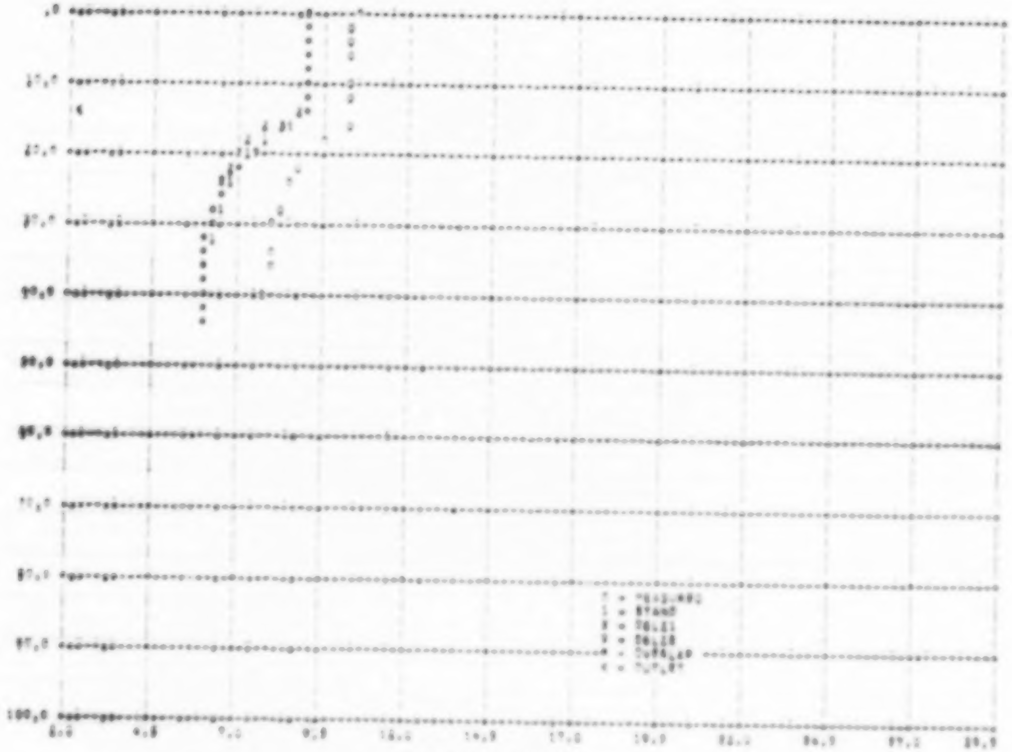

Figure 152

MIT MODEL * HIWASSEE RESERVOIR 1967--DAY: [illegible] --SURFACE ELEV: [illegible] M

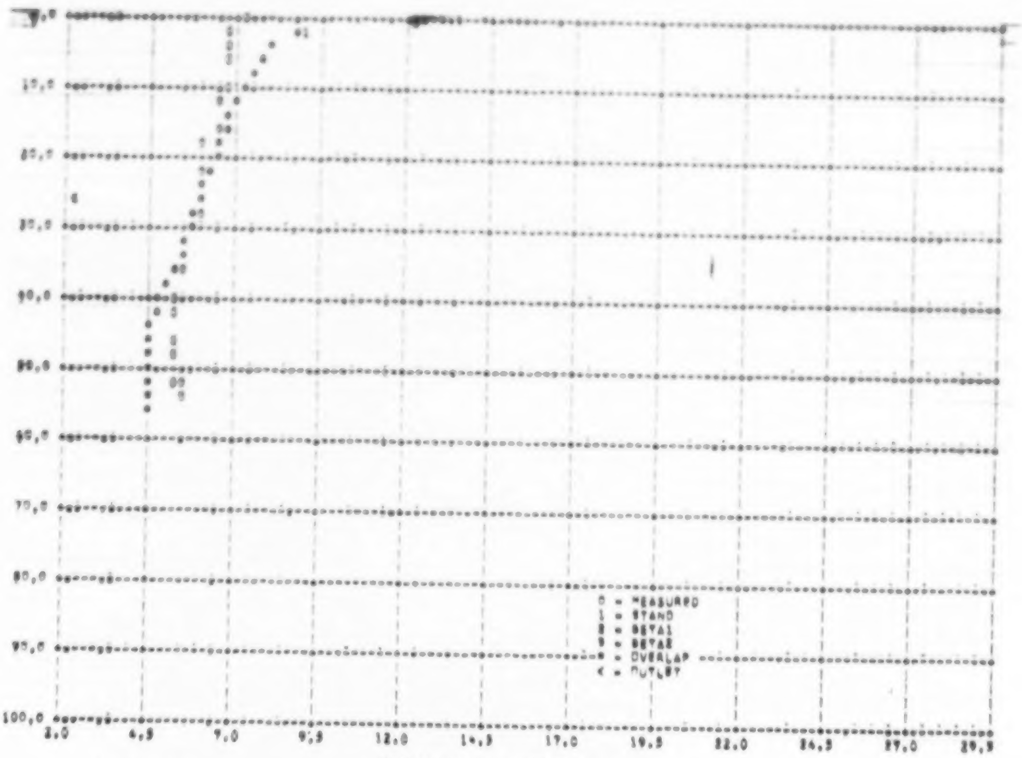

Figure 153

MIT MODEL * HIWASSEE RESERVOIR 1967--DAY: 90 --SURFACE ELEV: 446.0 M

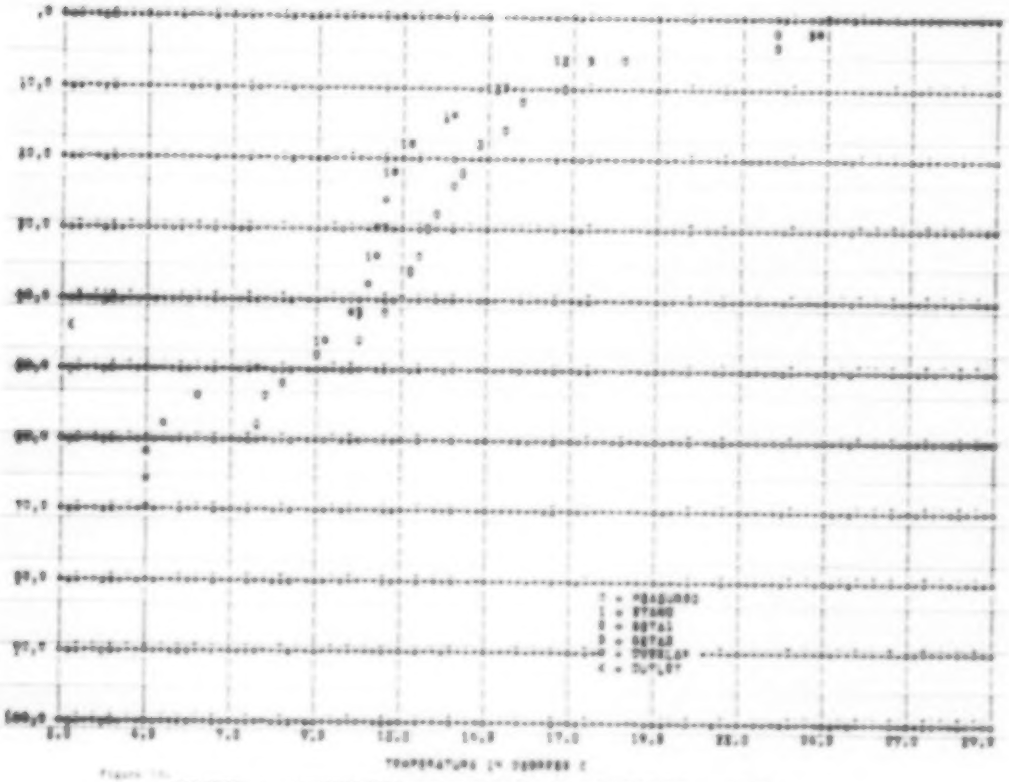

Figure 154

MIT MODEL - HIWASSEE RESERVOIR 1967--DAY:180 --SURFACE ELEV: 463.0 M

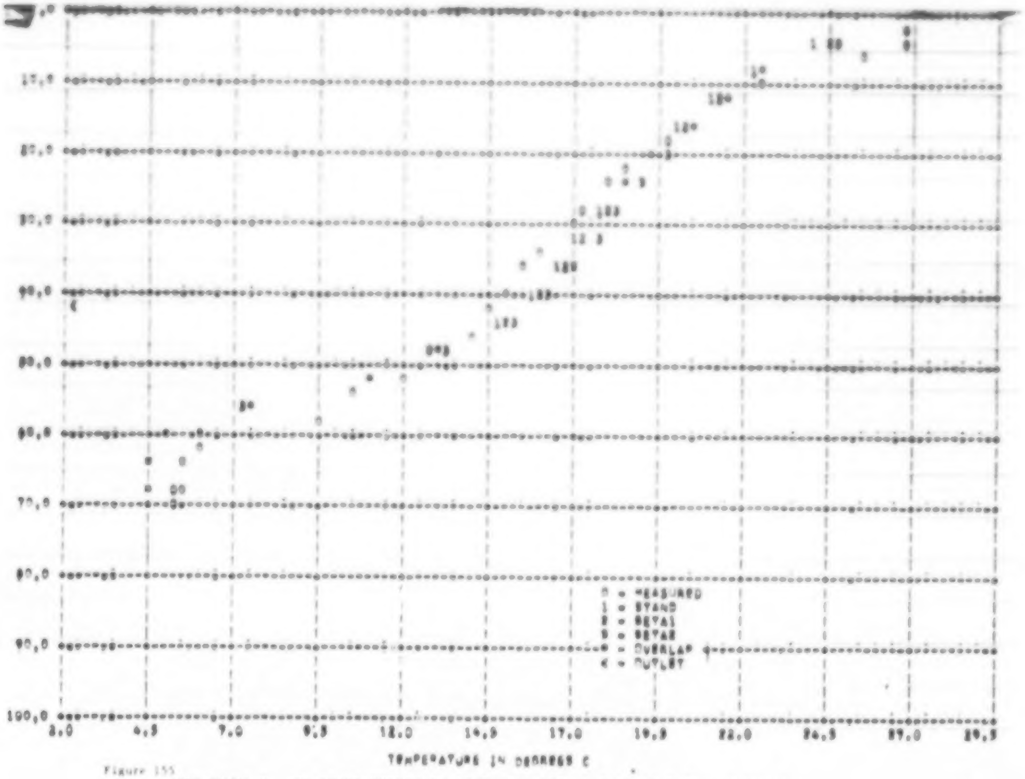

Figure 155

MIT MODEL - HIWASSEE RESERVOIR 1967--DAY:209 --SURFACE ELEV: 463.6 M

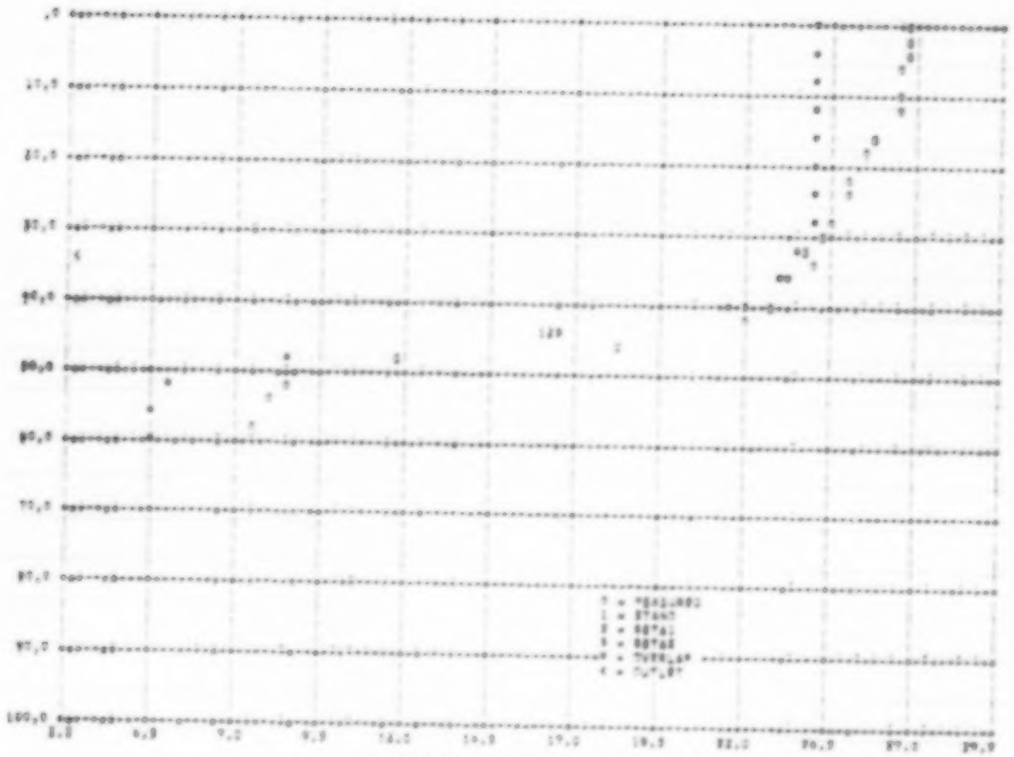

Figure [illegible]

MIT MODEL * HIWASSEE RESERVOIR [illegible] --SURFACE ELEV: [illegible] M

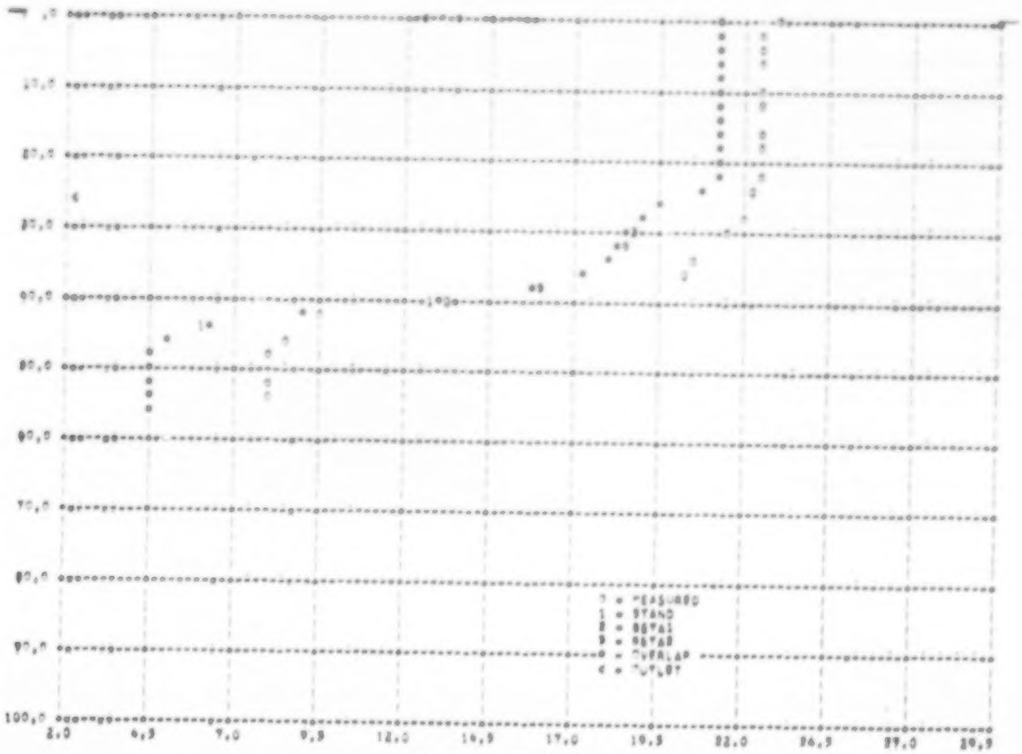

Figure [illegible]

MIT MODEL * HIWASSEE RESERVOIR [illegible] --SURFACE ELEV: [illegible] M

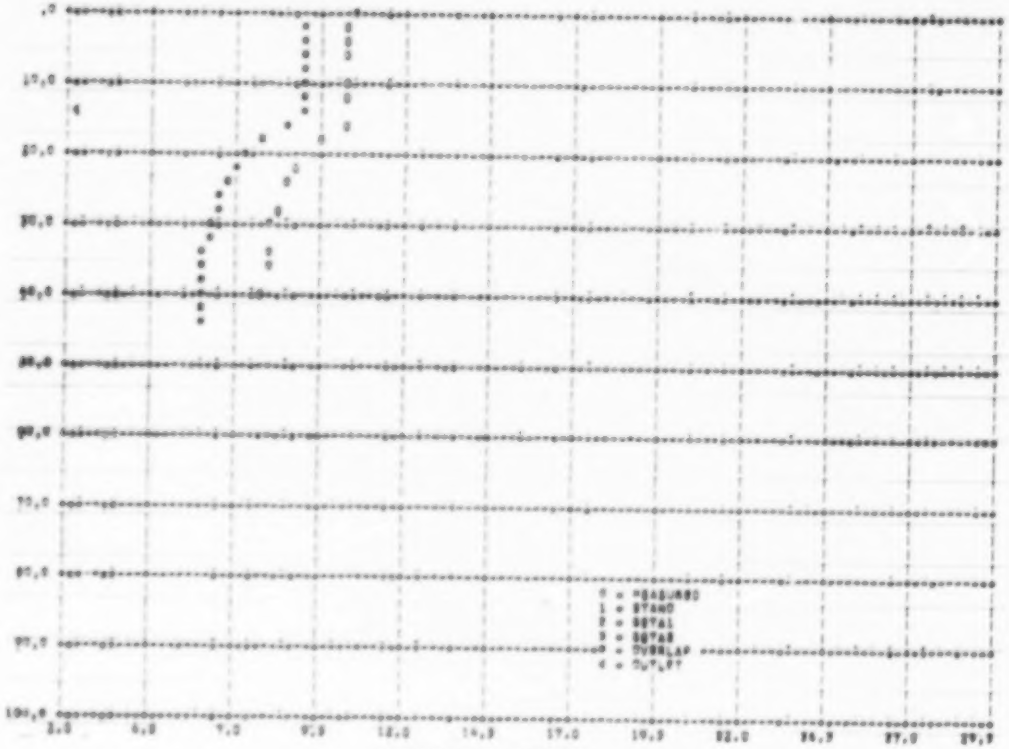

Figure 158

MIT MODEL - [illegible] RESERVOIR 1967--[illegible] --SURFACE ELEV: [illegible] M

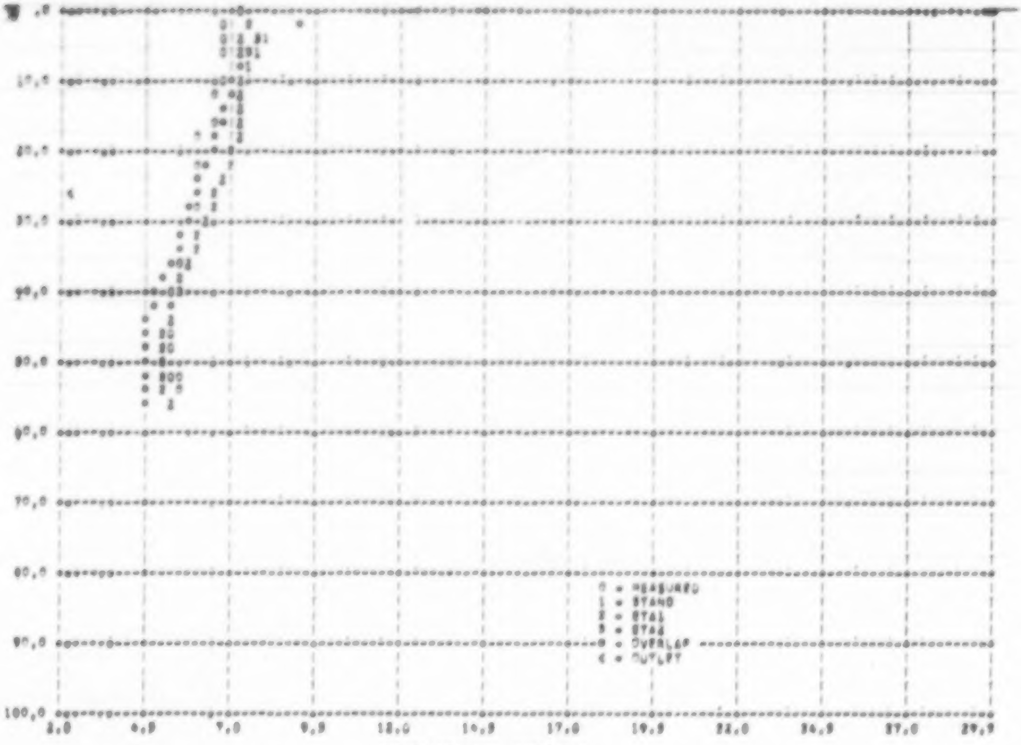

Figure 159

MIT MODEL - HIWASSEE RESERVOIR 1967--DAY: 80 --SURFACE ELEV: 446.0 M

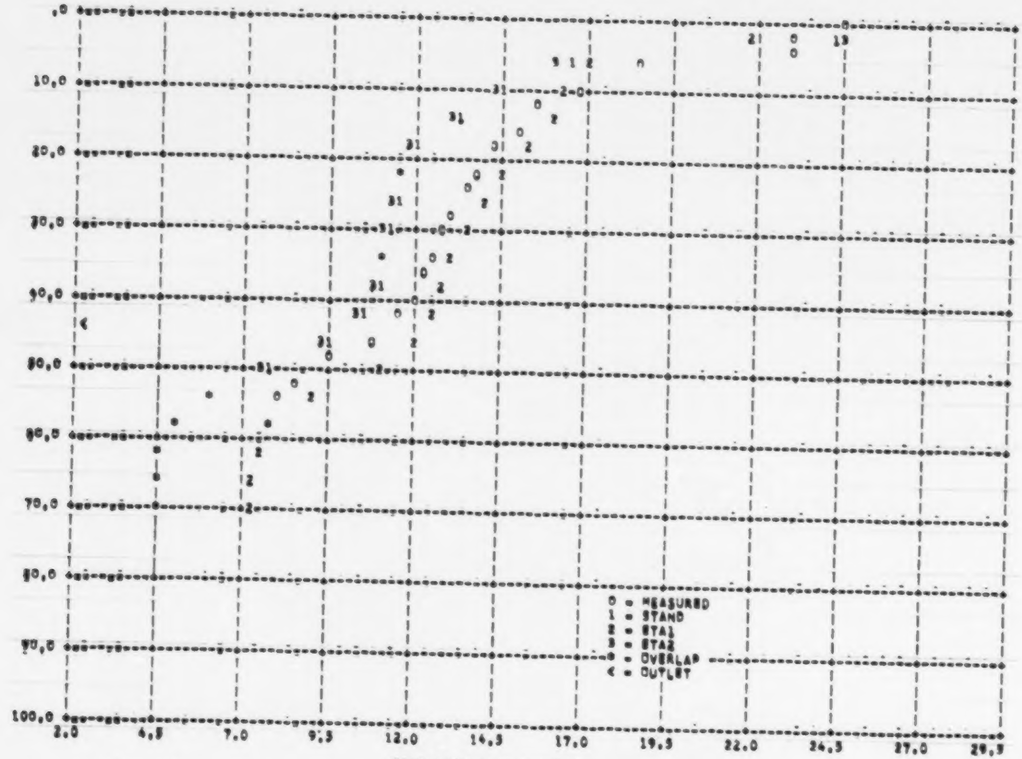

Figure 160

MIT MODEL = HIWASSEE RESERVOIR 1967--DAY:148 --SURFACE ELEV: 463.9 M

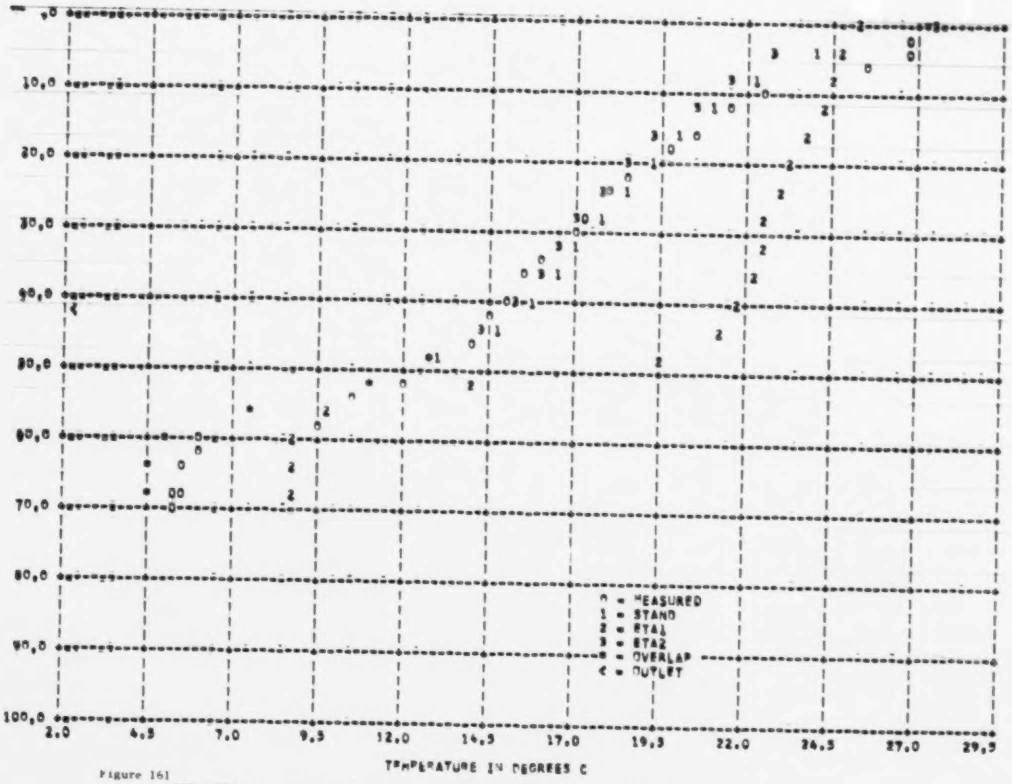

Figure 161

MIT MODEL = HIWASSEE RESERVOIR 1967--DAY:209 --SURFACE ELEV: 463.4 M

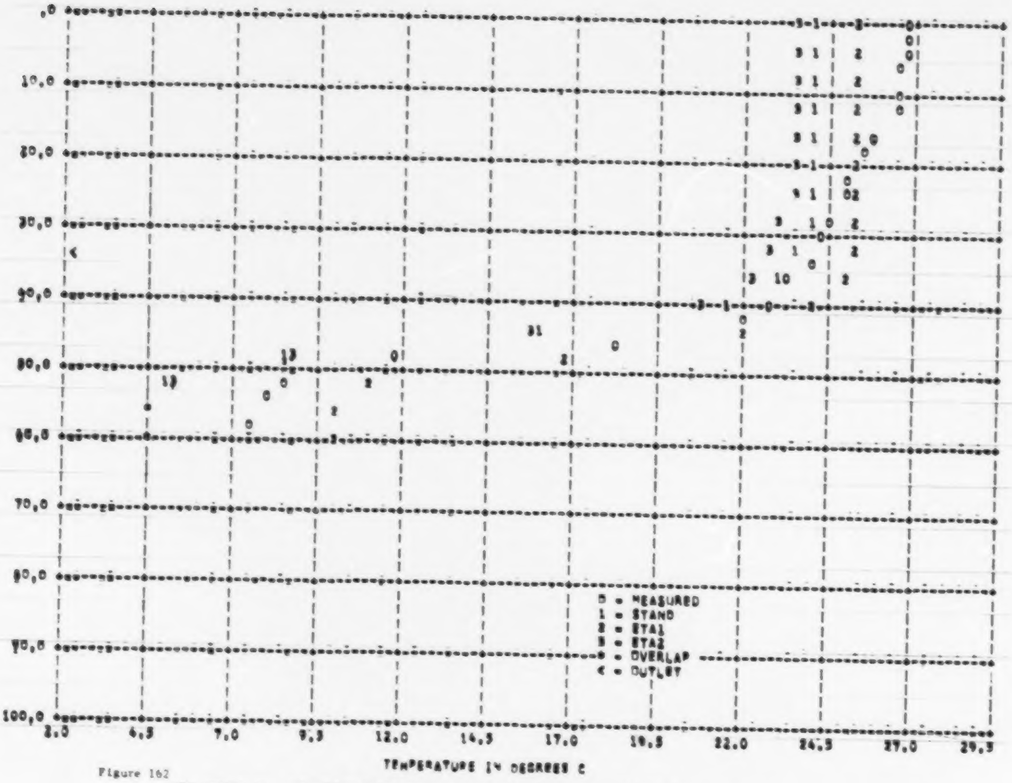

Figure 162

MIT MODEL * HIWASSEE RESERVOIR 1967--DAY:267 --SURFACE ELEV: 454.8 M

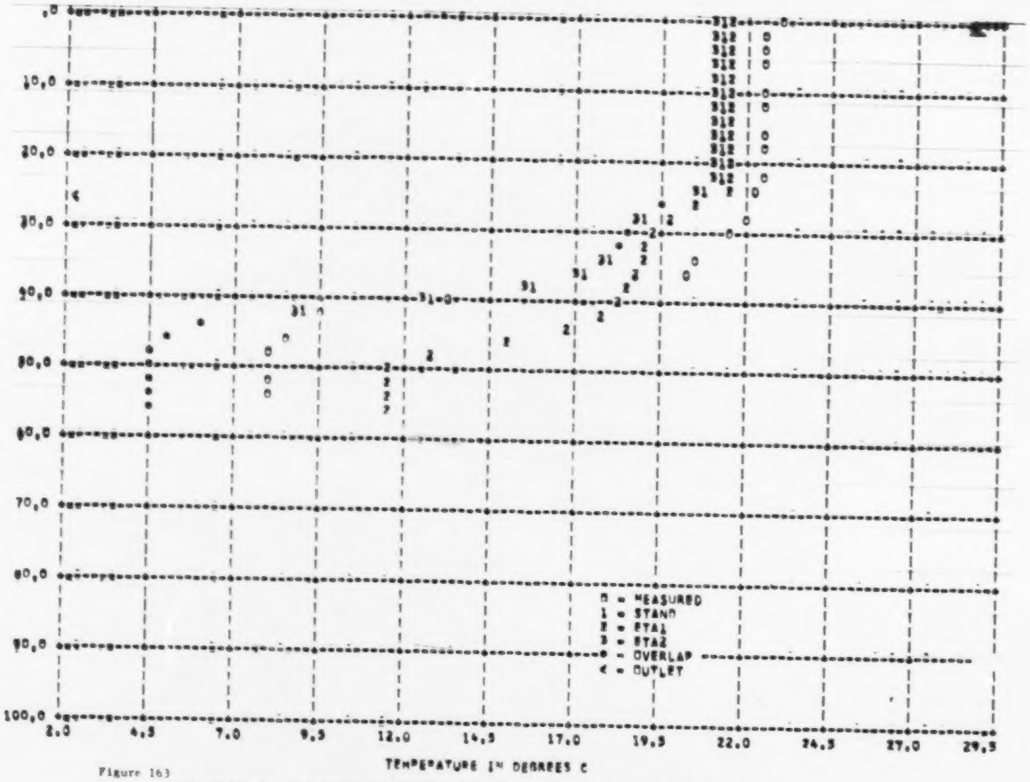

Figure 163

MIT MODEL * HIWASSEE RESERVOIR 1967--DAY:302 --SURFACE ELEV: 446.3 M

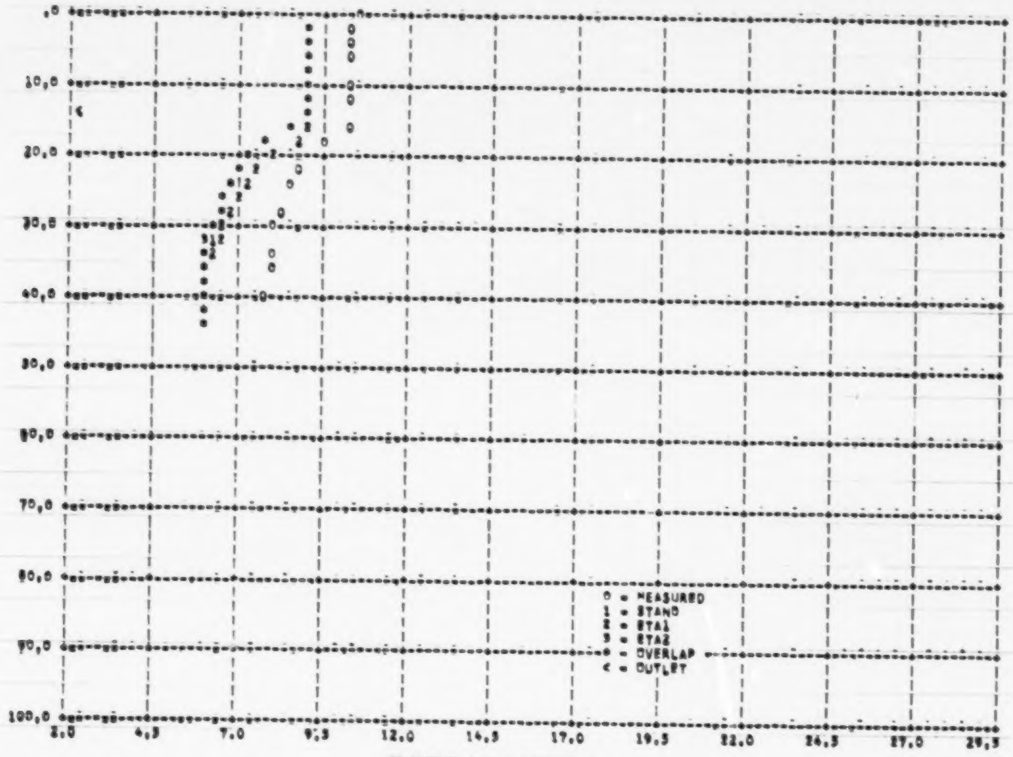

Figure 164

MIT MODEL * HIWASSEE RESERVOIR 1967--DAY:304 --SURFACE ELEV: 434.1 M

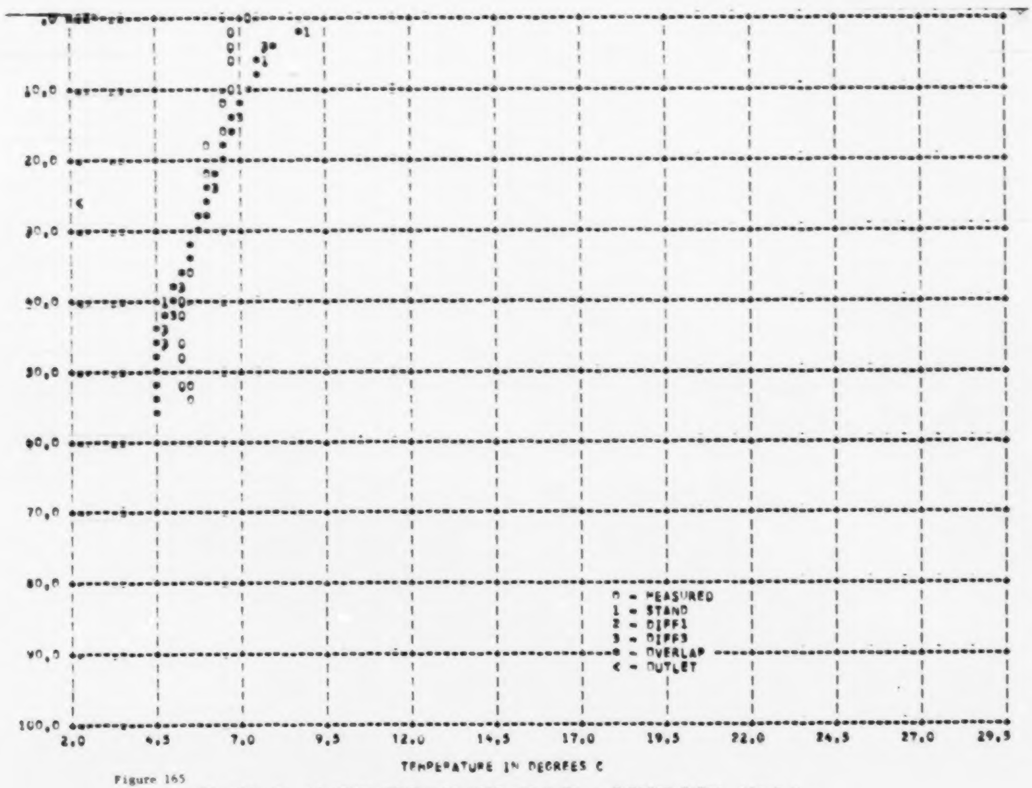

Figure 165

MIT MODEL * HIWASSEE RESERVOIR 1967--DAY: 90 --SURFACE ELEV: 446.0 M

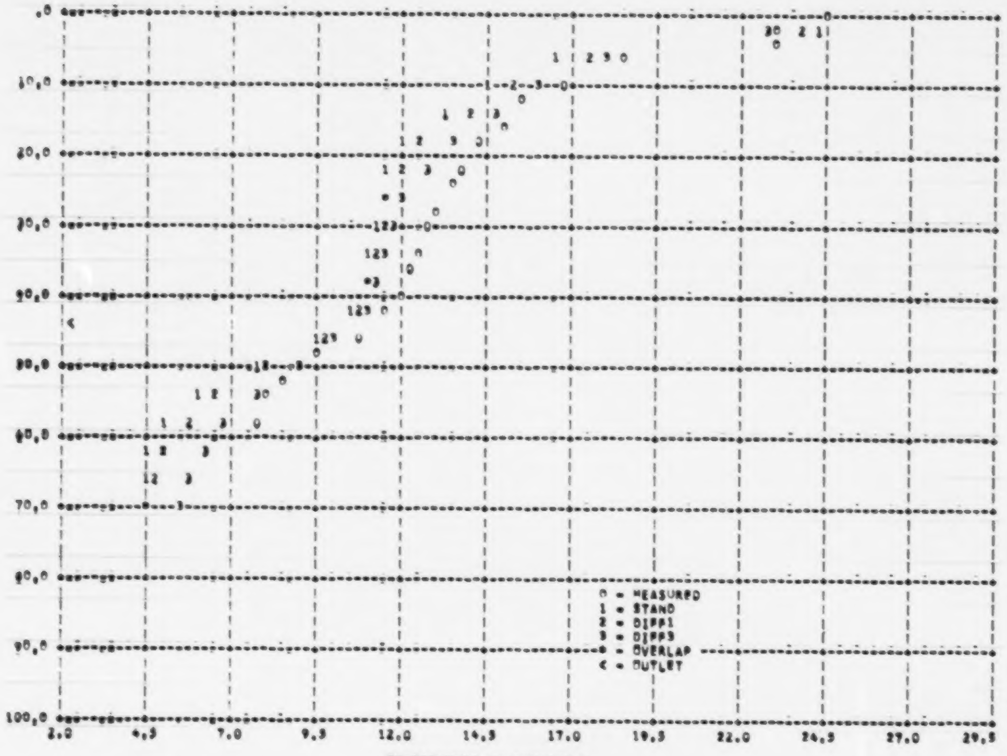

Figure 166

MIT MODEL * HIWASSEE RESERVOIR 1947--DAY:148 --SURFACE ELEV: 463.9 M

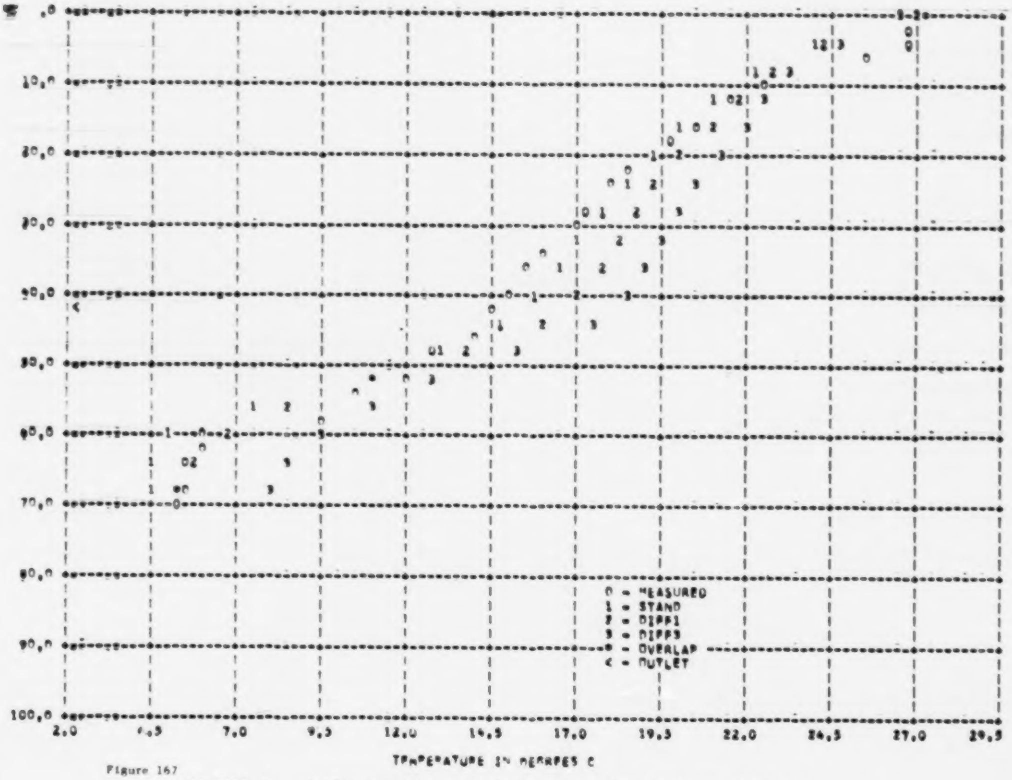

Figure 167

MIT MODEL * HIWASSEE RESERVOIR 1947--DAY:209 --SURFACE ELEV: 463.4 M

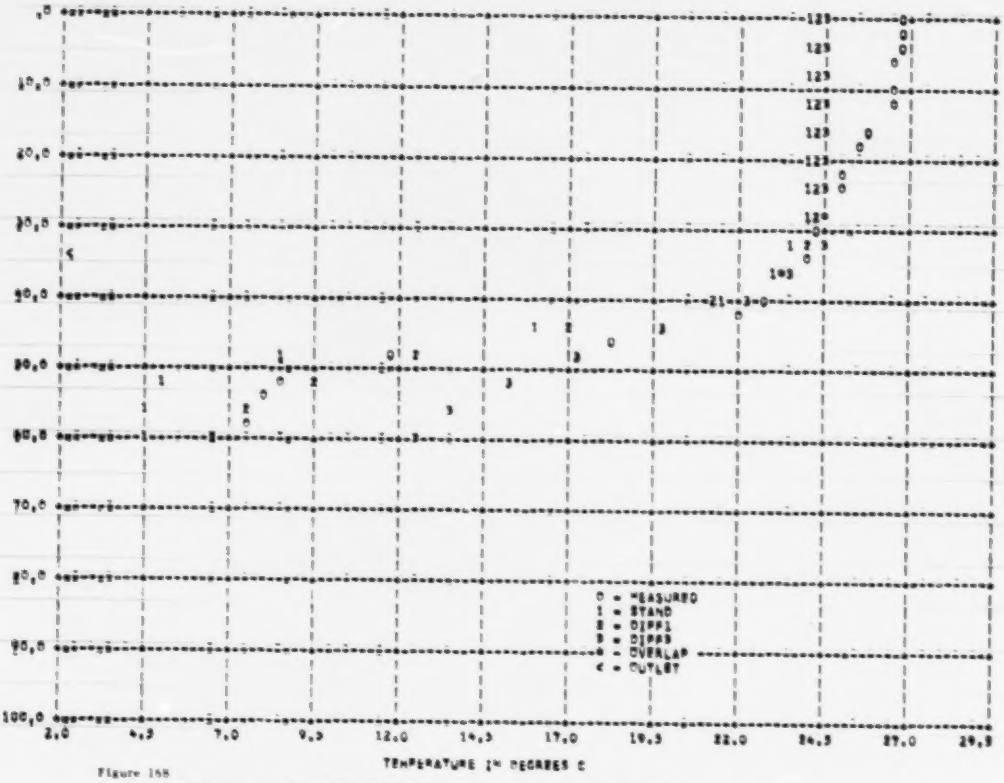

Figure 168

MIT MODEL * HIWASSEE RESERVOIR 1967--DAY:287 --SURFACE ELEV: 454.8 M

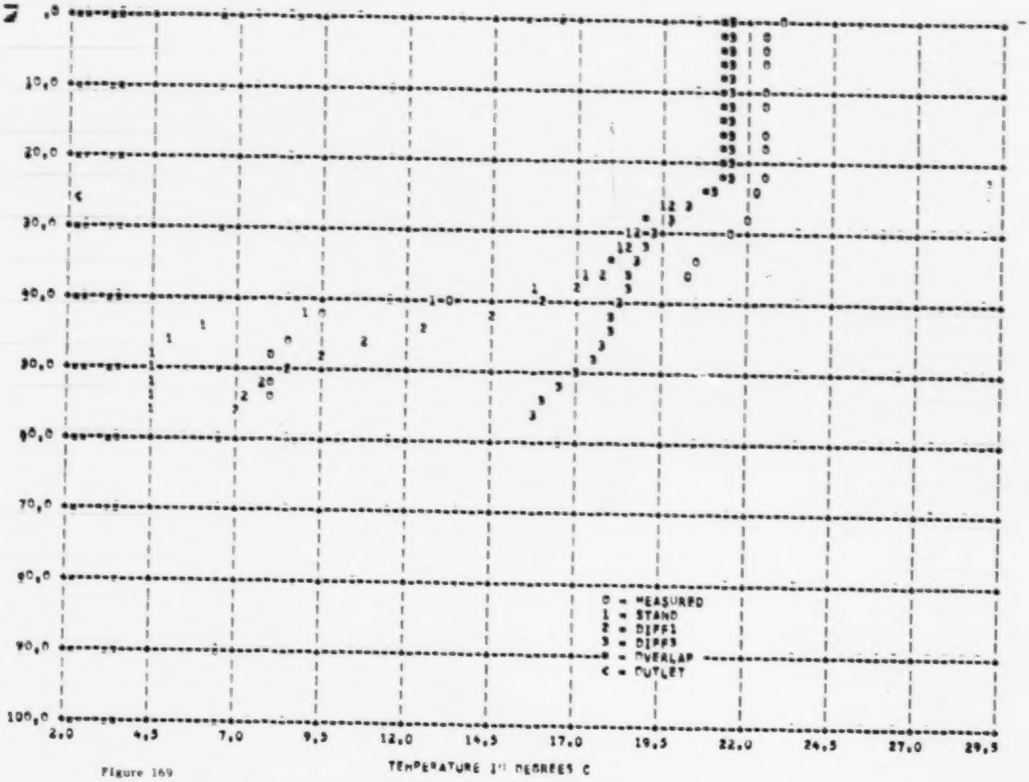

Figure 169

MIT MODEL * HIWASSEE RESERVOIR 1967--DAY:302 --SURFACE ELEV: 446.3 M

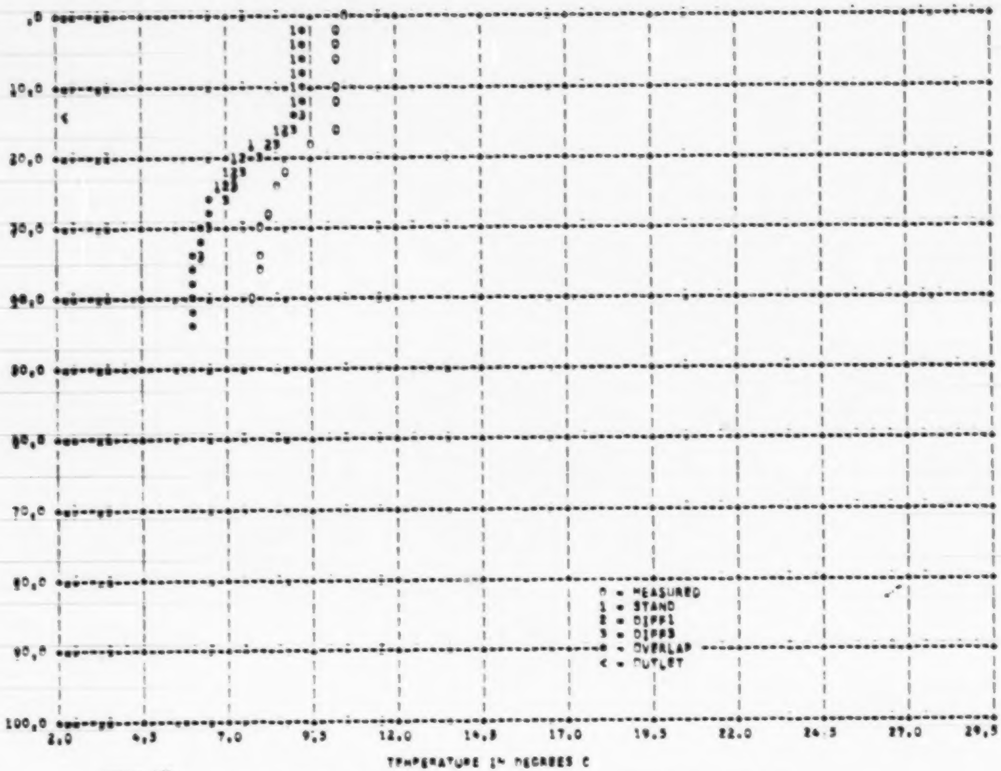

Figure 170

MIT MODEL * HIWASSEE RESERVOIR 1967--DAY:344 --SURFACE ELEV: 434.1 M

FORT LOUDON RESERVOIR

Figures 171 and 172 show the computed and measured temperature profiles for Fort Loudon Reservoir for 1971. It can be seen that the computed temperatures predict the water temperature at the outlet reasonably satisfactorily. The good fit of the predicted outlet water temperature is shown in Figure 173. These results are statistically verified in Tables 19 and 20 which show standard errors of estimate of 1.5°C and 3.0°C for the outlet and surface waters, respectively.

Figures 174 to 180 show the effect of the variation in the thickness of the horizontal segments from 1 to 3 meters. The change causes only minor differences in the predicted temperatures. This is verified in Tables 19 and 20 where the standard errors of estimate are only slightly different from those calculated using a 2 meter segment.

In Figures 181 to 187 the effect of the variation of β, the fraction of the solar radiation absorbed at the water surface, from 0.2 to 0.5 is shown to be negligible. This is verified in Tables 19 and 20 where the standard errors of estimate are shown to be similar to those obtained with the standard β of 0.5.

In Figures 188 to 194 is shown the effect of variation in η, the radiation absorption coefficient, from 0.05 to 1.40 per meter. It can be seen that the use of an absorption coefficient as low at 0.05 predicts the temperature poorly on day 132. On the other days the differences between the temperatures predicted using 0.05 and the other coefficients are relatively small. This is also verified in Tables 19 and 20 where the differences in the standard errors of estimate of temperatures are somewhat larger at the outlet than with the standard absorption coefficient of 0.75 per meter.

In Figures 195 to 201 are shown the effects in predicting temperature of varying the diffusion coefficient from molecular to 100 times molecular diffusion. It can be seen that the variation of the diffusion coefficient makes little difference in the predicted temperatures. This is verified in Tables 19 and 20 where the standard errors of estimate are all similar.

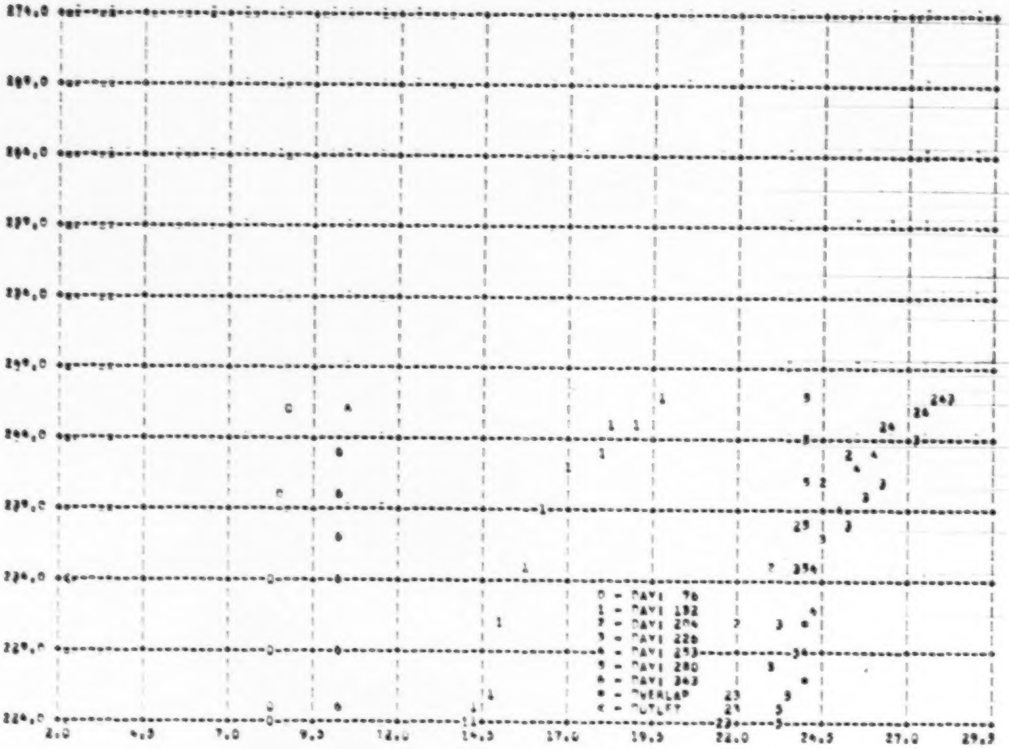

Figure 171 MIT MODEL - FORT LOUDOUN 1971 --MEASURED TEMPERATURE PROFILE--

Table 19

STATISTICAL ANALYSIS FOR THE PREDICTED WATER TEMPERATURE AT OUTLET LEVEL

Reservoir/Year: Fort Loudon/1971

Time Period Covered: 120th - 330th Julian Day

File Name	Std. error of estimate (^oC)	Correlation Coefficient
STAND	1.53	0.92
DELZ 1	1.56	0.92
DELZ 2	1.37	0.94
BETA 1	1.54	0.92
BETA 2	1.58	0.92
ETA 1	2.05	0.86
ETA 2	1.43	0.93
ETA 3	----	----
DIFF 1	1.59	0.92
DIFF 3	1.69	0.90

Table 20

STATISTICAL ANALYSIS FOR THE PREDICTED SURFACE WATER TEMPERATURE

Reservoir/Year: Fort Loudon/1971

Time Period Covered: 60th - 360th Julian Day

File Name	Std. error of estimate (°C)	Correlation Coefficient
STAND	2.98	0.86
DELZ 1	2.78	0.89
DELZ 2	3.09	0.85
BETA 1	2.86	0.88
BETA 2	2.88	0.88
ETA 1	2.81	0.89
ETA 2	3.38	0.81
ETA 3	----	----
DIFF 1	2.95	0.86
DIFF 3	2.92	0.87

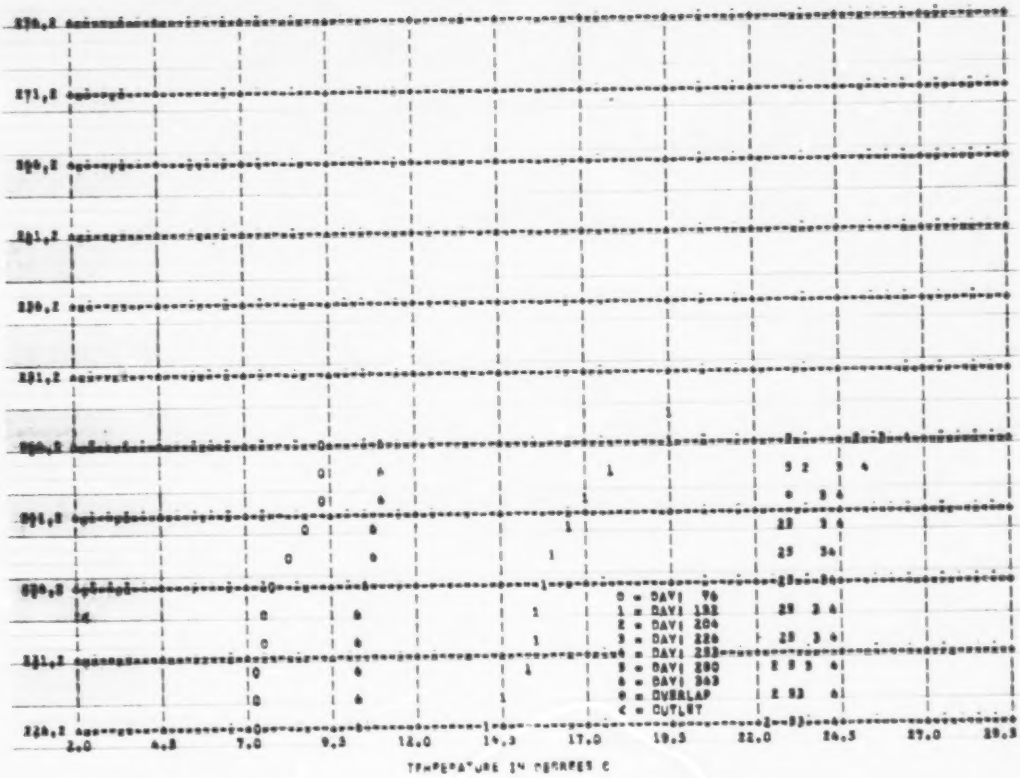

Figure 172 MIT MODEL 0 FORT LOUDOUN 1971 --COMPUTED TEMPERATURE PROFILE--

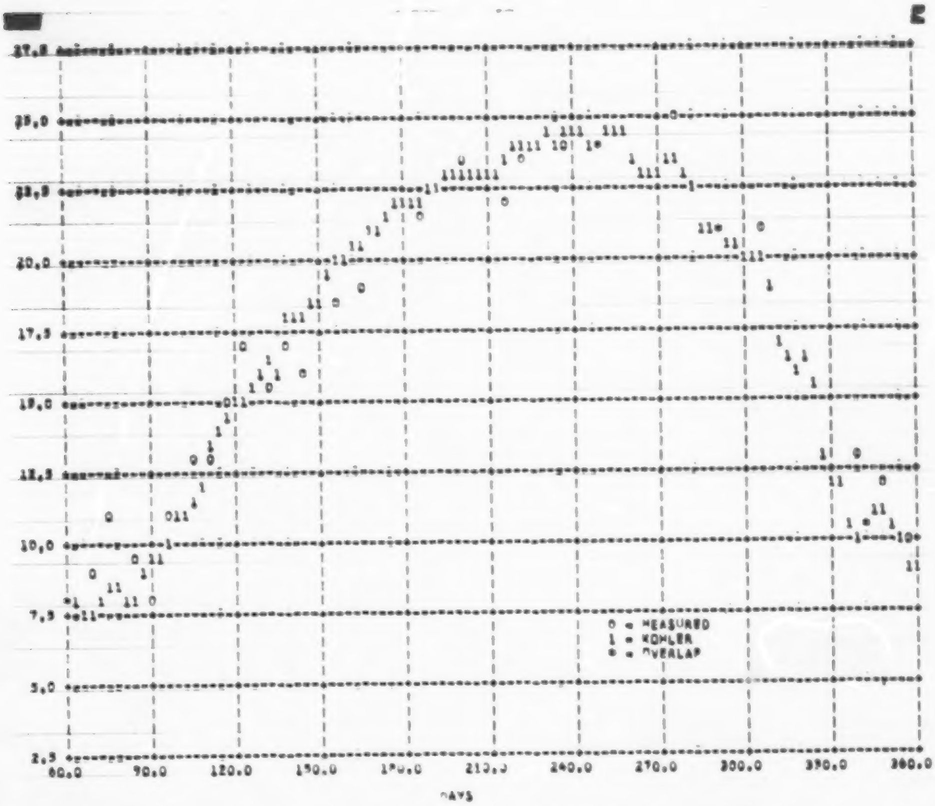

Figure 173 MIT MODEL 1 FORT LOUDOUN 1971 --COMPUTED OUTFLOW TEMPERATURE--

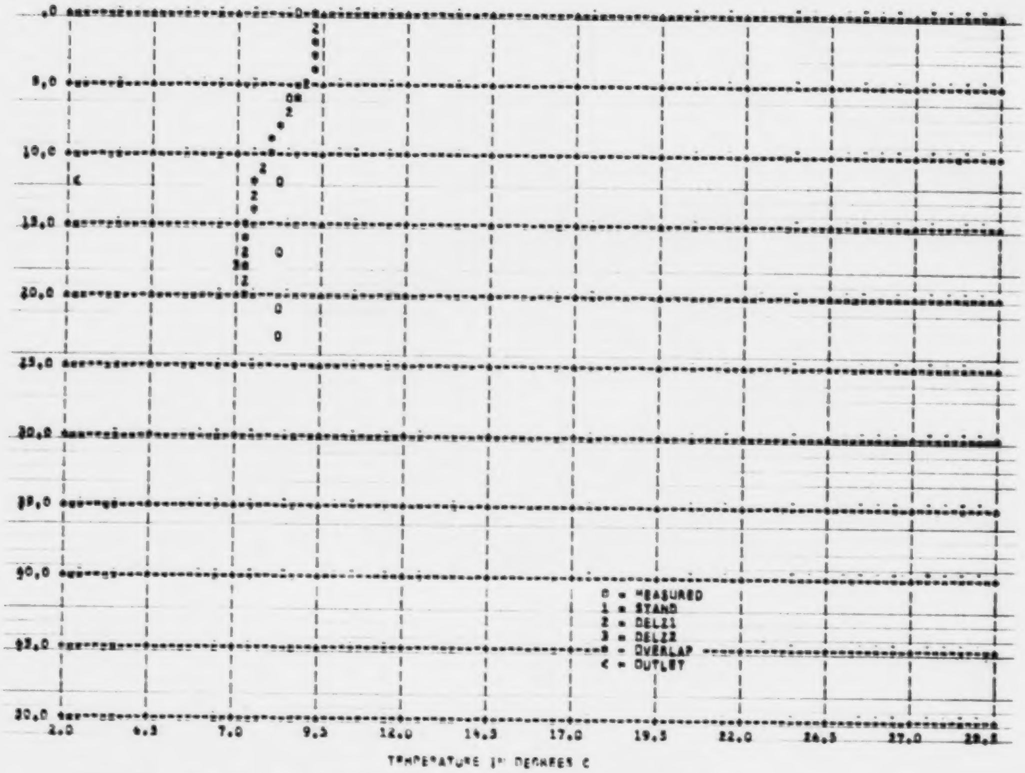

Figure 174 MIT MODEL * FORT LOUDOUN 1971 --DAY: 70 --SURFACE ELEV: 240.1 M

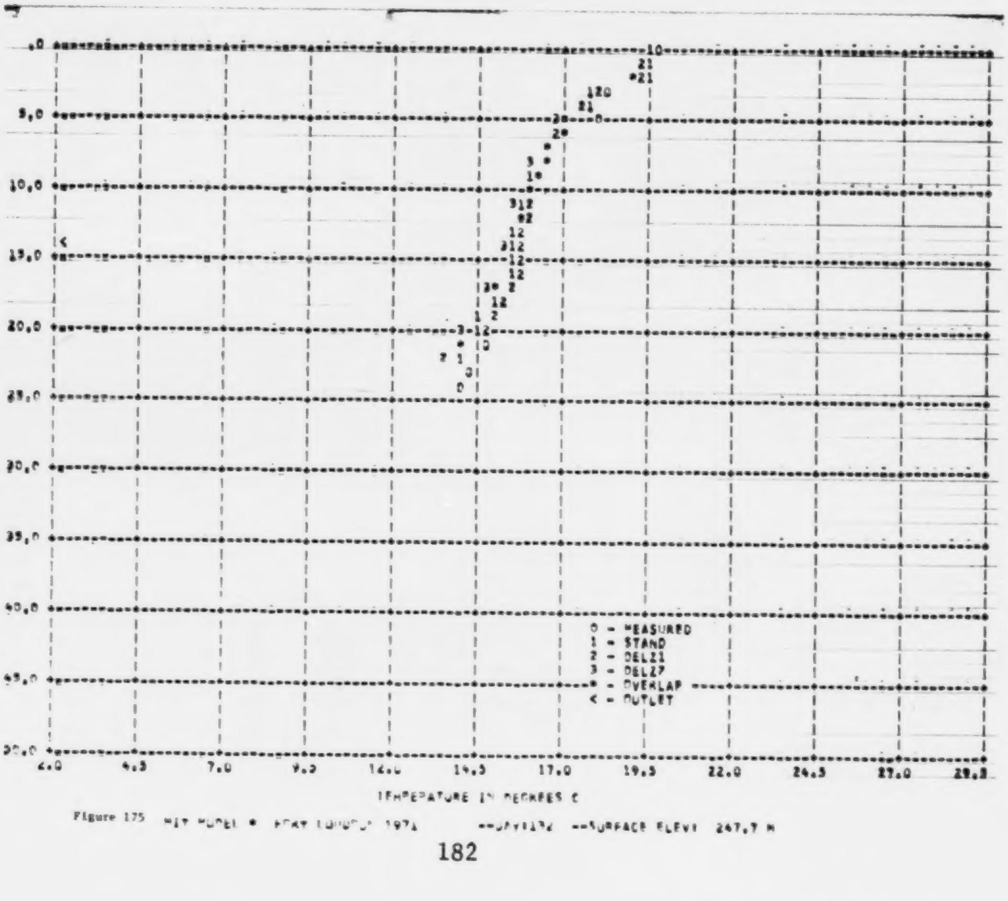

Figure 175 MIT MODEL * FORT LOUDOUN 1971 --DAY: 132 --SURFACE ELEV: 247.7 M

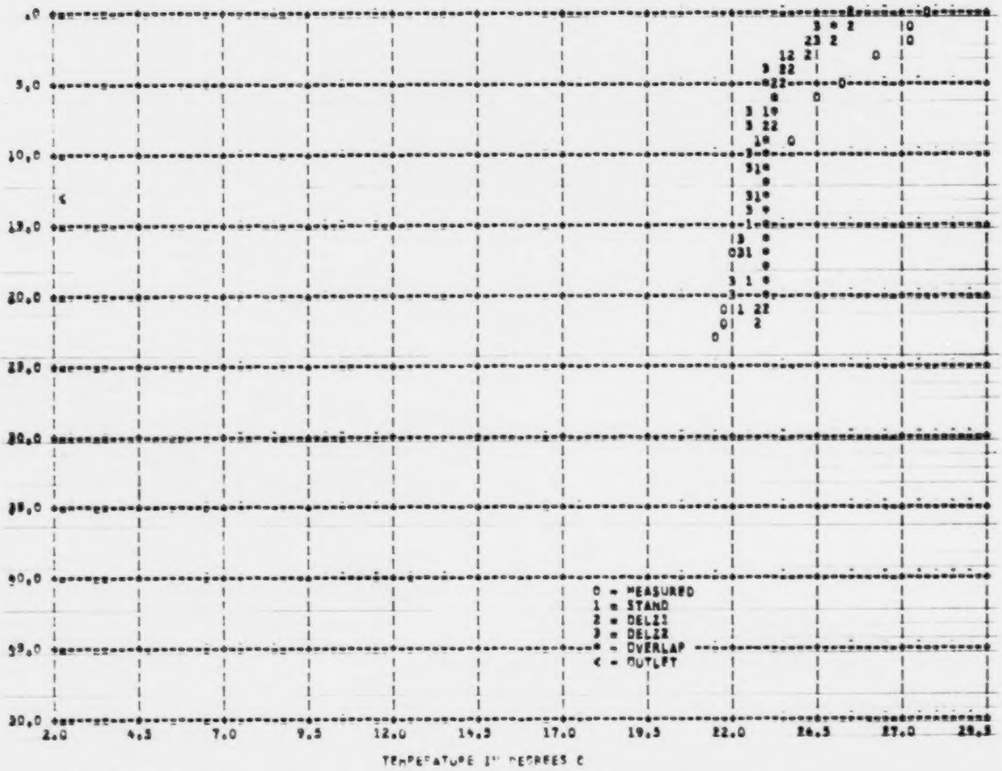

Figure 176 MIT MODEL • FORT LOUDOUN 1971 --DAY 204 --SURFACE ELEV 247.6 M

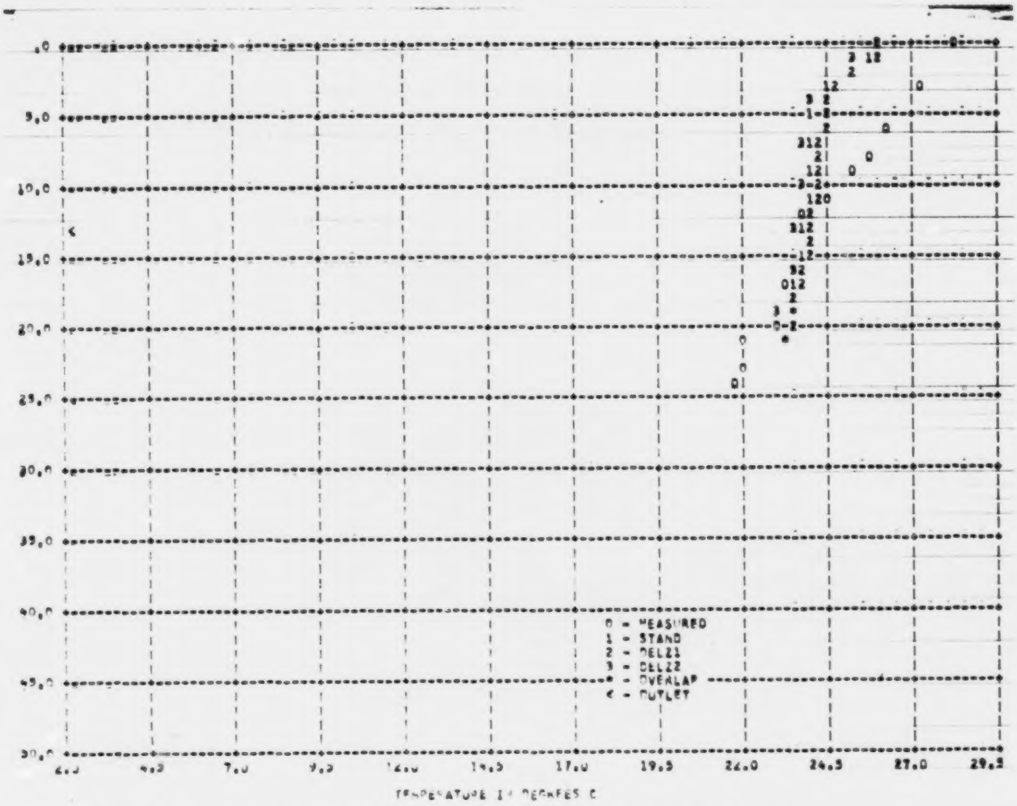

Figure 177 MIT MODEL • FORT LOUDOUN 1971 --DAY 226 --SURFACE ELEV 247.5 M

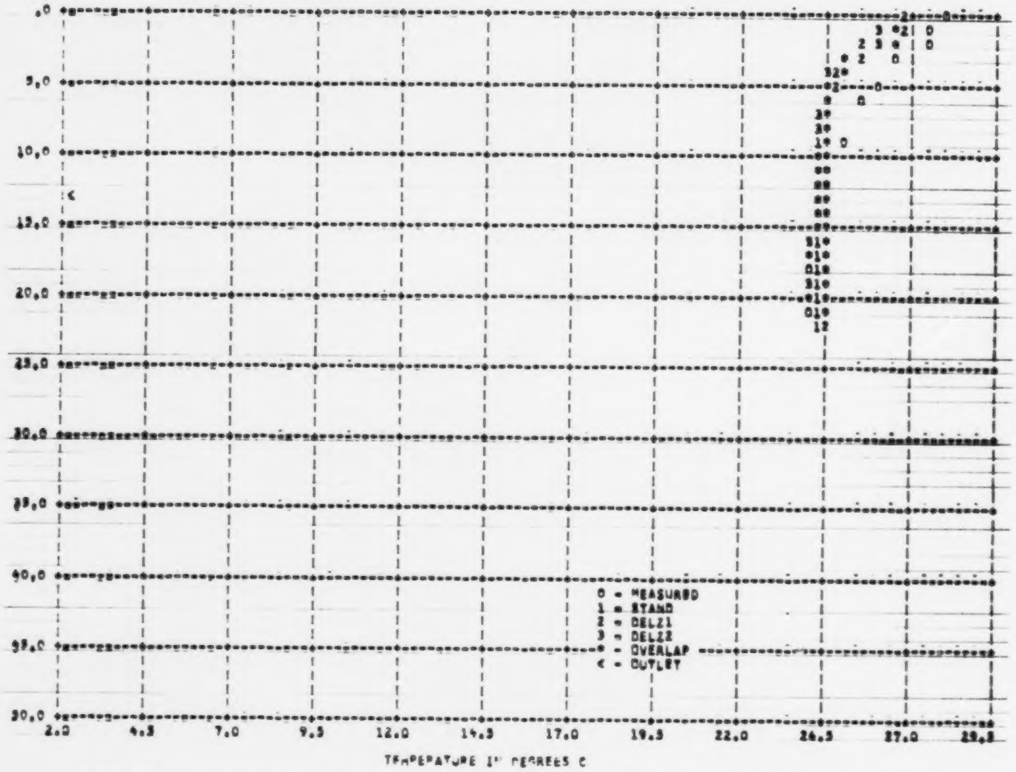

Figure 178 MIT MODEL * FORT LOUDOUN 1971 --DAY1253 --SURFACE ELEV: 247.6 M

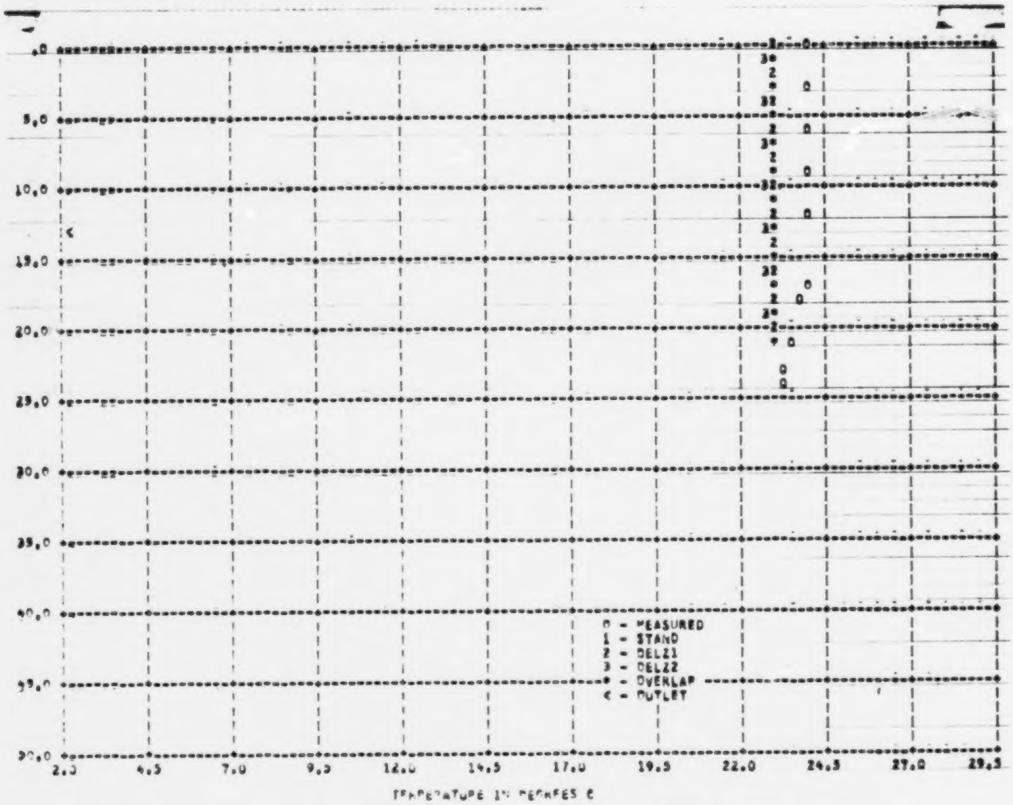

Figure 179 MIT MODEL * FORT LOUDOUN 1971 --DAY1260 --SURFACE ELEV: 247.5 M

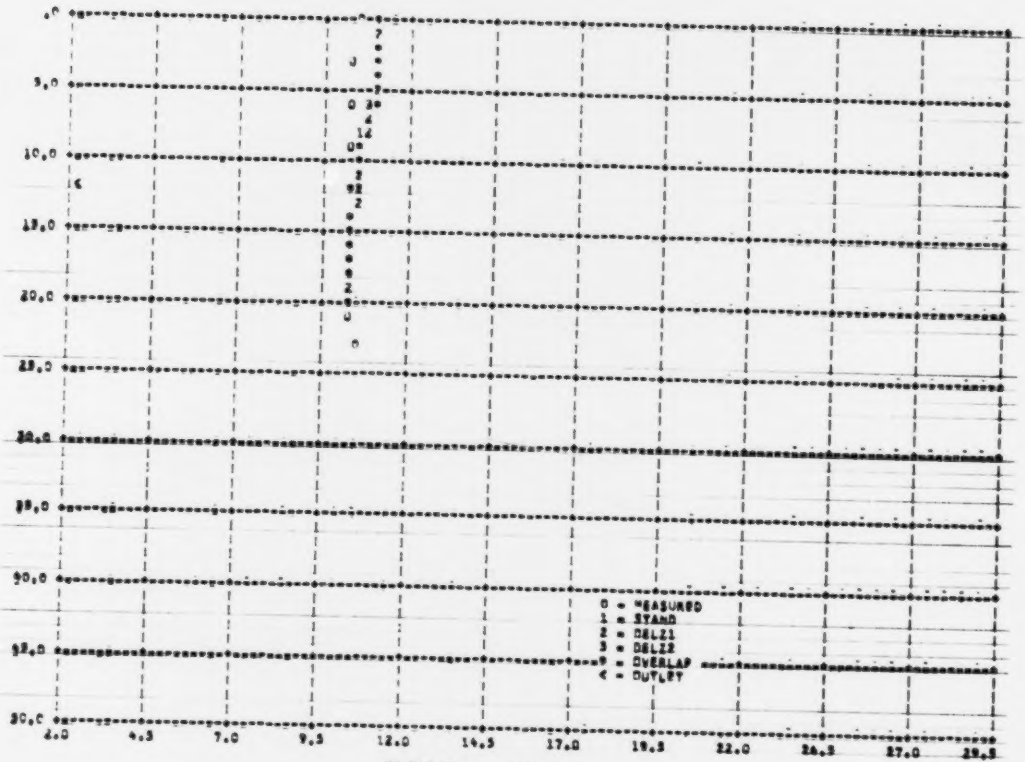

Figure 180 MIT MODEL * FORT LOUDOUN 1974 --DAY 343 --SURFACE ELEV: 246.1 M

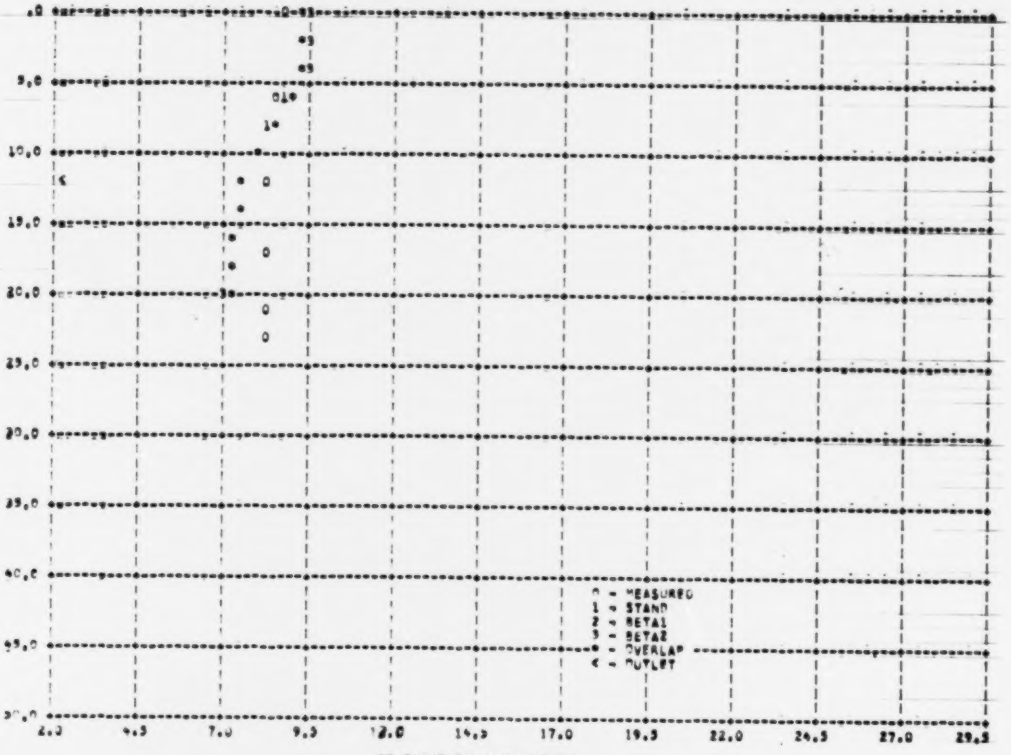

Figure 181 MIT MODEL * FORT LOUDOUN 1974 --DAY 78 --SURFACE ELEV: 246.1 M

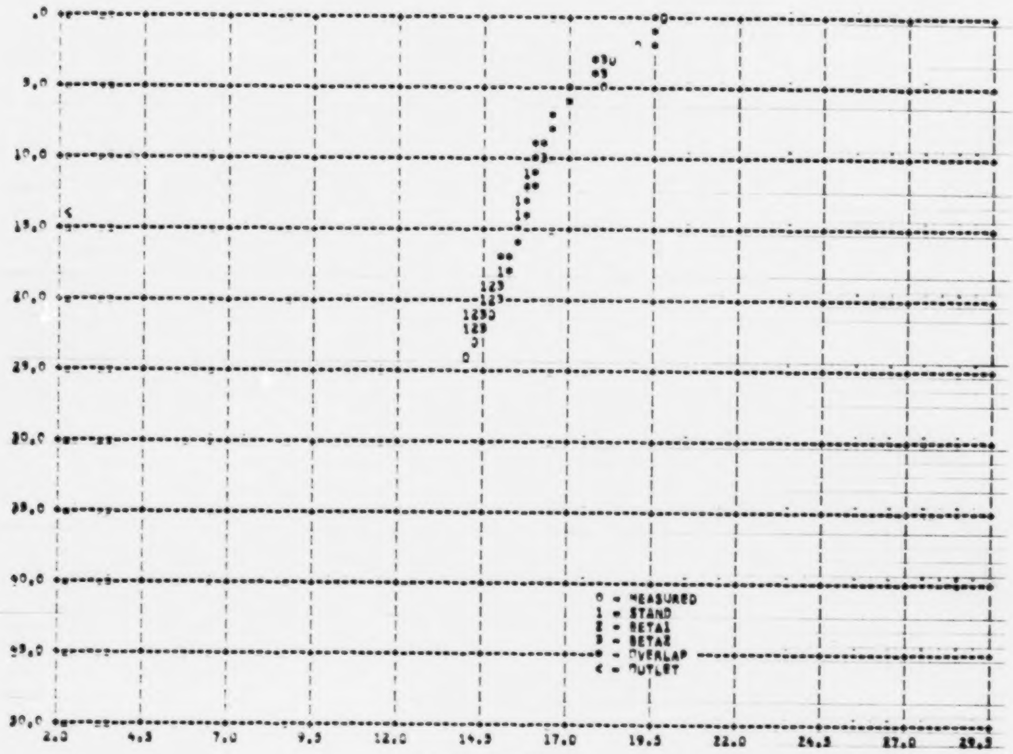

Figure 182 MIT MODEL * FORT LOUDOUN 1971 --DAY=192 --SURFACE ELEV= 247.7 M

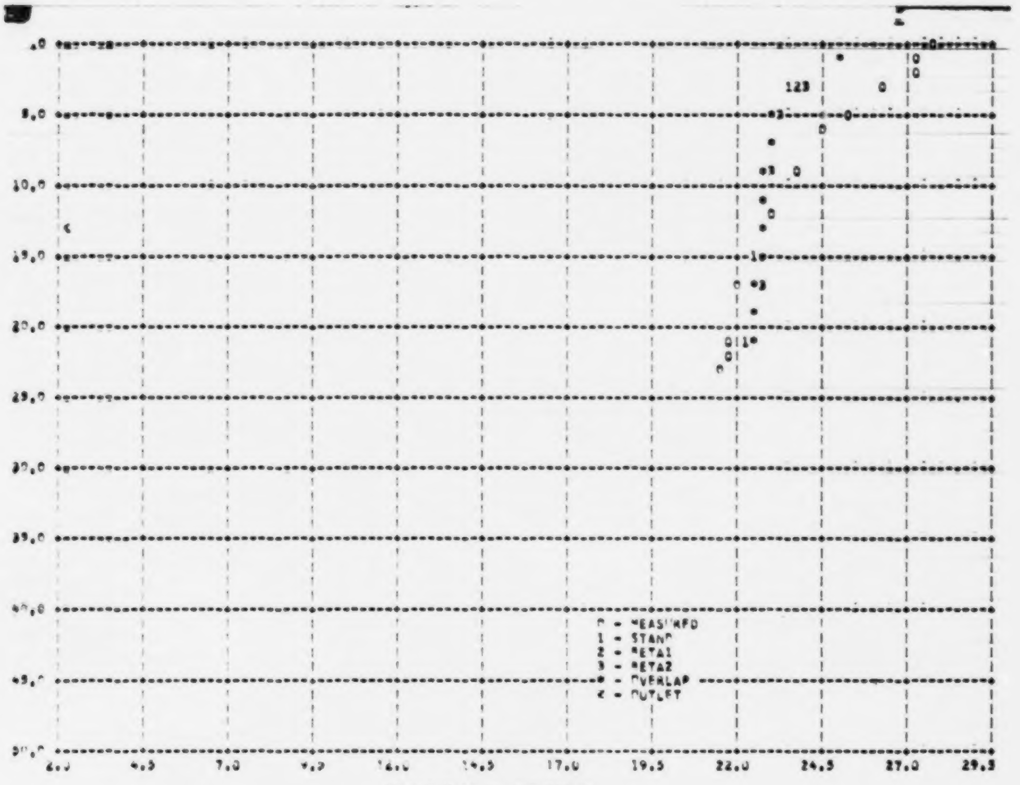

Figure 183 MIT MODEL * FORT LOUDOUN 1971 --DAY=204 --SURFACE ELEV= 247.6 M

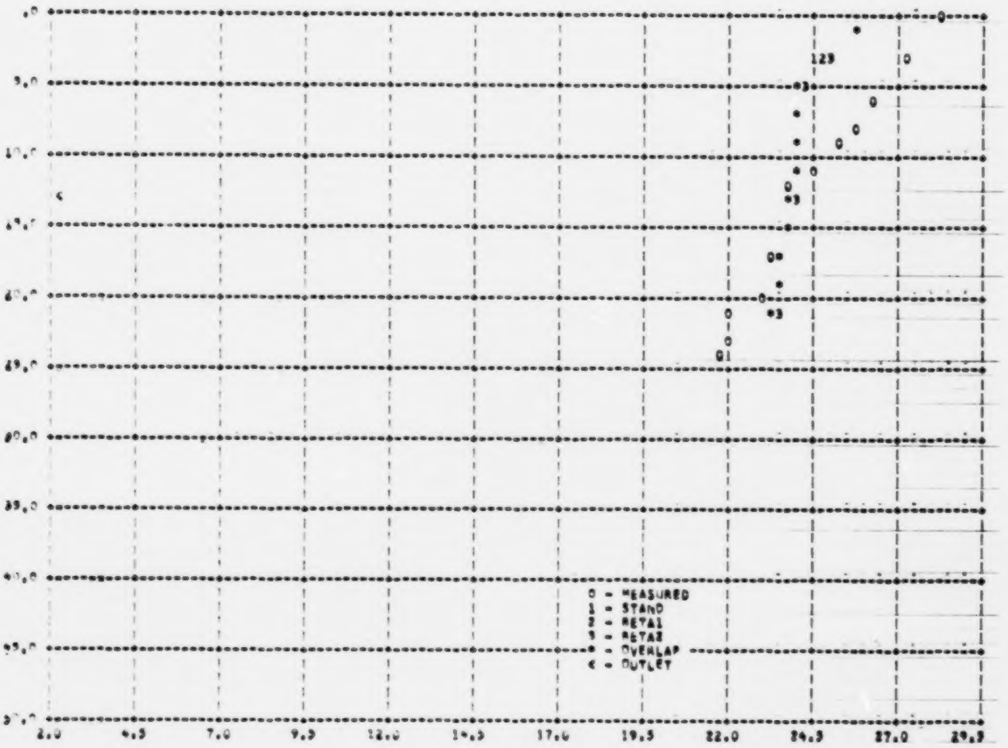

Figure 184 [illegible] 1974 --DAY1620 --SURFACE ELEV: 247.5 M

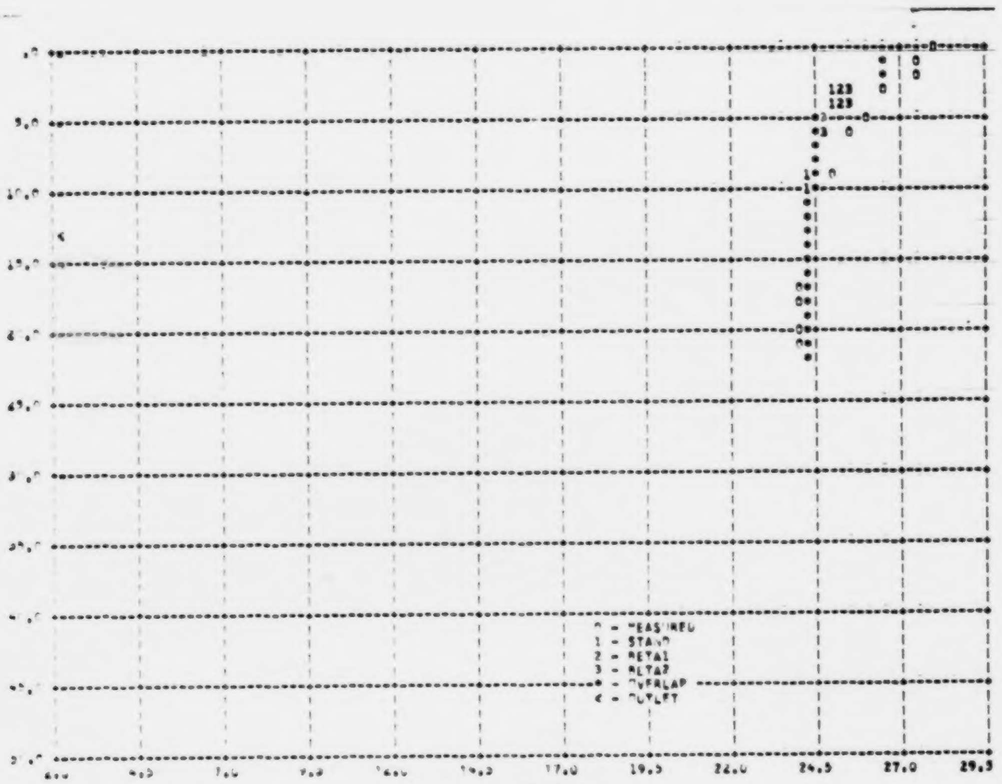

Figure 185 [illegible] 1974 [illegible] --SURFACE ELEV: 247.6 M

Reproduced from
best available copy.

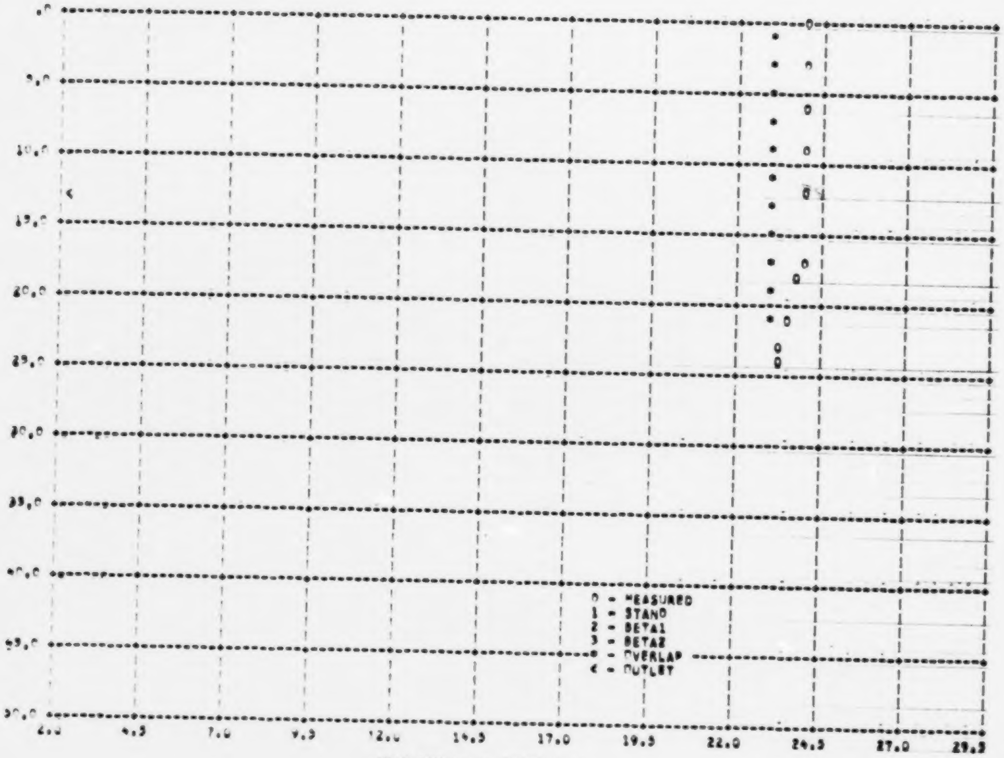

Figure 186 [illegible] 1971 --DAY120 --SURFACE ELEV. 247.5 M

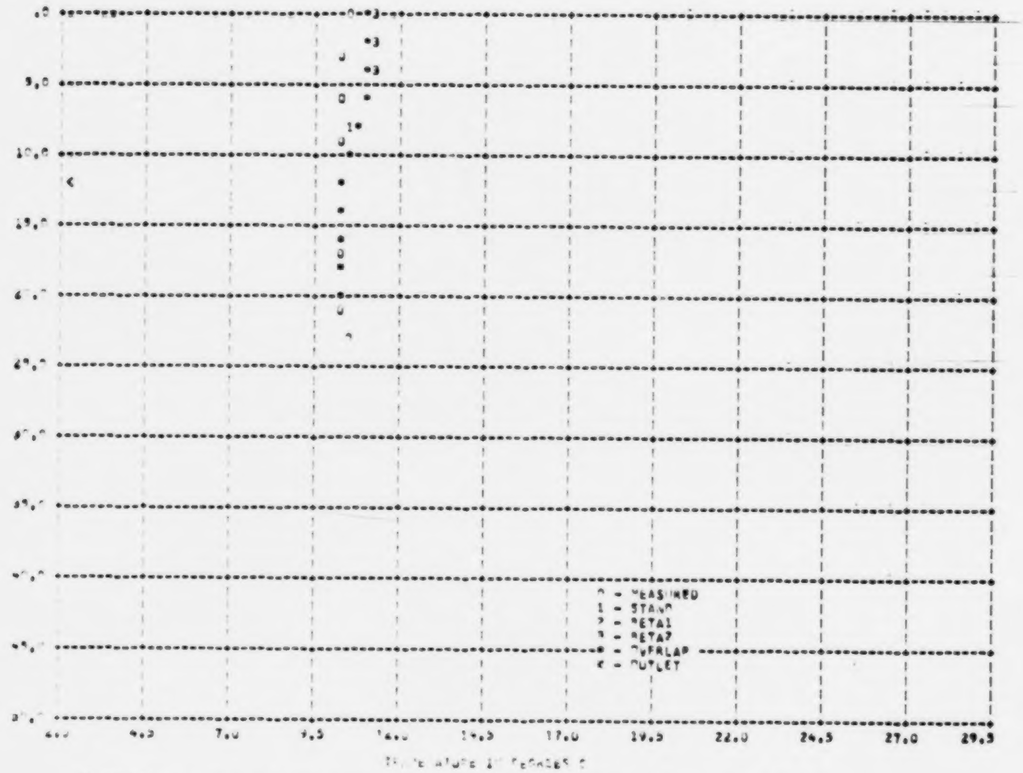

Figure 187 [illegible] 1971 --DAY134 --SURFACE ELEV. 246.1 M

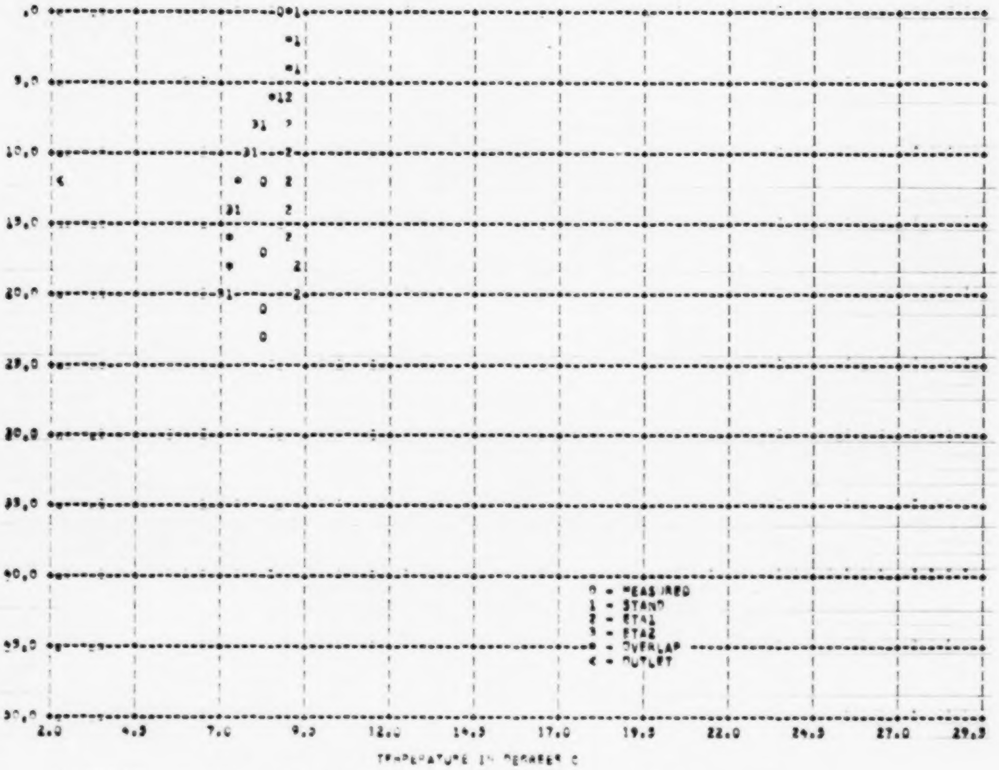

Figure 188 [illegible] 1971 --DAY 70 --SURFACE ELEV 246.1 M

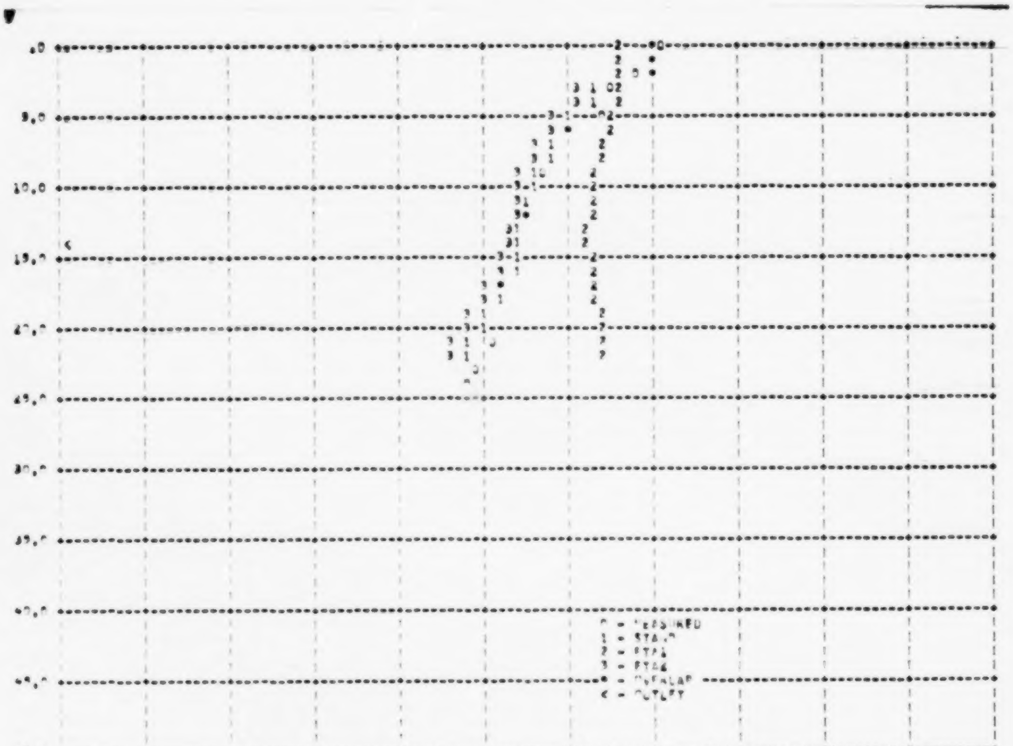

Figure 189 [illegible] 1971 --[illegible] --SURFACE ELEV 147.7 M

Reproduced from
best available copy.

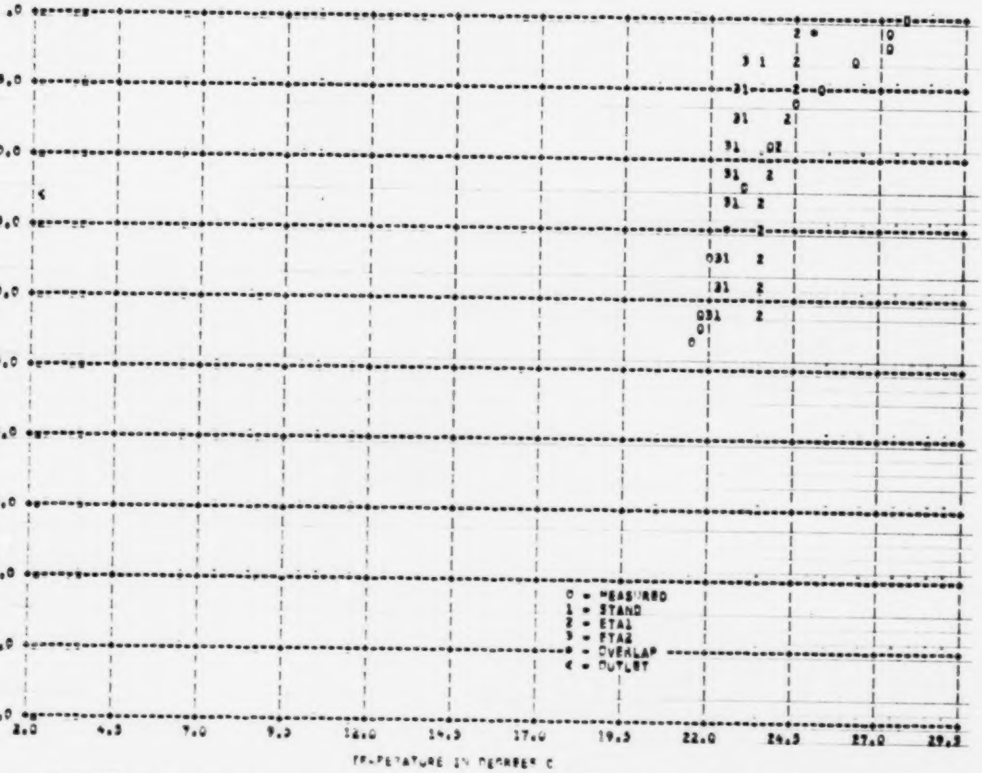

Figure 190 MIT MODEL * FORT LOUDOUN 1971 --DAY1204 --SURFACE ELEV: 247.6 M

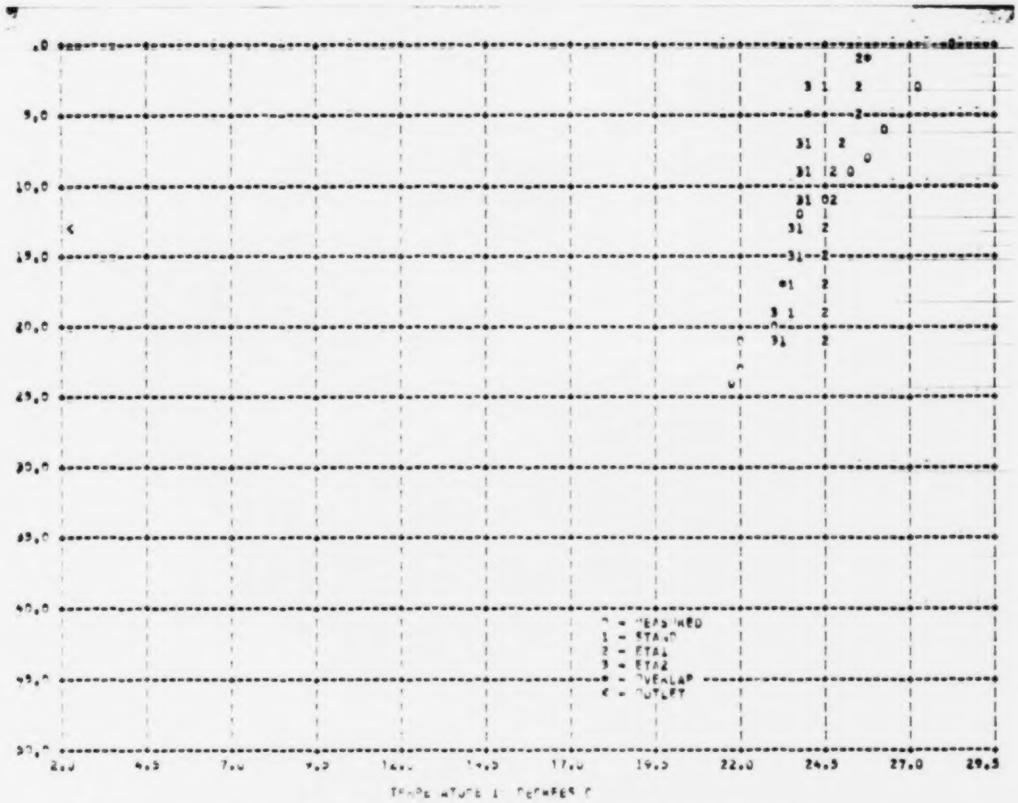

Figure 191 MIT MODEL * FORT LOUDOUN 1971 --DAY1226 --SURFACE ELEV: 247.5 M

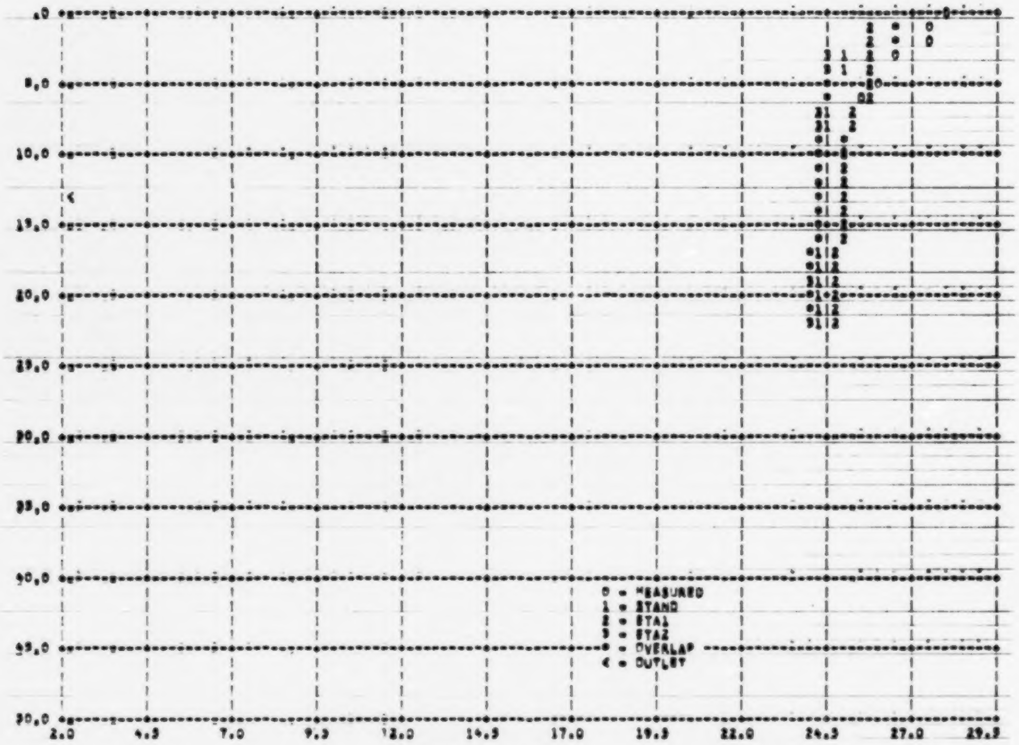

Figure 192 MIT MODEL * FORT LOUDOUN 1974 --DAY=253 --SURFACE ELEV: 247.6 M

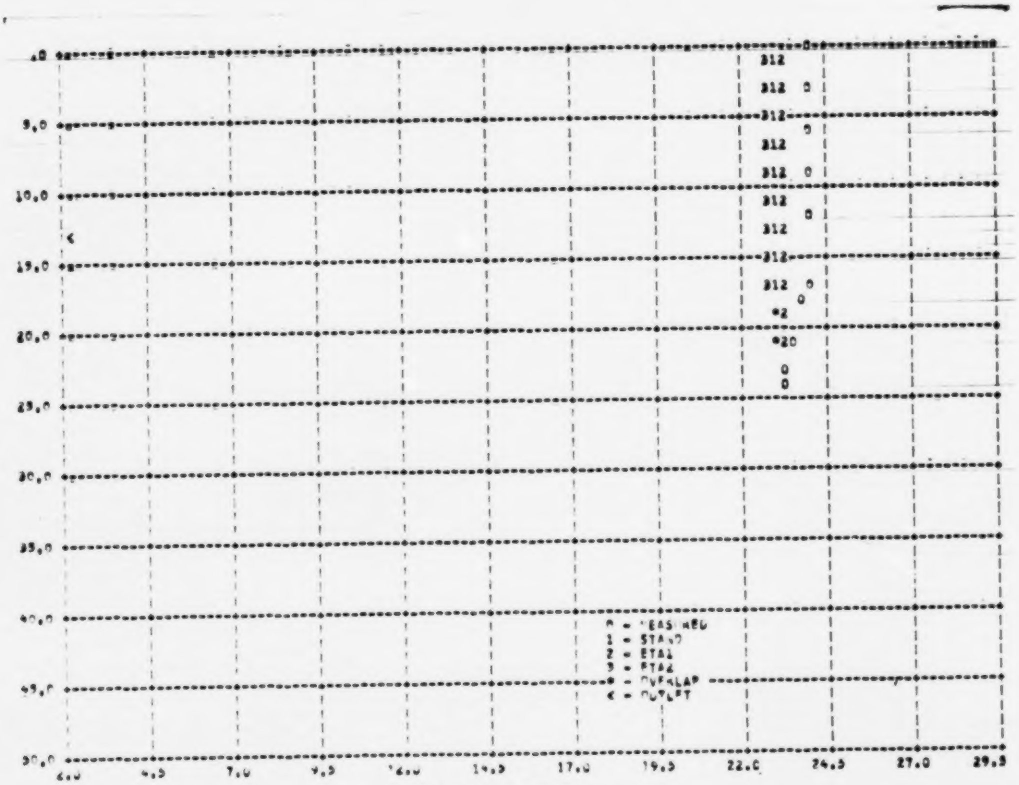

Figure 193 MIT MODEL * FORT LOUDOUN 1974 --DAY=260 --SURFACE ELEV: 247.5 M

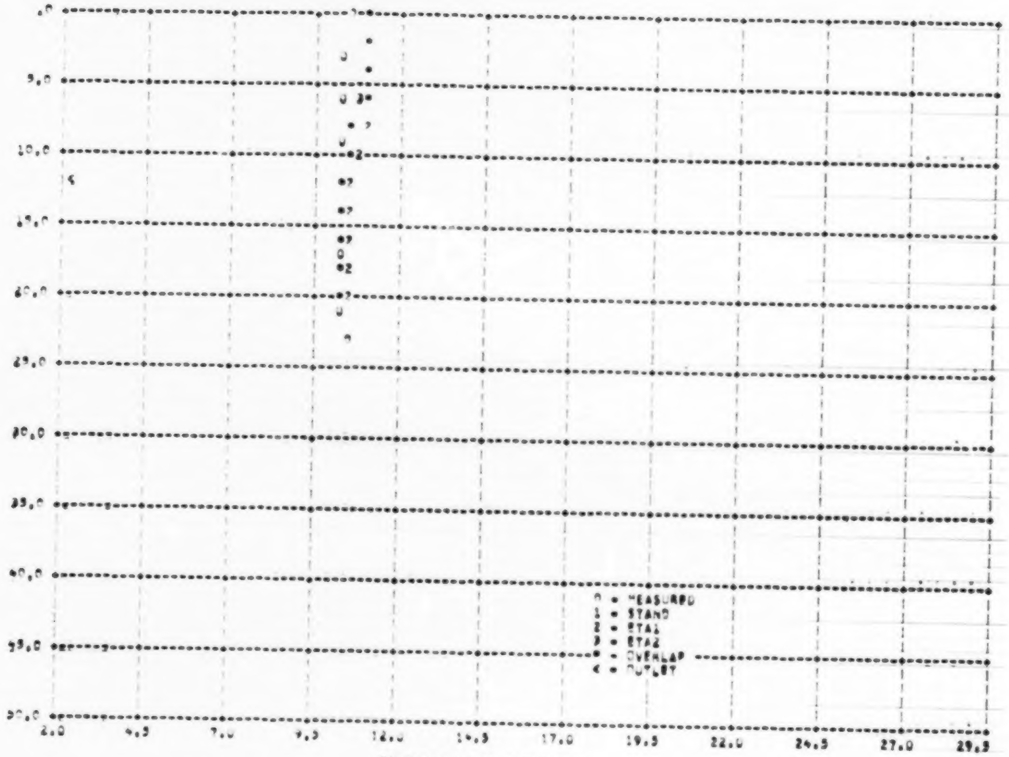

TEMPERATURE IN DEGREES C

Figure 194 [illegible] 1971 --DAY=134 --SURFACE ELEV 246.1 M

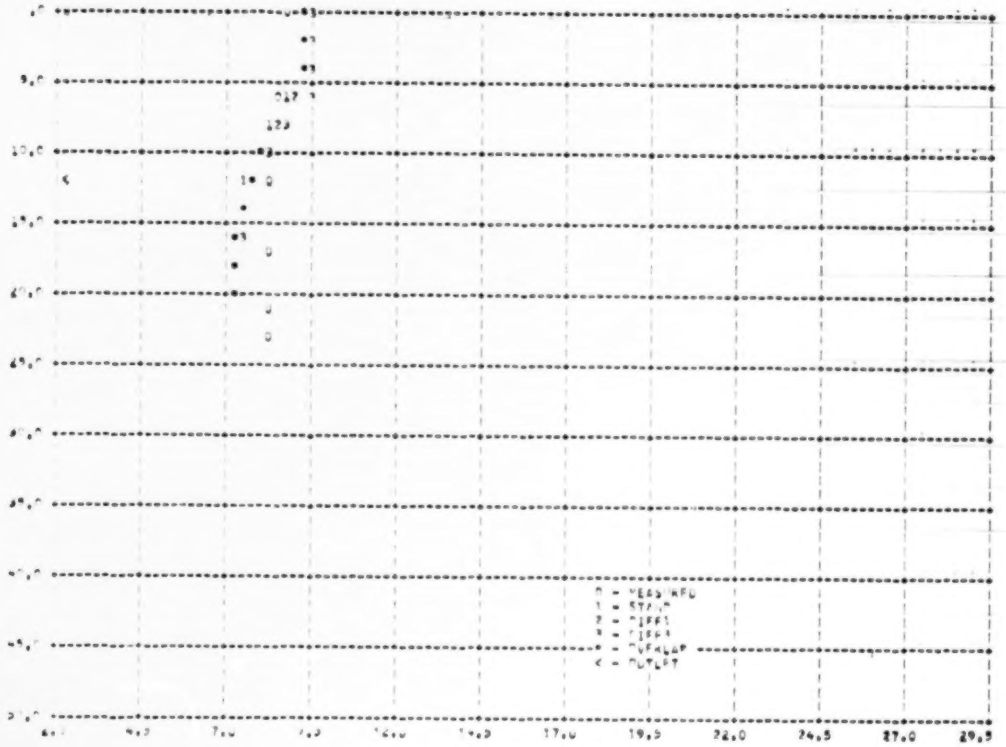

TEMPERATURE IN DEGREES C

Figure 195 [illegible] 1971 --DAY= 75 --SURFACE ELEV 246.1 M

Reproduced from
best available copy.

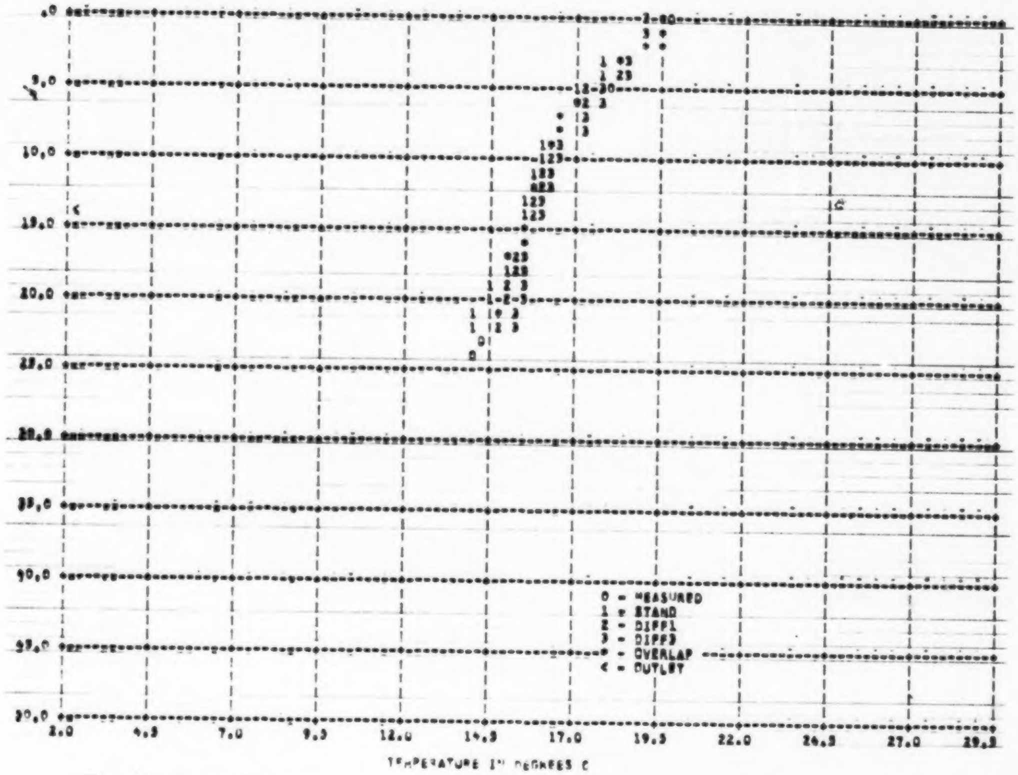

Figure 196 MIT MODEL * FORT LOUDOUN 1971 --DAY:132 --SURFACE ELEV: 247.7 M

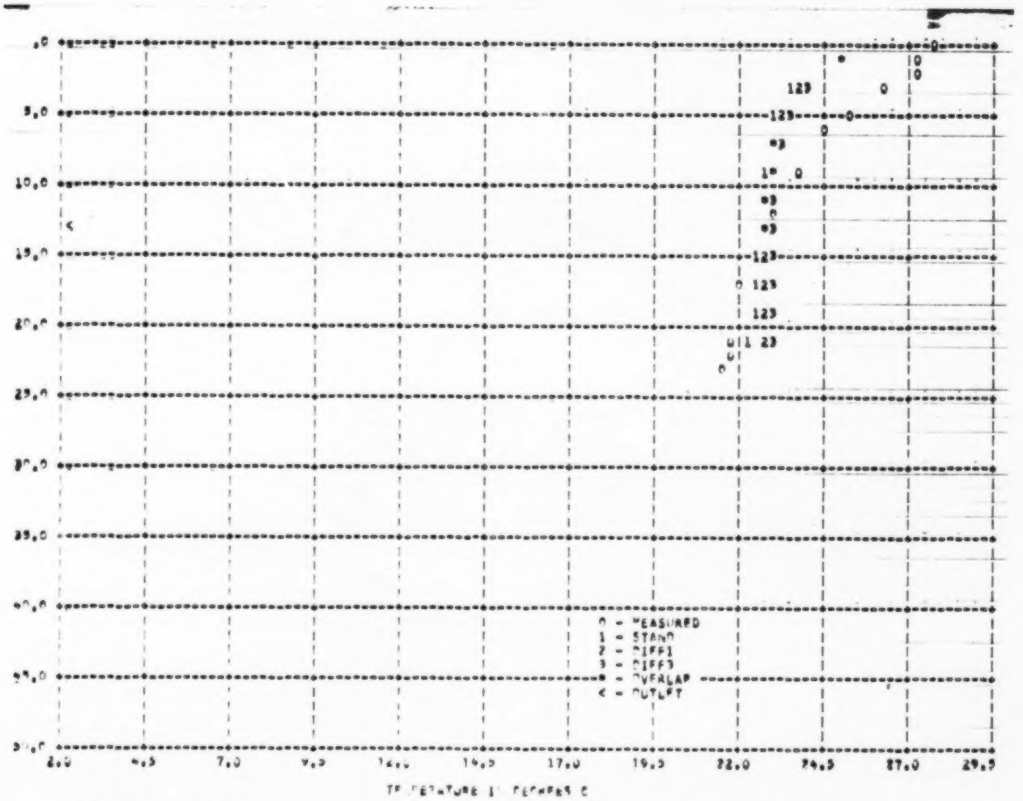

Figure 197 MIT MODEL * FORT LOUDOUN 1971 --DAY:216 --SURFACE ELEV: 247.6 M

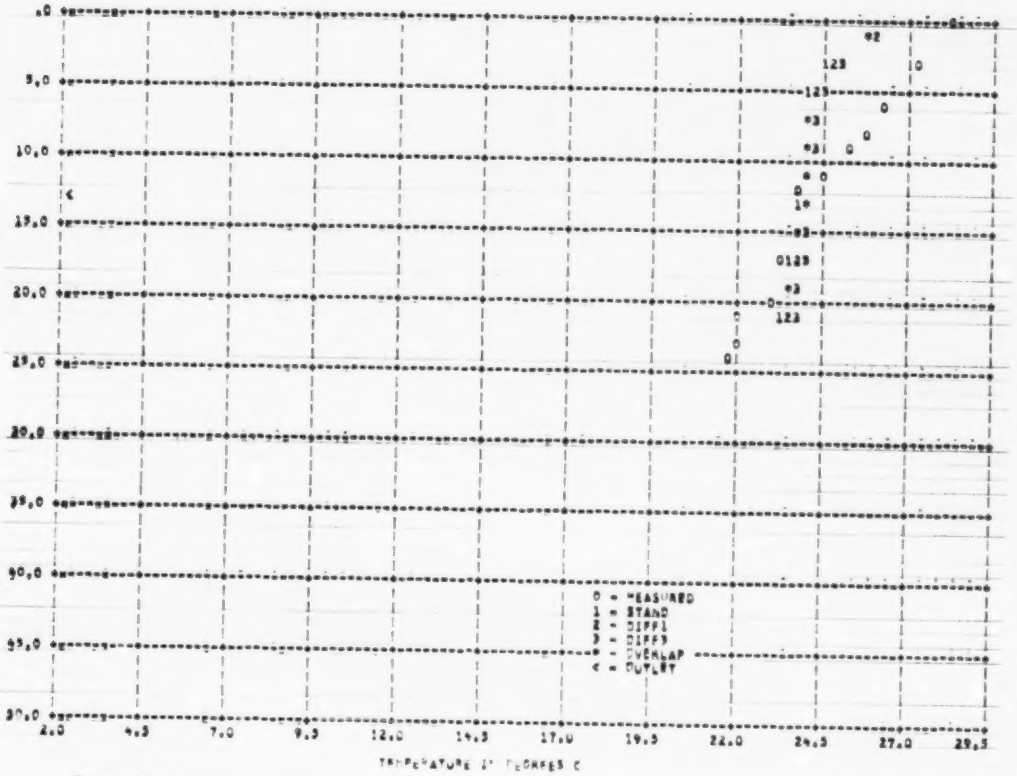

Figure 198 [illegible] MODEL * [illegible] 1971 --[illegible]1270 --SURFACE ELEV 247.5 M

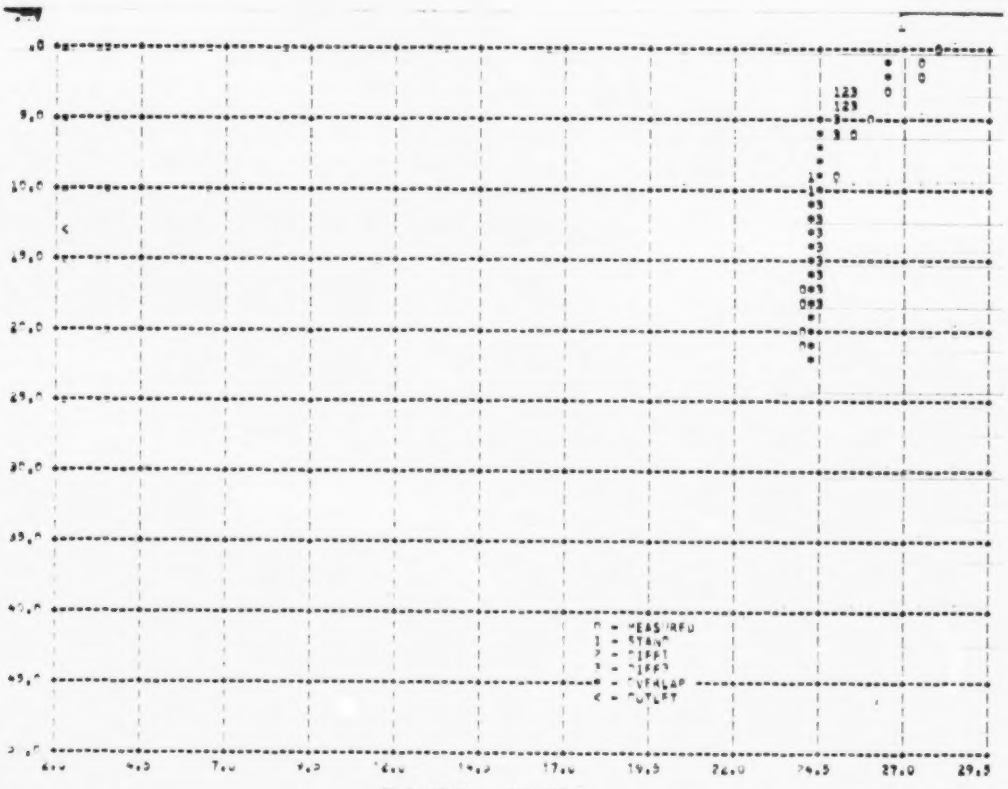

Figure 199 [illegible] MODEL * [illegible] 1971 --[illegible]1293 --SURFACE ELEV 247.0 M

Reproduced from best available copy.

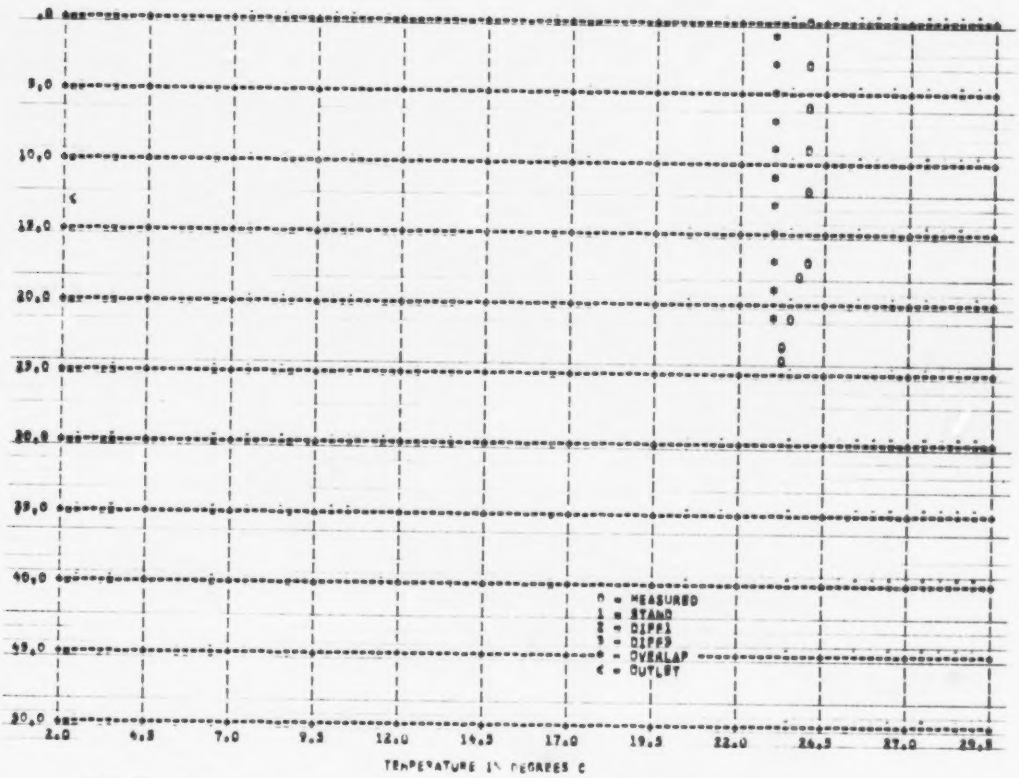

Figure 200 MIT MODEL - FORT LOUDOUN 1971 --DAY1280 --SURFACE ELEV: 247.5 M

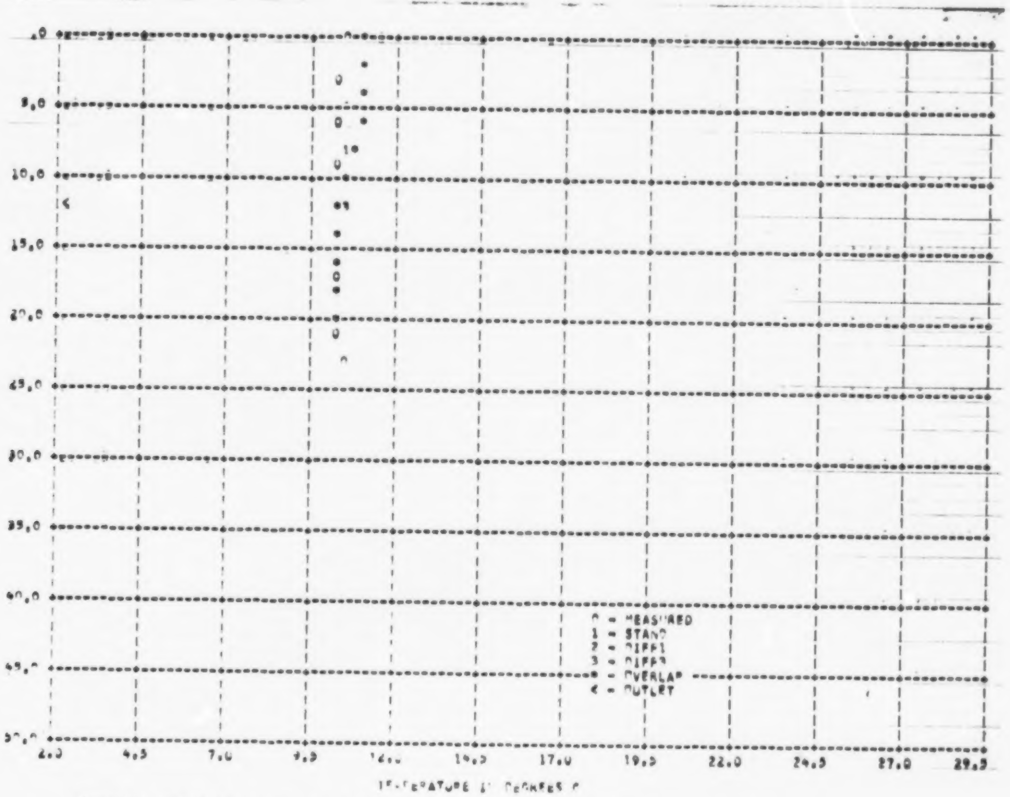

Figure 201 MIT MODEL - FORT LOUDOUN 1971 --DAY1343 --SURFACE ELEV: 240.1 M

SECTION VI

ANALYSIS OF DATA

The surface temperature, being related to the equilibrium temperature, can be well represented by a simple sinusoidal relationship. A sinusoidal type function was least square fitted to the measured surface water temperatures as shown in Table 21. The water temperature at the outlet level cannot be fitted as easily, because it is dependent upon several variables, e.g. time (day of the year), depth of outlet, outflow rate and variation of thermocline depth, etc. However, if the time period considered was shortened, such as using only the data between early summer and winter instead of the full year, a least square fit of a third degree polynomial can be fitted reasonably well. The results of a third degree polynomial fitted to the measured water temperatures at the outlet level are shown in Table 22. The average standard error of estimate for the curves fitted are 1.2°C for the measured surface temperature and 1.6°C for the measured water temperature at outlet level, respectively for seven TVA reservoirs. The predicted temperatures were then evaluated for the standard error of estimate with respect to the aforementioned fitted least square curves.

In general, the sensitivity analysis of the input parameters has shown that for:

1) Vertical Increments or Horizontal Layer Thickness, ΔY

The effects of variation of layer thickness on the temperature profile are different from one reservoir to another. The general trend is that the use of a smaller ΔY, 1 meter, yields temperature profiles a little lower in

Table 21

LEAST SQUARES CURVE* FIT FOR MEASURED SURFACE WATER TEMPERATURE

Reservoir/Year	No. of Data Points	Std. Error of estimate(^oC)	Correlation Coefficient	A (^oC)	B (^oC)	Ψ
Fontana/1966	27	1.22	0.98	16.96	- 9.72	0.927
Douglas/1969	31	2.23	0.97	17.60	-12.82	1.180
Cherokee/1967	37	1.53	0.97	16.70	-10.08	1.006
Norris/1971	48	1.30	0.97	17.46	-11.54	1.065
South Holston/1953	12	1.79	0.98	17.01	-11.63	0.970
Hiwassee/1947	12	1.70	0.98	19.07	-10.43	0.850
Fort Loudoun/1971	12	1.50	0.99	17.88	-12.32	0.992

*Curve Type: $A + B \sin (\frac{2\Pi}{365} t + \Psi)$

Table 22
LEAST SQUARES CURVE* FIT FOR MEASURED WATER TEMPERATURE AT OUTLET LEVEL

Reservoir/Year	No. of Data Points	Std. Error of Estimate (^oC)	Correlation Coefficient	Time Period of Fitted Curve (Julian Days)
Fontana/1966	22	0.96	0.97	103 - 341
Douglas/1969	27	1.10	0.98	69 - 352
Cherokee/1967	32	1.06	0.96	117 - 332
Norris/				
South Holston/1953	9	1.09	0.96	113 - 362
Hiwassee/1947	10	1.50	0.96	80 - 364
Fort Loudoun/1971	10	1.56	0.92	76 - 343

* Third Degree Polynomial

the middle or deep portion of the reservoir than the use of a larger increment. Because there is little difference in the predicted temperatures using either 1 or 2 meters, the use of 2 meters per layer is recommended since this reduces computing time considerably.

The MIT model recommends a minimum of twenty layers. From the results of this study, it is recommended that $\Delta Y = 2m$ be used unless this causes the number of layers to be much less than twenty. In a reservoir of one hundred meters or more, a thickness of 3 meters appears to be satisfactory.

2) Fraction of Solar Radiation Absorbed at the Water Surface, β

The value of the surface absorption ratio, β, is generally assumed to be about 0.4. Recent TVA field data suggests a value of 0.24 in Big Ridge Lake and Fontana Reservoir. The higher the value of β, the lower the temperature profile is likely to be, since a larger portion of the solar energy absorbed at the water surface means less energy geing transmitted downward into the body of water.

3) Radiation Absorption Coefficient, η

The value of η may vary with the time of year, being a function of turbidity of the water. The values selected for analyses ranged from 0.05 for clear water, 0.40 and 0.75 for intermediate waters to 1.4 for highly turbid water. Results on all reservoirs using 0.05 show that too much solar energy was transmitted to too great a depth. All reservoirs tested contained more turbidity than distilled water. Temperature profiles followed a general pattern, being lower for higher η values. Because of the temperature sensitivity to a change in η, a carefully measured value is important to thermal simulation. For prediction of temperatures in unbuilt reservoirs, η, between 0.75 and 1.40 can be used for the preliminary study.

4) Diffusion Coefficient, D

The MIT model authors recommend, based on their verification using Fontana Reservoir, the use of molecular diffusion for all depths at all times, which neglects turbulent diffusion. Other field data indicates diffusion coefficients higher than molecular diffusion. Diffusion coefficients are a function of density, gradient, depth, and time. Due to the approximate nature of the mathematical model and the complex interaction in diffusion, we are unable to assign a specific diffusion coefficient.

In this study molecular diffusion coefficients 30 times, 100 times, and 1000 times molecular diffusion were tested. The use of a coefficient 1000 times molecular diffusion always caused the model to malfunction. This was not unexpected since the stability criteria, Equation 58, is violated when $\Delta Y = 2m$ and $\Delta Y = 1$ day are used with this diffusion coefficient. The use of 100 times molecular diffusion also results in most cases, in predicted temperatures different from measured temperatures. The temperatures predicted with the use of 30 times molecular diffusion and with molecular diffusion are similar. It appears that an appropriate choice would be 15 to 20 times molecular diffusion.

5) Reservoir Classification

The criterion which is widely used for classification of a stratified reservoir, is that due to Orlob(3) who introduced a densimetric Froude number in the form

$$\mathrm{IF}_D = \frac{LQ}{DV} \sqrt{\frac{1}{g\varepsilon}} \qquad (86)$$

where:

L = length of reservoir in meters

Q = volumetric discharge through the reservoir in m^3/sec

D = mean reservoir depth in meters

V = reservoir volume in cubic meters

ε = average normalized density gradient in reservoir ($10^{-6}\ m^{-1}$)

g = gravitational constant (= $9.8\ m/sec^2$)

substituting the average values, we have

$$IF_D = 320 \frac{L}{D} \frac{Q}{V} \tag{87}$$

For $IF_D < \frac{1}{\Pi}$, the reservoir is considered strongly stratified.

The densimetric Froude numbers for the seven reservoirs tested are listed in Table 23. Except for Fort Loudoun Reservoir, the densimetric Froude numbers are much smaller than $1/\Pi$. Based on the Froude number criterion, all but one are considered to be strongly stratified.

When we compare the computed temperatures with measured temperatures, we note that an adequate simulation by the deep reservoir model for a particular reservoir does not solely depend on its densimetric Froude number.

The densimetric Froude numbers of the seven reservoirs do not extend over the whole range of interest. Therefore, no critical value can be established with regard to the applicability of the model. However, it appears that for a reservoir with large depth, low densimetric Froude number and small variation in surface elevation, such as Fontana Reservoir, small differences in predicted and measured temperatures result from the application of the MIT deep reservoir model. The greater the deviation from deep reservoir conditions, the less accurate the calculated temperatures will be.

TABLE 23 DENSIMETRIC FROUDE NUMBERS FOR SOME TVA RESERVOIRS

	Length of Lake Miles	Mean Annual Runoff at Dam, 10^3 acft/year	Normal Maximum Depth, Feet	Storage*, 10^3 acft	Reservoir Surface Area, Acres	Densimetric Froude Number
Fontana	29.0	2,667.7	432	1444.3	10,670	.006
Douglas	43.1	4,830.7	129	1514.1	30,600	.06
Cherokee	59.0	3,316.6	150	1565.4	30,200	.05
Norris	72.0**	2,956.1	196	2567.0	34,200	.02
South Holston	24.3	735.4	240	744.0	7,580	.005
Hiwassee	22.0	1,369.9	252	438.0	6,080	.01
Fort Loudoun	55.0	9,949.8	74	386.5	14,600	1.02

* At maximum controlled elevation

** Clinch River Arm Only

REFERENCES

1. Shirazi, Mostafa A. and Davis, Lorin R. Workbook of Thermal Plume Prediction, Volume 1: Submerged Discharge. National Environmental Research Center, Corvallis, Oregon. U.S. Environmental Protection Agency Technology Series EPA-R2-72-005a.August, 1972.

2. Shirazi, Mostafa A. and Davis, Lorin R. Workbook of Thermal Plume Prediction, Volume 2: Surface Discharge. National Environmental Research Center, Corvallis, Oregon. U.S. Environmental Protection Agency Technology Series EPA-R2-72-005b.1974.

3. Water Resources Engineers, Inc. Mathematical Models for the Prediction of Thermal Energy Changes in Impoundments. Federal Water Quality Administration, Washington, D.C. Water Pollution Control Research Series 16130EXT12/69. December, 1969.

4. Ryan, Patrick J. and Harleman, Donald R.F. Prediction of the Annual Cycle of Temperature Changes in a Stratified Lake or Reservoir: Massachusetts Institute of Technology, Cambridge, Mass. Mathematical Model and User's Manual, MIT Hydrodynamics Laboratory Report No. 137.April, 1971.

5. Sundaram, T.R. Rehm, R.G., Rudinger, G. and Merritt, G.E. A Study of Some Problems on the Physical Aspects of Thermal Pollution Report VT-2790-A-1.Cornell Aeronautical Laboratory, Buffalo, New York.June, 1970.

6. Hanford Engineering Development Laboratory The Colheat River Simulation Model. HEDL-TME 72-103.August, 1972.

7. Beard, Leo R. and Willey, R.G. An Approach to Reservoir Temperature Analysis. Water Resources Research 6(5): October, 1970.

8. World Meteorological Organization. Measurement and Estimation of Evaporation and Evapotranspiration. Geneva, Switzerland Technical Note 83. 1966.

9. Water Resources Engineers, Inc. Prediction of Thermal Energy Distribution in Streams and Reservoirs. Prepared for the Department of Fish and Game, State of California. Walnut Creek, California. June, 1967.

10. Debler, W.R. Stratified Flow into a Line Sink. Journal of Engineering Mechanics (ASCE)85(EM3): July, 1959.

11. Craya, A. Theoretical Research on the Flow of Non-Homogeneous Fluids. LaHouille Blanche 4(1):56-64 January-February, 1949.

12. Huber, W.C. and Harleman, D.R.F. Laboratory and Analytical Studies of Thermal Stratification of Reservoirs. Massachusetts Institute of Technology, Cambridge, Massachusetts Hydrodynamics Laboratory Technical Report No. 112 October, 1968.

13. Kao, T.W. The Phenomenon of Block in Stratified Flow. Journal of Geophysical Research 70(4): February, 1965.

14. Sundaram, T.R. Easterbrook, C.C., Piech, K.R. and Rudinger, G. An Investigation of the Physical Effects of Thermal Discharges into Cayuga Lake. Cornell Aeronautical Laboratory. Buffalo, New York Report VT-2616-0-2. November, 1969.

15. Rossey, C.C. and Montgomery, B.R. The Layer of Frictional Influence in Wind and Ocean Currents. Physical Oceanography 3(3):101. 1935.

16. Munk, W.H. and Anderson, E.R. Notes on the Theory of the Thermocline. Journal of Marine Research 1:276. 1948.

17. Tennessee Valley Authority Water Temperature Prediction Model for Deep Reservoirs. Water Resource Management Methods Staff. Technical Report No. A-2, October, 1973.

18. Tennessee Valley Authority. Temperature Predictions for TVA Reservoirs Graphical Presentations. Water Resources Management Methods Staff. Report A-6 December, 1973.

19. Tennessee Valley Authority. Heat and Mass Transfer Between a Water Surface and the Atmosphere. Water Resources Research Laboratory Report No. 14. April, 1972.